Western Australian School of Mines

Evaluation of Monorail Haulage Systems in Metalliferous Underground Mining

Bunda Besa

This thesis is presented for the Degree of
Doctor of Philosophy
of
Curtin University of Technology

July 2010

Declaration

To the best of my knowledge and belief, this thesis contains no material previously published by any other person except where due acknowledgment has been made. This thesis contains no material that has been accepted for the award of any other degree or diploma in any other University.

Signed: _____ Date: _____

BUNDA BESA

Publications

The following publications have been produced during the period of the PhD.

Internationally Refereed Journal Articles

1. Chanda, E. K. and **Besa, B.** (2010). **'A computer simulation model of a monorail based mining system for decline development'.** *International Journal of Mining, Reclamation and Environment*, Taylor & Francis Publishers; Print ISSN: 1748-0930; Online ISSN: 1748-0949; *(Accepted).*

2. Chanda, E. K. and **Besa, B.** (2009). '**Design of pneumatic loading system for monorail application**,' *International Journal of Mining and Mineral Engineering*, Vol. 1, No. 2, pp.181–203. ISSN (Online): 1754–8918; ISSN (Print): 1754–890X.

Locally Refereed Conference Papers

1. **Besa, B**., Kuruppu, M., and Chanda, E. K. (2010). **'Numerical modelling of monorail support requirements in decline development,'** *Paper submitted to 'Mine Planning & Equipment Selection (MPES 2010)'*, The AusIMM, 1 – 3 December 2010, Fremantle, Western Australia (***Submitted***).

2. Chanda, E. K., and **Besa, B**. (2008). '**Monorail technology – A rapid and cost effective method of decline development**' *Paper presented at 'Narrow Vein Mining Conference'*, The AusIMM. 14–15 Oct. 2008, Ballarat, Central Victoria, Australia. pp 129–141. ISBN: 978 1 920806 897.

3. Chanda, E. K., **Besa, B**. and Kuruppu, M. (2008). '**Design of a continuous monorail drilling system for decline development**' *Paper presented at 'The International Future Mining Conference'* 19–21 Nov. 2008, The University of New South Wales, The AusIMM, Sydney, Australia. pp 101–111. ISBN: 978 1 920806 910.

Internationally Conference Papers

1. **Besa, B**., Kuruppu, M., and Chanda, E. K. (2009). '**Risk assessment and hazard control for the monorail load-haul-system**' *Proceedings of the Eighteenth International Symposium on Mine Planning & Equipment Selection* (MPES 2009), Publisher: The Reading Matrix Inc. Irvine, CA, USA. November 16–19, 2009, Banff, Alberta, Canada. Pg. 163-179. ISSN 1913-6528.

2. Chanda, E. K., Darcey, W., Kuruppu, M. and **Besa, B.** (2007). '**Application Of Electro-Monorail Mine Haulage Systems In Underground Decline Development**' *Proceedings of the Sixteenth International Symposium on Mine Planning and Equipment Selection* (MPES 2007), 11–13 Dec. Bangkok, Thailand. pp 159–175. ISBN: 978 1 605603 261.

Technical Report

1. Chanda, E. K., Kuruppu, M. and **Besa, B.** (2009). '**Evaluation of Monorail Haulage in Metalliferous Underground Mining**.' Minerals and Energy Research Institute of Western Australia(MERIWA), Technical Report No. 276, Project No. M382. Crown Copyright. ISBN 1920981381.

Abstract

The decline is a major excavation in metalliferous mining since it provides the main means of access to the underground and serves as a haulage route for underground trucks. However, conventional mining of the decline to access the ore body poses economic and technical challenges that require innovative responses. The average cross-sectional area of mine declines in Australia is 5m wide x 5m high. The large excavations associated with current underground mining practices are economically and geotechnically inappropriate, especially for narrow vein mining conditions. The decline gradient of 1 in 7 (8^{o}) designed to accommodate truck haulage results in a significantly longer decline compared to a decline mined at a steeper gradient. Further, the current drill-blast-load-haul cycle does not allow rapid development of the decline to access the ore body since the cycle is made up of discontinuous segments. The use of diesel equipment poses health risks and increases ventilation requirements. The heat load and air borne exhaust contaminants emitted by large diesel engines create heavy demand on mine ventilation, sometimes resulting in substandard working conditions. As mines get deeper, there is a tendency to increase the truck and loader fleet – which results in traffic congestion in the decline. Metal prices in the recent boom may have helped to offset some of the shortcomings of current practices, and although the good times may continue, a down-turn could find many operations exposed. Federal government emissions trading scheme encourage mining companies to reduce carbon emissions in their operations.

This study was prompted by the need to investigate the potential of the monorail haulage system in metalliferous mining, particularly in decline development and main haulage in view of shortcomings of the current practices. Monorail systems are being used in mines around the world for material transport and man-riding but their utility in rock transport has not been fully investigated. Hence, it is proposed to replace non-shaft component of the mine haulage system with roof/back mounted monorail technology using continuous conductor technology to provide competitive haulage rates in substantially smaller excavations at

steeper gradient than is currently achievable. It is proposed that a suite of equipment can be adapted or modified to enable development of the decline supported by the monorail system.

To this end, a drill system mounted on the monorail accompanied by a pneumatic system for loading rock into monorail containers is proposed. The proposed decline gradient for the monorail decline is 1 in 3 (or 20^0) with a cross-sectional area of 4m wide x 4m high. Decline dimensions of size 4.0m x 4.0m (minimum opening for monorail system is 3m x 3m) are used in this design in order to leave enough working space (underneath and on the sidewalls) and to accommodate other mine services, such as, ventilation tubing, air and water pipes and cables. Systems analysis, engineering economics and computer simulation are used to evaluate the feasibility of the monorail mining system for decline development. Technical data relating to the operation of monorail systems in underground mining was obtained from Solutions for Mining Transport (SMT) – Scharf, of Germany, a company that manufactures monorail systems. Monorail haulage has definite advantages over conventional haulage; these include the use of electrical power instead of diesel, steeper gradients (up to 36^0), smaller excavations, tighter horizontal and vertical turning radii and potential for automation. The concepts are applied to a narrow vein ore deposit with results indicating that the monorail system delivers significant savings in terms of time and cost of decline development in this specific application.

Stability of the monorail drilling system is critical in ensuring high performance of the drilling system. Stabilisation of the system requires determination of the horizontal, vertical and lateral forces of the system. According to the findings, these forces depend on the vector position of the two drilling booms that will be mounted onto the monorail train. Therefore, the research provides minimum and maximum monorail system reaction forces in horizontal and vertical stabilisers that will stabilise the system during drilling operations. Because of the configuration and positioning of the monorail drilling system, the research has also shown that with appropriate swing angles and lifting angles that will enable the system to reach the whole drill face during drilling operations.

Since pneumatic or suction system is used during loading process, the research has revealed that the density of rock fragments, rock fragmentation, conveying air velocity and the negative pressure of the system would greatly influence the loading time and power consumption of the system. Therefore, the study has determined optimum fragmentation of the pneumatic system for various conveying air velocities. Additionally, for the efficient operations of the system, a range of conveying air velocities that give optimal mass flow rate (mass flow rate that give shorter loading time) and optimal power consumption have been determined at maximum negative pressure of 60kPa (0.6 bars).

Since the monorail drilling and loading systems move on the rail/monorail installed in the roof of the decline and supported by roof bolts, suspension chains and steel supports, the strength of the support system is critical. To avoid system failure, it is imperative that the force in each roof bolt, suspension chain and steel support capable of suspending the weight of the heaviest component of the system is determined. Through the models developed, this study has determined the minimum required strength of roof bolts, suspension chains and steel supports that can suspend and support the components of the drilling and loading systems.

To increase the efficiency and improve the safety of the two systems, the automation design for monorail drilling and loading systems' processes have been developed. The proposed automation system would increase productivity by improving operator performance through control of the two systems' processes. It is hoped that automation of the monorail drilling and loading systems will reduce the total drill-load-haul cycle time hence improving the efficiency of the systems.

The application of simulation techniques was deemed useful to determine the performance of the monorail system in mining operations. During modelling, a simulation programme was written using General Purpose Simulation System (GPSS/H) software and results of the simulation study were viewed and examined in PROOF animation software. According to simulation results, the

monorail system will have the same advance rate as conventional method since both systems have one blast per shift. However, the total drill-blast-load-haul cycle time for the monorail system is lower than for conventional method.

Since the monorail system poses health and safety challenges during operations, through risk analysis, this study has identified root factors that have the potential to cause monorail system risk and hazard failure. The research has revealed that lack of maintenance of the monorail system and the monorail installations, production pressure and insufficient training of personnel on monorail system use are the major root factors that have the potential to cause risk and hazard failure. In order to improve the health and safety of the system, the study has suggested risk and hazard control strategies which are aimed at reducing the level of risk by directing corrective measures at potential root causes as opposed to addressing the immediate obvious symptoms such as monorail falling from support system, monorail running out of control, and others.

A mine design case study using a monorail technology was conducted using one of 'South Deeps' gold deposits of Jundee mine operations (owned by Newmont Mining Corporations). Nexus deposit, one of 'South Deeps' deposits, was selected as case study area. The case study indicates that development of decline access to Nexus deposits using monorail technology is feasible. Compared with conventional decline development, results have shown that the monorail system has the potential of reducing the decline length to Nexus deposits by over 62.6% and decline costs by 63% (i.e., spiral decline and straight incline from the portal only). Furthermore, the study indicates that with the monorail system, there is a potential of reducing the total capital development costs to Nexus deposit by 22% (i.e., cost of developing the spiral decline, straight incline from the portal, crosscuts, ventilation network and installation and purchase of monorail train). Also, due to shorter decline length coupled with smaller decline openings, the duration of decline development reduces by 71.8%.

Dedication

This thesis is dedicated to my late mum

Mrs. Eunice Yumba Kapeya Besa

for showing me the value of education, the importance of perseverance and for the suffering she went through (after the death of my father) to make sure that I go to school.

I also dedicate this thesis to my beloved brother **Kanta Besa** who never saw an inside of a classroom because he passed away immediately he was taken to the village to start school.

To my beloved wife **Keddy Nambeye Besa** and my lovely children

– **Mwaba, Kanta, Bunda and Natasha**

- This is for you -

Acknowledgements

I wish to thank God Almighty for inspiring and giving me the guidance, discipline, strength, patience, perseverance and endurance until the end of my studies.

I also wish to sincerely thank my first supervisor Associate Professor Emmanuel Chanda for seeing the potential in me and for his valuable and excellent motivation, guidance and constructive input throughout this project. It was unfortunate that circumstances did not allow him to supervise the project to the end although he was constantly in touch with me and made sure that I finish the project. I also wish to express my deepest thanks to my second supervisor Dr. Mahinda Kuruppu for providing much needed enthusiasm and the high degree of expertise needed to guide me to the end. Special thanks also go to my co-supervisor, Dr. Andrew Jarosz, and my thesis chairperson, Professor Roger Thompson for their valuable contribution to this research.

This PhD research would not have been possible without the financial support from Curtin International Postgraduate Research Scholarship (CIPRS) and research funding from Minerals and Energy Research Institute of Western Australia (MERIWA), Newmont and Western Australian School of Mines (WASM). Many thanks also go to Professor Ernesto Villaescusa and the Rock Mechanics Research Group of Curtin University of Technology for extending financial support to the project.

I also wish to extend my deepest thanks to the following: Mr. Stefan Meyer and Solutions for Mining Transport (SMT) – Scharf, for providing technical data and cost information on the Electric Monorail Transport System (EMTS); Mr. William Darcey who worked on the project before I took over and Mr. Mick Roberts, for providing advice on practical aspects of the system. I would also like to acknowledge the support I received and the friendship afforded to me by WASM staff particularly from Mining Engineering and Mine Surveying Department during my studies.

Finally, I would like to mention that doing PhD studies for three years without my family nearby was so painful and sometimes disturbing. Therefore, my heartfelt thanks go to my loving family who have been there for me and for giving me the strength throughout the long process of completing PhD thesis. To my beloved wife Keddy Nambeye Besa, my deepest thanks for her love and inspiring and for looking after my four children well during my absence, sometimes under difficult and strenuous conditions. I am also deeply indebted to my four wonderful children Mwaba, Kanta, Bunda and Natasha who have been patient and understanding during this journey. Without their support and encouragement, which has been truly remarkable, this work would not have been possible.

Table of Contents

Page

Declaration ii
Publications iii
Abstract v
Dedication ix
Acknowledgements x
Table of Contents xii
List of Figures xxiii
List of Tables xxx
Nomenclature xxxii
Acronyms xxxvi

Chapter 1 1
1.0 Introduction 1
1.1 Underground mine access and haulage 1
1.2 The monorail system 2
1.3 Research objectives 3
1.4 Research approach 4
1.5 Significance of the study 5
1.6 Contribution 6
1.7 Thesis structure 6
Chapter 2 10
2.0 Monorail technology 10
2.1 Introduction 10
2.2 Background to monorail technology 10
2.2.1 Electric Monorail Transport System (EMTS) technology 11
2.2.1.1 What is EMTS technology? 11
2.2.1.2 Components of a monorail system 12
2.2.1.3 Electrical switches and power supply 20
2.2.1.4 Monorail switch points 21
2.2.1.5 Monorail train performance chart 21

2.2.1.6 EMTS automation and control system 23
2.2.1.7 Monorail system application in mining 23
2.2.1.8 An overview of monorail installation 25
2.2.2 Benefits of EMTS 25
2.3 Monorail system versus conventional decline development 26
2.3.1 What is a decline access? 26
2.3.2 Conventional decline development 27
2.3.2.1 Conventional decline design parameters 28
2.3.2.2 Effects of designed parameters on decline development 29
2.3.2.3 Productivity in conventional decline development 36
2.3.2.4 Conventional decline development costs 39
2.3.3 Application of monorail technology in decline development 40
2.3.3.1 Decline design parameters for monorail system application 41
2.3.3.2 Effects of designed parameters on decline development 43
2.3.3.3 Monorail system productivity 44
2.3.3.4 Monorail system costs 45
2.3.3.5 Power requirements for monorail system operations 47
2.3.4 Conventional versus monorail system decline development 49
2.3.5 Monorail system productivity 51
2.3.6 Conceptual monorail drilling and loading systems 52
2.4 Summary 54
Chapter 3 55
3.0 Pneumatic conveying system 55
3.1 Introduction 55
3.2 Pneumatics and its applications 55
3.3 Pneumatic conveying system 56
3.3.1 Types of pneumatic conveying systems 57
3.3.2 Components of pneumatic conveying system 58
3.3.3 Modes of pneumatic conveying 59
3.3.3.1 Dilute phase transport 60
3.3.3.2 Dense phase transport 61
3.3.4 Operations of pneumatic conveying system 62
3.3.4.1 Horizontal conveying 63

3.3.4.2 Vertical conveying 64
3.4 Fundamentals of pneumatic (suction) principles 65
3.4.1 Feeding and entry section 65
3.4.2 Pressure drop determination in pipes 67
3.4.2.1 Air-alone pressure drop 68
3.4.2.2 Pressure drop due to solids in straight inclined pipes 71
3.5 Force balance in incline suction pipe 76
3.6 Minimum entry velocity consideration 79
3.7 Effects of material physical characteristics 81
3.8 Gas-solid separation 84
3.9 Pneumatic conveying power requirement 84
3.10 Summary 85
Chapter 4 86
4.0 Design of monorail pneumatic loading system and surface infrastructure 86
4.1 Introduction 86
4.2 Structure of the conceptual monorail loading system 86
4.3 Design of monorail loading system 88
4.3.1 Design purpose and method 89
4.3.2 Suction pipe and material conveying characteristics 89
4.3.3 Mode of solid conveying 90
4.3.4 Solid loading ratio (m*) 90
4.3.5 Transport velocity 90
4.3.6 Mass flow rate of air 91
4.3.7 Mass flow rate of solids 92
4.3.8 Superficial velocity of solids in the suction pipe 94
4.3.9 Pressure drop in incline suction pipe 95
4.3.9.1 Pressure loss in acceleration zone 95
4.3.9.2 Pressure drop in steady state zone 97
4.4 Effects of particle size on design parameters 98
4.4.1 Effects of particle size on conveying velocity 98
4.4.2 Effects of particle size on mass flow rate of solids 100
4.4.3 Effects of particle size on power consumption 101

4.5 Optimum design parameters for the pneumatic loading system 103
4.5.1 Optimum mass flow rate of solids 103
4.5.2 Optimum power consumption 104
4.5.3 Optimum loading time 104
4.5.4 Optimum rock fragmentation 105
4.5.4.1 Post-blast material size distribution 106
4.5.4.2 Relationship between rock fragmentation, M_s and v_a 107
4.5.4.3 Dealing with oversize 109
4.5.4.4 Dust minimisation during conveyance 110
4.6 Handling of suction pipe during suction process 112
4.6.1 Suction pipe configuration 112
4.6.2 Movement and handling of suction pipe 114
4.6.3 Suction pipe connection and disconnection 115
4.7 Suction pump selection for pneumatic loading system 116
4.7.1 Pump capacity 116
4.7.2 Total head 117
4.7.2.1 Static head 118
4.7.2.2 Friction head 119
4.7.2.3 Pressure head 120
4.7.3 Pump performance curve 120
4.7.4 Brake-horsepower and pump efficiency 121
4.8 Monorail system surface infrastructure 123
4.8.1 Surface infrastructure arrangement 124
4.8.2 Surface material handling system 126
4.9 Summary 127
Chapter 5 128
5.0 Design of monorail drilling system 128
5.1 Introduction 128
5.2 Configuration of monorail drilling system 128
5.3 Components of the monorail drilling unit 129
5.3.1 Rock drill 130
5.3.2 Feed 131
5.3.3 Drill boom 133

5.4 Forces acting on the monorail drilling system 135
5.5 Reaction forces from the monorail drilling system 138
5.5.1 Forces in y-direction (longitudinal forces) 138
5.5.1.1 Forces due to weight of monorail drilling system 138
5.5.1.2 Brake force 138
5.5.1.3 Longitudinal frictional forces at base of horizontal stabilisers 139
5.5.2 Forces in z-direction (vertical forces) 140
5.5.2.1 Forces due to weight of monorail drilling system 141
5.5.2.2 Total force in roof bolts within span L_{md} 141
5.5.2.3 Vertical frictional forces at base of horizontal stabilisers 142
5.5.2.4 Forces in vertical stabilisers 142
5.5.3 Forces in x-direction (lateral forces) 142
5.5.3.1 Lateral forces in horizontal stabilisers 142
5.5.3.2 Lateral frictional forces at base of vertical stabilisers 143
5.6 Forces from the monorail drilling unit 143
5.6.1 Resolution of drilling force (F_M) into its components 144
5.6.2 Drilling boom vector definition 146
5.7 Stabilisation of the monorail drilling system 148
5.7.1 Stabilisation in y-direction 148
5.7.1.1 Minimum frictional forces in y-direction 150
5.7.1.2 Maximum frictional forces in y-direction 150
5.7.2 Stabilisation in z-direction 150
5.7.2.1 Minimum force in vertical stabilisers 153
5.7.2.2 Maximum force in vertical stabilisers 153
5.7.3 Stabilisation in x-direction 154
5.7.3.1 Minimum force in horizontal stabilisers 155
5.7.3.2 Maximum force in horizontal stabilisers 156
5.8 Stabilisation of monorail drilling system 156
5.8.1 Method 156
5.8.2 System assumptions 157
5.8.3 Stabilisation forces in y-direction 157
5.8.3.1 Minimum frictional forces 157

5.8.3.2 Maximum frictional forces 158
5.8.4 Stabilisation of forces in z-direction 159
5.8.4.1 Minimum force in vertical stabilisers 159
5.8.4.2 Maximum force in vertical stabilisers 160
5.8.5 Stabilisation of forces in x-direction 160
5.8.5.1 Minimum force in horizontal stabilisers 160
5.8.5.2 Maximum force in horizontal stabilisers 161
5.8.6 Coefficient of static friction at base of horizontal stabilisers 162
5.9 Factor of Safety 163
5.9.1 Factor of safety for monorail drilling system stabilisers 163
5.10 Summary 165
Chapter 6 166
6.0 Monorail installation and support system 166
6.1 Introduction 166
6.2 Decline support system for monorail installation 166
6.3 Monorail installation 168
6.3.1 Drilling of roof bolt support holes 170
6.3.2 Roof bolt installation and load transmission 171
6.3.3 Rail placement 173
6.3.4 Rail alignment 174
6.4 Weight of monorail system components in an incline versus required support system 176
6.4.1 Weight of monorail loading system components versus required support system 177
6.4.1.1 Total force in suspension chains within L_{part} 178
6.4.1.2 Weight of monorail loading system component 178
6.4.1.3 Required strength of suspension chains 179
6.4.1.4 Required strength of roof bolts 180
6.4.2 Weight of monorail drilling system components versus required support system 180
6.4.2.1 Total forces in suspension chains within L_{dpart} 181
6.4.2.2 Weight of monorail drilling system component 182
6.4.2.3 Required strength of suspension chains 183

6.4.2.4 Required strength of roof bolts 183
6.5 Strength of support system at horizontal and vertical curves 183
6.5.1 Strength of steel supports at vertical curves based on weight of monorail loading system components 184
6.5.1.1 Total axial force in steel supports at vertical curve 185
6.5.1.2 Required strength of steel supports at vertical curves 187
6.5.1.3 Required strength of roof bolts at vertical curves 187
6.5.2 Strength of steel supports at vertical curves based on weight of monorail drilling system component 187
6.5.2.1 Total axial force in steel supports at vertical curves 189
6.5.2.2 Weight of monorail drilling system component 189
6.5.2.3 Required strength of steel supports at vertical curve 189
6.5.2.4 Required strength in roof bolts at vertical curve 190
6.5.3 Strength of suspension chains at horizontal curves based on monorail loading system 190
6.5.3.1 Force and displacement of suspension chains at horizontal curves 190
6.5.3.2 Angular displacement (δ) of suspension chains due to monorail loading system 192
6.5.3.3 Horizontal displacement (X) of suspension chains due to monorail loading system 193
6.5.3.4 Force in suspension chains at horizontal curves 193
6.5.3.5 Axial force in roof bolts at horizontal curves 194
6.5.4 Strength of suspension chains at horizontal curves based on monorail drilling system 194
6.5.4.1 Force and displacement of suspension chains at horizontal curves 194
6.5.4.2 Required strength of suspension chains at horizontal curves 195
6.5.4.3 Axial force in roof bolts at horizontal curves 195
6.5.5 Summary of models to determine required support at curves 195
6.5.6 Variation of support system strength with change in decline gradient 197
6.5.6.1 Numerical values of support system strength 197

6.5.6.2 Strength of support system at 20^0 decline gradient 199
6.6 Summary 201
Chapter 7 202
7.0 Automation design for monorail system processes 202
7.1 Introduction 202
7.2 Process control engineering 202
7.3 What is automation? 203
7.4 Reasons for system automation 205
7.5 Fundamentals of open and closed-loop control system 206
7.5.1 Open-loop control system 206
7.5.2 Closed-loop control system 207
7.6 Automation design for monorail system processes 213
7.6.1 Overview of monorail system processes 213
7.6.2 Description of automation design for monorail loading process 215
7.6.3 Description of automation design for the monorail drilling system 217
7.7 Process control flow diagrams for monorail system 218
7.7.1 Process control flow diagram for monorail loading process 218
7.7.2 Process control flow diagram for material discharge process 219
7.7.3 Process control flow diagram for face marking process 221
7.8 Summary 222
Chapter 8 224
8.0 Simulation of monorail system 224
8.1 Introduction 224
8.2 Discrete-event simulation 224
8.3 Simulation model development 226
8.3.1 Problem formulation 227
8.3.2 Validity of conceptual model 228
8.3.3 Model programming 228
8.3.4 Model performance measure 229
8.3.4.1 System performance measure 229
8.3.4.2 Process performance measure 230
8.4 Simulation of monorail drilling and loading systems 231

8.4.1 Description of monorail system simulation processes 231
8.4.2 Model assumptions 234
8.4.3 Model programming 235
8.5 Results of monorail system simulation model 235
8.5.1 Effect of loading time on lashing speed 236
8.5.2 Effect of loading time on drilling speed 237
8.5.3 Effect of loading time on total drill-blast-load-haul cycle time 239
8.5.4 Effect of lashing time on the number of blasts per shift 240
8.5.5 Effect of lashing time on face advance rates 241
8.5.6 Effect of loading time on productivity of monorail system 242
8.6 Summary of monorail system simulation results 243
8.7 Conventional decline development versus monorail system 243
8.7.1 Time to drill and clean the development face 244
8.7.2 Charging, blasting and re-entry cycle time 245
8.7.3 Total drill-blast-load-haul cycle time 246
8.7.4 Advance rate per shift 247
8.8 Summary 248
Chapter 9 249
9.0 Monorail system risk analysis and hazard control 249
9.1 Introduction 249
9.2 Risk and hazard definitions 250
9.3 Risk assessment methodology – a theoretical approach 252
9.3.1 Hazard identification 253
9.3.2 System barrier identification 253
9.3.3 Risk analysis 254
9.3.4 Evaluation of failure consequence 256
9.3.5 Risk management and control 257
9.3.6 Risk communication 257
9.4 Risk assessment for monorail system 258
9.4.1 Risk assessment procedure 258
9.4.2 Identification of monorail system hazards 260
9.4.3 Existing hazard control measures and challenges 262
9.4.4 Likelihood and consequence risk factors 266

9.4.5 Likelihood analysis 266
9.4.6 Consequence analysis 269
9.4.7 Risk ranking 272
9.4.8 Risk level evaluation 273
9.4.9 Risk management and hazard control 276
9.4.9.1 Fault-tree analysis 276
9.4.9.2 Analysis of fault-tree results 280
9.4.9.3 Monorail system risk and hazard control strategies 286
9.5 Summary 290
Chapter 10 291
10.0 Mine design for monorail system application – Jundee Case Study 291
10.1 Introduction 291
10.2 Jundee "South Deeps" deposits 291
10.3 The Nexus orebody structure 293
10.4 Mine design for monorail system application 293
10.4.1 Mining method 293
10.4.2 Access design to Nexus structures 293
10.4.3 Design of cross-cuts to Nexus structures 294
10.4.4 Design of intake and exhaust ventilation network 295
10.4.5 Waste and ore handling 296
10.4.5.1 Waste handling 296
10.4.5.2 Ore handling 297
10.5 Results and analysis of the design 297
10.5.1 Development meters and tonnage to be removed 297
10.5.2 Capital development cost to Nexus structures 298
10.5.3 Conventional versus monorail system development meters 299
10.5.4 Conventional versus monorail system capital development costs 301
10.5.5 Purchase and monorail system installation costs 303
10.5.6 Duration of decline development to Nexus structures 304
10.6 Summary 304
Chapter 11 306
11.0 Conclusions and further work 306
11.1 Conclusions 306

11.2 Further work 310
References 311
Appendix 1 321
Appendix 2 339

List of Figures

Page

Figure 2.1: Aerial ropeway (a) Maamba Collieries Limited, Zambia (b) Brightling Aerial Ropeway 11
Figure 2.2: EMTS in an underground haulage 12
Figure 2.3: Components of a monorail system 13
Figure 2.4: Monorail train (a) driver's cabin with ergonomic operator seat; (b) Joystick with panel 14
Figure 2.5: Monorail train drive units (a) standard friction (b) rack–and–pinion 16
Figure 2.6: Monorail train power pack 17
Figure 2.7: Monorail system standard container 18
Figure 2.8: Monorail hoist system (a) single hoist unit; (b) series of hoist units 19
Figure 2.9: Monorail train power unit (a) switches (b) conductor bar 20
Figure 2.10: Monorail switch point 21
Figure 2.11: Monorail train typical performance chart 22
Figure 2.12: Conceptual applications of monorail system 24
Figure 2.13: Transport of men 24
Figure 2.14: Conventional decline access 27
Figure 2.15: Relationship between curvature and curve length 29
Figure 2.16: Relationship between gradient and length of a line 31
Figure 2.17: Effects of decline gradient on decline length 33
Figure 2.18: Relationship between decline gradient and development costs 35
Figure 2.19: Relationship between turning radius and curve length 35
Figure 2.20: Relationship between productivity of trucks and depth of mining .. 39
Figure 2.21: Decline opening requirements (a) one monorail train (b) two monorail trains 41
Figure 2.22: Solution to the minimum required curve radius 43
Figure 2.23: Effects of power on monorail system operating costs 48
Figure 2.24: Wattmeter chart for empty trip at faster monorail speed 49
Figure 2.25: Wattmeter chart for loaded trip at slow monorail speed 49
Figure 2.26: Cycle times for monorail and truck haulage systems 50

Figure 2.27: Capital and operating costs for monorail and truck haulage systems 51
Figure 2.28: Proposed conceptual monorail drill-load-haul system 52
Figure 3.1: Pneumatic (vacuum) conveying from open storage 58
Figure 3.2: Dilute phase transport 60
Figure 3.3: Horizontal flow conveying characteristic curves 63
Figure 3.4: Vertical flow conveying characteristic curves 64
Figure 3.5: Elements of a pneumatic conveying system 65
Figure 3.6: Moody chart 69
Figure 3.7: Schematic diagram of conveying in incline pipe (a) dense pneumatic condition (b) acting forces 73
Figure 3.8: Forces on a rock particle 77
Figure 3.9: Geldart's classification of materials 83
Figure 4.1: Structure and configuration of the conceptual monorail loading system. 87
Figure 4.2: Coupling and uncoupling mechanism 88
Figure 4.3: Mass flow rate of air at different conveying air velocities 92
Figure 4.4: Mass flow rate of solids at different conveying air velocities and solid loading ratios 93
Figure 4.5: Superficial velocity profile of solids in the suction pipe for different conveying air velocities and material densities 94
Figure 4.6: Pressure loss in acceleration zone for 200mm size rock particle of different densities 96
Figure 4.7: Pressure loss in acceleration zone for 50mm size rock particle of different densities 96
Figure 4.8: Pressure loss in steady state zone for material with 50mm particle diameter 97
Figure 4.9: Pressure loss in steady state zone for material with 200mm particle diameter 98
Figure 4.10: Effects of particle size on the required conveying air velocity for material with density 2400kg/m^3 99
Figure 4.11: Effects of particle size on the required conveying air velocity for material with density 3000kg/m^3 99

Figure 4.12: Effects of particle size on mass flow rate of solids for material with density 2400kg/m^3 100
Figure 4.13: Effects of particle size on mass flow rate of solids for material with density 3000kg/m^3 101
Figure 4.14: Effects of particle size on power consumption for material with density 2400kg/m^3 102
Figure 4.15: Effects of particle size on power consumption for material with density 3000kg/m^3 102
Figure 4.16: Optimum loading time for material with density 2400kg/m^3 104
Figure 4.17: Optimum loading time for material with density 3000kg/m^3 105
Figure 4.18: Size distribution curve 107
Figure 4.19: Rock fragmentation with corresponding mass flow rate at different conveying air velocities ρ = 2400kg/m^3 108
Figure 4.20: Rock fragmentation with corresponding mass flow rate at different conveying air velocities ρ = 3000kg/m^3 108
Figure 4.21: Size distribution curve showing optimum fragmentation range 109
Figure 4.22: Gravity settling chamber 111
Figure 4.23: Principle of cyclone separator 112
Figure 4.24: Longitudinal section across the suction pipe 113
Figure 4.25: Cross section view of the suction pipe 113
Figure 4.26: Connection and disconnection arrangement for suction pipe 115
Figure 4.27: Monorail loading system total head determination 118
Figure 4.28: Static head for the monorail loading system 119
Figure 4.29: Typical pump performance curve 121
Figure 4.30: Performance curve showing operating point (OP) for the monorail loading system pump 123
Figure 4.31: Schematic diagram showing monorail surface infrastructure arrangement 125
Figure 4.32: Schematic diagram showing ore and waste handling systems 126
Figure 4.33: Monorail system bottom dumping container 126
Figure 5.1: Configuration of conceptual monorail drilling system 129
Figure 5.2: Drilling boom with components 129
Figure 5.3: COP 1638 Rock drill 130

Figure 5.4: Feed with feed motor and cradle 131
Figure 5.5: Effects of thrust on penetration rate 133
Figure 5.6: BUT 28 drill boom 134
Figure 5.7: Longitudinal section showing forces on the monorail drilling system 136
Figure 5.8: Cross- section showing forces on the monorail drilling system 137
Figure 5.9: Static and kinetic frictional forces 139
Figure 5.10: Drilling boom represented as line segment in 3D space 143
Figure 5.11: Forces acting on the monorail drilling system from the drilling unit 145
Figure 5.12: Dimensions of decline opening showing position of monorail system for vector definition 147
Figure 6.1: Decline support system for monorail installation 168
Figure 6.2: Monorail installation 168
Figure 6.3: "Universal Flange Rail" type 169
Figure 6.4: Monorail profiles (a) I140E (b) I140V 170
Figure 6.5: Drilling of roof bolt support holes for monorail installation 171
Figure 6.6: Hilti OneStep® anchor bolt 172
Figure 6.7: Load transmission in roof bolts 172
Figure 6.8: Details of roof bolt and bracket 173
Figure 6.9: Levelling of irregular roof conditions 174
Figure 6.10: Chain angle cross to rail direction must be 0^0 175
Figure 6.11: Chain angle in rail direction must be maximum 30^0 175
Figure 6.12: Horizontal angle between two rails must be maximum 1^0 176
Figure 6.13: Vertical angle between two rails must be maximum 5^0 176
Figure 6.14: Axial forces in roof bolts and suspension chains for the monorail loading system components in an incline 177
Figure 6.15: Schematic diagram showing lengths and weights of monorail loading system components 179
Figure 6.16: Axial forces in roof bolts and suspension chains for the monorail drilling system components in an incline 181
Figure 6.17: Schematic diagram showing lengths and weights of monorail drilling system components 182

Figure 6.18: Schematic longitudinal-section view of required support system at vertical curve based on the weight of monorail loading system components 184
Figure 6.19: Schematic longitudinal-section view of required support system at vertical curve based on weight of monorail drilling system components 188
Figure 6.20: Plan view of forces at the horizontal curve 190
Figure 6.21: Displacement of suspension chain from vertical position at horizontal curve 191
Figure 6.22: Variation of force in support system with change in decline gradient for the monorail drilling system 198
Figure 6.23: Variation of force in support system with change in decline gradient for the monorail loading system 198
Figure 6.24: Strength of support system at 20^0 decline gradient 199
Figure 7.1: Components of an automated system 204
Figure 7.2: Open-loop control system 206
Figure 7.3: Closed-loop control system 207
Figure 7.4: Components of a closed-loop control system 207
Figure 7.5: Signals of a closed-loop control system 208
Figure 7.6: PID controller 209
Figure 7.7: Process variables versus time for three values of K_p with K_i and K_d held constant 210
Figure 7.8: Process variable versus time for three values of K_i with Kp and K_d held constant 211
Figure 7.9: Process variable versus time for three values of K_d with K_p and K_i held constant 212
Figure 7.10: Schematic description of automation design for the loading process 215
Figure 7.11: Schematic description of automation system for face marking 217
Figure 7.12: Process control flow diagram for monorail loading process 219
Figure 7.13: Process control flow diagram for monorail discharge process 220
Figure 7.14: Process control flow diagram for monorail loading and discharge processes 221

Figure 7.15: Process control flow automation diagram for face marking 222
Figure 8.1: Chronological periods of the model life cycle 226
Figure 8.2: Phases in chronological periods of the model life cycle 227
Figure 8.3: Process flow chart for monorail drill-load-haul system 232
Figure 8.4: Process flow chart for monorail loading operation 233
Figure 8.5: Process flow chart for material haulage to surface 234
Figure 8.6: Effect of loading time on the lashing speed 236
Figure 8.7: Effect of loading time on the drilling speed 237
Figure 8.8: Effect of loading time on face drilling and cleaning cycle time 238
Figure 8.9: Effects of loading time on total drill-blast-load-haul cycle time 239
Figure 8.10: Effects of lashing time on the number of blasts per shift 240
Figure 8.11: Effect of lashing time on advance rates 241
Figure 8.12: Effect of loading time on productivity of monorail system 242
Figure 8.13: Cleaning and drilling time of the development face 244
Figure 8.14: Charging, blasting and re-entry time for the two systems 245
Figure 8.15: Drill-blast-load-haul cycle time 247
Figure 8.16: Advance rates for conventional and monorail systems 247
Figure 9.1: Components of risk 251
Figure 9.2: Framework for managing risk 257
Figure 9.3: Monorail system hazard likelihood ranking 268
Figure 9.4: Monorail system hazard weighted consequence ranking 271
Figure 9.5: Monorail system risk ranking 275
Figure 9.6: Fault-tree diagram for monorail system failing from supports 277
Figure 9.7: Fault-tree diagram for monorail system running out of control 278
Figure 9.8: Fault-tree diagram for operational and maintenance hazards 279
Figure 9.9: Percent contribution of potential root causes to monorail system risk failure 281
Figure 10.1: Nim3 deposit of Jundee operations 292
Figure 10.2: Nim3 pit and South Deep deposits 292
Figure 10.3: Decline design to Nexus structures for monorail system application 294
Figure 10.4: Design of crosscuts from Nexus decline to the deposit 295

Figure 10.5: Design of intake and exhaust ventilation network to Nexus structures....296
Figure 10.6: Conventional versus monorail system development meters....300
Figure 10.7: Conventional versus monorail system tonnage to be removed....301
Figure 10.8: Conventional versus monorail system capital development costs.302
Figure 10.9: Conventional versus monorail system capital cost to access Nexus deposits....303

List of Tables

Page

Table 2.1: Drilling and blasting cycle times 37
Table 2.2: Truck cycle time to move waste from stockpile area to surface 38
Table 2.3: Total load-haul cycle time with stockpiling 38
Table 2.4: Operating costs for Hitachi AH400D truck 40
Table 2.5: Effects of monorail system design parameters 44
Table 2.6: Cycle time for loading and hauling using a monorail 45
Table 2.7: Capital costs for purchase of monorail train 46
Table 2.8: Capital costs for monorail train installation 46
Table 2.9: Operating costs for monorail train 46
Table 2.10: Power consumption for monorail train 47
Table 2.11: Steps of the loading / suction process 53
Table 2.12: Steps for material haulage 53
Table 4.1: Optimum mass flow rate of solids at maximum negative pressure 104
Table 4.2: Pressure head, static head, friction head and total head at maximum negative pressure (ρ=2400kg/m^3) 120
Table 4.3: Pump characteristics for monorail pneumatic loading system 123
Table 5.1: Rock drill parameters 131
Table 5.2: Feed types and technical parameters 132
Table 5.3: Drill boom types with respective technical parameters 134
Table 5.4: Minimum frictional force in y-direction at base of horizontal stabilisers 158
Table 5.5: Maximum frictional forces in y-direction at base of horizontal stabilisers 158
Table 5.6: Minimum force in vertical stabilisers 159
Table 5.7: Maximum force in vertical stabilisers 160
Table 5.8: Minimum force in horizontal stabilisers 161
Table 5.9: Maximum force in horizontal stabilisers 161
Table 5.10: Maximum and minimum reaction forces in hydraulic stabilisers .. 164
Table 5.11: Summary of design parameters for monorail drilling system 165
Table 6.1: Models for determining required support system 196

Table 6.2: Parameters of the monorail system 197
Table 6.3: Displacement of suspension chains at horizontal curves 200
Table 6.4: Required strength of the support system 200
Table 8.1: Time estimates for monorail system model simulation 235
Table 8.2: Parameters for monorail system model simulation 235
Table 8.3: Summary of monorail system simulation results 243
Table 8.4: Parameters used for model simulation 244
Table 9.1: Example of qualitative risk analysis matrix 255
Table 9.2: Consequence failure categories 256
Table 9.3: Existing control measure for identified hazards 264
Table 9.4: Likelihood range for monorail system hazards 267
Table 9.5: Likelihood ranking for monorail system hazards 267
Table 9.6: Consequences range for monorail system risks 269
Table 9.7: Monorail system hazard consequences ranking 270
Table 9.8: Weighted consequences range for monorail system risks 272
Table 9.9: Risk ranking matrix 273
Table 9.10: Risk recommended action 273
Table 9.11: Risk assessment levels for monorail system hazards 274
Table 9.12: Percent contribution of potential root causes to monorail system risk failure 280
Table 9.13: Recommended risk and hazard control strategies 286
Table 10.1: Access development meters and tonnages to be removed 297
Table 10.2: Capital development costs to Nexus structures using monorail technology 299

Nomenclature

Symbol	Description	Units
f	Friction factor	[-]
ρ	Density	[Kg/m^3]
μ	Viscosity of fluid	[kg/ms]
λ	Friction factor	[-]
μ_d	Dynamic internal friction factor	[-]
l_p	Plug length	[m]
ζ_p	Ratio of cross sectional area of conveying plug to that of pipe	[-]
ℓ_b	Bulky density of the material in the plug	[Kg/m^3]
ξ_i	Factor of internal friction	[-]
ξ_w	Factor of wall friction	[-]
u_a	Air velocity	[m/s]
u_k	Permeating air velocity	[m/s]
u_p	Plug velocity	[m/s]
l_a	Length of air cushion	[m]
η	Efficiency	[%]
h_f	Friction head loss	[m]
μ_k	Coefficient of kinetic friction	[-]
μ_s	Coefficient of static friction	[-]
p_c	Total conveying pressure	[kPa]
Δp_t	Total pressure drop in the suspension	[kPa]
Δp_a	Pressure drop due to gas (air-alone)	[kPa]
Δp_s	Pressure drop attributed to the solid particles	[kPa]
Δp_k	Permeating pressure drop in the plug	[kPa]
Δp_p	Conveying pressure related to a single plug.	[kPa]
ΔP_{acc}	Pressure loss in acceleration zone	[kPa]

ΔP_{sts}	Pressure loss in steady state zone	[kPa]
$\Delta\beta$	Angle change at vertical curve	[Degrees]
A	Cross sectional area of pipe	[m^2]
A	Particle projected area	[m^2]
A_h	Contact area between plug and retarded bed	[m^2]
A_w	Contact area between plug and the wall	[m^2]
C	Curve length	[m]
$C_{1,2}$	Constants with index 1 and 2	[-]
C_d	Development cost	[A$]
C_D	Drag coefficient	[-]
C_m	Decline development cost per meter	[A$/m]
D	Diameter of pipe	[m]
d	Drag diameter	[m]
D_{out}	Derivative output	[-]
d_p	Particle diameter	[m]
e	Pipe roughness	[m]
e(t)	Control error	[-]
E_c	Power of conveying system	[kW]
F_{BK}	Braking force	[kN]
F_C	Force in each suspension chain	[kN]
$F_{Cabin/train}$	Weight of driver's cabin or train	[kN]
F_{Cont}	Weight of loaded monorail container	[kN]
F_d	Drag force	[kN]
F_D	Net driving (propulsion) force	[kN]
F_{dpart}	Weight of monorail drilling system component	[kN]
F_{FR-HH}	Horizontal frictional forces at base of horizontal stabilisers	[kN]
F_{FR-HL}	Lateral frictional forces at base of vertical stabilisers	[kN]
F_{FR-HV}	Vertical frictional forces at base of horizontal stabilisers	[kN]
F_{FR-VH}	Horizontal frictional forces at base of vertical stabilisers	[kN]
F_{HS}	Forces in horizontal stabilisers	[kN]
F_M	Feed force from the monorail drilling system	[kN]
F_{MD}	Weight of monorail drilling system	[kN]
F_{ML}	Weight of monorail loading system train	[kN]

F_{MS}	Force in each roof bolts	[kN]
F_{part}	Weight of monorail loading system component	[kN]
$F_{Power\ pack}$	Weight of one power pack (with drive unit)	[kN]
Fr	Froude Number	[-]
F_S	Centrifugal force exerted on moving monorail system	[kN]
F_{SS}	Force in each steel support	[kN]
F_{VS}	Force in vertical stabilisers	[kN]
F_w	Gravitational force of rock particle	[kN]
H	Thickness of stagnant bed	[m]
H	Total head	[m]
H_T	Pump head	[m]
I_{out}	Integral output	[-]
K	Coefficient	[-]
K_d	Derivative gain	[-]
K_i	Integral gain	[-]
K_p	Proportional gain	[-]
L	Length	[m]
L_{dpart}	Length of monorail drilling system component	[m]
L_{md}	Length / span of monorail drilling system	[m]
L_{ml}	Total length / span of fully loaded monorail system	[m]
L_{part}	Length of monorail loading system component	[m]
M	Gradient	[-]
m*	Mass flow ratio	[-]
M_a	Mass flow rate of air	[kg/s]
m_{dpart}	Mass of monorail drilling system component	[kg]
M_p	Mass of plug	[kg]
m_{part}	Mass of the monorail loading system component	[kg]
M_s	Mass flow rate of solids	[kg/s]
P_1,P_2	Pressure at front and back side of plug	[kPa]
P_{out}	Proportional output	[-]
Pr	Normal pressure in the plug	[kPa]
Q	Conveying rate	[m^3/h]
R	Radius	[m]

Re	Reynolds Number	[-]
R_h	Friction resistance at the surface of stagnant bed	[N]
r_h	Horizontal curve radius	[m]
R_s	Roof bolt spacing	[m]
r_v	Vertical curve radius	[m]
R_W	Friction resistance at the inner surface of a pipe	[N]
T	Time	[sec]
U	Difference of permeating air velocity and plug velocity	[m/s]
u(t)	Manipulated signal	[-]
$u_c(t)$	Controlled signal	[-]
v	Velocity	[m/s]
V	Volumetric flow rate	[m^3/s]
v_s	Superficial velocity of solids	[m/s]
v_{term}	Terminal velocity of solids	[m/s]
v_t	Velocity of conveying air at entry point of the suction pipe	[m/s]
w(t)	Set point	[-]
y(t)	Controlled value	[-]
Z	Vertical displacement	[m]
z(t)	External disturbance	[-]
A	Decline gradient	[Degrees]
B	Angle of suction pipe inclination	[Degrees]
E	Porosity of conveying material	[-]
Φ	Shape factor	[-]

Acronyms

Symbol	Description
AC	Alternating Current
AusIMM	Australasian Institute of Mining and Metallurgy
BCM	Bank Cubic Metre
BEP	Best Efficiency Point
BHP	Brake Horsepower
CSIRO	Commonwealth Scientific and Industrial Research Organisation
DF	Design Factor
EMTS	Electric Monorail Transport System
FEL	Front End Loader
FoS	Factor of Safety
GPSS/H	General Purpose Simulation System / Henrikson
LHD	Load Haul Dump
MERIWA	Mineral and Energy Research Institute of Western Australia
NPSH	Net Positive Suction Head
NPV	Net Present Value
OP	Operating Point
PID	Proportional Integral Derivative
PLC	Programmable Logic Control
ROM	Run-Of-Mine
RPM	Revolutions Per Minute
SG	Specific Gravity
SI	International System of Units
SMART	Super Material Abrasive Resistant Tools
TH	Total Head
TSDC	Thermally Stable Diamond Composites
UFR	Universal Flange Rail
WA	Western Australia

Chapter 1

1.0 Introduction

1.1 Underground mine access and haulage

Underground mines in Australia are accessed by means of declines or shafts. However, the majority of mines in Western Australia (WA) adopt declines as a means of accessing underground resources. In conventional truck haulage mining, declines are usually excavated at a gradient of 1 in 7 (8^0) with an average width of 5m Wide x 5m High. From the decline, cross-cuts are mined at regular vertical intervals to access the orebody. Transportation of ore and waste from underground to surface as well as men and material to and from underground is done via the decline. The average cost of excavating a decline in Australia is in the order of A$2500/metre.

The decline method of accessing the orebody and its subsequent use as a transport excavation has been a huge success for the Australian underground mining industry. However, the system does not meet the specific needs of narrow vein mining and the challenge posed by mining at greater depths (greater than 600m) in the Australian context. Large excavations, typical of many Australian mines, are not suitable for narrow vein type deposit and are unlikely to be suitable at greater depths both from geotechnical and economic perspectives. Specific problems associated with conventional decline development and haulage include airborne exhaust contaminants emitted by large diesel engines, slow advance rates, increased ventilation requirements, increased rock reinforcement costs, traffic congestion and carbon footprint. Metal prices in the recent boom have helped to offset some of the challenges

associated with large declines; however, erosion in commodity prices could find many operations exposed. The need to develop innovative responses to these challenges is clearly evident.

1.2 The monorail system

One system that has the potential to overcome the above challenges, in part, is the monorail haulage system. This research work was conducted in order to determine the technical and economic feasibility of monorail system application in mine decline development. It is postulated that the monorail system would result in rapid decline development by reducing the mining cycle, hence accessing the orebodies faster and at a lower cost in comparison to conventional method of using jumbos, loaders and trucks. The monorail decline can be developed at steeper gradient of up to 36^0, hence reducing the total length of the decline. Furthermore, due to the reduction of excavation dimension, the monorail system would result in lower support costs, less seismic risk and lower excavated rock volumes. In relation to underground transport, the Electric Monorail Transport System (EMTS) will reduce reliance on diesel powered equipment by replacing it with quasi-mobile main powered electrical transport and development methods. Other benefits include reduction in ventilation air volumes, elimination of diesel exhaust fumes and reduction in heat load in underground workings, reduction in quantity of rock required to be mined and improved grade control by reducing the amount of external waste mined. Despite the economic benefits of the system, so far, no monorail system has been developed for mining operations (i.e., drilling and loading), hence, the need for this study. However, monorail technology has been used in the mining industry (in South Africa), specifically, for material and personnel transport and in a limited way for rock haulage.

The proposal of this project is to replace the non-shaft components of the mine transport system with roof/back mounted monorail system which provides mobile motive energy whilst simultaneously functioning as the second level electrical reticulation system. The system is designed to integrate drilling,

loading and hauling during the development of a decline, serving as the rock transport system from the underground to the surface.

It must be stated here that monorail haulage is not necessarily being proposed as a total replacement or direct competitor to the large tonnage autonomous machines currently in use, although the capability does exist and can be implemented as appropriate. The system has a lot of potential for narrow vein type of deposits and deep mines where large excavations pose seismic risks.

1.3 Research objectives

The primary objective of this project is to evaluate the technical and economic feasibility of the application of the EMTS in metalliferous underground mines in Australia.

Specific objects of this study are to:

- Design a drilling system that uses a monorail train to drill the decline face;
- Design a pneumatic loading system that uses a monorail train to clean the development face;
- Determine the support system strength for monorail installation;
- Conceptual design of process control and automation for the monorail system;
- Carry out risk analysis and suggest risk and hazard control strategies for the designed monorail system;
- Design decline haulage with application of the monorail system in ore bodies which cannot be economically accessed by existing practices; and
- Estimate capital and operating expenditures for the designed decline haulage and compare these with conventional decline haulage development.

1.4 Research approach

To achieve the stated objectives, the following approach was used: collection of technical, productivity and cost data from the manufacturer of the monorail train and some of the mines around the world where the system is currently being used.

Conceptual design of the drilling and loading systems based on monorail platform. The idea is to reduce the main cycle allowance for rapid development of the decline to access the orebody. The concept involves mounting a twin-boom drill jumbo on the roof-mounted monorail train and using a pneumatic suction system (that uses monorail technology) to load the broken rock into the monorail containers via a hopper. The containers are lifted by the monorail train and transported to the surface via the decline.

To determine the strength of the monorail support system, models that relate the weight of the monorail drilling and loading systems components to the required strength of each support system are established. The developed models are used to determine the required strength of support system for monorail installation in the decline. Determination of the required strength of monorail support system is critical to avoid monorail system failure as a result of its weight as well as to overcome dynamic forces.

The performance of the conceptual monorail system was determined using time and motion studies. This was done by developing monorail drilling and loading systems computer simulation model using General Purpose Simulation System (GPSS/H) software and PROOF animation software. The model was used to examine the performance of the two systems. To improve the efficiency of the two systems, critical processes performed by the two systems during mining operations were automated using aspects of system automation and control engineering.

Since the conceptual monorail drilling and loading systems have the potential to cause significant risks that require assessment, management and possibly regulating, risk analysis was conducted on the monorail system. Qualitative risk analysis approach was used during the assessment due to lack of actual data on monorail system operations for probabilistic treatment of such data. Risk analysis began by indentifying possible hazards that could occur during monorail system operations. The risks were then ranked (using risk ranking matrix) according to their likelihood of occurrence and consequences that may result from their release. Monorail system risk management and hazard control was performed using fault-tree analysis. This method was used because it addresses fundamental causes of risk and hazard failure as opposed to merely addressing the immediate obvious symptoms. By directing corrective measures at root causes of risk and hazard failure, it is hoped that the likelihood of failure will be minimized.

Conceptual mine design case study, using monorail technology, for a hypothetical decline development using Jundee mine orebody was conducted. Mine designs were completed using Datamine software. Capital costs, i.e., primary development costs as well as the cost for the purchase and installation of the monorail system in the decline were determined. The costs for the monorail system were estimated from first principle using the data supplied. The results for the case study were compared to those based on conventional decline development.

1.5 Significance of the study

Current haulage methods put enormous cost pressure on the profitability of mining operations. This is especially so in the case of narrow vein ore bodies where conventional haulage systems and mine design may be too expensive to support economic extraction of the ore. Therefore, the monorail haulage system offers better ways to handle materials underground and also takes into account safety and cost advantages in terms of return on investments. The system has potential to improve profitability of suitable ore bodies and could be

implemented as an economic alternative to conventional haulage systems such as trucks and trains (Jagger, 1997; Rupprecht, 2003; Buyens, 2005; Chanda and Roberts, 2005). In addition, the monorail system could augment other mobile equipment and conveyor systems to achieve better economic outcomes in underground materials handling. Since monorail has the ability to negotiate steeper gradients than the conventional 1 in 7 common in underground mining in Australia, the monorail system could provide significant cost reduction in decline development as decline length will be shorter with monorail system application. This also means that ore deposits will be accessed cheaply and quickly. Since the decline size will also be reduced, less material will be extracted further reducing development costs. This is particularly important for narrow deep ore bodies that are currently uneconomical due to high levels of development costs.

1.6 Contribution

The original contributions made in this thesis include the following:

- Design of an underground transport system that combines drilling, loading and hauling using monorail technology; and
- This research has brought about new and cost effective ways of developing decline access to underground deposits which cannot be accessed using expensive conventional method. Using this method, most deposits that are uneconomical will become economically viable due to reduced cost of capital developments for such deposits.

1.7 Thesis structure

The outline of this thesis is as follows:

Chapter 1 serves as an introduction to the study, elaborating the importance of the study. It details the objectives of the research and the approach taken to achieve the stated objectives. The Chapter also highlights the significance of the study.

Chapter 2 reviews existing literature on monorail technology and its application in mining. The Chapter is intended to provide background information on the monorail technology and the design of conventional decline access in Western Australian mines. The Chapter also discusses decline access design parameters as they relate to the research objectives being investigated in this study. Advantages and operations of the monorail system are discussed in comparison with the conventional method. An introduction of the conceptual monorail drilling and loading systems has also been highlighted in this Chapter.

Chapter 3 provides a detailed description of the available mathematical models and experimental explanations of pneumatic conveying systems. Since loading of broken rock from the development face will be done using a pneumatic suction unit, this Chapter reviews literature on pneumatic suction principle. The Chapter highlights the pneumatic suction theory used in the design of the monorail pneumatic loading system.

In **Chapter 4** the conceptual pneumatic loading system that uses monorail technology has been described. The system is based on the principle of a vacuum cleaner or vacuum lift system. With this system, rock fragments are sucked from the development face, through the suction pipe, into the hopper which loads the monorail containers. Loaded monorail containers are transported to the surface using the monorail train. The use of pneumatic loading provides a much more continuous system compared to the use of trucks. The Chapter also describes the required surface infrastructure for monorail system operations which include surface ore and waste handling structures.

In **Chapter 5**, conceptual designs of monorail drilling system has been described. The drilling system consists of two drilling jumbos mounted on a monorail train. The system is also composed of horizontal and vertical hydraulic stabilisers (props) to be used as supports during drilling operations. Since the drilling system will be unstable due to resultant forces from the two drilling jumbos, this Chapter focuses on stabilising the monorail drilling system during drilling operations. In particular, it looks at determining equal and opposite reaction

forces in horizontal and vertical hydraulic stabilisers that will oppose the drilling forces.

Chapter 6 looks at the strength of the support system used during monorail installation, i.e., roof bolts, suspension chains and steel supports. The aim of this Chapter is to determine the minimum required strength of the roof bolt, suspension chain and steel supports for suspending and supporting the monorail drilling and loading systems (i.e., two systems) components during operations. This is in order to avoid failure of the two systems from the support systems as well as to overcome dynamic forces. During the study, models that relate the weight of the monorail drilling and loading systems components to the required strength in each roof bolt, suspension chain and steel support are developed. Using the developed models, numerical values of the minimum required strength in each roof bolt, suspension chain and steel supports to suspend and support the components of the two systems is determined. Variation of support system strength with changes in decline gradient is also established in the Chapter. The Chapter also highlights correct monorail installation procedure in the decline.

In **Chapter 7**, automation designs for monorail drilling and loading system processes are developed using aspects of system automation and control engineering. This is in order to increase the performance of the monorail drilling and loading systems by improving the efficiency of various processes performed by the two systems. Automation of monorail drilling system involves automatic face marking by projecting laser beams of the desired drill pattern onto the drill face by the system. For the monorail loading system, the two processes automated include pneumatic loading and material discharge into monorail containers.

Chapter 8 is devoted to determining capabilities and performance of the drilling and pneumatic loading systems through time and motion studies. In this Chapter, modelling of the conceptual monorail loading and drilling systems described in Chapters 4 and 5 respectively was done. A simulation model was developed using GPSS/H software and results of the simulation study were viewed and

examined using PROOF animation software. Computer simulation was used to determine the capability of the system in terms of drilling and loading cycle time, number of blasts/shift, advance rates/shift and the total drill-blast-load-haul cycle time against which operational performance is measured. The Chapter also presents the results of the comparison between the performance of the monorail drilling and loading systems and conventional truck haulage system.

In **Chapter 9** risk analysis of monorail system hazards is performed. The aim of the Chapter is to identify potential hazards and risks associated with the operations and use of the monorail system in underground mining. Potential root causes of risk and hazard failure were also determined and evaluated by carrying out fault-tree analysis to assist in risk management. Strategies to mitigate and control risks and hazards associated with the monorail system operations have also been discussed in this Chapter.

Chapter 10 discusses the application of monorail technology to a mine design case study using "Jundee – South Deeps" deposit. In 2004, Jundee Mine Planning Group investigated the potential of South Deeps deposits by designing capital developments to the deposits using the conventional 1 in 7 decline gradient. However, following the optimisation of the South Deeps deposits, resources were found to be far from becoming potentially economic. Therefore, in an effort to making the deposits economical, monorail technology is used to design capital developments to Nexus deposit of the South Deeps deposit. Datamine software is used during the design process. Decline access was designed with a gradient of 1 in 3 (20^0) and a turning radius of 6m suitable for monorail application. The economic analysis of the designed mine was made and results compared with conventional method.

Chapter 11 brings together the findings of this thesis and highlights the original contributions to knowledge. Some areas requiring further research are also identified.

Chapter 2

2.0 Monorail technology

2.1 Introduction

This Chapter reviews existing literature on monorail technology and its application in underground mining. The Chapter provides background information on monorail technology and the design of conventional decline access in Western Australian mines. Design parameters for conventional decline access development are also discussed as they relate to the research objectives being investigated in this study. Advantages and operations of the monorail system are discussed in comparison with the conventional truck haulage method.

2.2 Background to monorail technology

Aerial ropeways (Figure 2.1), which can be considered as early forerunners of monorails, have long been recognised as less expensive transportation devices than road and rail transport (Oguz and Stefanko, 1971). According to Oguz and Stefanko (1971), the first aerial ropeway was installed for surface transportation in Germany in 1860. However, the most important disadvantage of an aerial ropeway installation for underground application is slack in the carrying rope and the difficult arrangement of pulling at horizontal curves. An important underground aerial rope installation was constructed in the San Francisco Mine of Mexico Limited at San Francisco Del Oro, Chihuahua, in Mexico (Metzger, 1940). According to Metzger (1940) the underground portion of this installation was 930m (3054 ft).

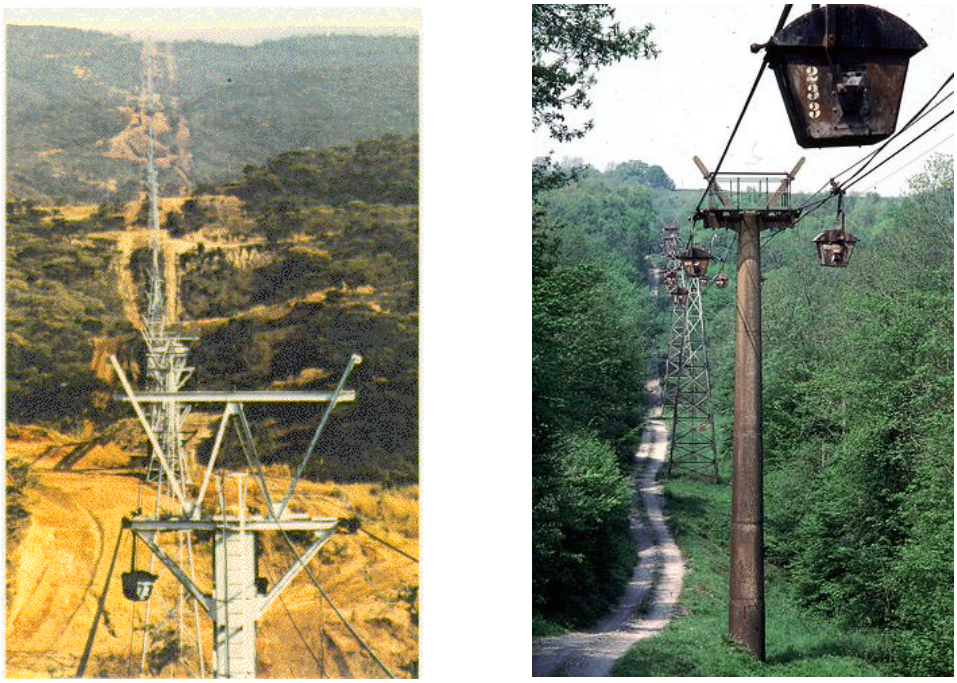

(a) (b)

Figure 2.1: Aerial ropeway (a) Maamba Collieries Limited, Zambia (Boyd, 1993) (b) Brightling Aerial Ropeway (http://www.flickr.com)

One of the first monorail systems was developed in Germany early during Second World War using old, flat-bottomed rails to transport relatively heavy material (Oguz and Stefanko, 1971). This was the beginning of the old Bacorite monorail system (Parfitt and Griffin, 1963). The more recent developments of monorail systems at the end of the 1950's and early 1960's in Germany and in England are also remarkable, i.e., had high productivity (Oguz and Stefanko, 1971).

2.2.1 Electric Monorail Transport System (EMTS) technology

2.2.1.1 What is EMTS technology?

Monorail haulage systems are not new in the world of materials handling (Oguz and Stefanko, 1971). Their early application can be traced to Germany during the Second World War (Toler, 1965). The EMTS system consists of a track of jointed section rails, which can easily be extended to the desired length and suspended by means of suspension chains or steel support (or rigid brackets) attached to roof bolts (Figure 2.2).

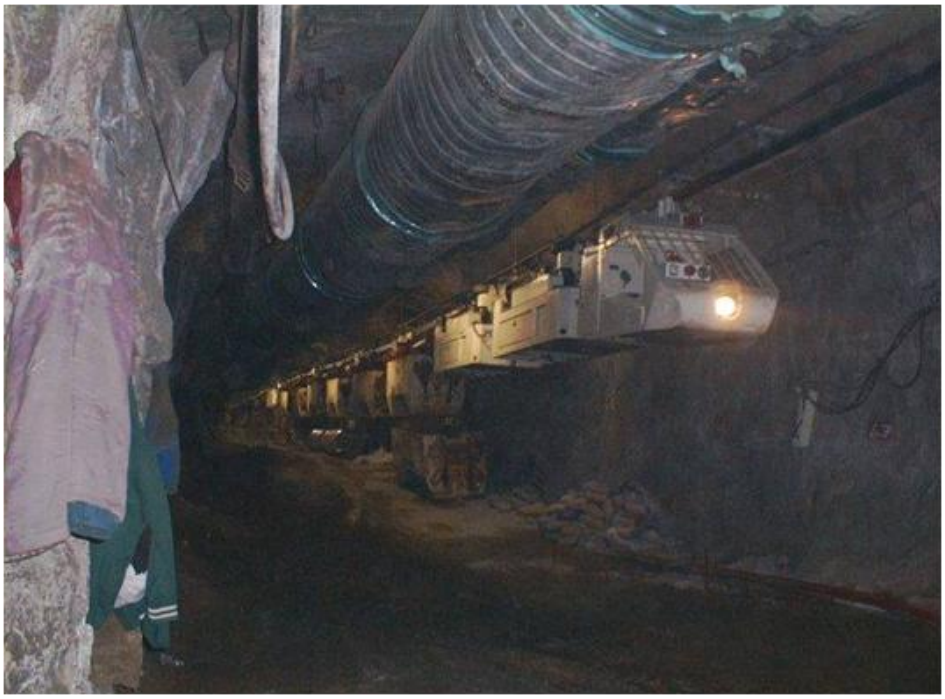

Figure 2.2: EMTS in an underground haulage (Scharf, 2007)

The containers or carriages hang by their wheels on the bottom flange of the track and are powered by electric motors. Monorail systems use a roof suspended I–profile rail, which fully prevents any derailment of the train. Depending on the transportation task, the monorail system can be equipped with man-riding cabins, material container and bottom discharge hoppers (Guse and Weibezhn, 1997). With a load carrying capacity of up to 30 tonnes and the ability to negotiate gradients of up to 36^0, the EMTS can make transport in decline development considerably more efficient than conventional truck haulage system. Variable drive units and load–carrying beams with payload capacities of up to 30 tonnes allow the monorail system to negotiate horizontal and vertical curves with a minimum radius of 4m and 10m, respectively.

2.2.1.2 Components of a monorail system

The monorail system consists of the following main components (Figure 2.3), which are flexibly joined to each other via coupling rods:

(a) Operator or driver's cabin;

(b) Drive units;

(c) Power pack;

(d) Bulk material containers; and

(e) Hoist units.

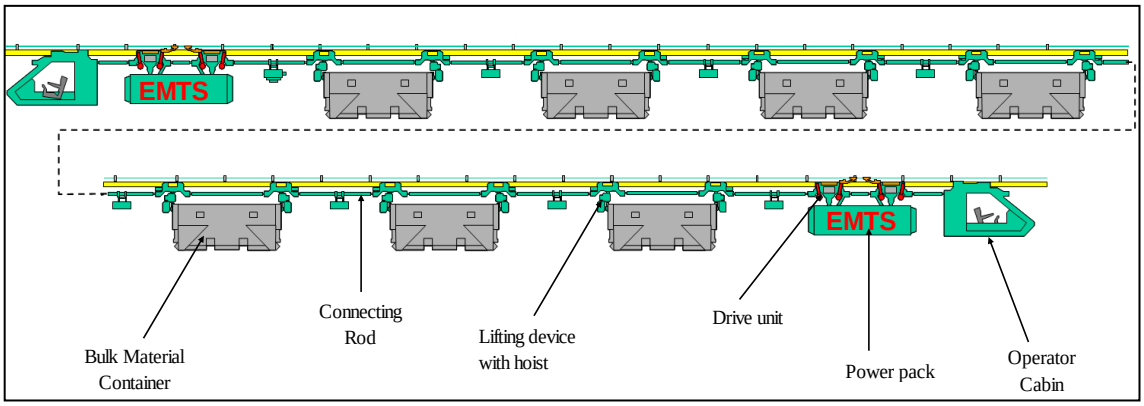

Figure 2.3: Components of a monorail system (Scharf, 2007)

(a) Operator or driver's cabin

On at least one end of the monorail system, there is an operator or driver's cabin (Figure 2.4), which serves to control and operate the system. The cabin contains an ergonomic operator seat (equipped with seat belt), a joystick and a panel with the signalling and control devices. Additionally, each cabin is equipped with a head light and a tail light which can be switched according to the travelling direction. The cabin weighs approximately 1 tonne and has a maximum length of 2.6m.

(a)

(b)

Figure 2.4: Monorail train (a) driver's cabin with ergonomic operator seat; (b) Joystick with panel (Scharf, 2007)

The following is additional technical data for the standard driver's cabin:

- Height to surface of rail – 1300mm;
- Width – 1100mm;
- Emergency and stop brakes – spring-loaded rail brakes; and
- Number of brake callipers – 1.

(b) Drive units

Figure 2.5 shows the monorail system standard friction and rack–and–pinion drive units. Standard friction drives are used for gradients up to 24^0 while rack–and–pinion drives are used for gradients steeper than 24^0, i.e., up to 36^0. Each drive unit consists of 2 x 29kW electric motors that are coupled to the drive wheel through gears.

The electric motors are controlled by frequency converters and Programmable Logic Controllers (PLC); the special design drive units using frequency converter powered motors allows to feed back electrical power into the power supply. This results in approximately 30% average power saving of the electrical power needed for the operation of the train. The drive unit is controlled from either end of the train from the operator's cabins. The number of drive units is determined by the total train weight and gradient.

Monorail trains operated by friction drives are generally equipped with 2 or 3 drive units each with a nominal traction force of 40kN. Because the monorail train can have up to four drive units, each electric motor propels one drive unit, which subsequently runs one pair of friction drive wheels. Each drive unit also comprises two spring tensioned hydraulically released brakes. The drive unit weighs approximately 3.8 tonnes and has maximum length of 3m.

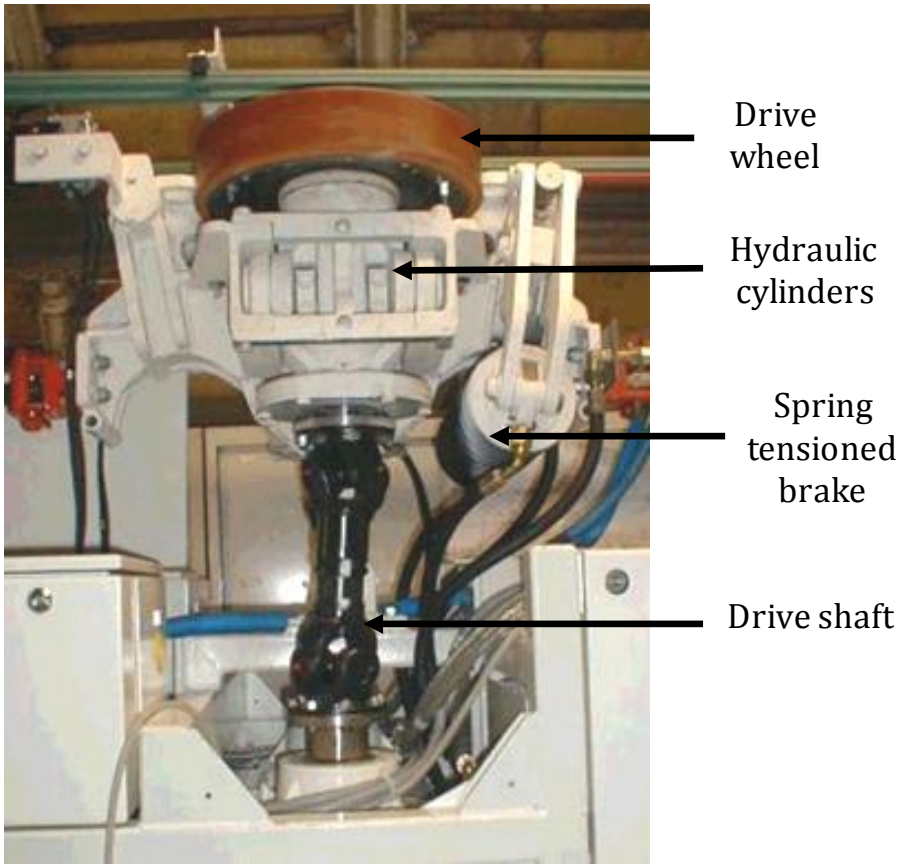

(a)

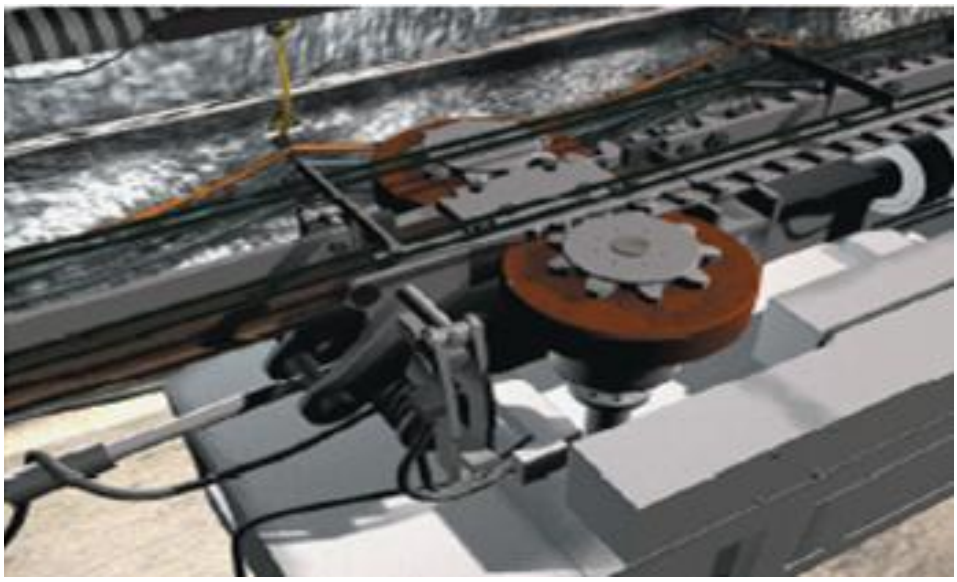

(b)

Figure 2.5: Monorail train drive units (a) standard friction (b) rack–and–pinion (Scharf, 2007)

The following is additional technical data for the drive units:

- Maximum speed – 3.50m/s;
- Height to surface of rail – 1300mm;
- Width – 1100mm;
- Diameter of friction wheels – 450mm;
- Number of friction wheels – 4;
- Coefficient of friction (friction wheel) – 0.3; and
- Number of brake callipers – 2.

(c) Power pack

The monorail system drive unit consists of two electric motors. Therefore, the power pack (Figure 2.6) provides power to the two electric motors which then propel the drive units. There is also a small hydraulic power pack mounted on the rear of the driver's cabin that provides power to the hydraulic release cylinders of the spring loaded brake system.

Figure 2.6: Monorail train power pack (Scharf, 2007)

(d) Bulk material containers

Figure 2.7 shows the monorail system standard container. The standard containers are 1.2m high, 1.1m wide and 3.5m in length. Each container holds 2.5m^3 of material, weighs 1 tonne when empty and has lifting devices that are designed to handle a payload of 5 tonnes. The monorail train can carry a maximum of 6 containers.

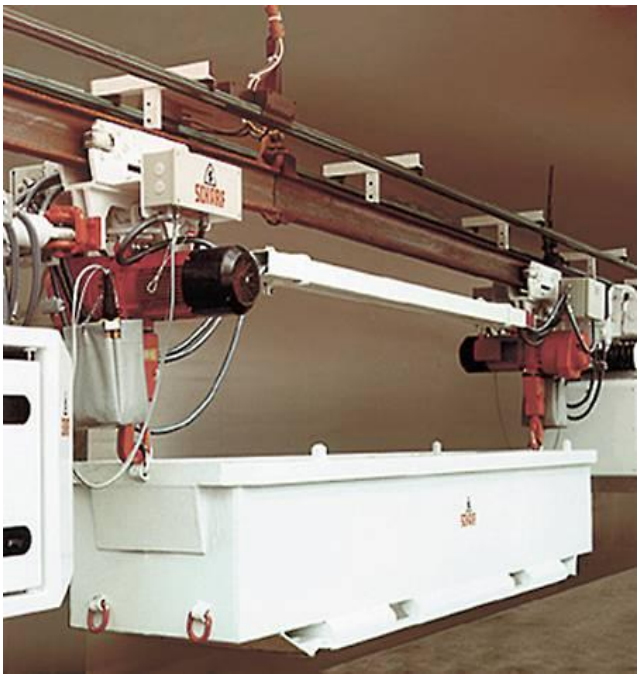

Figure 2.7: Monorail system standard container (Scharf, 2007)

The payload may be increased by upgrading the lifting beams which requires the use of stronger chains and use of twin trolley on each lifting beam. Customised containers and carrying frames for heavy loads as well as rock containers can easily be coupled to the lifting beams. This permits a great deal of flexibility and high utilisation of the machine. A system of load distribution limits the roof bolt/suspension chain or bracket load to 50kN. This allows single load of maximum 30 tonnes to be transported. The lifting beams are available with load measuring devices to prevent an overloaded train from being operated. The load measuring system allows the internal PLC to adapt the system's setting according to the actual total train weight.

(e) Hoist units

The monorail system is equipped with hoist unit or carriage (Figure 2.8). Each unit incorporates a hoist able to take load up to maximum of 30 tonnes. The hoists are controlled either from the operator's cabin or directly from the hoist unit.

(a)

(b)

Figure 2.8: Monorail hoist system (a) single hoist unit; (b) series of hoist units (Scharf, 2007)

2.2.1.3 Electrical switches and power supply

All components of the power supply and the control unit are installed in switch boxes. Supply of power to the monorail train is through the current conductor bars (Figure 2.9). There are a total of four conductor bars, i.e., 2 on each side of the runner rail. Conductor bars are made of copper and the voltage on the bars is rated at 525V.

(a)

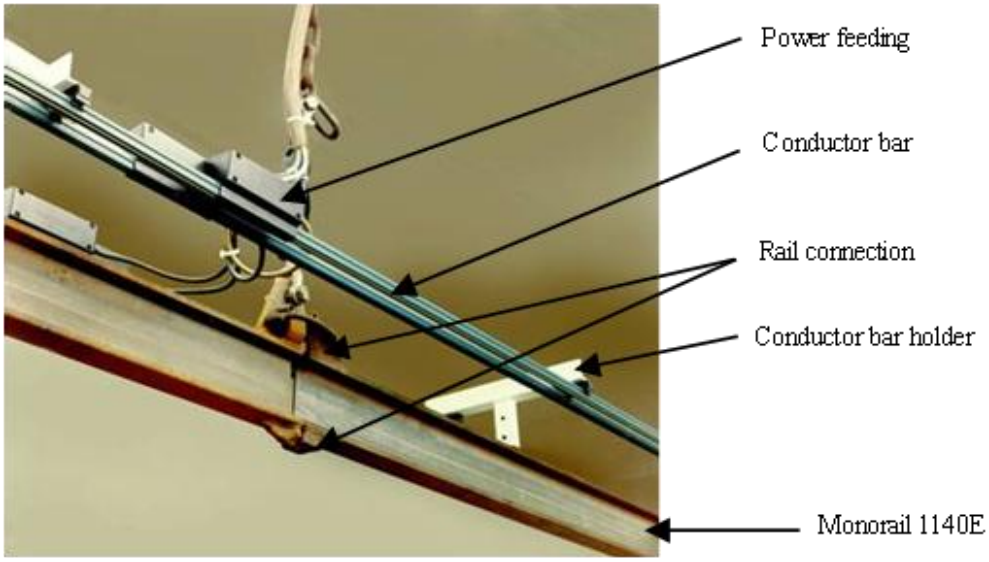

(b)

Figure 2.9: Monorail train power unit (a) switches (b) conductor bar (Scharf, 2007)

2.2.1.4 Monorail switch points

Monorail switch points are mechanical installations that enable the monorail train to be guided from one rail track to another at a rail junction (Figure 2.10). Several types of swiches are avalaible which can be remote controlled by the driver or by a dispatcher. The switches can also be activated hydraulically, pneumatically or electrically and consists of fail–safe locking system. Different types of switches allow adaptation to any mine layout.

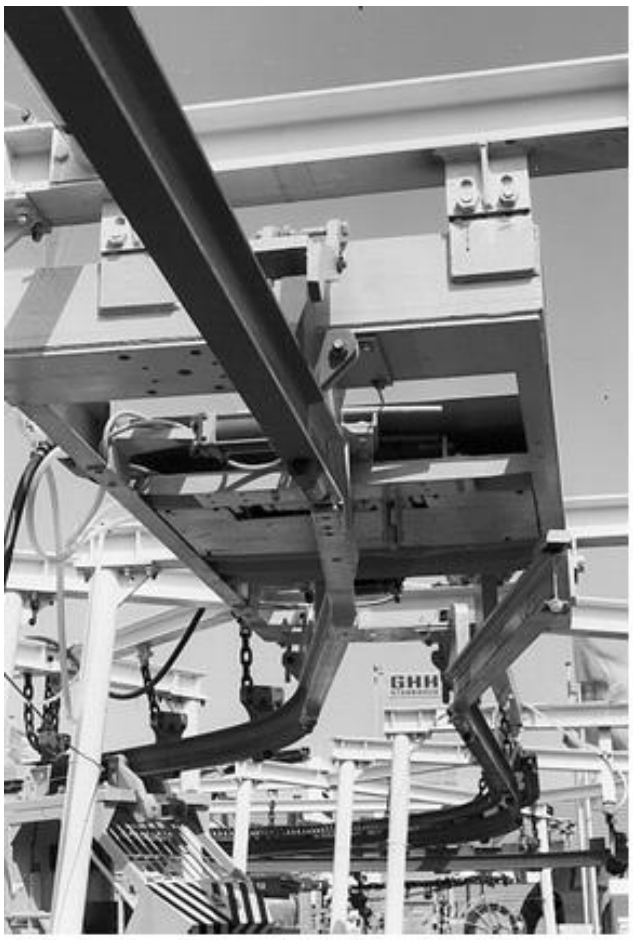

Figure 2.10: Monorail switch point (Scharf, 2007)

2.2.1.5 Monorail train performance chart

Generally, monorail trains are designed to carry loads in gradients of up to 24^0 with standard friction drives and up to 36^0 with specially installed rack–and–

pinion drives. Therefore, the performance of the monorail train depends on the weight of the train (payload), pulling force and the inclination (or gradient). Figure 2.11 shows the performance chart for the monorail train. The chart indicates the relationship between pulling force, train weight, inclination and the speed of the monorail train with 4 drive units.

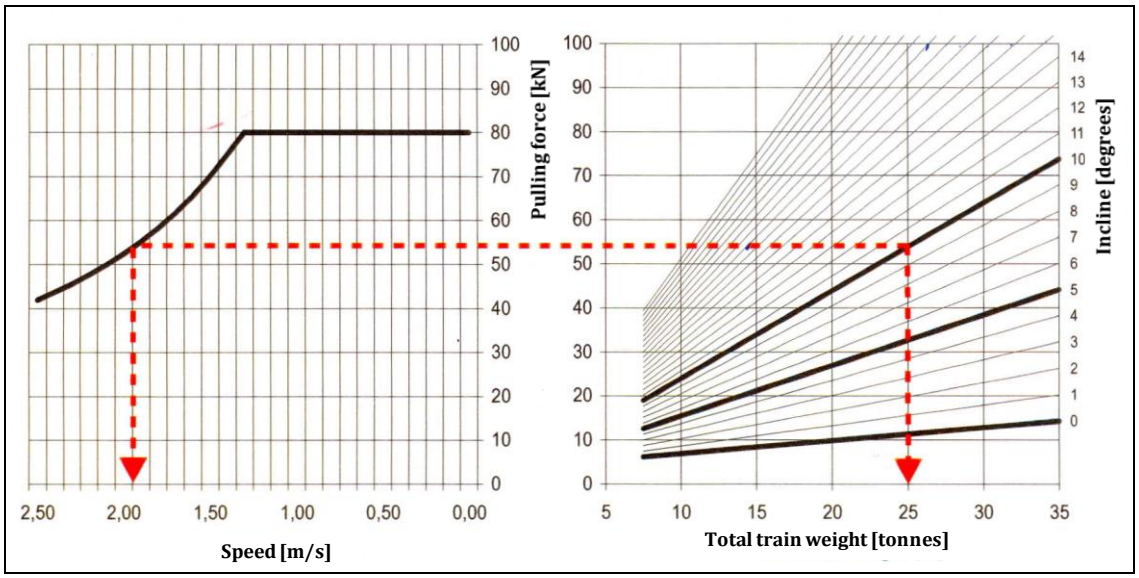

Figure 2.11: Monorail train typical performance chart (Scharf, 2007)

According to Figure 2.11, the pulling force required to move the monorail train with a weight (payload) of 25 tonnes up an incline of 10^0 is approximately 55kN to achieve a speed of 2m/s. The installed power on the monorail train is calculated from the formula:

Power = Pulling force required **x** resultant velocity

Therefore, the power required to move the loaded train up an incline of 10^0 is 110 kW per 2 drive units or 220kW per monorail train (with 4 drive units). Generally, a train with two drive units has an installed power of 116kW and a pulling force of 80kN.

2.2.1.6 EMTS automation and control system

The heart of the EMTS control is a PLC that controls the entire monorail system through a programme or software. The PLC manages different drive modes in which the EMTS operates including the ascending and descending functions. The software also incorporates a fault-finding facility and records all operational details. The EMTS can also apply soft and emergency braking modes through the PLC system. PLC systems have proven to be extremely reliable in mining environments and their application in longwall controllers and belt starters have become commonplace (Novak and Kohler, 1998). Safety features incorporated in the PLC include the ability to control and limit speed of train which can be slowed down automatically when approaching rail switches or stations. Furthermore, the operations of the system can be remote–controlled combined with video cameras. This could result in the removal of personnel from hazardous underground environment increasing the safety of the workers.

2.2.1.7 Monorail system application in mining

The following are some of the potential applications of the monorail system in mining:

- In horizontal development, ore stoping operations and in ore/waste haulage from underground to the surface;
- In some instances, the monorail system may replace truck and/or train haulage;
- The monorail system could also be installed in combination with conveyor haulage system;
- It is also conceivable that the system could be used in lateral haulage to the ore pass system for further materials handling;
- Transport of material (mine and non–mine), machinery and equipment up to 30 tonnes per single load (Figure 2.12); and
- Transport of personnel by mounting man-riding carrier of up to 20 men per carrier (Figure 2.13).

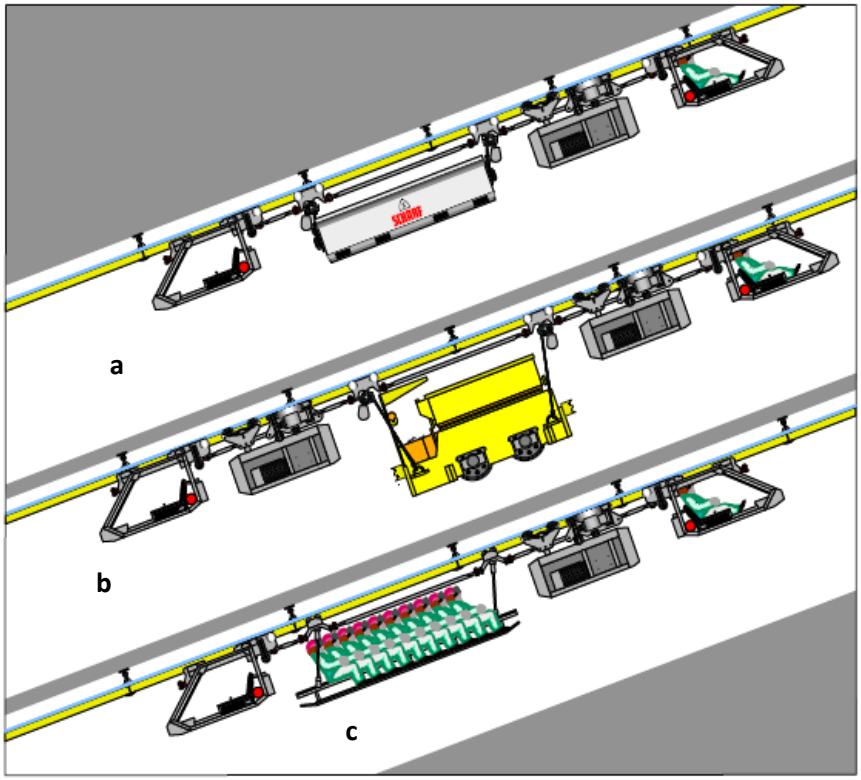

Figure 2.12: Conceptual applications of monorail system (a) Bulk transport (b) Machinery and equipment and (c) Transport of men (Scharf, 2007)

Figure 2.13: Transport of men (Scharf, 2007)

2.2.1.8 An overview of monorail installation

Monorail installation is a combination of three major activities, i.e., drilling of roof bolt support holes, roof bolting and placing new rail section. It is reported (Oguz and Stefanko, 1971) that preparatory activities such as lining, marking the hole and collaring of drill holes are important phases in drilling of holes for monorail installation. Drill holes for monorail installation are normally drilled to a depth of 2m and require a 41mm diameter hole. Collaring and eventually drilling a hole precisely are very important because incorrect drilling results in the monorail being off-line and this creates unnecessary friction on the monorail by the rollers.

Once holes are drilled, roof bolts are inserted into the holes. Selecting the support structure for the monorail deserves attention. This is to avoid roof bolts coming out of the sockets due to the weight of the rail and the monorail system. The Hilti OneStep® anchor bolts are used as suspension bolts for the monorail. These types of anchor bolts have increased working safety and have reduced anchor settling time. After installing the roof anchor bolt, a special eyebolt is attached on the threaded end of the bolt. A shackle provides easy connection of the chain to the roof bolt. From the shackle the distance is carefully measured to obtain the length of the chain for horizontal track installation. This restricts the lateral movement of the rail during monorail system movements. Details of monorail installation and support system are discussed in Chapter 6.

2.2.2 Benefits of EMTS

Monorail haulage system has many more benefits as compared to conventional truck haulage system. The following are some of the potential benefits of the monorail system:

- Ability to negotiate declines at steeper gradients up to 36^0 with less power demand. This has an effect of reducing the decline length;

- Ability to negotiate horizontal curves to the radius of 4m and vertical radius of 10m;
- Reduction in size of excavations – minimum operating drive dimension is 3mW and 3mH – this improves stability of underground excavations;
- Small excavations and non–usage of diesel engines translate into reduced ventilation and need for air conditioning;
- Reduced haulage costs per tonne per kilometre because of less power consumption (generally, rail transport systems have low friction energy loss);
- High availability of more than 95%;
- Multi-purpose haulage system for men, material and rock;
- Small and medium sized ore bodies can be mined with less initial investment;
- Require no floor preparation and are not affected by wet or weak floor conditions;
- No diesel fumes since it uses electricity for operations; and
- Can be controlled by PLC system which opens the possibility of significant personnel savings and hence cost saving.

2.3 Monorail system versus conventional decline development

2.3.1 What is a decline access?

In underground mining, accessing the ore body can be achieved via a decline or ramp system, vertical shaft or adit (Hartman, 2002). The decisions related to the primary development openings of a mine must be made early in the mine planning stage. The decisions normally concern the type, shape and size of main openings. In Australia, most underground mines are accessed by means of declines. Declines are spiral, which are in rectangular form and which circle either the flank of the deposit or the deposit itself (Figure 2.14).

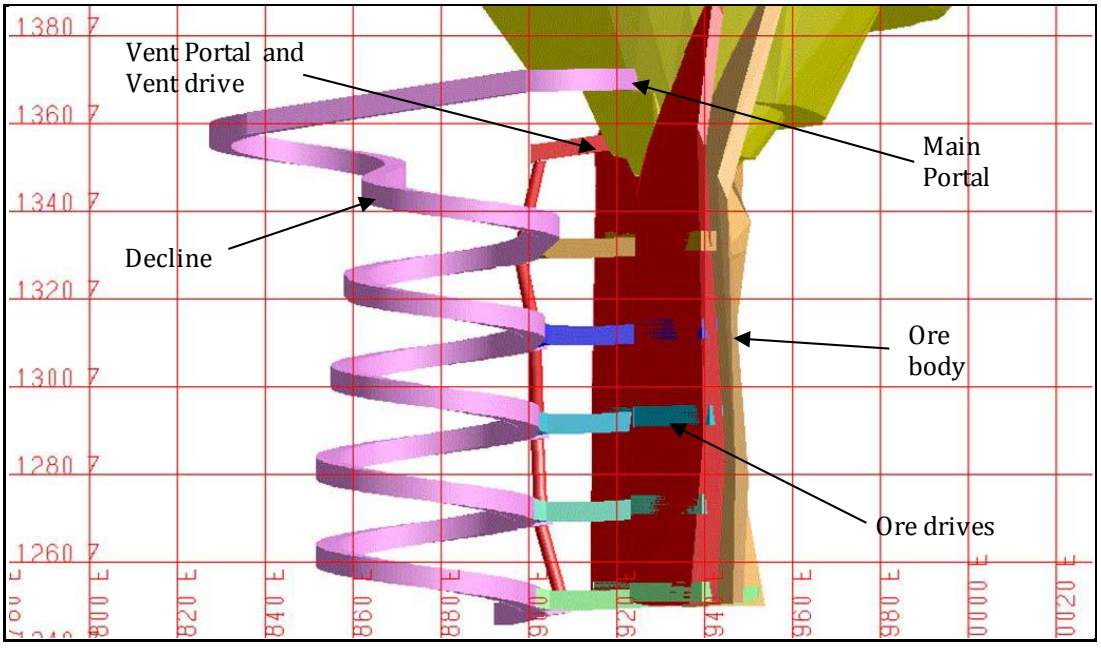

Figure 2.14: Conventional decline access (Chanda and Roberts, 2005)

The decline begins with a box cut, which is the portal to the surface, or from an open pit. A box cut is a small open cut created to provide a secure and safe portal as access to a decline in an underground mine. Levels are then excavated horizontally off the decline to access the ore body. Australia is a world leader in the design and operation of mine accessed by declines and the number of metaliferous underground mines using the decline system are increasing steadily (Chanda and Roberts, 2005). This increase has generated a great deal of interest in future underground haulage systems.

2.3.2 Conventional decline development

Australian underground mines utilise hybrid system of underground haulage (i.e., decline or shaft) appropriate to the ore body being mined and layout (Isokangas and White, 1993). However, most mines in Australia adapt decline access and the use of truck haulage (Medhurst, 2004; Robertson, 1998). Therefore, mine planning and design parameters for decline access are greatly influenced by available haulage system that the mining engineer can choose from. In this Section, conventional decline design parameters and their effects on decline development are presented.

2.3.2.1 Conventional decline design parameters

(a) Size of decline access

In most Australian mines, the size of the decline access is designed for truck haulage with the average standard opening cross-sectional area of 5mW x 5mH. Declines are ordinarily driven to allow free access to any level of the mine with diesel-powered equipment. The size of the decline provides a means of utilising mobile equipment throughout the mine without limitations. Generally, declines are sized to accommodate the largest equipment to be used with added room for ventilation, drainage and personnel (Pond, 2000). This means that the bigger the equipment, the bigger the decline dimensions. Therefore, the size of these openings and the design of curves must be carefully matched to the equipment used in the mine and must allow room for tubing that is used for ventilation. Thus, for narrow deposits the minimum dimension requirement of decline development and material handling are costly and as a result, they fail to clear economic hurdles.

(b) Decline gradient

Decline gradient generally refers to the slope of the decline access. It is used to express the steepness of slope of the decline where zero indicates level (horizontal) and increasing (or decreasing) numbers correlate to more vertical inclinations upwards or downwards. Decline gradient has fundamental importance in decline access development because it affects the length of the decline. In Australian mines, the standard decline gradient used in conventional decline development is 1 in 7 (8^0). According to Chanda and Corbett (2003) steeper gradients require trucks to operate under higher loads for longer periods per kilometre travelled, thereby increasing maintenance and operating costs.

(c) Turning radius

The turning radius of an underground decline access is the radius of the smallest circular turn that the truck is capable of traversing. This is illustrated in Figure 2.15.

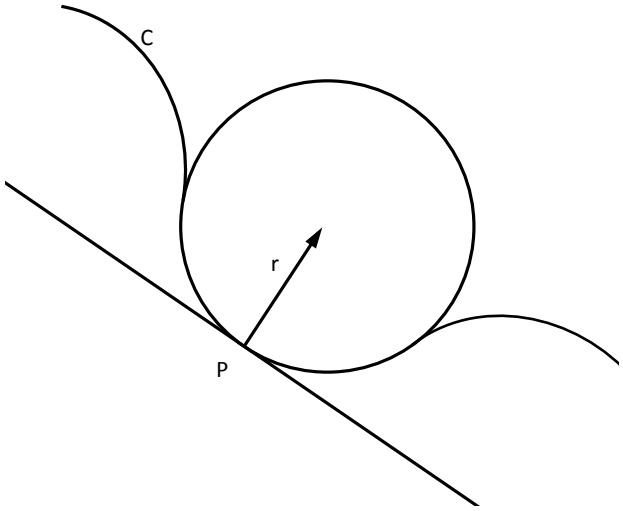

Figure 2.15: Relationship between curvature and curve length (Wikipedia, 2007)

For a plane curve ***C***, the curvature at a given point ***P*** has a magnitude equal to the reciprocal of the radius (**1/*r***) of an oscillating circle (Wikipedia, 2007). The smaller the radius ***r*** of the oscillating circle the larger the magnitude of the curvature. Therefore, where a curve is 'nearly straight', the curvature will be close to zero, i.e., length of the curve will be longer, and where the curve undergoes a tight turn, the curvature will be large in magnitude giving smaller curve radius.

2.3.2.2 Effects of designed parameters on decline development

Decline access design parameters affect decline length, waste material excavated and duration of decline development. These parameters also influence decline development costs. The following are the effects of design parameters on decline development.

(a) Effects of size of decline

The size of decline access has fundamental impacts on decline development. Reduction in decline dimension has the effects of reducing both the costs and duration of decline development. It can also be argued that large dimensions speed up the rate of development through the use of large and more productive machines. However, large and more productive machines have an effect of increasing both the initial capital costs and the development cost per meter. Similarly, with large machines, mining of thin and narrow vein type of deposits become very expensive making mining operations uneconomic. According to Chanda and Burke (2007) the large access excavations typical of many Western Australian mines are likely to be unsustainable at increased mining depths, from both geotechnical and economic perspectives. This means, for decline dimensions smaller than the conventional 5mW x 5mH, development costs will decrease. This also implies that narrow vein deposits can be extracted with minimal mining dilution as sited by Chanda and Roberts (2005) and Granholm et al (1990).

A smaller excavation reduces the need for costly ground support, increases the safety of mine workers and reduces ventilation requirements. However, smaller decline dimension entails finding suitable haulage equipment since truck haulage can no longer be applicable. Other effects of large size decline opening are:

- Infrastructure requirements to support large openings for decline truck haulage may be too expensive to economically extract narrow ore bodies;
- The amount of development outside the ore body is large resulting in more waste material being excavated. The increase in waste development has an effect of increasing development costs as well as transport costs; and
- The duration of decline development is also excessively longer for declines with large dimensions than those with smaller ones. This is because more time is spent excavating large quantity of material in declines with larger dimensions.

(b) Effects of decline gradient

In this Section, the effects of decline gradient as they relate to decline development parameters are discussed.

(i) Effects on decline length

Decline gradient has significant effects on decline length. According to Chanda and Burke (2007) with increasing depths of mining and further tightening on safety requirements, the price of a typical decline excavation in Australia is likely to increase further. It is reported that at decline gradient of 1 in 7, to reach a theoretical 700m vertical depth ore body, the decline length would be 4950m while at steeper gradient the decline length would be relatively less. This is illustrated using Figure 2.16:

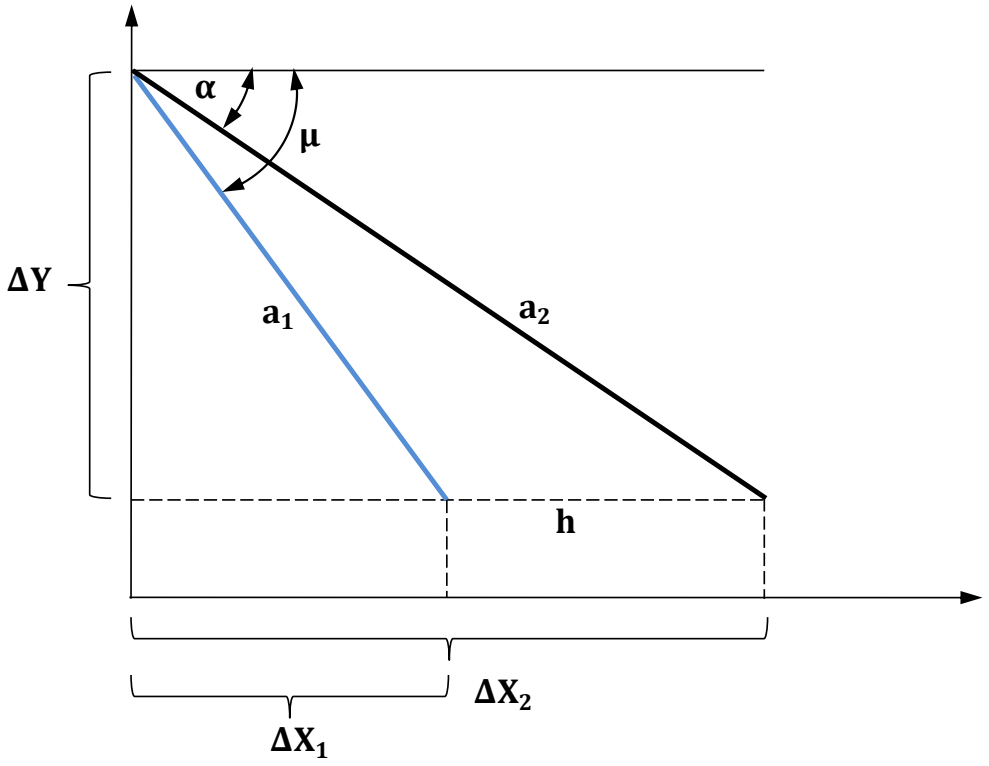

Figure 2.16: Relationship between gradient and length of a line

According to Figure 2.16, for linear functions, the gradient of a line (**m**) is calculated as indicated in Equation 2.1:

$$m = \frac{\Delta y}{\Delta x} \qquad 2.1$$

and according to Figure 2.16, a_1 has steeper gradient than a_2. The length of a_1 and a_2 is calculated using Equation 2.2 and 2.3 respectively.

$$a_1 = \frac{\Delta Y}{\sin\mu} \qquad 2.2$$

$$a_2 = \frac{\Delta Y}{\sin\alpha} \qquad 2.3$$

According to Equation 2.2 and 2.3, it can be seen that to reach horizontal level ***h***, the length a_1 will be less than a_2 because a_1 has steeper gradient than a_2. This is also confirmed by numerical calculations of *Euclidean Length*, **L**, using Equation 2.4 (Brazil et al., 2003). From Equation 2.4, it is evident that as decline gradient increases, the decline length reduces and vice versa.

$$L = Z\sqrt{1 + \frac{1}{m^2}} \qquad 2.4$$

where:

L is the Euclidean Length;
m is the decline gradient; and
Z is the vertical displacement.

Although the gradient in Equation 2.4 varies between 1 in 9 and 1 in 7 for conventional mining, the equation also applies for steeper gradients, i.e., to gradients less than 1 in 7. Thus, if decline gradient is reduced below the conventional 1 in 7, the decline length will be shorter. Figure 2.17 shows the effects of decline gradient on decline lengths. According to a study by Chanda and Roberts (2005), an increase in decline gradient from 1 in 7 (8^0) to 1 in 3 (20^0) resulted in 50% reduction in decline length.

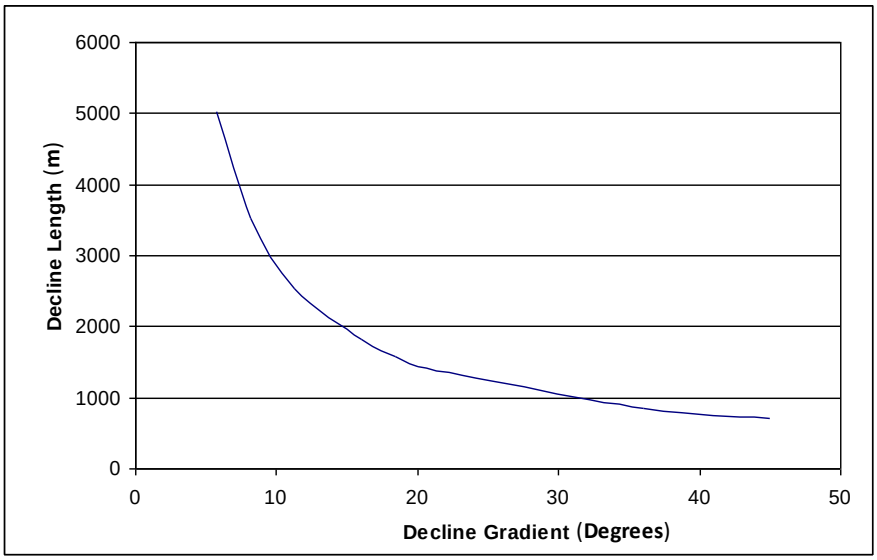

Figure 2.17: Effects of decline gradient on decline length (Chanda and Roberts, 2005)

(ii) Effects on duration of decline development

Duration of decline development is also inversely proportional with decline gradient. This means that, as the decline gradient increases, the duration of decline development reduces and vice versa. Thus, if we let **X** be the average decline development advance per day, the duration of development can be determined using Equation 2.5:

$$\text{Duration of development} = \left[\frac{Z\sqrt{1+\frac{1}{m^2}}}{X} \right] \qquad 2.5$$

A study conducted by Chanda and Roberts (2005) indicates that it would take approximately 825 days to develop a decline to a depth of 700m with conventional 1 in 7 decline gradient at 6m advance per day. However, with a gradient of 1 in 3, it would take approximately 451 days with the same advance rate. The study, therefore, shows that there is a reduction of almost 50% in decline development period with the reduction of decline gradient from 1 in 7 to 1 in 3.

(iii) Effects on decline development cost

The cost of decline development is also directly related to the decline gradient. As indicated earlier, the steeper the decline gradient, the less the decline length required to reach the ore body and vice versa. It is reported (Brazil et al., 2003) that with steeper gradient, the development costs decrease because of the reduction in decline length, thereby reducing the total development cost. Equation 2.6 (Brazil et al., 2003) confirms the reduction in development costs as the decline gradient is increased.

$$C_d = C_m\left[\mathrm{Z}\sqrt{1+\frac{1}{m^2}}\right] \qquad 2.6$$

Where:

$\boldsymbol{C_d}$ is the development cost; and

$\boldsymbol{C_m}$ is the decline development costs per meter.

According to literature (Chanda and Roberts, 2005) development cost per meter for conventional decline development (5.5mW x 5.5mW) is approximately A$2500. At such cost, the longer the decline length (low decline gradient), the more development costs will be incurred as compared to steep decline gradient (Figure 2.18). The results also indicate that an increase in decline gradient from 1 in 7 to 1 in 3 resulted in more than 50% reduction in development costs.

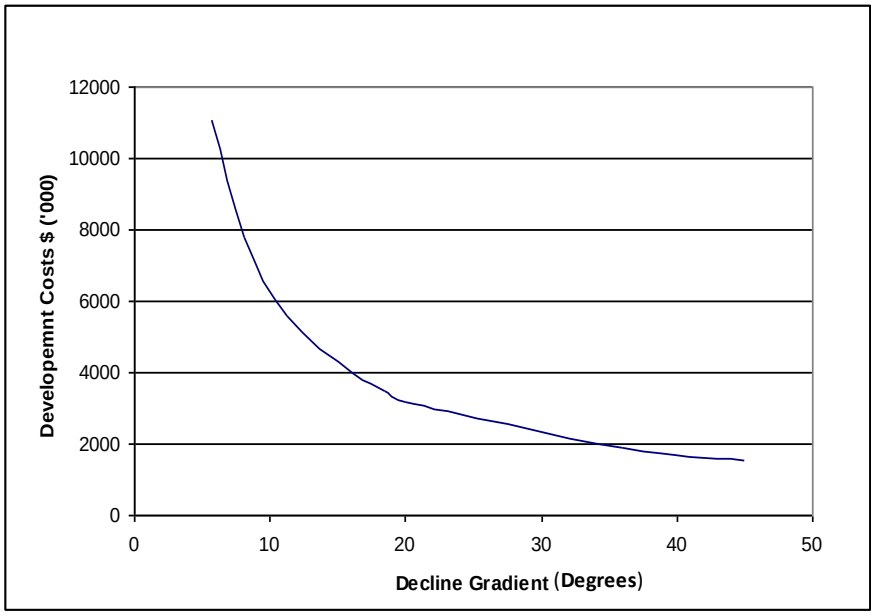

Figure 2.18: Relationship between decline gradient and development costs (Chanda and Roberts, 2005)

(c) Effects of turning radius

The effects of the turning radius can be illustrated by calculating the arc length ***AB*** using Figure 2.19.

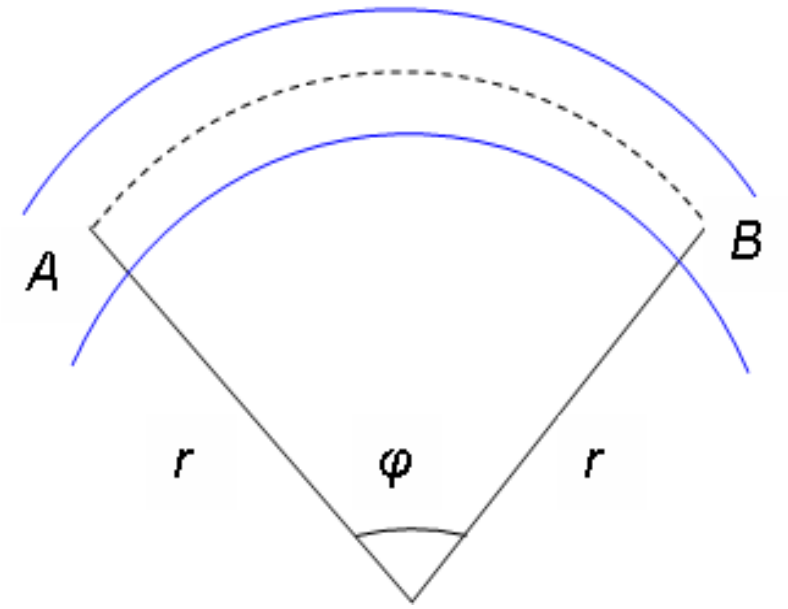

Figure 2.19: Relationship between turning radius and curve length

In Figure 2.19, considering ***AB*** as the curve length with turning radius ***r***, the distance between ***A*** and ***B*** is found using Equation 2.7.

$$C = \frac{\varphi}{180}\pi r \qquad 2.7$$

where:

C is the curve length between **A** and **B**;
r is the curve radius; and
φ angle formed by arc **AB** (degrees).

From Equation 2.7, it can be seen that the larger the turning radius ***r***, the longer will be the curve length. Although the effect of turning radius is not greatly felt at steep gradient, it will still increase curve lengths. In Australian underground mines, a turning radius of 15 – 20m is adopted for decline access. This means curve lengths in conventional decline development are relatively longer compared with a monorail system which can negotiate horizontal curve radius of 4m.

2.3.2.3 Productivity in conventional decline development

Productivity in conventional decline development involves the following unit operations:

- Drilling and blasting;
- Waste removal from the face to stockpile area; and
- Loading and transporting of waste from stockpile area to the surface.

(a) Drilling and blasting

Table 2.1 shows the drilling and blasting cycle time according to the studies conducted in Western Australia by Leppkes (2005).

Table 2.1: Drilling and blasting cycle times (Leppkes, 2005)

No	Unit operation	Cycle time (Minutes)
1	Drill face - using twin boom jumbo (48 face holes and 32 support holes @ 4 min per hole)	320
2	Charging the face	39
3	Other activities (e.g. mark face, tie blast, evacuate blast area, evacuate blast fumes etc)	114
	Total cycle time	**473**

According to Leppkes (2005), in competent ground surface, ground support with a wire mesh is only required by statutory regulations in Western Australia where the height of the face exceed 3.5m. Therefore, since the development face studied by Leppkes was 3m x 3m in competent ground surface, no time to install wire mesh was allowed as indicated in Table 2.1. However, where the height of the decline exceeds 3.5 metres, as later indicated, the time to install support would be included in the mining cycle.

(b) Waste removal from the face to stockpile area

In conventional decline development, Load Haul Dump (LHD) units are used for waste removal at face in combination with Front End Loaders (FELs). Cycle time at the face involves loading muck from the development face into LHD units and transporting the waste material to a stockpile area at another level. When all the muck pile is removed, face drilling commences. According to studies by Leppkes (2005), the cycle time to load one truck ranged from 3.6 minutes to 6 minutes. However, to load and transport waste from a 3.7m cut to the stockpile area was estimated to take 78 minutes (1.3 hours).

(c) Waste removal from stockpile area to the surface

When all waste is removed from the face, stockpiled waste is then loaded into a 32.4 tonne payload trucks and transported to the surface. Table 2.2 shows an example of cycle times to transport muck from the stockpile area to the surface.

Table 2.2: Truck cycle time to move waste from stockpile area to surface (Leppkes, 2005)

No	Unit operation	Cycle time (Minutes)
1	Loading time	6.00
2	Travel time (loaded) – 2000m @ 6.8km/h	17.64
3	Dump time	1.00
4	Travel time (Unloaded) - 2000m @ 23km/h	5.22
	Total cycle time	**29.86**

According to Leppkes (2005) a 3m wide by 3m high by 3.7m long cut produces a muck pile of 33.3 Bank Cubic Metre (BCM) of material or 93.2 tonnes at Specific Gravity (SG) of 2.8. Therefore, with a 32.4 tonne Hitachi 400D payload truck and 29.9 min/cycle, the total cycle time to load and transport 93.2 tonnes from the stockpile to the surface in conventional truck haulage system takes approximately 90 minutes (1.5 hours) for a 2000m spiral decline length. Therefore, the total cycle time to load muck from face to surface with stockpiling in a 3.7m cut is 168 minutes (2.8 hours) as shown in Table 2.3.

Table 2.3: Total load-haul cycle time with stockpiling

No	Unit operation	Cycle time (Minutes)
1	Total cycle time to load and transport muck to stockpile area.	78
2	Total cycle time to load and transport muck from stockpile to surface	90
	Total cycle time	**168**

(d) Truck productivity versus decline length

Decline access is normally attractive for shallow ore bodies. However, as the depth of mining operations increases, productivity of trucks decreases. McCarthy and Livingstone (1993) simulated the productivity of 50 tonne and 40 tonne trucks and the results of their modelling showed that productivity of trucks reduces as the depth of mining increases (Figure 2.20). The decrease in

truck production is attributed to long truck cycle times due to increase in decline length.

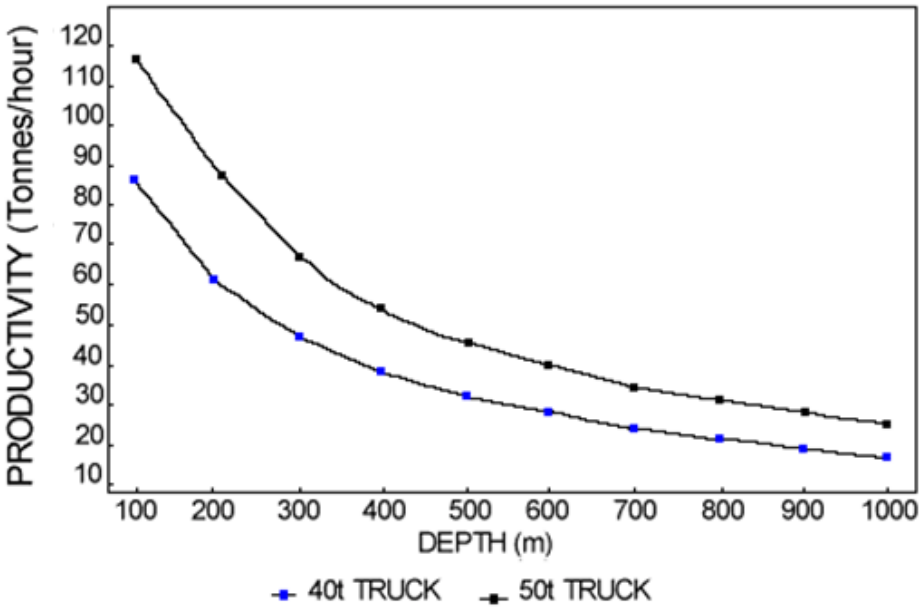

Figure 2.20: Relationship between productivity of trucks and depth of mining (McCarthy and Livingstone, 1993)

According to studies (Leppkes, 2005) of truck cycle times conducted in Western Australia where a 32.4 tonne payload Hitachi 400D trucks was loaded with Elphinstone R1700G, two trucks were required to develop a decline up to a vertical depth of 377m and three trucks were required to develop a decline thereafter. This confirms results by McCarthy and Livingstone (2005) that productivity of trucks reduces with increase in mining depths. It is a well known fact that the LHDs in decline development have limitations, which include the need for dump bays, not effective over distances exceeding 100m, soft floors, confined to certain gradients and the need for constant road maintenance.

2.3.2.4 Conventional decline development costs

Generally, mining costs are governed by the ratio of excavated tonnes of ore to tonnes of excavated waste including waste resulting from capital development. With respect to the recent liberal use of decline as mine access, the ratio of

capital waste development tonnes to mined ore tonnes has been excessive, especially in narrow vein, high grade small deposits (Brazil et al., 2003). In conventional decline, access development costs are categorised in two types, i.e., capital costs and operating costs for LHD trucks.

(a) Capital Costs

Capital costs for conventional decline development involves purchase of LHD trucks as well as boggers/loaders. According to literature (Leppkes, 2005), the cost of an underground Hitachi AH400D truck is A$720,000.

(b) Operating costs

Operating costs associated with operations of a 32.4 tonne payload Hitachi AH400D truck commonly used in conventional decline development are summarised in Tables 2.4.

Table 2.4: Operating costs for Hitachi AH400D truck (Leppkes, 2005)

No.	Description	Operating costs (A$/h)
1	Maintenance parts	13.36
2	Fuel	21.00
3	Tyres	7.74
4	Maintenance labour	6.14
5	Oil and Lubricants	0.94
	Total	**49.18**

2.3.3 Application of monorail technology in decline development

Application of monorail technology in decline development requires changes to design parameters of the decline access. This Section, therefore, reviews literature as it relates to design parameters of the decline access with monorail system application.

2.3.3.1 Decline design parameters for monorail system application

(a) Size of decline

The monorail system is designed to operate on declines of cross-sectional area less than the 5.5mW x 5.5mH used in conventional decline development. According to Scharf (i.e., manufacturers of monorail train), the monorail system has dimensions 1.1mW x 1.3mH but considering safety and ventilation requirements of the decline access, decline dimension of 3mW x 3mH is recommended by Scharf as being suitable for single monorail system application (Figure 2.21). For two monorail trains, decline dimension of 3.8mW x 3.0mH is recommended. An allowance has also been made for locating an overhead air or ventilation bag.

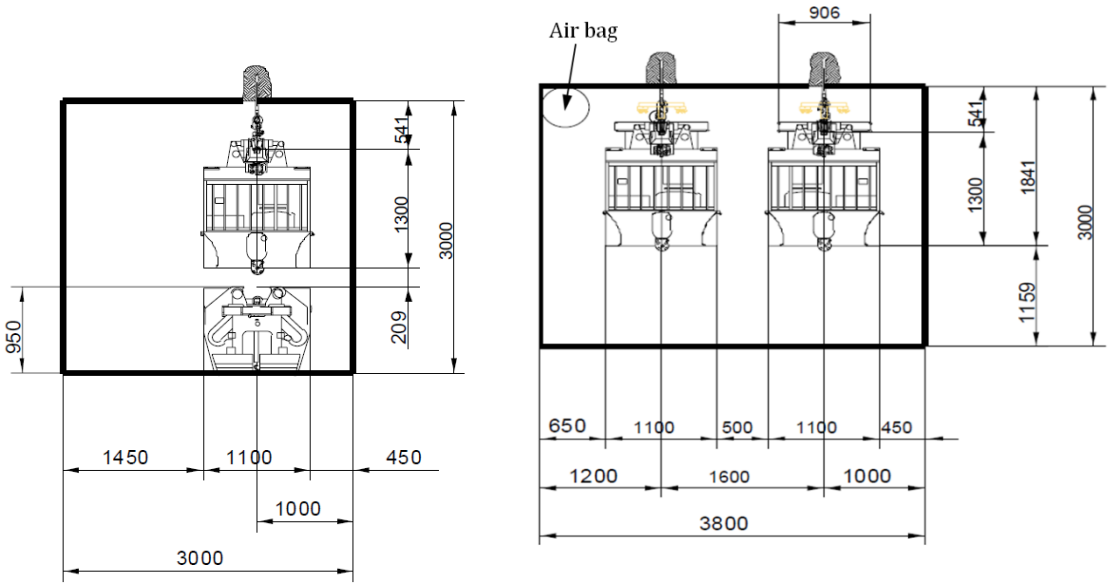

(a) (b)

Figure 2.21: Decline opening requirements (a) one monorail train (b) two monorail trains (Scharf, 2007)

Therefore, the smaller decline dimensions with monorail system application reduces the need for costly ground support – an important measure for health and safety of mine workers and for energy savings – and reduces ventilation requirements. Generally, the implication of smaller cross-sectional area of

decline access is that considerable savings can be made in underground development.

(b) Decline gradient

Decline access for monorail system application is developed at a steeper gradient than 1 in 7 (8^0) used in conventional decline development. This is because the monorail system has the ability to negotiate steeper gradients. It is reported (Scharf, 2007; Chanda and Roberts, 2005) that monorail train can negotiate gradients of up to 36^0 when specially installed rack–and–pinion drives are used. At such gradient, it is reported (Scharf, 2007; Meyer, 2007) that the monorail speed can go up to 12.6km/h with a load of up to 30 tonnes.

(c) Turning radius consideration

Design of vertical and horizontal radius for monorail system application is also of paramount importance in decline development. According to Scharf (2007), horizontal curves with minimum radius of 4m as well as vertical curves of 10m can easily be negotiated by the monorail containers of width 1.1m and length 3.5m. Networks can also be built using manually or pneumatically operated rail switches. However, calculations for turning radius (***r***) for monorail cars with varying dimensions can be done as per Figure 2.22.

According to Figure 2.22, the minimum turning radius (r) between two monorail containers can be determined given the following parameters:

- Width of the car (given as ***a*** in Figure 2.22) ;
- Length of drawbars between two containers (given as $\mathbf{AA^1}$ in Figure 2.22); and
- Distance from hanging point to the edge of the car (shown as ***b*** in Figure 2.22).

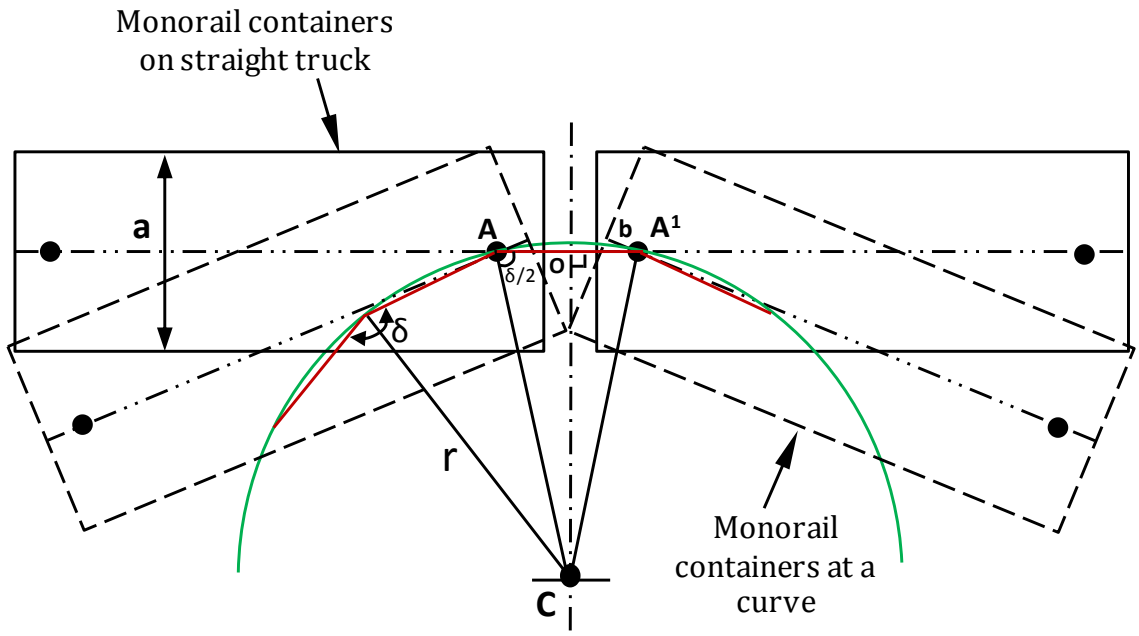

Figure 2.22: Solution to the minimum required curve radius (Oguz and Stefanko, 1971)

With angle **δ** known (from trigonometry), the radius of the curve (***r***) is determined using triangle AOC which is right angled at O as indicated below:

$$r = \frac{AO}{Cos\left(\frac{\delta}{2}\right)} \qquad 2.8$$

This means that at turning radius ***r***, the monorail containers will just touch on a curve. Therefore, for the safety of the system, any curve for the monorail system should be more than ***r***. As reported by Oguz and Stefanko (1971), a turning radius less than 4m develops unnecessary stresses on the truck beam and on the rollers, causing excessive wear on the track and damage to the roller bearings.

2.3.3.2 Effects of designed parameters on decline development

Decline design parameters for monorail system application have effects on decline development. Table 2.5 summarises the effects of the parameters and the benefits resulting from their use.

Table 2.5: Effects of monorail system design parameters

No	Design Parameter	Effects	Benefits
1	Decline dimension (Small cross-sectional area)	• Less waste to be drilled and blasted; • Less waste to be transported; • Less ground support needed;	• Less development costs; • Less ventilation costs;
2	Decline gradient (Steep gradient)	• Reduced decline length;	• Faster developments; • Less development costs; • Less waste to be transported;
3	Turning radius (Small radius)	• Reduced decline length;	• Faster developments; • Less development costs; • Less waste to be transported;

2.3.3.3 Monorail system productivity

The rock loading subsystem is a critical component of monorail haulage system. Loading is part of the mining cycle that involves drilling and blasting as well as removal of rock from the development face. However, the cycle times of the drill and blast operation are dependent on the efficiency of the mucking and transport system. A fully installed underground monorail system in decline development consists of the following unit operations:

- Loading of monorail containers with Front End Loader; and
- Transport of material to the surface by monorail train.

(a) Monorail system productivity with Front End Loader (FEL)

Productivity of the monorail system with FEL at a workface consists of a loader (Side Dump Loader) that loads material from the face directly into monorail containers. Therefore, the cycle time for the loader is the total time to load all 6 containers of the monorail train. According to Leppkes (2005), it takes approximately 33 minutes to load all 6 monorail containers (in horizontal crosscut) of 5 tonne capacity using a side dump FEL. This is based on monorail

containers located 20m from the face. The loading time of the FEL is likely to increase when loading from a decline face (which is inclined).

(b) Transport of material to the surface by monorail train

Once all the monorail containers are loaded, they are lifted up by the lifting beam of the monorail train and transported to surface. The cycle time for the monorail system, therefore, involves lifting of containers and transporting material from the development face to the surface. Table 2.6 shows the cycle times for loading and hauling muck using a monorail system for a 3.7m cut development face.

Table 2.6: Cycle time for loading and hauling using a monorail

No	Unit operation	Cycle time (Minutes)
1	Loading time	33.00
2	Travel time (loaded) – 2000m @ 6.5km/h	18.46
3	Dump time (1 minute / container)	6.00
4	Travel time (Unloaded) – 2000m @ 12.6km/h	9.52
	Total Cycle time	**66.98**

Therefore, with 93.2 tonne material from the 3.7m box cut, it would take 208 minutes (3.5 hours) to clean the face with monorail system of payload 30 tonnes.

2.3.3.4 Monorail system costs

The costs associated with operations of the monorail system are classified into two:

- Capital costs; and
- Operating costs.

(a) Capital Costs

Capital costs for monorail system operations consist of purchase and installation of a monorail train in the decline. Table 2.7 shows capital costs, for the purchase

of a monorail train with two driver's cabins, four drive units and six lifting beams and containers with a payload of 30 tonnes (Meyer, 2008). Table 2.8 shows the capital costs for monorail installation per meter.

Table 2.7: Capital costs for purchase of monorail train (Meyer, 2008)

No.	Unit	A$	Comments
1	Monorail Train	1,200,000	Price by Scharf
2	Containers	16,000	Price by Scharf
3	Monorail Tools	25,000	Price by Scharf
4	Shunting Trolley	49,000	Price by Scharf
5	Dispenser (For roof bolt installation)	26,000	Price by Hilti
	Total	**1,316,000**	

Table 2.8: Capital costs for monorail train installation (Meyer, 2008)

No.	Unit	A$/m	Comments
1	Rail component	125.00	Price by Scharf
2	Electrical Components	250.00	Price by Scharf
3	Bolts (2 bolts / 3m section)	72.00	Price by Hilti
4	Rail Suspension components	75.00	Price by Scharf
5	Labour	51.04	Estimated by Scharf
6	Jumbo Drill (for roof bolt installation)	4.45	Estimated by Scharf
	Total	**577.49**	

(b) Operating costs

Table 2.9 shows operating costs for the monorail train. The installed power on the train is 232kW.

Table 2.9: Operating costs for monorail train (Leppkes, 2005)

No.	Description	Operating costs (A$/h)
1	Maintenance parts	12.00
2	Power	34.40
3	Maintenance labour	2.59
	Total	48.99

2.3.3.5 Power requirements for monorail system operations

Monorail trains are controlled from the driver's cabin at either end of the train. Each monorail train has a power pack equipped with 2 x 29kW electric motors providing a total of 58kW power to each drive unit. The monorail trains are controlled by frequency converters and PLC, coupled to the drive wheels through gears to control the speed of the train. When the train is braking, the EMTS is working in a generating mode. That means the braking forces are not entirely wasted by creating heat but they generate electrical power which is fed back into the power supply system. The average saving by generating electrical power is approximately 30% of the electrical power needed for the operation of the trains. This special design feature of the frequency converters allows such a cost saving mode of operation. There are also emergency and parking brakes and a twin 3-phase alternating current (AC) power pick-up. Up to four drive units are implemented into one monorail train for more traction forces. Therefore, the total power installed on one monorail train is 232kW.

(a) Monorail power consumption

A single monorail train with 232kW of installed power requires a transformer with a minimum capacity of 167kVA every 800m although a 200kVA transformer is selected for a single monorail system (World Mining Equipment, 1996). According to Leppkes (2005), power alone contributes to 70% of total operating costs (Table 2.9) based on power costs of A$0.29 per kWh using site based diesel power generators. Table 2.10 shows power consumption for the monorail train.

Table 2.10: Power consumption for monorail train (Leppkes, 2005)

Description	Units	Value	Comments
Installed power	kW	232.0	4 drives at 58kW per drive
Power required	kWhrs	170.1	40 minutes per hour full load and 20 minutes per hour 20% of load
Power saved (in generating mode)	kWhrs	51.0	30% of full load power recovered
Power required	kWhrs	119.1	Power Required minus power saved

Leppkes (2005) assumed that for 40 minutes in an hour, power would be consumed at the full installed power and for 20 minutes in the hour, 20% of installed power would be consumed. He also assumed that one third of the full load power consumed would be saved when the train is operating in generating mode. Therefore, the total power consumption for four drive units is 119.1kWh (or 29.7kWh for each drive unit). The results by Leppkes (2005) coincided with results obtained by Oguz and Stefanko (1971) who obtained a power consumption of 30kWh per drive unit during their study of monorail train.

(b) Effects of power on monorail operating costs

Cost of power has the effect of increasing operating costs of monorail train depending on its cost per kWh. Figure 2.23 shows the relationship between power cost and monorail operating cost. According to Figure 2.23, monorail system operating costs are directly proportional to the cost of power. Thus, operating costs for monorail system would be less than a similar payload truck if the cost of power was significantly reduced.

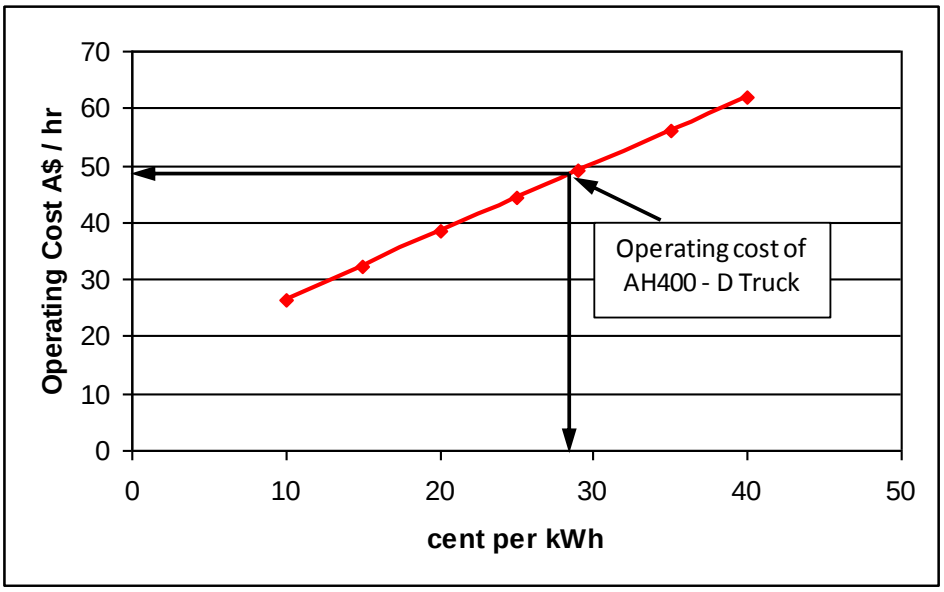

Figure 2.23: Effects of power on monorail system operating costs (Leppkes, 2005)

(c) Effects of monorail speed on power consumption

According to the study (Oguz and Stefanko, 1971), acceleration and speed of the monorail train affects power consumption; power demand for empty run was higher than for the loaded run because of the higher travel speed of the former (Figures 2.24 and 2.25).

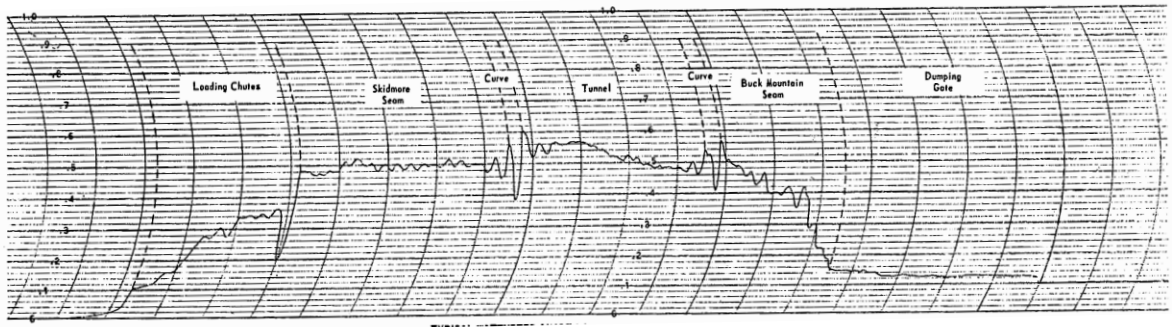

Figure 2.24: Wattmeter chart for empty trip at faster monorail speed (Oguz and Stefanko, 1971)

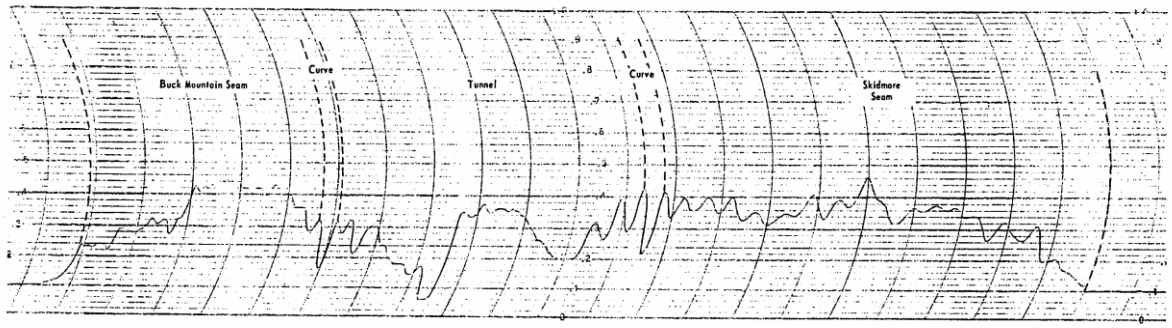

Figure 2.25: Wattmeter chart for loaded trip at slow monorail speed (Oguz and Stefanko, 1971)

2.3.4 Conventional versus monorail system decline development

A comparison on decline development between conventional (truck) haulage method and monorail haulage system was made. This Section presents the results of the comparisons.

Literature has revealed that to reach the ore body in conventional decline development, significant amount of waste material is excavated. However, with

monorail application less amount of waste material would be extracted due to smaller size of the decline opening and steeper gradient, reducing both the development costs and the duration of development. It is also evident that decline gradient and turning radius play an important role in reducing the decline length. Therefore, with monorail system application, there is significant reduction in development meters and ore bodies will be accessed more quickly and cheaply.

Monorail system productivity is greatly affected by the loading mechanism. According to literature, it takes longer time to load monorail containers when compared to trucks and this increases monorail cycle times (Figure 2.26).

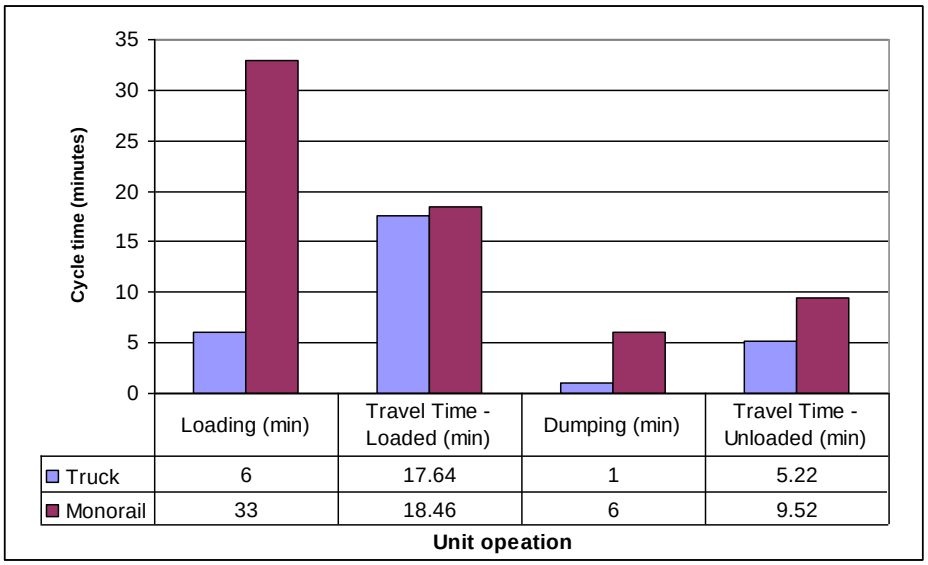

Figure 2.26: Cycle times for monorail and truck haulage systems

However, significant reduction in cycle times will be achieved if the monorail system is loaded with some continuous loading system. The system will make monorail system cycle times comparable with conventional LHD truck techniques whilst eliminating the need for stockpiling. Capital cost for monorail is significantly higher than for a similar payload truck (Figure 2.27). However, the higher capital costs of monorail system will be overshadowed by the huge saving resulting from decline development.

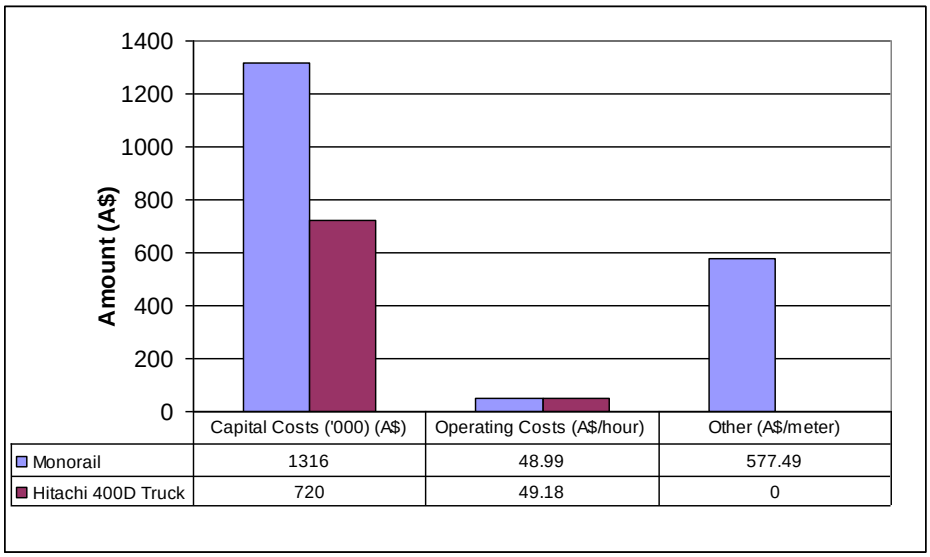

Figure 2.27: Capital and operating costs for monorail and truck haulage systems

Although power consumption is critical in monorail system operations, operating cost of the monorail system was estimated to be the same as a similar payload underground truck, i.e., A$49 per hour. Mining operations using monorail system have proved to be very cost-effective in most major mining countries of the world (Leppkes, 2004).

2.3.5 Monorail system productivity

From the reviewed literature (Leppkes, 2005; Leppkes, 2004), it has been determined that loading time is the main drawback to high advance rates with monorail system application. Therefore, to improve advance rates, the monorail system should be loaded by some continuous system that will quickly remove the rock from the face onto the monorail containers. According to literature (Leppkes, 2005), the cycle time for the development of a decline using monorail system without stockpiling was greater than using conventional LHD and truck in combination with stockpiles. The increase in cycle time for monorail system resulted from the inefficiency of the loader and the number of cycles the loader had to make to fill the monorail containers. In Chapter 10, a detailed comparison

of the two systems over the same decline length of 2000m has been made using simulation studies.

2.3.6 Conceptual monorail drilling and loading systems

This Section summarises the developed concept for drilling, loading, hauling and dumping operations using the monorail technology. The concept is composed of two systems, i.e., the drilling system and the loading system (which cleans the development face, transports and dumps material to surface). Each of the two systems is powered by an independent power supply to make the systems flexible. The concept is illustrated in Figure 2.28.

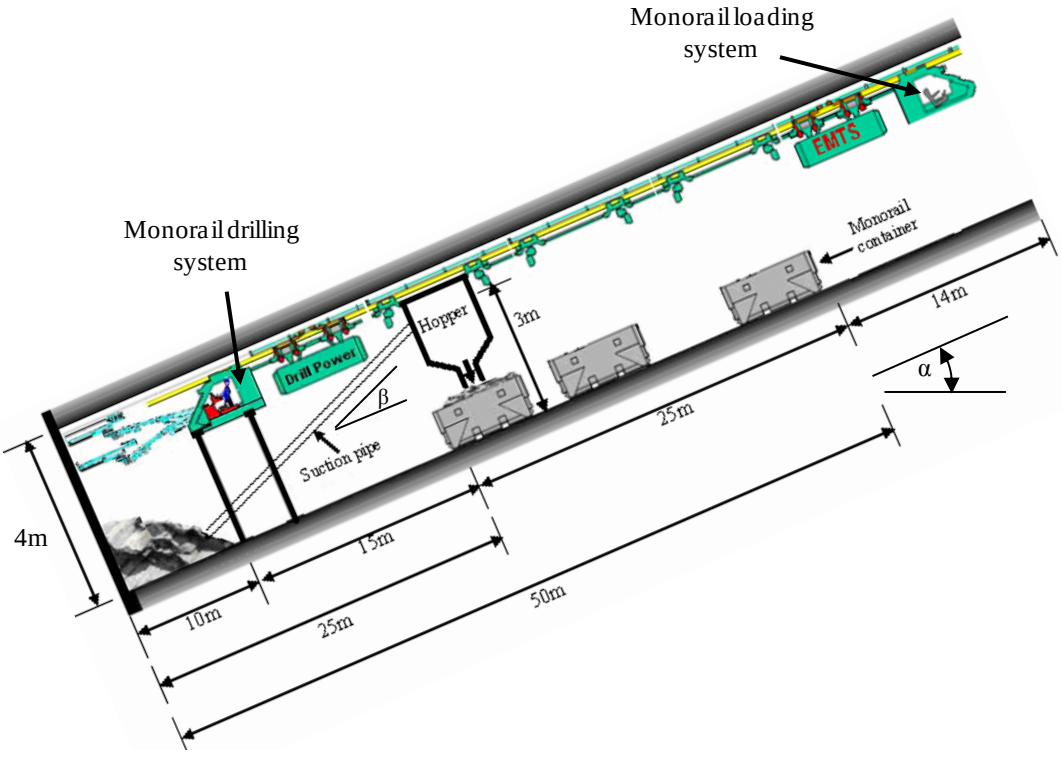

β is inclination of suction pipe from the decline floor to hopper; **α** is the decline gradient

Figure 2.28: Proposed conceptual monorail drill-load-haul system

In this concept, the loading system consists of a pneumatic suction unit that uses vacuum to load (suck) rock fragments from the development face into the hopper through the suction pipe. Table 2.11 summarises the steps of the loading

process in the order in which they appear. Details of the conceptual design of the monorail loading system are discussed in Chapter 4.

Table 2.11: Steps of the loading / suction process

Step No.	Description of process
1	Prime mover creates negative pressure inside the hopper;
2	Loading / suction of blasted material from the face into the hopper through suction pipe;
3	Disconnection of suction pipe from the hopper when the hopper is fully loaded.
4	Pulling of loaded hopper by the monorail train to position of empty container;
5	Automatic discharge of material from the hopper into the container;
6	Pushing of empty hopper by the monorail train to the loading position;
7	Reconnection of suction pipe to the hopper;
8	Loading process resumes;

Once all the six monorail containers are loaded, material is transported to surface by the monorail train for dumping. Table 2.12 summarises steps of material haulage process.

Table 2.12: Steps for material haulage

Step No.	Description of process
1	Disconnection of hopper from the monorail train when all six monorail containers are loaded;
2	Monorail train moves to container lifting position and lifts the loaded containers;
3	Pulling of loaded containers to surface by the monorail train (for material dumping);
4	Monorail train returns underground with empty containers after material is dumped on surface;
5	Containers are lowered at the loading position;
6	Reconnection of the hopper to the monorail train;
7	Loading of material at face resumes until the face is completely cleaned;

The proposed monorail drilling system consists of two independent drilling booms mounted on the monorail train. The system also consists of two horizontal and two vertical stabilisers (props) to act as supports during drilling process. This concept would allow the top part of the face to be drilled while

blasted material is being loaded. As can be seen from Figure 2.28, the drilling system will drill the face at maximum distance of 10m with a possibility of the system drilling closer to the face. Details of the conceptual design of the monorail drilling system are discussed in Chapter 5.

The advantage of this concept is that as the development face is being cleaned and as the material is being transported to surface, the monorail drilling system will be drilling the top part of the face without waiting for the material to be completely removed from the face. It is envisaged that this method will reduce the total drill-blast-load-haul cycle time when compared with the conventional method.

2.4 Summary

The reviewed literature shows that the current method of accessing ore bodies by conventional decline method has proved to be expensive. It suggests that more waste material is being extracted because of the size of decline openings adopted. The conventional 1 in 7 decline gradient and turning radius of 20m makes the decline excessively longer whereas at steeper gradients and small turning radius, decline lengths will be reduced and ore bodies will be accessed more cheaply and quickly. It is also evident that the monorail system offers an alternative to truck haulage system at reduced costs. However, the rock loading system is a critical component of monorail system haulage. The cycle time is dependent on the efficiency of the loading and transport system. In monorail system operations, the loading time is the main drawback to high advance rates. It is, therefore, suggested that the monorail system be loaded by some type of continuous system that will quickly remove the rock from the face onto the monorail containers. The proposed pneumatic loading system offers fundamental reduction in capital expenditure and significant savings in mine operating costs. Therefore, in Chapter 3, an extensive literature review regarding pneumatic conveying system is presented. The results of the review are used in Chapter 4 during the design of a pneumatic loading system that uses monorail technology.

Chapter 3

3.0 Pneumatic conveying system

3.1 Introduction

A continuous monorail loading system is fundamental in improving advance rates in decline development. In Chapter 2, it was revealed that to improve advance rates in decline development, the monorail system should be loaded by some continuous system that quickly removes blasted rock fragments from the development face onto the monorail containers. The proposed monorail loading system uses pneumatic (vacuum) conveying system to suck blasted rock fragments (via inclined suction pipe) into the hopper. Thus, the design of the system involves an analysis of the application of fluid flow. Although classic hydraulic principles apply, the monorail pneumatic loading system is complicated since suction involves solids, which make significant changes in the rheological or flow characteristics of the liquid. Therefore, in order to gain an understanding of the flow phenomenon in different sections of pneumatic conveying system and how different research addressed these issues, a detailed literature survey was undertaken on the gas-solids flow in a pipeline. This Chapter, therefore, reviews literature regarding pneumatic conveying system.

3.2 Pneumatics and its applications

Pneumatics comes from the Greek word "*Pneumatikos"*, which means coming from the wind. It is a branch of physics dealing with systems that use pressurized gas, especially air, as a power source. It was first successfully used

in 1860s for transporting lightweight material, such as, wood shavings, sawdust and waste papers.

The technology of pneumatic transport has steadily improved and found increasing use in the last 150 years. Currently, the applications of pneumatic conveying systems can be seen in many industrial sectors, such as, transportation of pulverised and crushed Run-Of-Mine (ROM) coal through pipelines (Wypych et al., 1990; Kerttu, 1985). Pneumatic conveying is also used at harbours, barge terminals and rail terminals for loading and unloading bulky material, such as, grain, cement, fertilisers, etc. Other applications include chemical process industry, pharmaceutical industry, mining industry, agricultural industry, etc. Pneumatic transport system also finds wide application in dredging of sand and other sea-bottom materials (Herbich, 2000). According to Ratnayake (2005), a list of more than 380 different products have been successfully conveyed pneumatically including very fine powders as well as big crystals, such as, quartz rock of size 80 mm.

3.3 Pneumatic conveying system

Pneumatic conveying system is the use of air or another gas to transport powdered or granular solids through pipes (Kraus, 1980). This is a counterpart of slurry pipeline, using a gas instead of a liquid as the medium to transport solids. Using either positive or negative pressure of air or other gases, the material to be transported is forced through pipes and finally separated from the carrier gas and deposited at the desired destination. Because of high intensity of pneumatic transport and the abrasion (wear) of material transported, such pipelines are for transport over short distances only, usually less than 1km, although most often only a few hundred meters or shorter. The following are some of the advantages of pneumatic conveying:

- Economical over short-distance transport of bulk material;
- Automatic and labour-saving;

- Elimination or reduction human contact with the material being transported, thus enhancing safety and security;
- Easy automation and control;
- Low maintenance and low manpower costs;
- Flexibility in routing; and
- Dust free conveying system.

3.3.1 Types of pneumatic conveying systems

Generally, there are three types of pneumatic pipeline conveying systems, i.e., negative pressure (or suction) system, positive pressure system and combined (negative-positive pressure) system (Mills, 2004). In this study, only details of negative pressure system are discussed in detail. This is because negative pressure systems are used to convey material from an open storage which is the case of the development face studied in this research.

Negative pressure systems are sometimes called the suction systems and they behave like a vacuum cleaner. With this method, the absolute gas pressure inside the system is lower than atmospheric pressure. The vacuum inside the hopper and the suction pipe is created by the prime mover (e.g. air pump) such that the solid-air mixture is sucked through the pipe and solids discharged into the receiving hopper. Because the maximum pressure differential across a pipe and hopper that can be developed by suction system is always less than one atmospheric pressure, the suction can only be used for relatively short distances, normally not more than 30m (Liu, 2003). According to Liu (2003), the smallest suction system is the vacuum cleaner while the largest suction systems are those used at Disney World in Orlando, Florida. The latter system consists of an underground network of pipes for collecting the trash from various buildings to a central station. Figure 3.1 shows the schematic configuration of the negative pressure system.

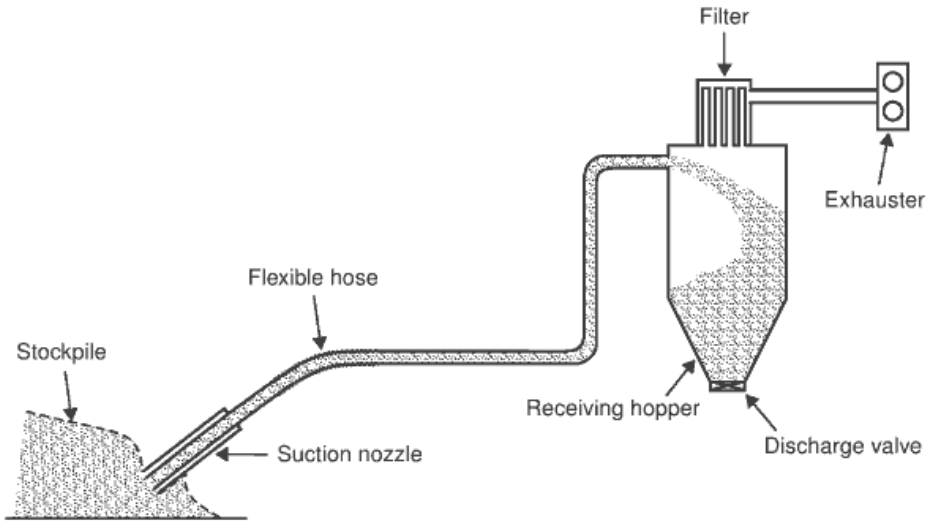

Figure 3.1: Pneumatic (vacuum) conveying from open storage (Mills, 2004)

3.3.2 Components of pneumatic conveying system

A number of different components exist in a pneumatic conveying plant. A typical conveying system comprises different zones where distinct operations are carried out. In each of these zones, some specialised pieces of equipment are required for the successful operation of the plant. According to Klinzing et al. (1997), typical modern pneumatic conveying system consists of the following major components:

(a) The prime mover

The prime mover is an essential element in pneumatic conveying system. A wide range of compressors, blowers, fans and vacuum pumps are used to provide the necessary energy to the conveying gas.

(b) Feeding, mixing and acceleration zone

This zone is considered critical in pneumatic conveying system. In this zone, the solids are introduced into the flowing gas stream. Initially, the solids are essentially at rest and a change in momentum occurs when solids are mixed with

the flowing gas. Associated with this momentum change is the need to provide an acceleration zone. According to Mills (2004), the acceleration zone consists of a horizontal pipe of certain length designed such that the solids are accelerated to some 'steady' flow state.

(c) The conveying zone

Once the solids have passed through the acceleration zone, they enter into the conveying zone. The conveying zone consists of a pipe to convey the solids from point **A** to point **B** over a certain distance. The selection of piping is based on a number of factors including the abrasiveness of the product and the pressure required.

(d) Gas-solid separation zone

At the end of any negative or positive pneumatic conveying system, a separator is needed that separates the solids from the carrier gas or air in order to recover the solids transported. The selection of an adequate gas-solid separation system is dependent upon a number of factors, the primary factor being the size of solids requiring to be separated from the gas stream.

3.3.3 Modes of pneumatic conveying

The pneumatic conveying of particulate solids is broadly classified into three categories, i.e., dilute, medium or dense phase. The classification is based on flow regimes and concentration of solids in the pipeline, i.e., according to the mass flow ratio or solid loading ratio (m*) which is defined as the ratio of the mass of solids (M_s) to the mass of conveying air (M_a). The classifications are indicated in Table 3.1. In this study, only two regimes, i.e., dilute-phase and dense-phase are discussed in detail.

Table 3.1: Classification of pneumatic conveying regimes (Jones, 1989)

Description	Solid loading ratio – m*
Dilute (lean) phase	m*<15
Medium phase	15<m*<50
Dense phase.	m*>50

(m* is the solid loading ratio - See Equation 4.3)

3.3.3.1 Dilute phase transport

Rhodes (2001) described dilute phase transport system as a system which is characterised by high gas velocities (greater than 20m/s), low solid concentration (less than 1% by volume) and low pressure drop per unit length of transport line. With this method, the bulk material is carried by an air stream of sufficient velocity to entrain and re-entrain it for a distance depending on the available pressure. Under these dilute conditions, the solid particles behave independently fully suspended in the gas and fluid-particle forces dominate. Until quite recently, most pneumatic transport was done in dilute suspension using large volume of air at high velocity. Figure 3.2 shows an example of dilute phase transport of fines.

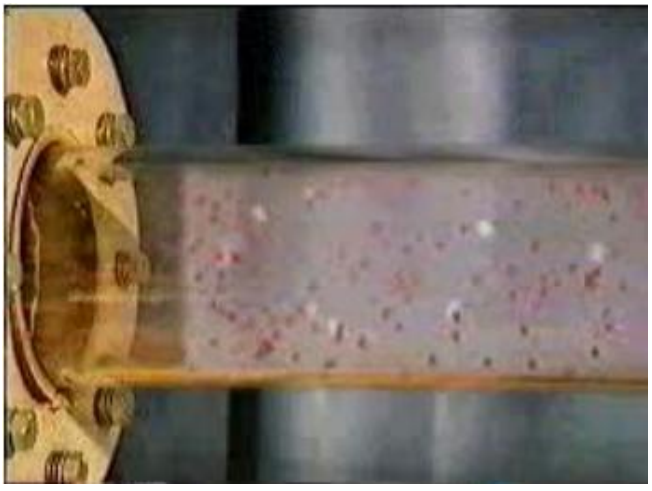

Figure 3.2: Dilute phase transport (Rhodes, 2001)

Dilute phase transport systems are comparatively cheap to install and operate, use low pressure compressed air and can be used over long distances. On the

other hand their relatively high conveying velocities cause degradation (wear) of material and they are low tonnage systems.

3.3.3.2 Dense phase transport

Dense phase involves reduction of gas velocity such that bulk materials are transported in stratification mode with non-uniform concentration of solids over the pipe cross-section (Wypych and Arnold, 1984). With this method, the material is pushed through a pipeline as a plug which occupies the whole cross-section or as a moving bed for a pressure dependant distance. Thus, in this method, particles in a pipeline are not fully suspended and there is much interaction between particles. Dense phase pneumatic transportation of bulk solids is continually gaining interest and popularity for a variety of industrial applications. Examples include coal-fired power stations, blast furnace injection, dry disposal of fly ash and the transportation of materials in the plug phase mode. The attraction of dense phase transport lies in its low air requirements meaning low energy requirement. Also, according to Liu (2003), in dense phase conveyance, most of the pipe interior is filled with the solids to be transported or solid-to-air weight ratio is very high, i.e., greater than 100.

Several researchers have adopted m* as the basis of definition for dilute and dense phase conveyance e.g. Mason et al. (1980) have suggested that dense phase conveyances normally operate with m* greater than 40 whilst Jones (1989) indicates that m* for dense phase is greater than 50. Wypych (1994) also revealed that m* of 20 is typical of dilute phase contrary to classification of pneumatic conveying regimes in Table 3.1. Wypych and Arnold (1984) also suggests that the above forms of definitions are inadequate since m* is dependent upon the pipeline length for a given air mass flow rate (as highlighted by Mills et al., 1982). Thus, based on the above, in this study, it was assumed, that m* for dense phase conveyance is above 50 whilst for dilute/medium phase m* is less than 50. According to Jones (1989), dilute phase systems are the most common applicable method of broken rock conveyance in the mines. These methods are comparatively cheap to install and operate but have relatively low

productivity. Therefore, since dilute/medium phase has been proven in suction of broken rock from the mines, it is adopted in this design.

3.3.4 Operations of pneumatic conveying system

Various flow regimes exist inside the pipeline in a pneumatic conveying system, spanning the entire range of conveying conditions from extrusion flow to fully dilute suspension flow. Through numerous experimental studies together with visual observations using glass tubes, etc., scientists (Rhodes, 2001; Liu, 2003) have deduced these varieties of flow regimes. It has been seen that these different flow regimes could be explained easily in terms of variations of gas velocity, solids mass flow rate and system pressure drop. This clarification also explains the general operation of a pneumatic conveying system.

Most researchers and industrial system designers have used a special graphical technique to explain the basic operation of a pneumatic conveying system. This technique utilises the interaction of gas-solid experienced inside the conveying pipeline in terms of gas velocity, solids mass flow rate and pressure gradient in pipe sections in a way of graphical presentation, which was initially introduced by Zenz and Othmer (1960) and Zenz (1964). Some researchers named this diagram 'pneumatic conveying characteristics curves', (Rhodes, 2001; Liu, 2003) while others call them 'phase diagrams' (Mills, 2004). The superficial air velocity and pressure gradient of the concerned pipe section are usually selected as the X and Y axes of the diagram and a number of different curves are produced on this set of axes in terms of different mass flow rates of solids. There is a distinguishable difference between the relevant flow regimes for horizontal and vertical pipe sections. In addition, the particle size and particle size distribution also have influence on the flow patterns inside the pipelines.

3.3.4.1 Horizontal conveying

Figure 3.3 shows a typical horizontal conveying phase diagram with various cross-sectional diagrams showing the state of possible flow patterns at different flow situations.

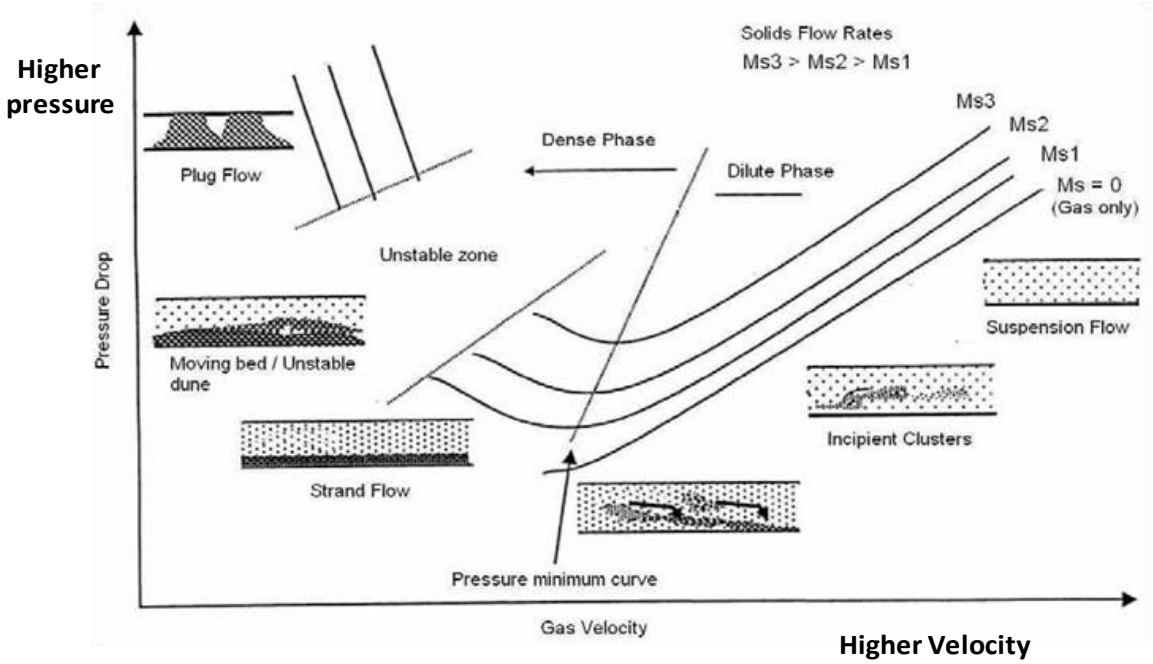

Figure 3.3: Horizontal flow conveying characteristic curves (Ratnayake 2005)

The curves in Figure 3.3 show the variations of constant solids mass flow rate contours, when the conveying gas velocity and system pressure drop varies independently. The gas only line shows the pressure drop versus gas velocity curve, which is characteristically a single phase flow. When the solids particles are introduced to the system with a particular solids mass flow value, the pressure drop increases to a higher value than in case of gas only transport even though the gas velocity is maintained constant. By keeping the solid flow rate constant and reducing the gas velocity further, pressure drop decreases down to a certain point where the minimum pressure drop is experienced. The pressure minimum curve connects such points for different solid flow rate values. Generally, the flow regimes up to this point from higher velocity could be categorized as the dilute phase flow with low values of mass loading ratios.

Further reduction of gas velocity leads to particle deposition in pipe bottom and then the flow mode is called dense phase conveying. Pressure drop is increasing when gas velocity is decreasing. After an unstable flow region, the conveying pattern shows a plug flow characteristic, which will cause the pipeline to be totally blocked if further reduction of gas velocity occurs.

Figure 3.3 also shows the different boundaries of the conveying characteristic curves. One boundary is the extreme right hand side limitation, which depends on the air volume flow capacity of the prime mover. The upper limit of the solid flow rate is influenced by the allowable pressure value of compressed air supply. The left-hand side boundary is fixed by the minimum conveying velocity, which will be discussed in detail in Section 3.6.

3.3.4.2 Vertical conveying

Figure 3.4 shows a typical vertical conveying phase diagram with various cross-sectional diagrams showing the state of possible flow patterns at different flow situations.

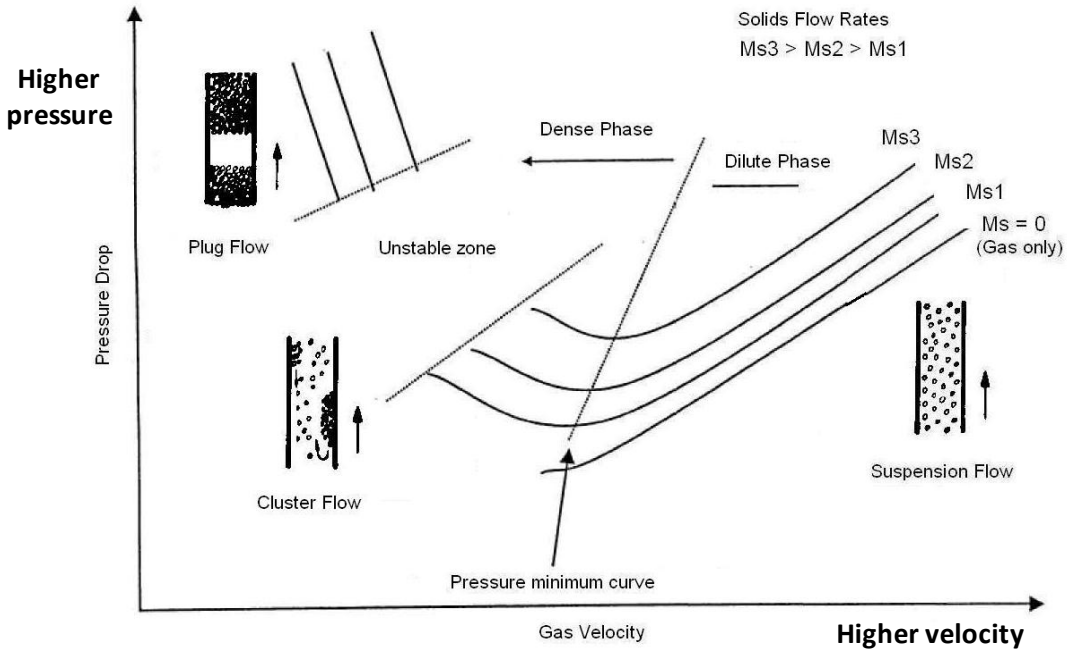

Figure 3.4: Vertical flow conveying characteristic curves (Ratnayake, 2005)

The orientation of the pipe has a considerable effect on the flow patterns and conveying regimes, because of the influence of gravity force. Consequently, the cross-sectional diagrams are totally different for the vertical pipe sections from those of horizontal sections, although the general appearances of the mass flow rate contours are similar to each other.

3.4 Fundamentals of pneumatic (suction) principles

All pneumatic conveying systems, whether they are of the positive or negative pressure type, conveying continuously or in a batch-wise mode can be considered to consist of the basic elements, i.e., feeding system, air and material pipeline (horizontal, vertical or inclined) and separation system (Figure 3.5)

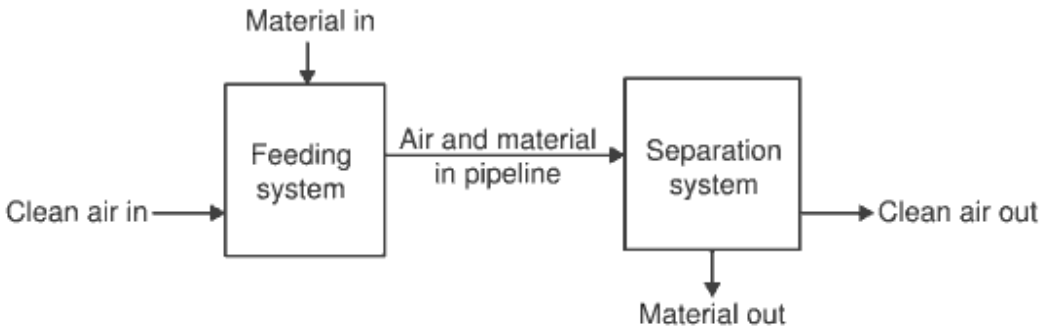

Figure 3.5: Elements of a pneumatic conveying system (Mills, 2004)

Therefore, in order to gain an understanding of the flow phenomenon in different sections of pneumatic conveying system, a literature survey was undertaken on the gas-solids flow in pipes. The review commences from the beginning of the conveying line and proceeds along the pipeline up to the end of transport line by considering different sections.

3.4.1 Feeding and entry section

Material feeding device is particularly critical to the successful operation of the pneumatic loading system. According to Klinzing and Dhodapkar (1993), the nature of the pressure fluctuation and smoothness of the flow are strongly

dependent on the design of the feed section. According to their research, the feed section plays an important role in the development of flow pattern. Thus, the basic requirement of any feeding device is that the pressure loss across the device should be as low as possible in low pressure systems and as small a proportion of the total as possible in high pressure systems (Mills, 2004). Thus, if the feeder takes an unnecessary proportion of the total pressure drop from the air source, less pressure will be available for conveying the material from the pipeline.

In vacuum systems, the material feeding is invariably at atmospheric pressure and so the pipeline can either be fed directly from a supply hopper or by means of suction nozzles from a storage vessel or stockpile (Figure 3.1). In this case, there will be no adverse pressure gradient against which the material has to be fed. This means that there will be no leakage of air across the device when feeding material in the pipeline. Usually, the feeding systems are classified on the basis of pressure limitations. In terms of commercially available feeding devices, it is convenient to classify feeders in three pressure ranges:

- Low pressure – maximum 100 kPa;
- Medium pressure – maximum 300 kPa; and
- High pressure – maximum 1000 kPa.

Below are commonly used feeding devices with their relevant pressure ranges:

- Rotary valves – low pressure;
- Screw feeders – medium pressure;
- Venturi feeder – low pressure (operate up to 20 kPa);
- Vacuum nozzle – negative pressure; and
- Blow tanks – high pressure.

3.4.2 Pressure drop determination in pipes

Since the suction pipe for monorail loading system is inclined, the analysis should be based on pressure loss determination through straight sections of an inclined pipe.

The accurate prediction of pressure drop is becoming an increasingly important requirement for many pneumatic conveying applications. According to Pan and Wypych (1992), to predict accurately the total pipeline air pressure drop in pneumatic conveying, an essential step involves the determination of pressure drop due to the solids-air flow in each straight section of pipe. In the literature, there is no lack of theoretical and empirical studies on the determination of the pressure drop across the pipe. However, most of these studies have their limitations. For example, a number of theoretical models are restricted to the dilute-phase conveying of coarse particles of relatively narrow size distribution (Yang, 1977; Tsuji, 1982).

The usual assumption of pressure drop determination in gas-solid two-phase flow is correlated best when expressed as the sum of two functions (Morikawa et al., 1978; Bradley, 1989; Mills, 1990; Pan and Wypych, 1992; Pan and Wypych, 1997) as indicated in Equation 3.1.

$$\Delta p_t = \Delta p_a + \Delta p_s \qquad 3.1$$

where:

Δp_t is the total pressure drop in the suspension;

Δp_a is pressure drop due to gas (air-alone); and

Δp_s is pressure drop attributed to the solid particles.

Determination of each of these components of pressure drop is considered separately and is presented in this Section.

3.4.2.1 Air-alone pressure drop

Determination of the air-only pressure drop is straightforward in single phase flow. As gas flows along a pipeline, the pressure resulting from the frictional resistance to the flow causes the gas to expand, i.e., the density of the gas decreases and, consequently, the average velocity of the gas across a section of the pipe must increase in the direction of the flow. Thus, using the Darcy formula, the pressure drop due to air is given as follows:

$$\Delta P_a = 4f\frac{L}{D}\frac{\rho_a \mathrm{v}_a^2}{2} \qquad 3.2$$

where:

v_a is the average velocity of the flowing gas;

f is the friction coefficient for the gas;

D is diameter of pipe;

L is length of pipe; and

ρ_a is density of air.

According to Schlichting (1960), the friction coefficient for the gas f can be determined using the Blasius equation (for Re < 10^5) as follows:

$$f = \frac{0.316}{\mathrm{Re}^{0.25}} \qquad 3.3$$

where **Re** is the Reynolds number determined as follows:

$$\mathrm{Re} = \frac{\rho_a \mathrm{v} D}{\mu} \qquad 3.4$$

where:

$\boldsymbol{\mu}$ is the viscosity of the fluid.

Alternatively, according to Irving (1989), the value of f can be calculated using Colebrook formula as indicated in Equation 3.5 or using Moody chart (Figure 3.6).

$$\frac{1}{\sqrt{f}} = -2 \cdot \log\left[\frac{e/D}{3.7} + \frac{2.51}{\mathrm{Re}\sqrt{f}}\right] \qquad 3.5$$

where:

e is relative roughness of pipe.

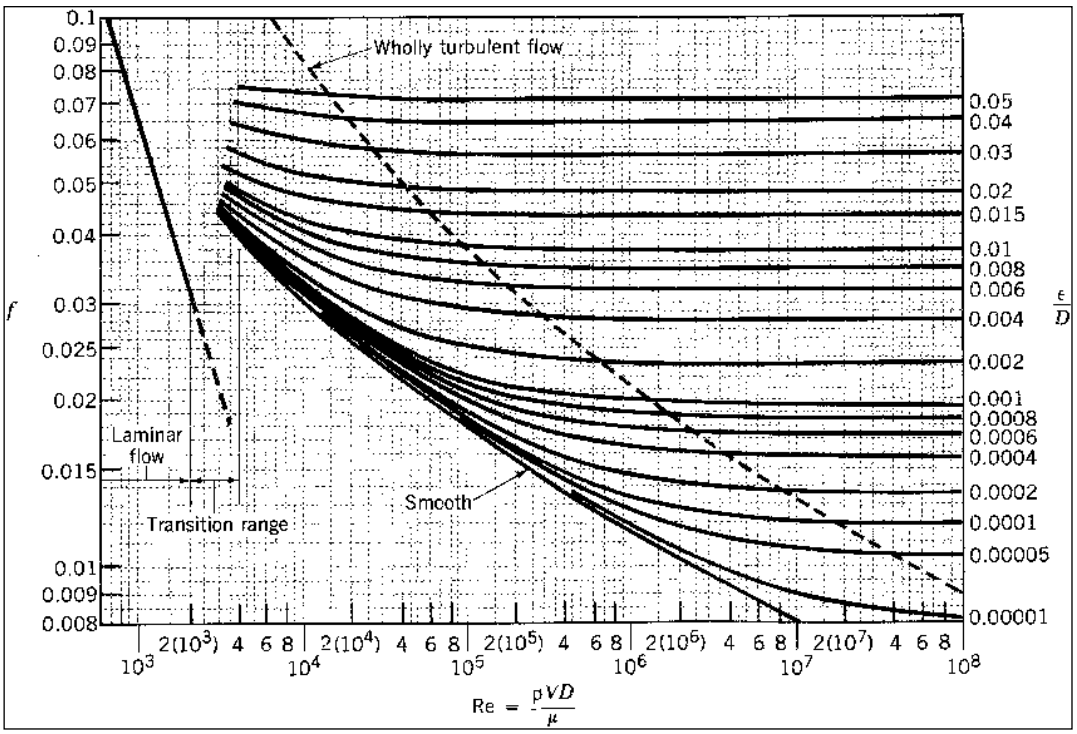

Figure 3.6: Moody chart (Klinzing and Dhodapkar, 1993)

The Koo equation (Klinzing, 1981) can also be used to determine the friction coefficient f for the gas for turbulent flow as:

$$f = 0.0014 + \frac{0.125}{\mathrm{Re}^{0.32}} \qquad 3.6$$

For incompressible flow, the following general formula for pressure drop in pipes as developed by Darcy is used:

$$\Delta P_a = \lambda_a \rho_a v_a^2 \frac{L}{2D} \qquad 3.7$$

where:

λ_a is the friction factor (Note that $\lambda_a = 4f$)

(a) Friction factor for Laminar flow

In the range 0 < Re < 2300 the friction factor:

$$\lambda_a = \frac{64}{Re}$$

(b) Friction factor for turbulent flow

In the range Re > 2300, λ_a is found using Figure 3.6 relating the friction factor to the Reynolds number or can be calculated as follows:

$$\lambda_a = \frac{1.325}{\left[In\left(\frac{\varepsilon}{3.7D} + \frac{5.74}{Re^{0.9}} \right) \right]^2} \qquad 3.8$$

(For $10^{-6} \leq \varepsilon/D \leq 10^{-2}$ and $5 \times 10^3 \leq Re \leq 10^8$)

Wypych and Pan (1991) modified Equations 3.3 and Equation 3.8 and proposed to replace the values of constants of Equation 3.8 by a number of coefficients (i.e., $x_1 \ldots x_5$), which could be determined by minimising the sum of squared errors of pressures at different points along the conveying line.

$$\lambda_a = \frac{x_1}{\left[In\left(\frac{\varepsilon}{3.7D} + \frac{x_2}{Re^{x_3}} \right) \right]^2} \qquad 3.9$$

$$f = \frac{x_4}{\mathrm{Re}^{x_5}} \qquad 3.10$$

Based on an empirical relationship, Klinzing et al. (1997) proposed the following equation to calculate the pressure drop in straight pipe for compressed air pipe works.

$$\Delta P_a = 1.6 \times 10^3 V^{1.85} \frac{L}{D^5 P_1} \qquad 3.11$$

where:

V is volumetric flow rate;

L is pipe length; and

P_1 is initial pressure.

To calculate the air-only pressure drop in the pipeline, Wypych and Arnold (1984) proposed the following empirical formula:

$$\Delta P_a = 0.5\left[\left(101^2 + 0.004567 M_a^{1.85} L D^{-5}\right) - 101\right] \qquad 3.12$$

where:

M_a is mass flow rate of air.

3.4.2.2 Pressure drop due to solids in straight inclined pipes

According to Pan and Wypych (1992), the pressure drop due to solids through a straight section of pipe can be considered as a function of many variables, such as superficial air velocity v_a, air density ρ_a, pipe diameter D, pipe length ΔL, air viscosity μ_a, pipe roughness ***e,*** mass flow rate of solid M_s, particle density ρ_s, mean particle diameter d_p, particle shape factor φ, friction coefficient between pipe wall and the particles. Inclination of conveying pipe also affects the pressure during gas-solid fluid flow (Mills, 2004). For a given product and pipe material, it can be assumed that d_p, v_s, ρ_s and the vertical displacement (Z) are constant. Although the possibility of the existence of a unique mathematical model to

determine the pressure drop component due to the presence of dispersed solid particles is very low because of the complex nature of two-phase gas-solid flow in pipes, many correlating equations have been proposed by various authors in different publications. When the friction factor of gas-solid mixture is considered, the total pressure drop for horizontal pipes as presented by Pan and Wypych (1992) can be presented as below:

$$\Delta P_s = \mathrm{m}^* \lambda_s \frac{\rho_s \Delta \mathrm{L} v_s^2}{2D} \qquad 3.13$$

λ_s is the frictional factor of solids. According to Pan and Wypych (1992), λ_s can be calculated, in horizontal pipes, as follows:

$$\lambda_s = 2\mathrm{k}\left(\frac{\pi}{4}\right)\mathrm{Re}\left(\frac{\varepsilon}{D}\right)\left(\frac{\Delta \mathrm{L}}{D}\right) \qquad 3.14$$

Since Equation 3.14 is applicable for horizontal pipes, Aziz and Klinzing (1990) proposed the frictional approach for the inclined sections and used the following equation to determine the friction factor λ_s:

$$\lambda_s = \frac{D}{2\mathrm{v}_s^2}\left[\frac{3C_D \varepsilon_s^{-4.7} \rho(\mathrm{v}_a - \mathrm{v}_s)^2}{4(\rho_s - \rho_a)d_p} - g\sin\theta\right] \qquad 3.15$$

where:

θ is the inclination of the suction pipe;

v_a is the average velocity of the flowing gas; and

v_s is the average velocity of solids in a pipe.

Hirota et al. (2002) carried out an experimental investigation on inclined conveying of solids in high-dense and low-velocity. They found a linear relationship between the Froude number (Fr) and the friction factor of the gas-solid mixture, which can be presented in the following form.

$$\lambda_s = 2(\sin\theta + C_1\mu_d \cos\theta)\frac{1}{\mathrm{Fr}} \qquad 3.16$$

where:

μ_d *is* the dynamic internal friction factor; and

C_1 is a constant and varies between 1 and 2 (1.5 is recommended).

Hirota et al. (2002) found that the pressure drop is maximum when pipe inclination angle is between 30°and 45°. Pneumatic pressure loss in incline pipes for dense phase was also investigated by Kano (1985). Figure 3.7 shows the basis for which his study was based. In the force pattern, a plug of length l_p slides successively on a stagnant bed of thickness h piled up at the bottom of an inclined pipe of thickness D .

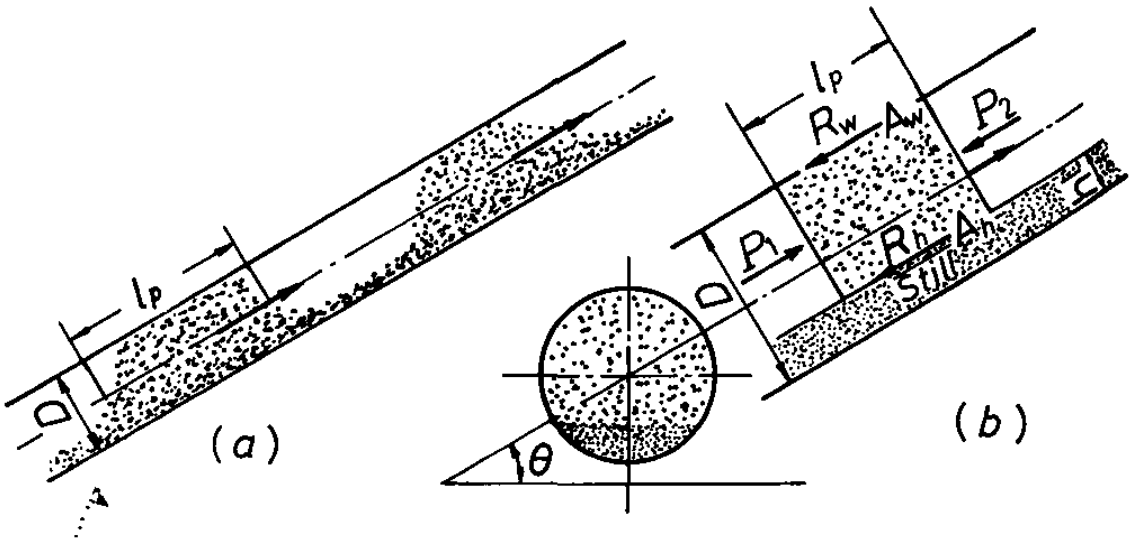

Figure 3.7: Schematic diagram of conveying in incline pipe (a) dense pneumatic condition (b) acting forces (Kano, 1985)

The pressure at the front and back side of the plug are p_1 and p_2 respectively and their difference $\Delta p_p = p_1 - p_2$. Kano (1985) assumed balance of the forces acting at the plug in the flow direction, the pressure difference and related to the component of gravity $M_p.g.\sin\theta$, the wall friction resistance R_w and the frictional resistance R_h at the surface of the retarded bed as follows:

$$\Delta p_p \zeta_p A = M_p g \sin\theta + R_w + R_h \qquad 3.17$$

where:

ζ_p is ratio of the cross sectional area of conveying plug to that of a pipe;

M_p is mass of plug; and

A is cross sectional area of pipe.

The above parameters are calculated as indicated below:

$$M_p = \zeta_p A l_p \ell_b \qquad 3.18$$

where:

ℓ_b is bulk density of the material in the plug.

$$R_w = \xi_w p_r A_w \qquad 3.19$$

where:

ξ_w is a factor of wall friction; and

p_r is a normal pressure to the pipe wall.

$$R_h = \xi_i \left(M_p g \cos\theta + p_r A_h \right) \qquad 3.20$$

where:

ξ_i is a factor of internal friction; and

A_h is the contact area between plug and retarder bed calculated as follows:

$$A_h = 2 l_p \sqrt{(2D - h)h} \qquad 3.21$$

Kano (1985) also determined the contact area A_w between the plug and the wall as:

$$A_w = \left(1 - \frac{\cos^{-1}\left(1 - \frac{2h}{D}\right)}{\pi}\right)\pi D l_p \qquad 3.22$$

Thus, the pressure loss over the entire plug as determined by Kano (1985) is:

$$\Delta p_p = \left[\ell_b g \sin\theta + \xi_w \frac{4p_r}{\zeta_p D}\left(1 - \frac{\cos^{-1}\left(1 - \frac{2h}{D}\right)}{\pi}\right) + \xi_i\left(\ell_b g \cos\theta + \frac{8p_r\sqrt{(2D-h)h}}{\zeta_p \pi D^2}\right)\right] l_p \qquad 3.23$$

As cited by Kano (1985), Ergun (1952) expressed Δp_p as:

$$\Delta p_p = \Delta p_k + \frac{\rho_a}{2}\left(u_a^2 - u_k^2\right) \qquad 3.24$$

where Δp_k denotes the permeating pressure drop in the plug and can be calculated as shown below:

$$\Delta p_k = \left(1.75 + \frac{1.50(1-\varepsilon)}{\mathrm{Re}}\right)\frac{\rho_a U}{d_s}\left(\frac{1-\varepsilon}{\varepsilon^3}\right) l_p \qquad 3.25$$

where ρ_a is the air density, and U and u_p is determined according to the equation below:

$$U = u_k - u_p = \frac{u_a}{\varepsilon} - u_p \qquad 3.26$$

where:

U is difference of permeating air velocity and plug velocity

And

$$\mathrm{Re} = \frac{U\rho_a d_s}{\mu} \qquad 3.27$$

where:

u_a is calculated mean air velocity, i.e., the quotient of the total air volume; divided by the cross-sectional area of the pipe;

u_k is permeating air velocity;

u_p is plug velocity; and

ε is porosity of the conveying material in the pipe.

If it is assumed that the length l_p and l_a of the plugs and the air cushions between the plugs, respectively, stay constant over the whole pipe length L, the total conveying pressure p_c in the pipe is determined as follows:

$$p_c = \Delta p_p \frac{L}{l_p + l_a} \qquad 3.28$$

where:

Δp_p is the conveying pressure related to a single plug.

3.5 Force balance in incline suction pipe

This Section provides an overview of force balance of solids in incline suction pipe during solid transport in pneumatic conveying system. The equations of fluid dynamics that are required have been well known for centuries and have been presented by many researchers (Dorricott and Jones, 1984; Biegaj, 2002; Jones, 1989). Figure 3.8 shows the principle on which these equations are based.

As shown in Figure 3.8, the movement of a particle in a fluid is subjected to two forces, i.e., gravitational force and drag force (Biegaj, 2002; Jones, 1989). Gravitational force is due to of the particle weight while drag force is the force that resists the movement of solid particles through a fluid. Drag force is made up of frictional forces and pressure forces. Therefore, for transport of solid particle into and along the pipe to take place, the suction pressure across the particle must exceed its weight:

$$F_w \sin(\alpha + \beta) < F_d \qquad 3.29$$

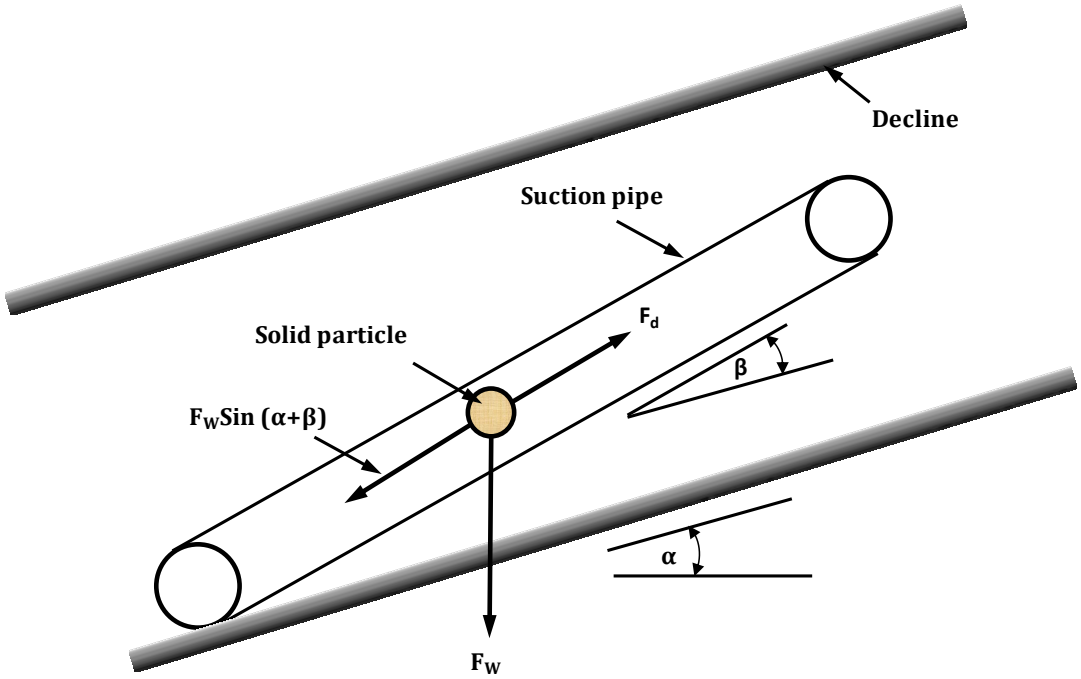

F_w = Gravitational force of rock particles
F_d = Drag force of rock particles
β = Inclination of suction pipe (degrees)
α = Decline gradient (degrees)

Figure 3.8: Forces on a rock particle

The gravitational force on a spherical particle as given by Terence (1997) is provided by Equation 3.30:

$$F_w = \frac{4}{3}\pi r^3 g \rho_s \qquad 3.30$$

where:

ρ_s is the density of solid; and

$\boldsymbol{g}$ is the acceleration due to gravity.

However, in laminar flow, i.e., fluid flow in which the fluid travels smoothly or in regular paths along a vertical tube, the particle is subjected to air resistance as indicated in Equation 3.31:

$$F_w = \frac{4}{3}\pi r^3 g(\rho_s - \rho_a) \qquad 3.31$$

where:

ρ_a is the density of air.

With inclined suction pipe, gravitational force is given as indicated in Equation 3.32:

$$F_w = \frac{4}{3}\pi r^3 g(\rho_s - \rho_a)\sin(\alpha + \beta) \qquad 3.32$$

Therefore, with inclined suction pipe the gravitational force on a spherical particle is given by Equation 3.33:

$$F_w = \frac{\pi d^3}{6}(\rho_s - \rho_a)g\sin(\alpha + \beta) \qquad 3.33$$

where:

d is the drag diameter (i.e., diameter of the cross-sectional area of the particle perpendicular to the direction of motion).

However, according to Terence (1997), the movement of solid particles in a stream gives rise to drag force, which acts in the opposite direction to motion. It comprises frictional forces and pressure forces and is given by Equation 3.34.

$$F_d = \frac{1}{2}C_D\rho_a v_s^2 A \qquad 3.34$$

where:

F_d is drag force on a particle;

C_D is the drag coefficient (for rough unstreamlined objects CD is 1 and for smooth objects it is much less (Terence, 1997));

v_s is the velocity of the rock particle in a suction pipe; and

A is particle projected area.

Many experiments have been carried out (Terence, 1997) to determine the relationship between settling velocity of particle and unique relationship

between drag coefficient and Reynolds number which reduces to the Stokes' equation at low Reynolds numbers.

Stokes' Law states that,

> *"if particles are falling in the viscous fluid by their own weight, then a terminal velocity is reached when drag force exactly balance the gravitational force."*

At high velocities, the drag increases above that predicted by Stokes' equations due to high turbulence and particles settle more slowly than the Law predicts (Terence, 1997). Therefore, in order for Stokes' Law to apply, solid particles must be small enough to have terminal velocities in laminar region. Thus, the terminal velocity of particles is found in Stokes' Law by equating drag and gravitational forces on the particle as given by Equation 3.35 for the case of flow through vertical pipes.

$$F_w = F_d \qquad 3.35$$

3.6 Minimum entry velocity consideration

Mills (2004) described entry velocity as the superficial velocity at the point where the material is fed into the pipeline. Because of the continuous expansion of the conveying gas over the conveying distance, the gas velocity at the start of the pipeline is the lowest gas velocity in the conveying system having a constant bore size. Thus, the entry velocity must be greater than the required minimum conveying velocity to ensure successful conveying of material. In a vacuum conveying system, it is approximately equal to the free air velocity, i.e., the superficial velocity of the air when evaluated at free air condition. Thus, to avoid pipeline blockages and to facilitate an efficient conveying without high particle degradation, an optimum value of the start gas velocity should be chosen at the entry section of the conveying line.

In vacuum conveying systems, the pickup velocity is defined as the air velocity required to cause solids initially at rest to be totally suspended by the air flow. From theory of pneumatic transport of solids, it is known that particles become suspended when the vertical component of turbulence (i.e., turbulent velocity fluctuation) is greater than the settling velocity of the particle in the fluid in the case of flow through vertical pipes. Considerable literature has been published by various authors (Dorricott and Jones, 1984; Biegaj, 2002; Jones, 1989) on the determination of minimum air velocity required to convey material in a pipe in gas-solid pneumatic transport system. According to Jones (1989), the minimum air velocity in the conveying pipeline must exceed the terminal velocity of the largest particle if choking is to be avoided. The terminal velocity for spherical particles in vertical pipes can therefore be obtained as follows:

$$v_{term} = \sqrt{\frac{4d(\rho_s - \rho_a)g}{3C_D\rho_a}} \qquad 3.36$$

where:

v_{term} is the terminal velocity of solid particles

Therefore, with inclined suction pipe Equation 3.36 can be written as follows:

$$v_{term} = \sqrt{\frac{4d(\rho_s - \rho_a)g\sin(\alpha+\beta)}{3C_D\rho_a}} \qquad 3.37$$

However, according to literature (Dorricott and Jones, 1984; Biegaj, 2002; Jones, 1989), the upward velocity of the air stream must exceed this value by a Design Factor (DF) for the largest particle to be transported satisfactorily:

$$v_t = DF\left[\sqrt{\frac{4d(\rho_s - \rho_a)g\sin(\alpha+\beta)}{3C_D\rho_a}}\right] \qquad 3.38$$

where:

DF is the design factor; and

v_t is the velocity of air stream at entry of the pipe.

For design purposes, it is unwise to have superficial velocities too near the critical velocity because of the danger of choking the system. Therefore, to avoid choking, Jones (1989) recommended a design factor of 1.5 – 2.0, although, at high velocities, high frictional losses prevail. As an example, when conveying rock fragments in shaft sinking, high air velocity in suction pipes, i.e., 150m/s – 200m/s gives rise to high frictional losses (Jones, 1989). Since the rock particles are non-spherical and will be in turbulent flow, the difficulty arises in which particles will fall in random orientation in the laminar flow region. However, according to Terence (1997), particles will orientate themselves to give maximum resistance to drag in the turbulent region. Therefore, the velocity of air stream as given by Holland (1973) is calculated from Equation 3.39:

$$v_t = DF\left[\sqrt{\frac{4\varphi d(\rho_s - \rho_a) g \sin(\alpha + \beta)}{3 C_D \rho_a}}\right] \qquad 3.39$$

where:

φ is factor of smoothness and varies from 0.5 – 1, where 0.5 is very rough material and 1.0 is perfectly smooth material (Alwyn, 1991).

3.7 Effects of material physical characteristics

The characterization of the material to be conveyed plays a very large part in the selection of the velocity regime. The conveying velocity and hence air flow rate is greatly influenced by material characteristics. Particle size distribution, hardness and particle density, all have an effect on minimum conveying velocity, pressure drop, air flow, etc. Properties such as moisture content, cohesiveness and adhesiveness may cause flow problems during conveyance. This Section highlights the effects of material physical characteristics on the conveying system.

(a) Particle size distribution

Particle size distribution for a product can be readily measured by various means and is considered to be one of the most important material properties in relation to dense phase conveying. In conventional systems, materials with a wide size distribution are generally more problematic than fine powders such as cement or pulverized fuel ash. Also the natural force of attraction increases with the decreasing particle size. Mean, volume, surface and Stokes diameters are a few of the commonly used terms to define the particle size.

(b) Particle shape

The particle shape is a more difficult parameter to measure, but a qualitative assessment of the particle shapes of a material can often be made. It is evident, however, that particle shape distribution has to be considered in conjunction with particle size distribution. Usually, the shape of the constituent particles in a bulk solid is an important characteristic as it has a significant influence on their packing and flowing behaviour. Highly irregular-shaped and fibrous particles can interlock, thereby, increasing the resistance of a bulk solid to flow.

(c) Hardness

Particle hardness, like shape and size, has a superficially obvious effect on wear rate of a pipeline. Thus, it is important to take it into account when a pneumatic conveying installation is being designed to avoid undue erosive wear of the system components.

(d) Density of particles

The density of particles in gas-solid pneumatic conveying systems is also an important parameter to be considered. Like hardness, the density of the particle will have effects on wear rate of the suction pipe. In pneumatic conveying, many different kinds of materials can be transported. The properties of these materials

are different from one to another but the materials can be classified in a few groups. Geldart's work (Geldart, 1973), which has been used as a base for many other experiments, is worthwhile to take into account. Based on experimental evidence, Geldart found that most products, when fluidised by a gas, are likely to behave in a manner similar to one of four recognisable groups and these groups of materials can be represented graphically as shown in Figure 3.9.

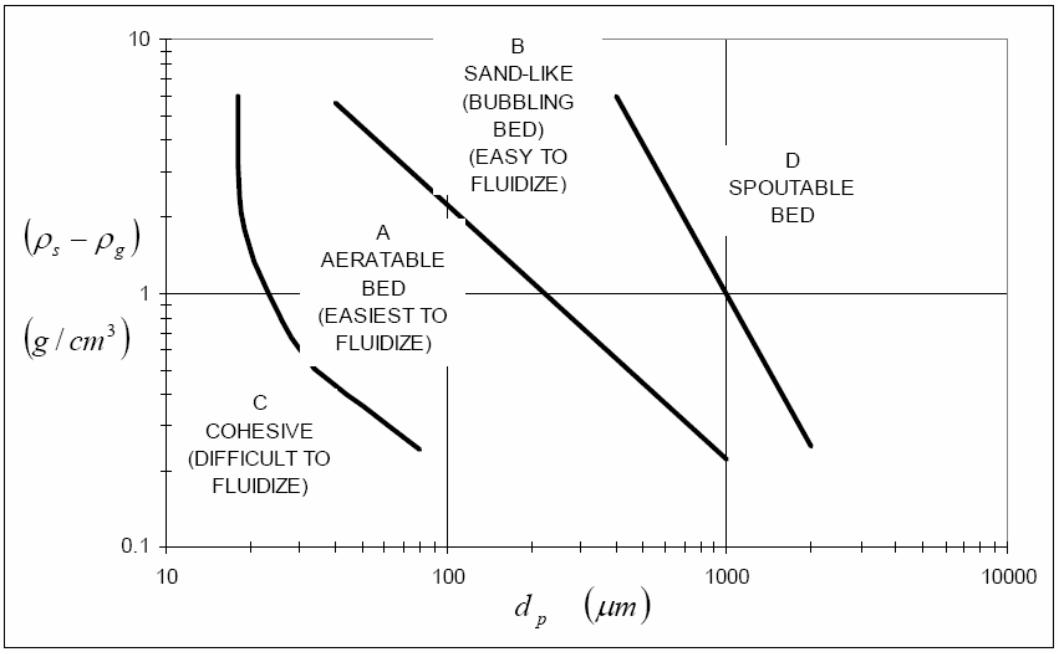

Figure 3.9: Geldart's classification of materials (Geldart, 1973)

Geldart found that materials can be classified by four characterized groups (called Groups **A**, **B**, **C**, and **D**) by the size and density difference between particle and gas. Each material group has its own characteristic property as follows:

(i) **Group A**: Powders, ideal for fluidization, the non-bubbling fluidization occurs at the minimum fluidization gas velocity and bubbling occurs as fluidization gas velocity increases.

(ii) **Group B**: Start bubbling at minimum fluidization velocity.

(iii) **Group C**: Very fine and cohesive material, very hard to be fluidized.

(iv) **Group D**: Coarse solids.

3.8 Gas-solid separation

Transportation of solids is terminated in the gas-solid separation zone. In gas-solid separation zone, the solids are separated from the gas stream in which they have been conveyed. Particles in this zone are decelerated and are separated from the gas stream by means of a cyclone. Therefore, the separation unit is critical in gas-solid phase and should receive attention in pneumatic conveying system. According to Klinzing et al. (1997), the gas solid separation unit can have profound influence on the performance of a pneumatic system. The selection of adequate gas-solid separation system depends on a number of factors, the most important being the size of solids requiring to be separated.

3.9 Pneumatic conveying power requirement

Pneumatic conveying power requirement is also critical in ensuring smooth flow of material in the suction pipe. The power consumption of the prime mover is the rate at which work is done to convey rock fragments through the suction pipe over a vertical distance. Therefore, the amount of work done by the prime mover is the product of the weight of material moved and the vertical distance through which it is moved (Sharp, 1988). According to Kano (1985), the power requirement for pneumatic conveying system E_c is calculated as indicated in Equation 3.40:

$$E_c = \frac{Q\Delta p}{60\times 1000\eta} \qquad 3.40$$

where:

E_c is power required by the pneumatic conveying system;

Q is the air conveying rate;

Δp is pressure loss in all pneumatic lines of the system; and

η is total efficiency of blower (usually in the range 0.6 – 0.75).

3.10 Summary

Literature review indicates that pneumatic (vacuum) conveying of solids is possible in mines. However, many factors such as pressure loss and minimum transport velocity in the suction pipe and material characteristics must be considered during the design of the pneumatic conveying system. It is also important that the mode of pneumatic conveyance, i.e., whether dense-phase or dilute phase is considered during the design process. Selection of the pump to give the required negative pressure is also critical in smooth conveyance of the solids in the pipeline. The type of pump selected will determine the efficiency of the pneumatic conveyance system. Since pneumatic conveying is generally suited to the conveyance of fine and lighter particles, it has a limitation in terms of productivity when larger and denser particles are being conveyed, i.e., it gives low productivity for larger particles. Therefore, it is necessary to set up a pilot plant, where the performance in terms of productivity of the pneumatic system is determined. In Chapter 4, pneumatic loading system that uses the monorail technology is developed based on the reviewed literature.

Chapter 4

4.0 Design of monorail pneumatic loading system and surface infrastructure

4.1 Introduction

Transportation of broken rock in mines is often discontinuous involving the use of expensive equipment, which takes up considerable space and injects pollutants into the air stream. In Chapter 2, the literature review revealed that a continuous monorail loading system could become fundamental in improving advance rates in decline development. According to the literature, to improve advance rates in decline development, the monorail should be loaded by some continuous loading system that quickly removes blasted rock fragments from the development face and onto the monorail containers. In Chapter 3, extensive literature has been reviewed on pneumatic conveying theory which is used in the design of monorail pneumatic loading system. This Chapter focuses on the design of monorail loading system that uses pneumatic (vacuum) conveying principles to suck broken rocks from the decline face into the hopper via a suction pipe. Pneumatic transport systems are increasingly being used in a wide variety of industries and their wider use in the mining industry could lead to more efficient and cost effective rock loading system and better ventilated mines. Surface ore and waste handling infrastructure are also described in this Chapter.

4.2 Structure of the conceptual monorail loading system

Figure 4.1 shows the structure and configuration of the conceptual monorail loading system. The loading system consists of an incline suction pipe that is

connected to the storage hopper. Rock fragments from the development face are sucked into the hopper through the incline suction pipe. The high pressure fan connected to the storage hopper creates negative pressure inside the hopper that enables transport of blasted material from the development face into the hopper to take place.

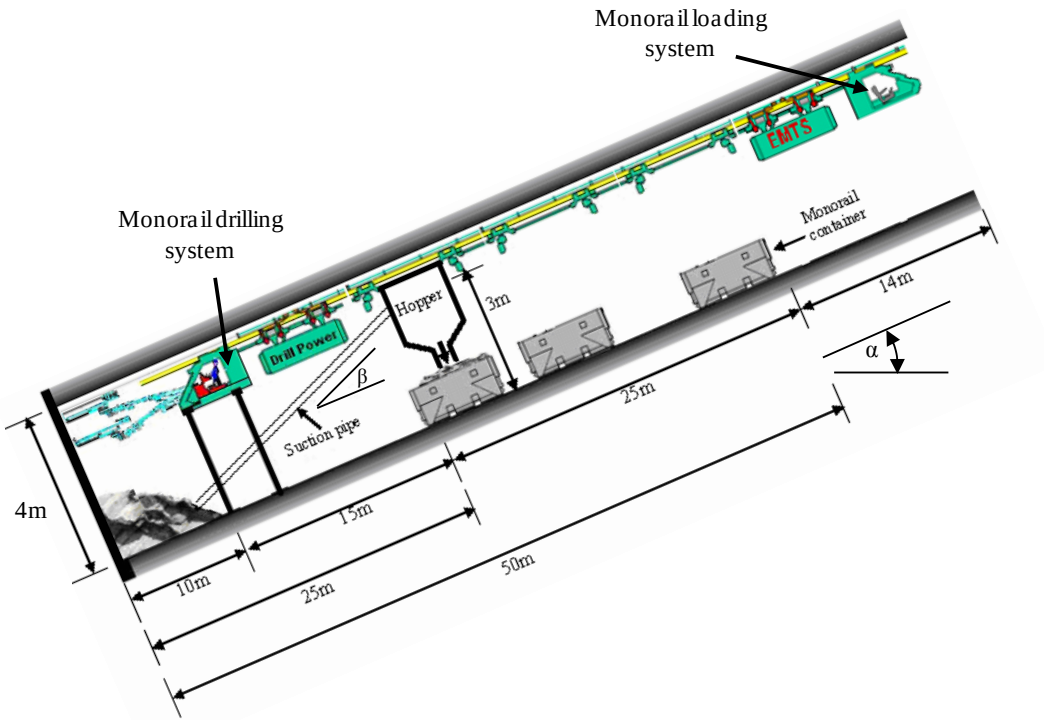

β is inclination of suction pipe from the decline floor to hopper; α is the decline gradient

Figure 4.1: Structure and configuration of the conceptual monorail loading system.

The loading process is such that, once the hopper is full, the suction pipe is disconnected from the hopper. The hopper will have a mechanism that allows connecting and disconnecting of the suction pipe. When the suction pipe is disconnected, the hopper is connected to the monorail train, which pulls the loaded hopper to the position of an empty container, where automatic discharge of material takes place (Figure 4.2). In order to facilitate this, the monorail train will also have a mechanism that allows coupling and uncoupling of the hopper. Once the material is discharged, the empty hopper is pushed by the monorail train back to the loading position, where the suction pipe is reconnected to the hopper to restart the loading process.

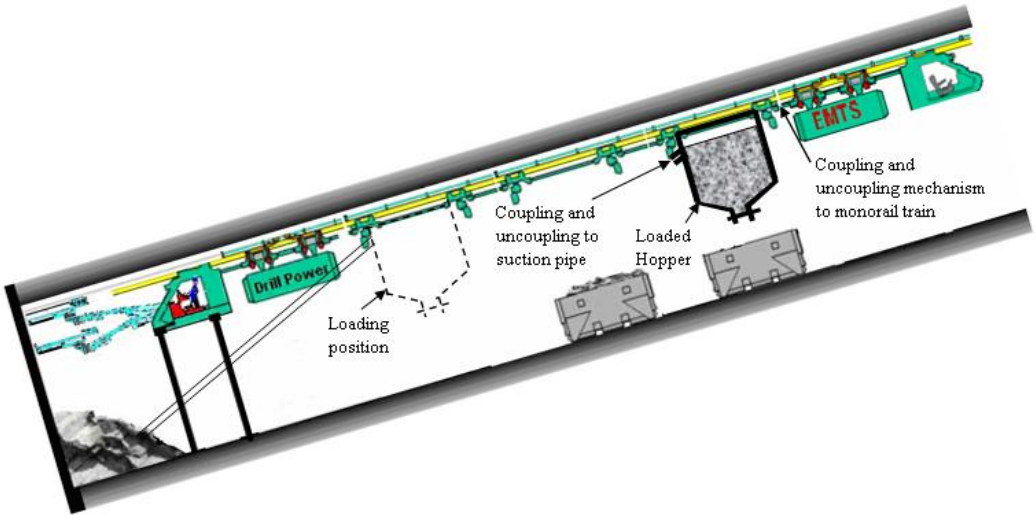

Figure 4.2: Coupling and uncoupling mechanism

According to Scharf (2007), the dead weight of each monorail container is 1 tonne and the maximum payload per container is 4 tonnes. Therefore, in this study, the storage hopper is designed with a capacity of 4 tonnes. This is in order to allow material from the hopper to be loaded in each monorail container in one pass.

4.3 Design of monorail loading system

As highlighted by Mills (2004), design of any pneumatic conveying system for a new application is always difficult due to lack of sufficient knowledge and published data. Determination of parameters such as type of solids to be transported, pipe diameter, length and fittings need a pilot plant test or a full-length test. This is in order to determine accurately the design parameters such as what conveying speed should be used, and at what loading rate. Data must be available to accurately predict pressure drop along the pipe. With the pressure drop known, one can then size the air pump and determine its horsepower. However, without the above information, it is difficult to accurately design the new system. Therefore, due to absence of the pilot test, only theory is used in this study to design the monorail pneumatic loading system. This means that where information is lacking assumptions have been made, which may affect the results obtained.

4.3.1 Design purpose and method

The purpose of the monorail loading system is to load blasted rock fragments from the decline development face into the hopper and subsequently into monorail containers. The system will load 25m from the development face while the suction pipe is connected to the hopper 3m from decline floor giving a pipe inclination from the decline floor of 6.84^0 (calculated using trigonometry). A decline gradient of 20^0 is adopted since it is the gradient at which decline access is developed during mine design case study. At this gradient, the total pipe inclination from the horizontal will be 26.8^0. This means also that material will be conveyed from the development face into the hopper a vertical distance of 11.4m (see also Section 4.7.2.1). In designing the monorail loading system, a model was created in an Excel spreadsheet in which the relationship between theoretical suction principle equations presented in Chapter 3 and the loading parameters were studied. The sensitivity of each loading parameter on the performance of the loading system was examined using this model.

4.3.2 Suction pipe and material conveying characteristics

According to research on units used in suction of broken rocks in shaft sinking (Jones, 1989), the ideal average diameter of suction pipes used varies from 203mm - 258mm. In this study, a suction pipe diameter of 220mm is adopted, because this pipe size will allow most of the blasted rock fragments from the face to pass without choking the pipe and it is also anticipated that the pipe size will be easier to handle during the suction process. However, larger size rock fragments, i.e., those that cannot pass through the suction pipe, will be reduced in size using various methods (see Section 4.5.4.3). During the analysis, material density is varied from $2400kg/m^3$ – $3000kg/m^3$ while the size of rock fragments (i.e., particle diameter) is varied from 50mm to 200mm. It is also assumed that a total of 4 tonnes is loaded in each monorail container, which is the maximum payload per monorail container. Therefore, in this study, the loading time of the monorail loading system refers to loading 4 tonnes of blasted material into the hopper.

4.3.3 Mode of solid conveying

Jones (1989) found that dilute phase systems are the most common applicable method of broken rock conveyance in mines. These methods are comparatively cheap to install and operate although they have relatively low productivity. In this study, a dilute phase method is adopted during the design of the monorail pneumatic loading system. This is because the method is proven and works well in suction of broken rock, such as, in shaft sinking.

4.3.4 Solid loading ratio (m*)

Since dilute phase mode of conveyance has been adopted as the mode of solid conveyance during the design of the loading system, solid loading ratio (**m***) of the system should not be more than 50. To avoid choking the suction pipe a voidage of 0.7 was used.

4.3.5 Transport velocity

Though a considerable number of research works has been carried out in the field of pneumatic conveying, currently there is no general procedure to predict the minimum conveying velocity. Since this study is theoretical, the transport velocity used was based on results of some experimental work, which give good correlations with the theory (Jones, 1989). According to Jones (1989), the conveying air velocity in suction pipes used in shaft sinking maybe as high as 150 m/s - 200m/s (i.e., for vertical distance of 100m<) although this velocity results in high frictional losses.

Determining the terminal velocity of the largest particle (i.e., 200mm) in the suction pipe using Equation 3.39, with solid loading ratio of 50 and voidage of 0.7, the largest particle (i.e., with maximum density of 3000kg/m^3) will only be suspended in the suction pipe at velocity of 66.4m/s. Therefore, for the largest particle to be transported as well as to avoid choking, the upward velocity of the conveying air should be higher than the terminal velocity of the largest particle

in the suction pipe, i.e., should be larger than 66.4m/s. Using 1.5 as design factor of safety as recommended by Jones (1989), the minimum upward conveying air velocity was determined as 100m/s. This air velocity is used as minimum conveying air velocity in the model with maximum being 300m/s. However, since the maximum negative pressure cannot exceed 60kPa (0.6 bars), the range of conveying air velocities at maximum negative pressure for different sizes of rock fragments and density is determined during the study.

4.3.6 Mass flow rate of air

To determine the mass flow rate of air through the conveying line, the minimum conveying air velocity of 100m/s and pipe diameter of 220mm (as discussed in Section 4.3.5) are used. Using the relationships shown in Equation 4.1 and 4.2 (assuming incompressible flow), the mass flow rate of air in the suction pipe at different air velocities was determined. Figure 4.3 shows mass flow rate of air at different air velocities.

$$Q_a = A.v_a \qquad 4.1$$

where:

Q_a is the volume flow rate of air;

A is the cross-section area of suction pipe; and

v_a is the conveying air velocity.

$$M_a = Q_a.\rho_a \qquad 4.2$$

where:

M_a is the mass flow rate of air; and

ρ_a is the density of air (1.2kg/m^3) and was assumed constant.

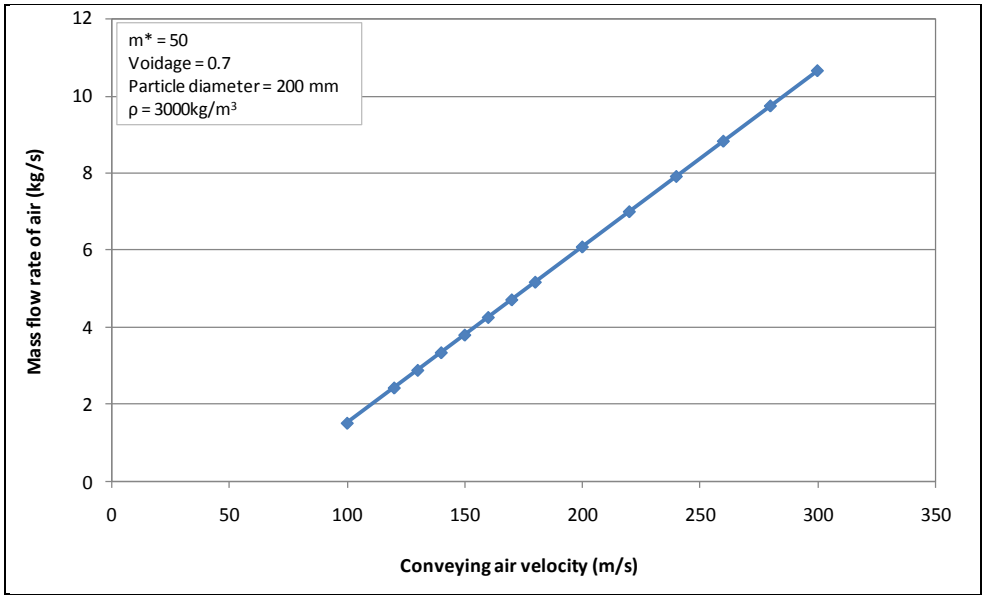

Figure 4.3: Mass flow rate of air at different conveying air velocities

Figure 4.3 shows that conveying air velocity is directly proportional to the mass flow rate of air in the suction pipe, i.e., as air velocity increases, the mass flow rate of air in the suction pipe also increases linearly.

4.3.7 Mass flow rate of solids

Since the mass flow rate of air ($\mathbf{M_a}$) and solid loading ratio (**m***) are known, the mass flow rate of solids in the suction pipe can be determined using the relationship in Equation 4.3:

$$m^* = \frac{M_s}{M_a} \qquad 4.3$$

where:

$\mathbf{M_s}$ is the mass flow rate of solids in the suction pipe;

$\mathbf{M_a}$ is the mass flow rate of air in the suction pipe; and

m* is the solid loading ratio.

Determining $\mathbf{M_s}$ as a function of **m***, **A**, $\mathbf{V_a}$ and $\boldsymbol{\rho_a}$ by combining Equations 4.1, 4.2 and 4.3 gives the following:

$$M_s = m^* A.v_a \rho_a \qquad 4.4$$

Figure 4.4 shows the relationship between mass flow rate of solids ($\mathbf{M_s}$) at different conveying air velocities for different solid loading ratios (m*) in the suction pipe. The cross-section area of suction pipe (A) and the density of air ($\boldsymbol{\rho_a}$) were held constant.

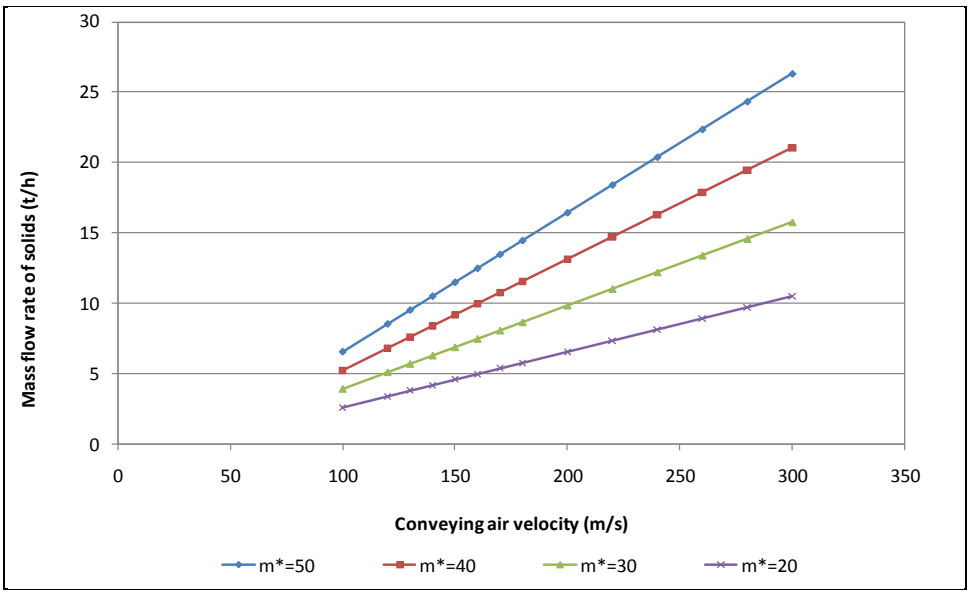

Figure 4.4: Mass flow rate of solids at different conveying air velocities and solid loading ratios

As shown in Figure 4.4, the mass flow rate of solids in the suction pipe increases with increase in conveying air velocity. This is due to the fact that with increase in conveying air velocity, the volume flow rate of air in the suction pipe also increases, thereby, increasing the mass flow rate of air in the pipe. At constant solid loading ratio, this increase in mass flow rate of air would result in an increase in the mass flow rate of solids in the pipe. Figure 4.4 also reveals that as the solid loading ratio increases, the more solids will be transported in the suction pipe resulting in higher tonnage.

4.3.8 Superficial velocity of solids in the suction pipe

To estimate the superficial velocity of solids in the suction pipe, Equation 4.5 as proposed by Dorricott and Jones (1984) is used. Figure 4.5 shows the superficial velocity profile of solid phase at different conveying air velocities in the suction pipe according to the density of the material being conveyed with m*, A, D and $\boldsymbol{\rho_a}$ held constant.

$$v_s = \frac{4M_s}{\pi D^2 \rho_s} = \frac{4m^* A.v_a \rho_a}{\pi D^2 \rho_s} \qquad 4.5$$

where:

$\mathbf{v_s}$ is the superficial velocity of solids in the pipe; and

D is the diameter of suction pipe.

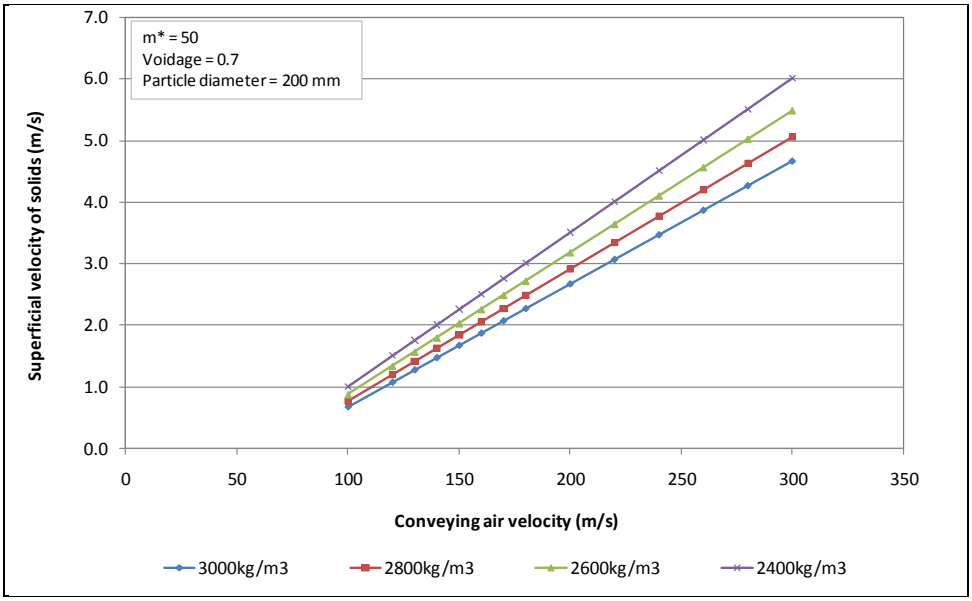

Figure 4.5: Superficial velocity profile of solids in the suction pipe for different conveying air velocities and material densities

Figure 4.5 indicates that superficial velocity of solids in the suction pipe is directly proportional to the conveying air velocity and also to the density of the material being transported. Thus, as the conveying air velocity increases, superficial velocity of solids in the suction pipe also increases. Results also show

that particles with higher density have less superficial velocity as compared to particles with smaller density.

4.3.9 Pressure drop in incline suction pipe

The pressure drop prediction in incline suction pipe of the monorail pneumatic conveying system is divided into three zones: acceleration, conveying and separation zones. However, since this study is theoretical and due to the difficult nature of predicting pressure loss in the separation zone, only the pressure losses in acceleration and conveying zones are determined. Equation 4.6 is used to determine the total pressure loss of the system during material conveyance:

$$\Delta p_t = \Delta p_{acc} + \Delta p_{sts} \qquad 4.6$$

where:

Δp_t is total pressure loss in the suction pipe;

Δp_{acc} is pressure loss in acceleration zone; and

Δp_{sts} is pressure loss in steady state zone (conveying zone).

4.3.9.1 Pressure loss in acceleration zone

The solids to be transported by the monorail conveying system are initially at rest and at atmospheric pressure. However, as the rock fragments are accelerated from rest to some average conveying velocity, a rapid change in momentum takes place with associated high pressure loss. To determine the pressure loss in the acceleration zone, Equation 4.7 as recommended by Ottjes et al. (1976) is used, with m*, A, D, v_s and $\boldsymbol{\rho_a}$ held constant. Results of the pressure loss determination in an acceleration zone for materials of different density are shown in Figure 4.6 and Figure 4.7.

$$\Delta p_{acc} = \frac{4M_s v_s}{\pi D^2} = \frac{4m^* A.v_a \rho_a v_s}{\pi D^2} \qquad 4.7$$

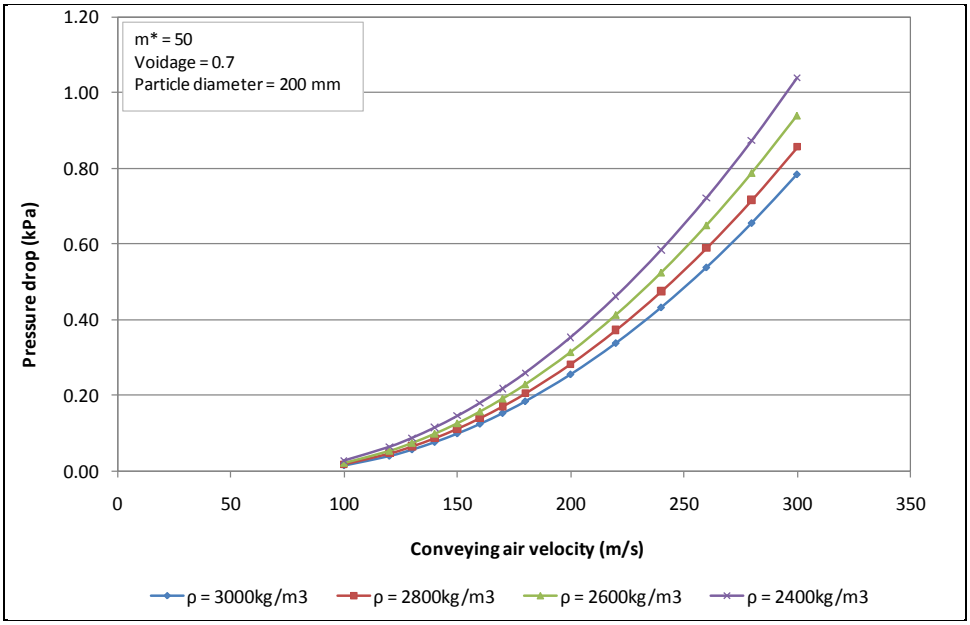

Figure 4.6: Pressure loss in acceleration zone for 200mm size rock particle of different densities

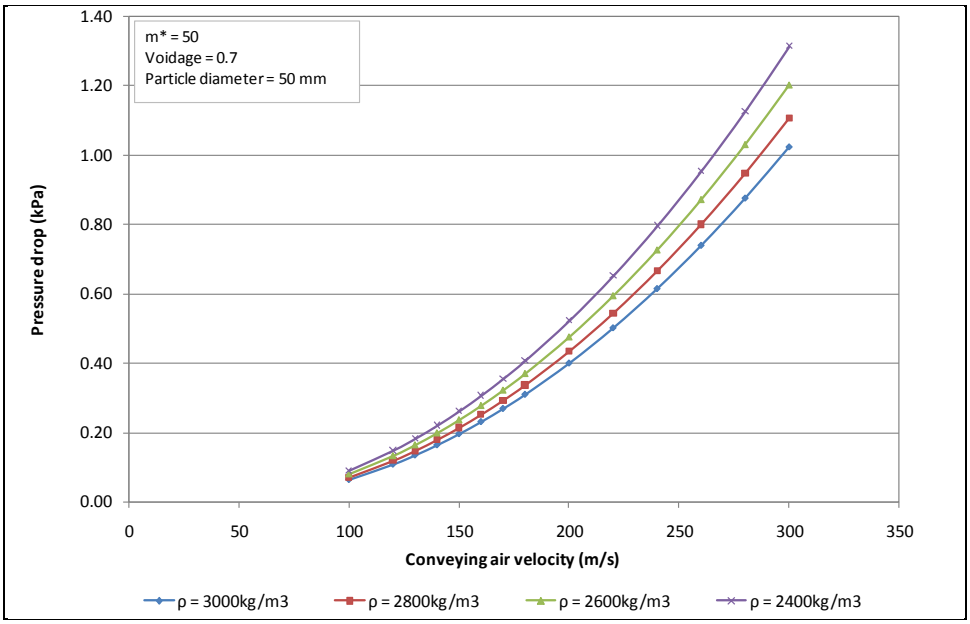

Figure 4.7: Pressure loss in acceleration zone for 50mm size rock particle of different densities

Figure 4.6 and Figure 4.7 show that as the conveying air velocity increases, the pressure loss in the acceleration zone also increases. Results also reveal that the pressure drop in the acceleration zone increases with decrease in particle

density. This is as a result of high superficial velocity of smaller particles compared to larger particles in the suction pipe.

4.3.9.2 Pressure drop in steady state zone

Pressure drop in steady state zone is determined using the Darcy equation (Equation 3.13). To avoid choking in the suction pipe, a voidage of 0.7 with drag coefficient of 1 are used. Since the suction pipe for the loading system is inclined, Equation 3.15, as suggested by Aziz and Klinzing (1990), is used to determine the friction factor (λ_s). In Figure 4.8 and Figure 4.9, the pressure drop per unit length of conveying pipe is shown as a function of the conveying air velocity in steady state zone. The maximum achievable negative pressure of 60kPa (0.6 bars) is also indicated in the two figures.

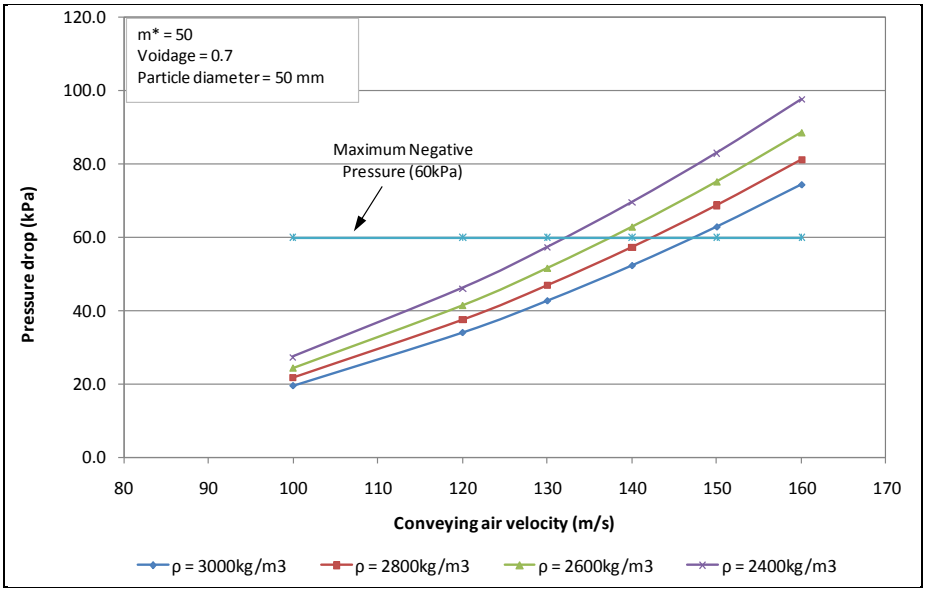

Figure 4.8: Pressure loss in steady state zone for material with 50mm particle diameter

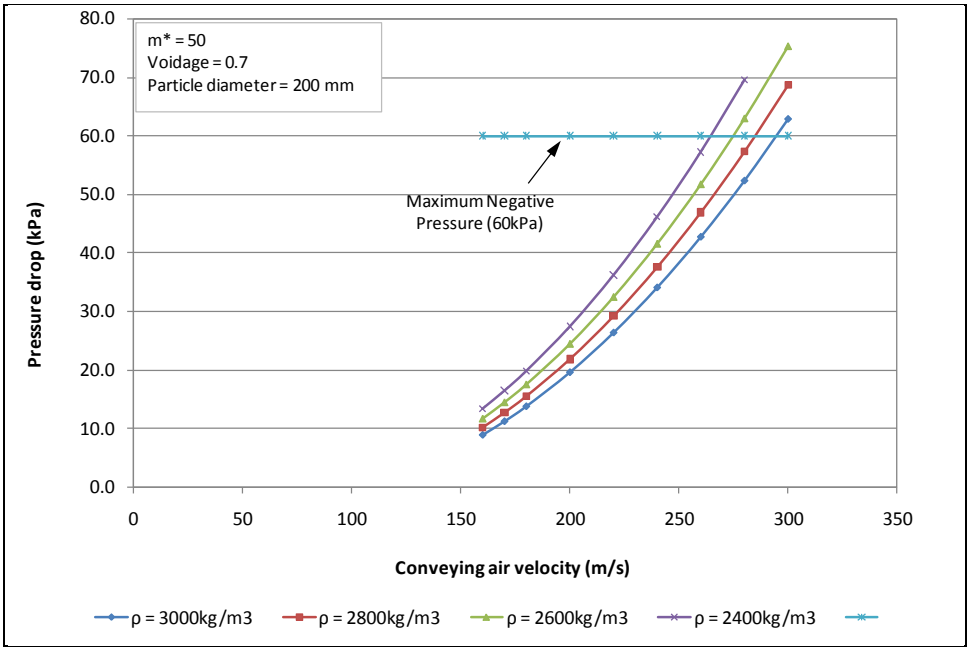

Figure 4.9: Pressure loss in steady state zone for material with 200mm particle diameter

4.4 Effects of particle size on design parameters

4.4.1 Effects of particle size on conveying velocity

Fragmentation (particle size) is the rock breakage carried out to fragment masses of rock. It attempts to break rocks into manageable sizes by chemical energy in blasting (Hartman, 2002). It should be recognized that particle size being conveyed (sucked) has strong effects on the productivity of the pneumatic loading system. Additionally, the size of particles being sucked by the system at maximum negative pressure will have an effect on the required conveying air velocity. In view of this, the effects of particle size on the required conveying air velocity at maximum negative pressure was evaluated using the model. The result of the evaluation is shown in Figure 4.10 and Figure 4.11.

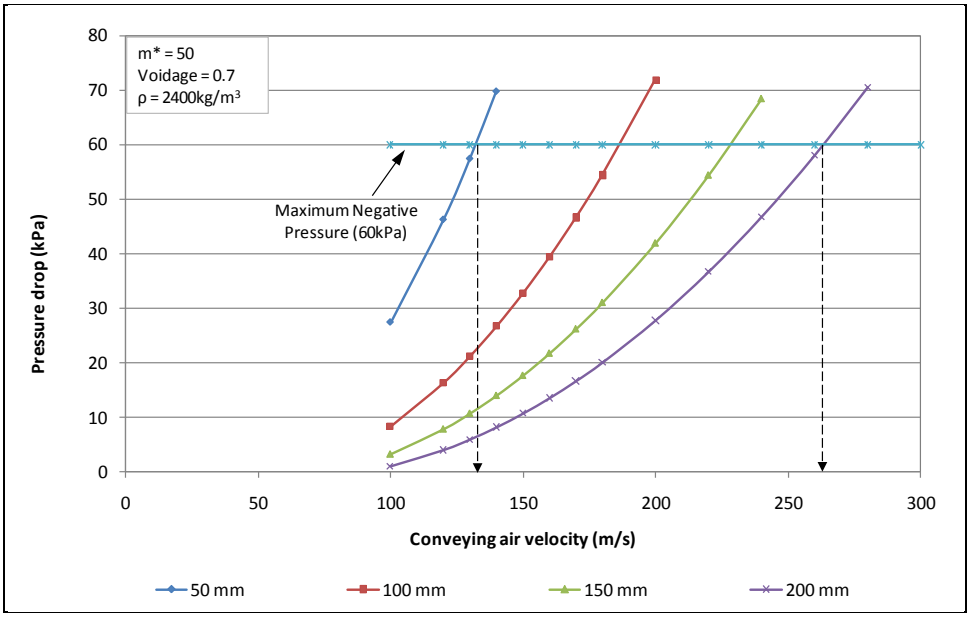

Figure 4.10: Effects of particle size on the required conveying air velocity for material with density 2400kg/m^3

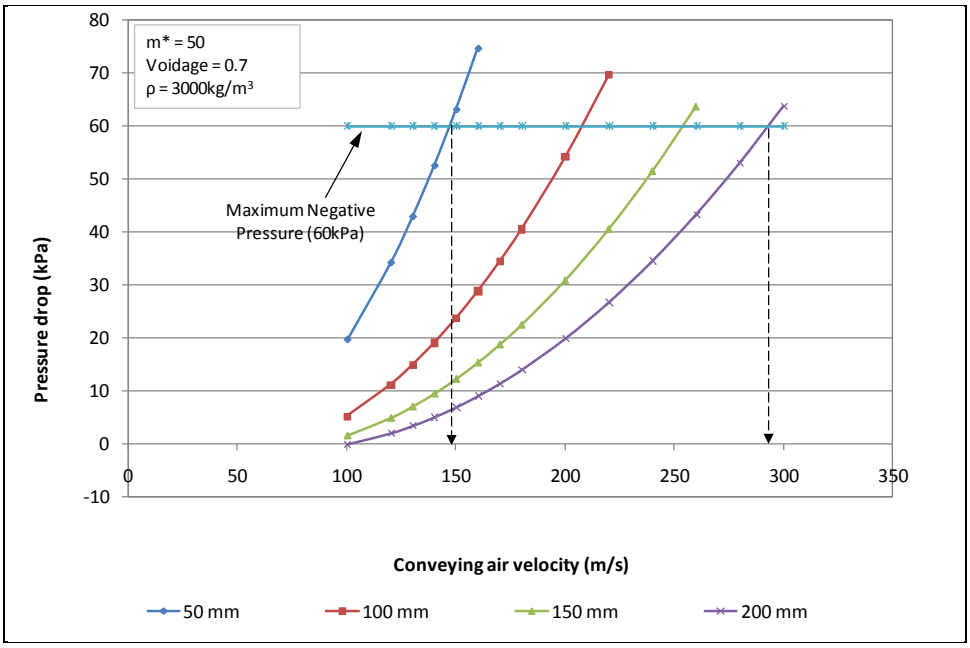

Figure 4.11: Effects of particle size on the required conveying air velocity for material with density 3000kg/m^3

Figure 4.10 and Figure 4.11 reveal that the required conveying air velocity for particles with smaller size at maximum negative pressure is lower than that for larger particles. According to Figure 4.10 (for material with density 2400kg/m^3), at maximum negative pressure, the conveying air velocity of the system varies

from 132m/s (for 50mm particle size) to 263m/s (for 200mm particle size). For material with density 3000kg/m^3 (Figure 4.11), the conveying velocity varies from 147m/s to 293m/s for 50mm and 200mm size particles, respectively. Results also indicate that the pressure drop of the system increases as the size of rock fragments reduces (satisfying the Darcy's equation). The increase in pressure drop for smaller particle size is attributed to the fact that as the particle size reduces, its mass also reduces, thereby, increasing the transport or superficial velocity of the particle in the suction pipe.

4.4.2 Effects of particle size on mass flow rate of solids

The effects of particle size on mass flow rate of solids of the pneumatic loading system at maximum negative pressure were also studied. Figure 4.12 and Figure 4.13 show the results obtained.

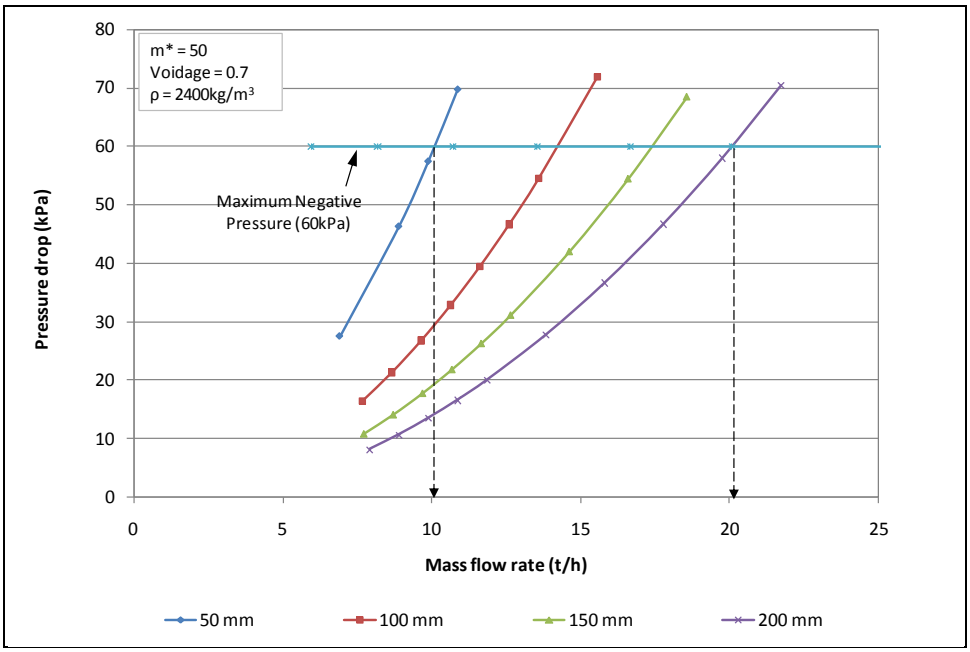

Figure 4.12: Effects of particle size on mass flow rate of solids for material with density 2400kg/m^3

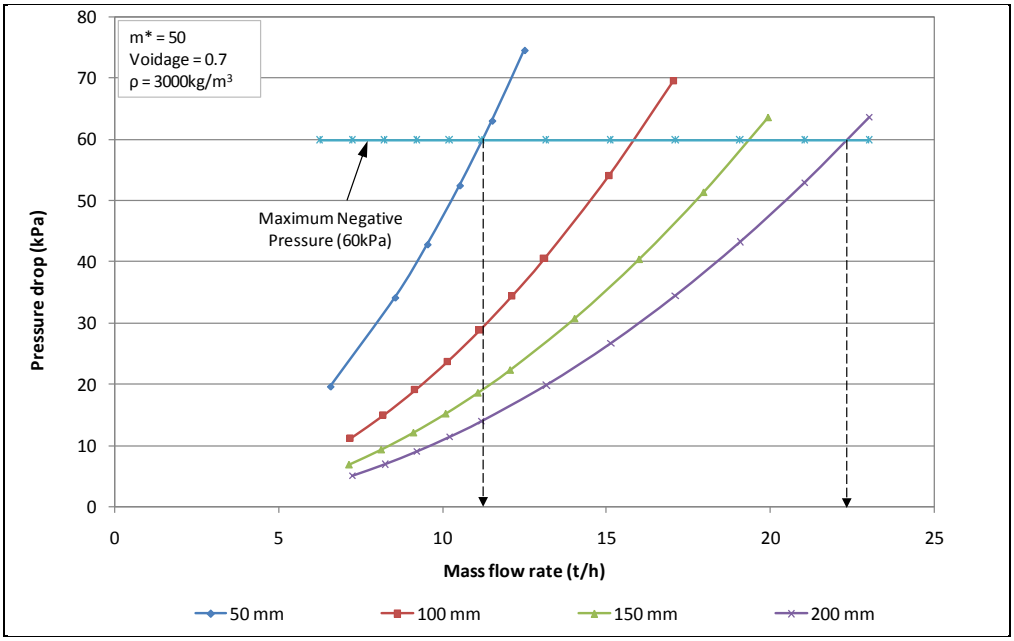

Figure 4.13: Effects of particle size on mass flow rate of solids for material with density 3000kg/m^3

According to the results shown in Figures 4.12 and 4.13, at maximum negative pressure, rock fragments with 50mm particle diameter result in lower mass flow rate than particles with size 200mm. From Figure 4.12 (rock density 2400kg/m^3), it is clear that particles with 50mm size result in mass flow rate of 10t/h while rock fragments with size 200mm gives 20t/h. Similarly, particles with density 3000kg/m^3 result in mass flow rate of 11t/h (for 50mm size particles) and 23t/h (for 200mm size particles). The larger mass flow rate due to larger particle size is attributed to the fact that at maximum negative pressure, larger particles require larger conveying air velocity than smaller particles.

4.4.3 Effects of particle size on power consumption

The power input to a pneumatic conveying system is through the air supply. Therefore, the power of the system is a function of air flow rate and pressure drop of the system. Equation 3.40 is used to determine the power consumption of the pneumatic conveying system. Figures 4.14 and 4.15 show the results obtained.

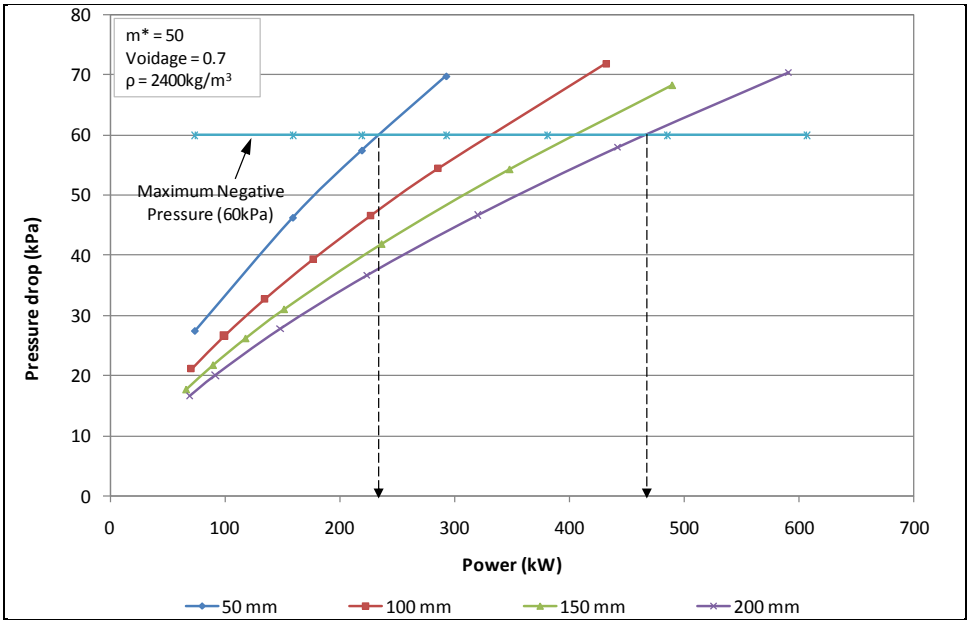

Figure 4.14: Effects of particle size on power consumption for material with density 2400kg/m^3

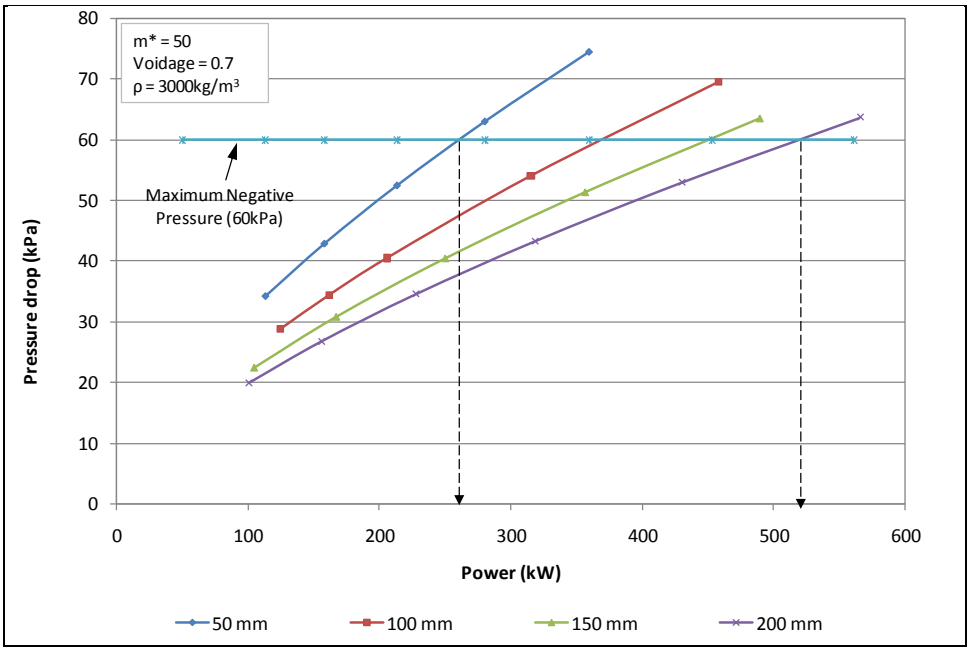

Figure 4.15: Effects of particle size on power consumption for material with density 3000kg/m^3

According to Figure 4.14 and Figure 4.15, the power required by the loading system increases in proportion to the density and size of rock fragment being conveyed. At maximum negative pressure, rock particles (with density

2400kg/m^3 and 3000kg/m^3) with smaller diameter (i.e., 50mm) result in smaller power consumption than larger particles (i.e., 200mm). As can be seen from Figure 4.14 (ρ= 2400kg/m^3), at maximum negative pressure, the power varies from approximately 220kW to 460kW for 50mm and 200mm particle size, respectively. Similarly, for rock fragments with density 3000kg/m^3, power varies from approximately 270kW to 540kW for 50mm and 200mm rock particles respectively. The increase in power is attributed to the high conveying air velocity required to transport larger and denser particles as compared to lighter and smaller particles.

4.5 Optimum design parameters for the pneumatic loading system

This Section presents optimum design parameters for the pneumatic loading system. Optimum parameters in this study are defined as the parameters that will enable the loading system achieve maximum productivity during suction process.

4.5.1 Optimum mass flow rate of solids

As shown in Figure 4.12 and Figure 4.13, the mass flow rate of solids in the suction pipe of the loading system depends on the conveying air velocity at maximum negative pressure, the density of rock fragments and also on rock fragmentation. Studies show that the optimum mass flow rate of solids in the suction pipe at maximum negative pressure would vary from 10t/h to 23t/h depending on the rock density and rock fragmentation. Table 4.1 summarises the optimum mass flow rate of the pneumatic loading system at maximum negative pressure for different sizes of rock fragments and conveying air velocity.

Table 4.1: Optimum mass flow rate of solids at maximum negative pressure

Air Vel. (m/s)	Density of rock fragments (kg/m³)	Particle size (mm)	Max. Negative Pressure (kPa)	Mass flow rate (t/h)
132.0	2400	50	60	10.0
147.0	3000	50	60	11.2
263.0	2400	200	60	20.0
293.0	3000	200	60	23.0

4.5.2 Optimum power consumption

In Section 4.4.3, the effects of rock density as well as rock fragmentation on system power consumption was discussed. According to the results, at maximum negative pressure, the optimum power would vary from 220kW to 540kW depending on the density and particle size of the rock fragments being conveyed.

4.5.3 Optimum loading time

In this study, the loading time refers to loading 4 tonnes of rock fragments from the development face into the hopper via the suction pipe. Figure 4.16 and Figure 4.17 show the optimum loading time of the pneumatic loading system at maximum negative pressure for different rock fragments and rock density.

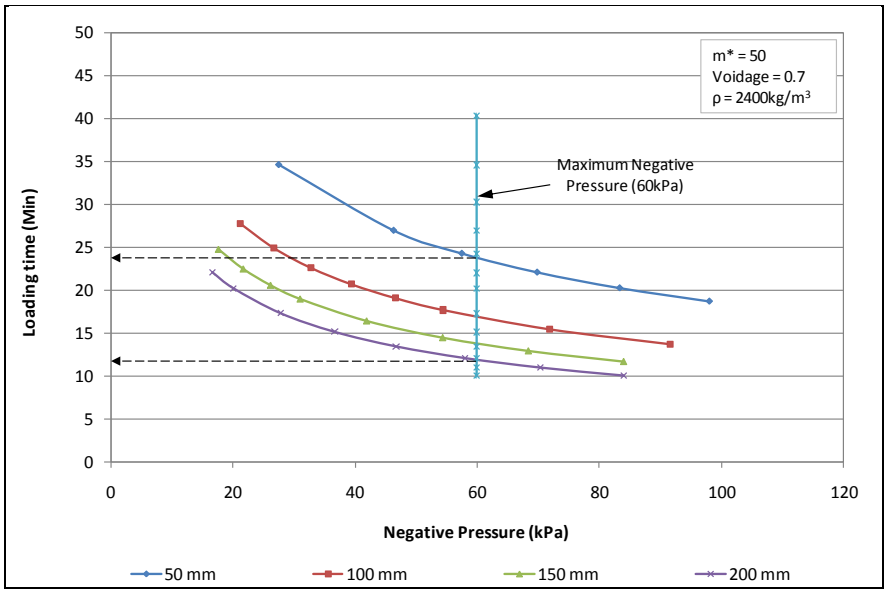

Figure 4.16: Optimum loading time for material with density 2400kg/m³

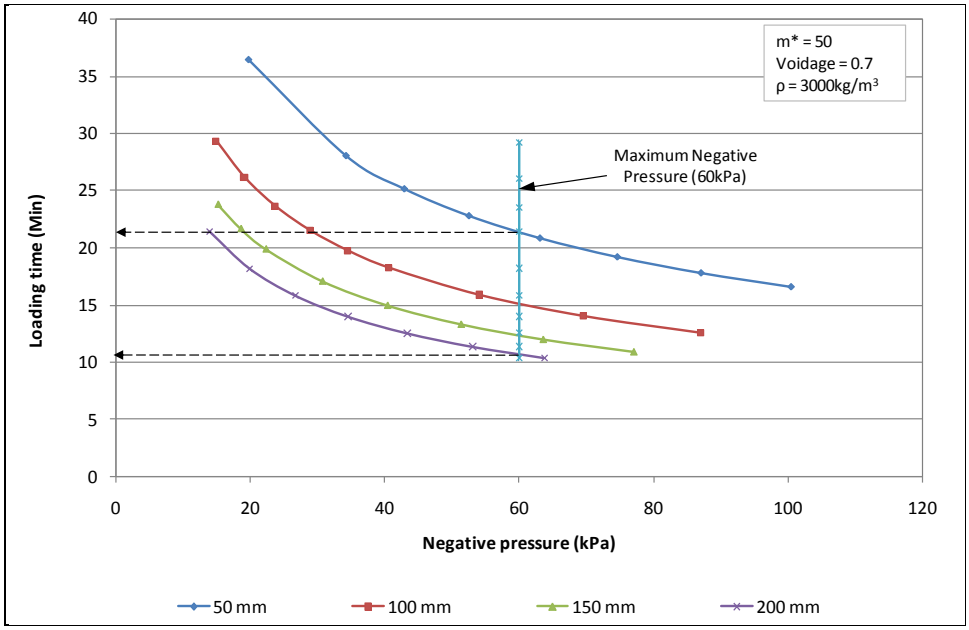

Figure 4.17: Optimum loading time for material with density 3000kg/m^3

Studies show that the loading time of the pneumatic loading system depends on the conveying air velocity (or operating negative pressure), the density of rock fragments as well as the fragmentation of the rocks being conveyed. At maximum negative pressure, Figure 4.16 and Figure 4.17 reveal that the loading time for lighter and more fragmented rock is higher than for heavier and less fragmented rocks. As shown in Figure 4.16 (ρ = 2400kg/m^3), the loading time of the system varies from 12 minutes (for 200mm rock fragments) to 24 minutes (for 50 mm rock fragments). However, for rock fragments of density 3000kg/m^3 (Figure 4.17), the loading time varies from 11 minutes (for 200mm rock fragments) to 22 minutes (for 50mm rock fragments). Therefore, the optimum loading time for the pneumatic system would vary from 11 minutes to 24 minutes, depending on the density and size of rock fragments being conveyed.

4.5.4 Optimum rock fragmentation

According to Franklin and Katsabanis (1996), rock fragmentation can mean anything from 'the limit of breaking' to 'the percentage passing, above or below a certain size' (page 14). During pneumatic suction of broken rock, it should be recognised that rock fragmentation have strong effects on system productivity.

Therefore, with a monorail loading system, control of rock fragmentation is critical in ensuring smooth suction of rock fragments by the pneumatic system. This means also that rock fragments after blasting should be carefully handled to avoid choking of the suction pipe during the suction process. The blast design of the decline face for monorail loading system application should, thus, optimise rock fragmentation so as to optimise the productivity of the suction system.

4.5.4.1 Post-blast material size distribution

Fragment size measurement of blasted rock has become an active research field as computers, digitizing and image analysis techniques progress (Franklin and Katsabanis, 1996). In fragment size distribution, the creation of new surface in blast-fragmented rock, energy consumption and rock strength properties are the most important interrelated variables. According to Franklin and Katsabanis, (1996), the significant fractions after rock blasting can usually be classified as oversize, fines and mid-range. In underground mines, the oversize can be boulder size above which secondary breakage is necessary before further handling, normally above 300mm. Kuznestov characteristic-size and Roslin-Rammler distribution equations are valid starting points for modelling fragment distribution in rock blasting and their combination has resulted in the development of the Kuz-Ram model. Figure 4.18 shows an example of size distribution curve after rock blasting.

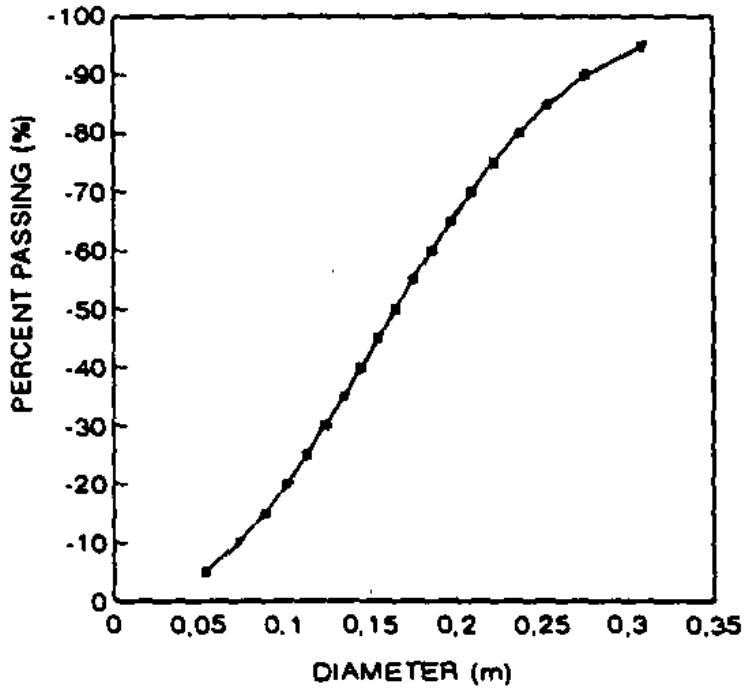

Figure 4.18: Size distribution curve (Franklin and Katsabanis, 1996)

4.5.4.2 Relationship between rock fragmentation, M_s and v_a

The size of rock fragments to be sucked by the pneumatic conveying system plays an important role during conveyance. This means that the efficiency and performance of the pneumatic conveying system does not only depend on the conveying air velocity and density of rock fragments but also on the particle size (rock fragmentation) being transported. Therefore, it is important that the relationship between rock fragmentation, mass flow rate of solids in the pipe, and the velocity of conveying air be determined. In this Section, the relationship between rock fragmentation, mass flow rate of solids and the velocity of conveying air of the pneumatic loading system is determined at maximum negative pressure (i.e., at 60kPa) and at m* equal to 50. For each conveying air velocity, the size of rock fragments that gave the maximum mass flow rate in the suction pipe was determined. Figures 4.19 and 4.20 show the results obtained.

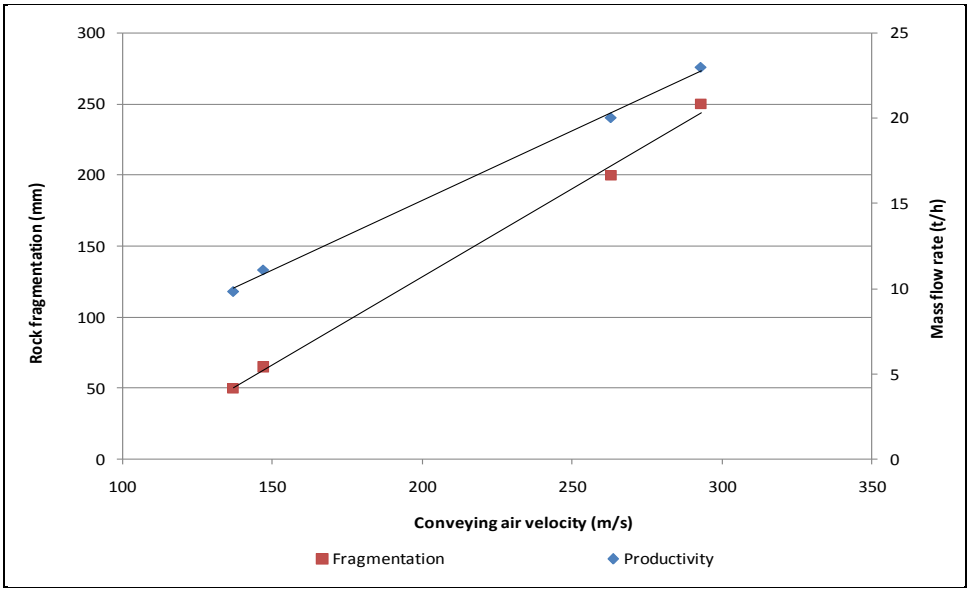

Figure 4.19: Rock fragmentation with corresponding mass flow rate at different conveying air velocities ρ = 2400kg/m^3 (Voidage = 0.7; Pipe diameter = 220mm)

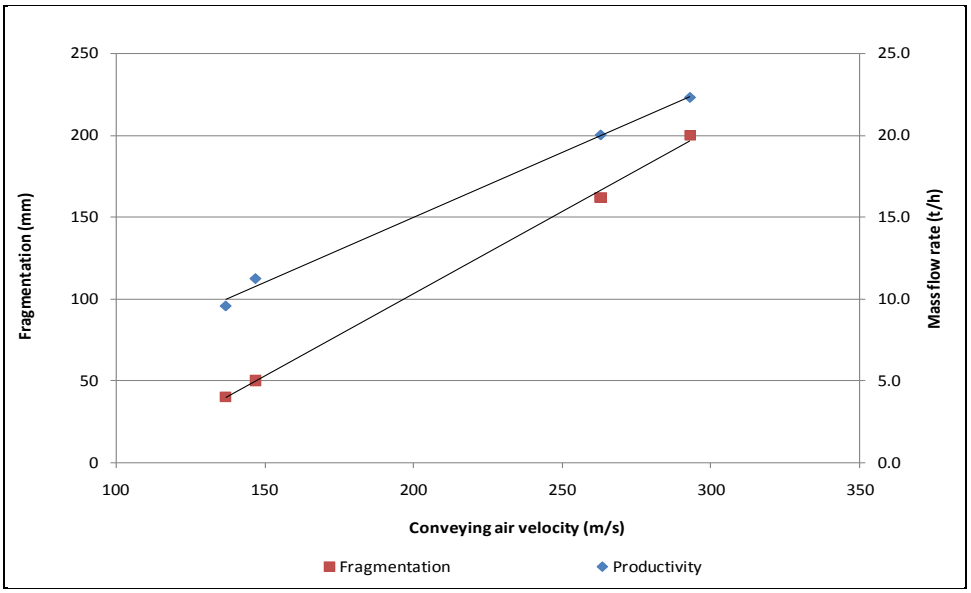

Figure 4.20: Rock fragmentation with corresponding mass flow rate at different conveying air velocities ρ = 3000kg/m^3 (Voidage = 0.7; Pipe diameter = 220 mm)

Figure 4.19 and Figure 4.20 show that optimal rock fragmentation is directly proportional to the conveying air velocity of the loading system. This means that as the conveying air velocity increases, the optimum rock fragment size being sucked by the system also steadily increases. Results also indicate that rock fragmentation has direct effect on the mass flow rate (i.e., productivity) of the

suction system. According to the results obtained, the more fragmented rock particles result in low productivity while larger particles have higher productivity. Therefore, based on this study, optimal rock fragmentation for the monorail loading system would vary from 50mm to 200mm (Figure 4.21) depending on the conveying air velocity adopted.

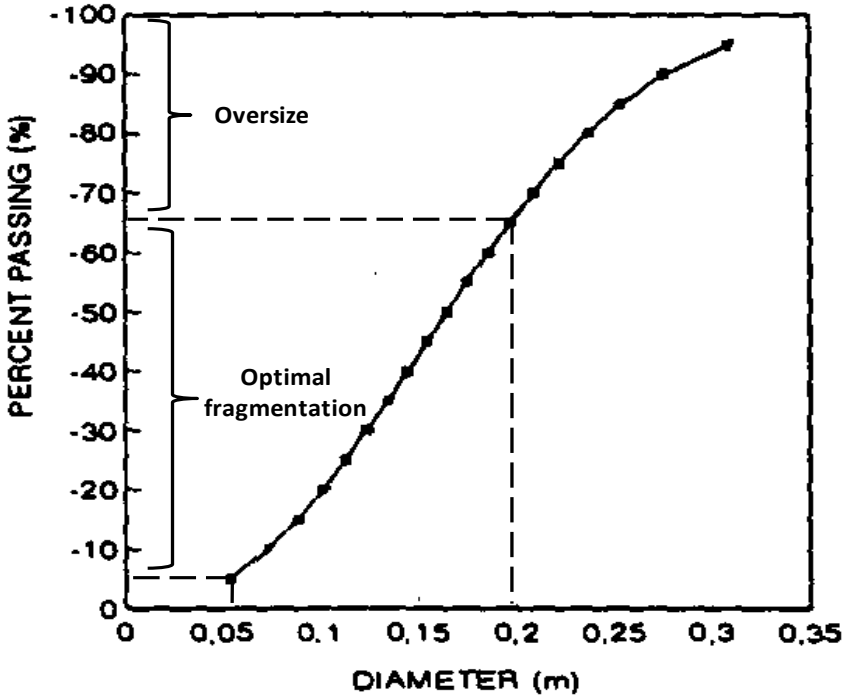

Figure 4.21: Size distribution curve showing optimum fragmentation range

Figure 4.21 also shows that only 65% of the rock fragments in a muck pile will be sucked by the loading system at maximum conveying air velocity (i.e., at maximum negative pressure). This will also leave 35% of rock fragments as oversize material.

4.5.4.3 Dealing with oversize

As highlighted in Section 4.5.4.2, 35% of rock fragments at the development face will not be sucked in by the pneumatic loading system. These rock fragments will remain as oversize material at the face. The oversized materials would affect pneumatic loading operations through entrance blockage of suction pipe, smaller particles blockage preventing suction as well as pipe movement restrictions at

the face. Therefore, oversized rock fragments must be reduced to manageable size (i.e., size that can be sucked by the pneumatic system) by secondary breaking at the face. The following are the suggested methods of reducing oversize rock fragments to size fractions that can be sucked by the system:

- Segregating oversize material at the face and using secondary blasting to reduce them to manageable size;
- Use impact hammer to fragment the oversize material at the face; and
- Rock cutting at the face.

It is also suggested that to control rock fragmentation at the development face, more research be conducted into blast design pattern that will reduce or minimize the percentage of oversize rock fragments after blasting.

4.5.4.4 Dust minimisation during conveyance

With pneumatic conveying system application, dust is generated during gas-solid separation as well as during discharge of material from the hopper into monorail containers. Most of the dust from the system is due to suction of fine dust resulting from blasting operations and degradation of rock fragments during conveyance. Thus, the amount of dust generated during suction and discharge processes is a function of conveying conditions in terms of conveying air velocity (or operating negative pressure) and the fineness of the material being conveyed. Therefore, with the monorail pneumatic loading system, the gas-solid separation device (i.e., the hopper) should be designed to perform two functions:

- To store conveyed rock fragments; and
- To minimise dust pollution of the working environment by the conveyed material especially during discharge process.

This means that extreme measures must be taken to prevent the escape of dust particles from the hopper into the working environment during conveying and discharge process, particularly, if potentially hazardous rock fragments are being

conveyed. It is suggested that the storage hopper should be designed with dust control mechanism to prevent dust emissions into the underground environment. The following dust control mechanism has been suggested for the monorail loading system.

(a) Use of gravity settling chambers

The gravity settling chambers are used to separate solid material from gas stream. With this equipment, the velocity of the gas-solid stream is reduced and the residence time is increased. This allows particles to fall under gravity as the gas containing dust is collected as indicated in Figure 4.22.

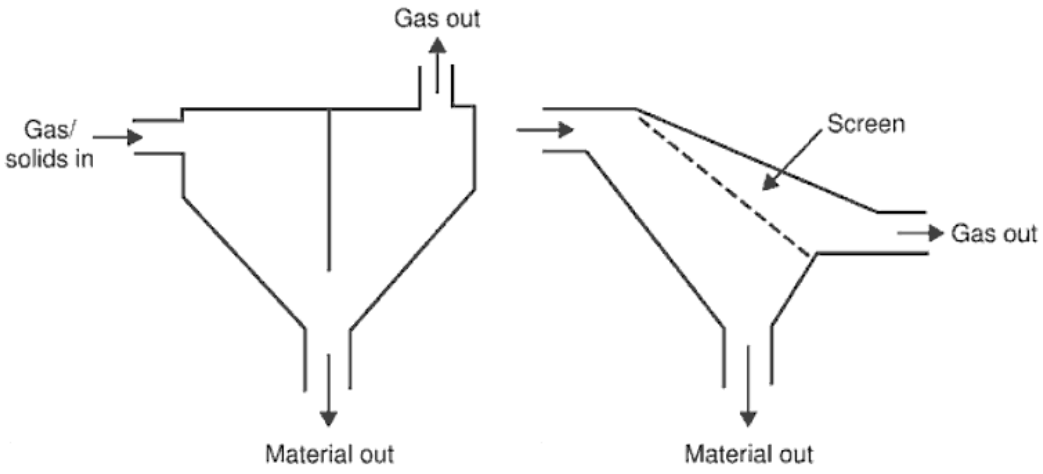

(a) (b)

Figure 4.22: Gravity settling chamber; (a) basic system (b) design incorporating screen (Mills, 2004)

(a) Use of cyclone separators

Depending on rock fragmentation after blasting, a cyclone separator can be employed if medium to fine particulate material exists in the muck pile. Since the cyclone separator is dependent upon the mass of the particulate for its separation, the forces that discharge the solid particles from the conveying gas are developed by imparting a spinning motion on the incoming stream. This

allows particles to migrate outwards and downwards under the influence of centrifugal and gravitational effects. This arrangement is shown in Figure 4.23.

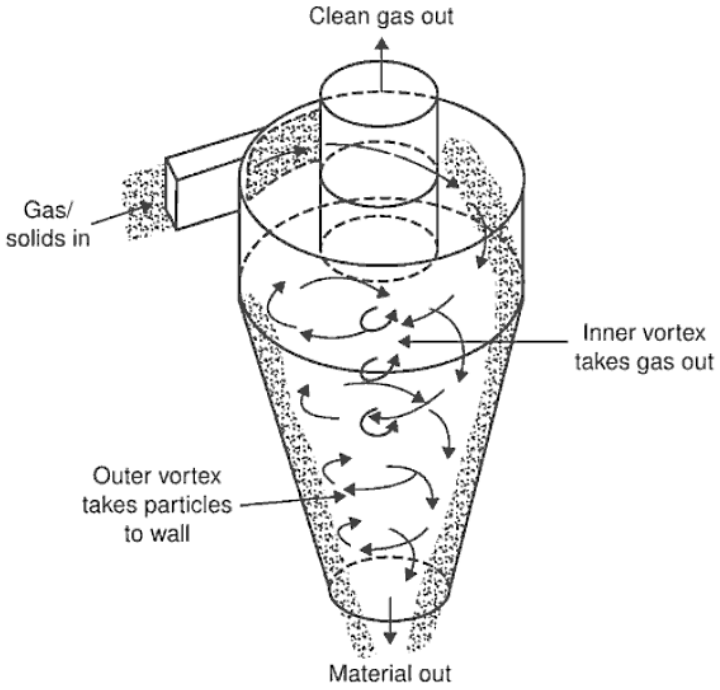

Figure 4.23: Principle of cyclone separator (Mills, 2004)

4.6 Handling of suction pipe during suction process

The configuration of the suction pipe and the process of handling it during suction are critical in ensuring smooth flow of rock fragments from the face into the hopper. It is, therefore, important that configuration, handling and movement of the suction pipe and the mechanism of connecting and disconnecting the pipe to and from the hopper during suction process are outlined. In this Section, pipe configuration, process of handling and the mechanism of connecting and disconnecting to and from the hopper during suction process are described.

4.6.1 Suction pipe configuration

Figure 4.24 and Figure 4.25 show the schematic configuration of the suction pipe for the monorail loading system.

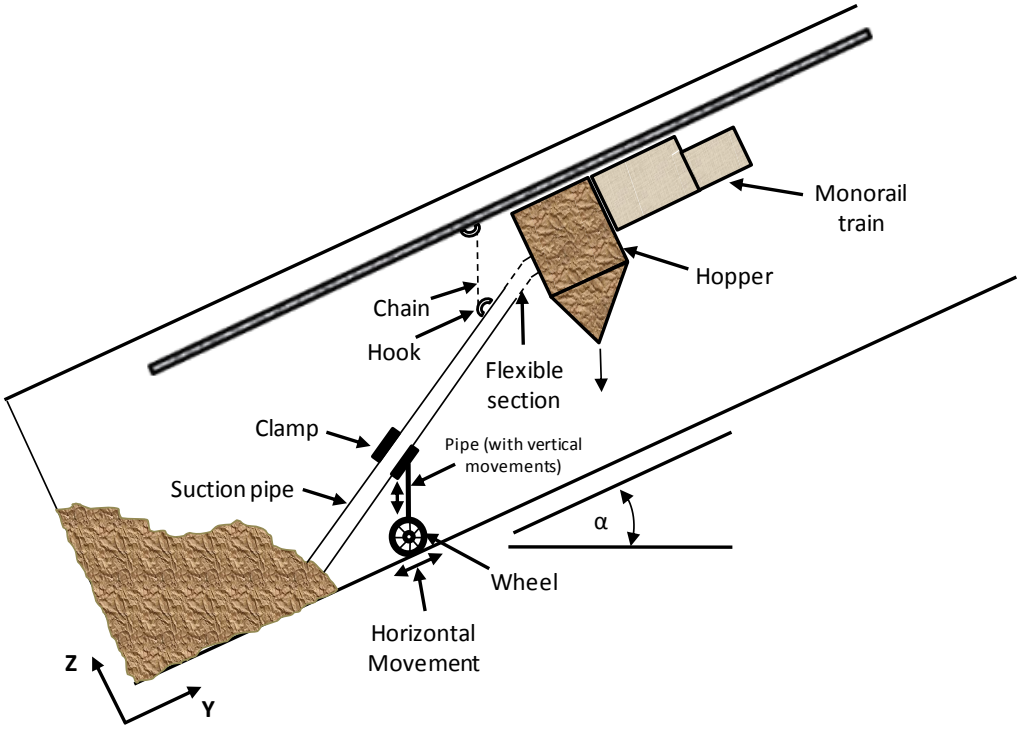

Figure 4.24: Longitudinal section across the suction pipe

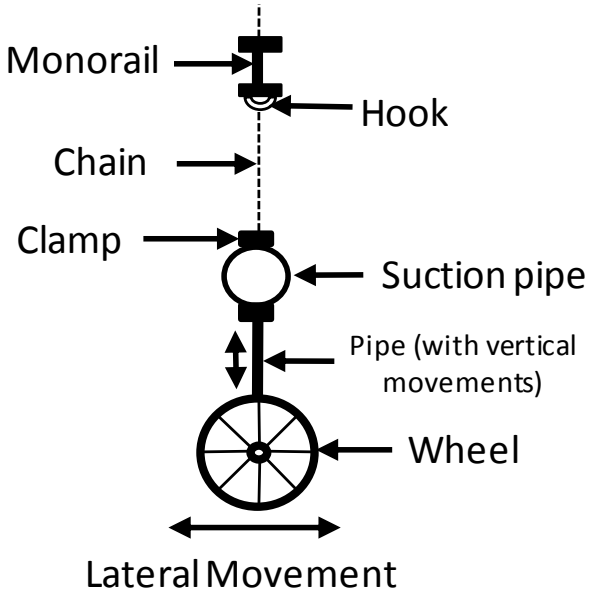

Figure 4.25: Cross section view of the suction pipe

As can be seen from Figure 4.24, the suction pipe is composed of two sections i.e., the rigid and flexible sections. The flexible section allows the suction pipe to be positioned in any direction during suction process. It should also be noted that the inside part of the flexible section should be made of a strong lining to reduce

wear and tear due to friction during suction process. The rigid part is the metal section of the suction pipe connected to one end of the flexible section through which the material enters from the development face.

As shown in Figures 4.24 and 4.25, the rigid metal section is clamped onto the vertical adjustable pipe connected to the wheel at the bottom. The wheel allows horizontal and lateral movement of the suction pipe at the face while the vertical adjustable pipe has a mechanism that allows upwards and downwards pipe movement. The vertical movement allows vertical positioning of the suction pipe to be done correctly at the face. The pipe has also a fixed hook on the metal section closer to the flexible section of the pipe. The hook is a means of holding the pipe in fixed position during suction process as well as after disconnecting it from the hopper. Thus, by using a chain, the pipe is hooked and held securely onto the monorail segment as indicated in Figures 4.24 and 4.25.

4.6.2 Movement and handling of suction pipe

The process of pipe movement and handling during suction is significant for easy and fast flow of material from the face into the hopper. It should also be pointed out that the easier and faster it is to manoeuvre the pipe at the face, the quicker will the material flow into the hopper and vice versa. In this Section, the process of suction pipe movement and handling at the face is outlined.

During suction process, lateral and horizontal movement of suction pipe is provided by the wheel attached to the vertical adjustable pipe. This indicates that to move the suction pipe in lateral direction, i.e., across the development face, the wheel is adjusted in lateral direction. Similarly, the wheel is adjusted in horizontal direction for horizontal movement of the suction pipe. Movement of the suction pipe can be done either manually by pushing the pipe in the desired direction or by attaching a motor to the wheel to aid its movements. Alternatively, pneumatic control system such as the hydraulic control systems used in most underground drills can be used to control the suction pipe.

4.6.3 Suction pipe connection and disconnection

The process of connecting and disconnecting the suction pipe to and from the hopper during suction process is also important in reducing the total loading cycle time for the system. It should be noted that the more time it takes to connect and disconnect the suction pipe, the more time it would take to clean the face and vice versa. Hence, a simple mechanism that allows quick connection and disconnection of the suction pipe to and from the hopper is essential. Figure 4.26 shows the required connections between the flexible section of the pipe and the hopper.

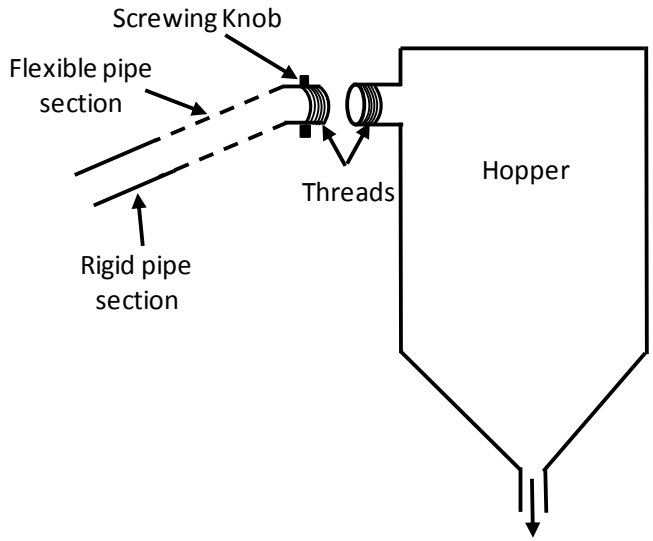

Figure 4.26: Connection and disconnection arrangement for suction pipe

As can be seen from Figure 4.26, one end of the flexible section has a threaded metal section which serves as the male part of the connection with the hopper. The threaded metal section has a screwing knob that is used for tightening and loosening the pipe during connection and disconnection to and from the hopper. Therefore, to connect the pipe, the threaded metal part of the hopper is inserted into the threaded end of the flexible section. The screwing knob is then used for tightening the pipe. To disconnect the pipe, the screwing knob is loosened and threaded metal part of the flexible section removed from the threaded end of the hopper. It should also be pointed out that due to the flow of rocks in the pipe and

the expansion of the threaded metal section resulting from heat inside the pipe, screwing and unscrewing will sometimes be difficult.

4.7 Suction pump selection for pneumatic loading system

Pump selection can be both arbitrary and specific, i.e., for a given duty requirement, several alternative types of pumps may be suitable when the choice of type may be based on "accept practice" or individual preference, such as, based on costs and performance. The choice can also be made purely on technical grounds. Based on technical grounds, pump selection for monorail loading system can be done by analysis of the hydraulic system and the pump location and function. Therefore, the initial decision that must be made in applying a pump is the decision regarding the type of pump to use. According to literature (Bankston and Baker, 1994), centrifugal pumps are used in pneumatic suction systems during shaft sinking. Therefore, a centrifugal pump is adopted for the design of monorail loading system. According to Bankston and Baker (1994), before selecting a pump that fits one's needs, the following must be known:

1. The desired flow rate (pump capacity);
2. The total head or pressure against which it must operate;
3. The suction lift; and
4. Characteristics of the fluid.

4.7.1 Pump capacity

In order to select a pump that meets the requirements of the system in an efficient manner, the pump must be matched to the piping system and required flow rate. Therefore, the required capacity of the pump is dictated by the requirements of the system in which the pump is located. Normally, a process system is designed for a particular throughput. Therefore, in determining the pump capacity of the monorail pneumatic loading system, the maximum mass flow rate is used as pump capacity of the system. As shown in Table 4.1, at

maximum negative pressure, the pneumatic loading system has minimum mass flow rate or capacity of 10t/h with maximum being 23t/h depending on the rock fragments being conveyed. Therefore, the maximum value is used to determine the pump capacity for the system.

4.7.2 Total head

To determine the required size of a centrifugal pump for a particular application, all components of the system head in which the pump is to operate must be added up to determine the pump total head (TH). The monorail pneumatic loading system consists of three separate components of total head, i.e.:

1. Static head;
2. Friction head; and
3. Pressure head.

Each of these three components must be considered for the system in which the pump is to operate, and the sum of these is the total head of the pump. Determination of total head for the monorail system is achieved by the application of Bernoulli's equation (Equation 4.8) to the system shown in Figure 4.27:

$$\frac{P_1}{\rho g} + \frac{v_1^2}{2g} + Z_1 = \frac{P_2}{\rho g} + \frac{v_2^2}{2g} + Z_2 + h_f - H_T \qquad 4.8$$

where:

$\mathbf{H_T}$ is total pump head;

$\mathbf{h_f}$ is friction head loss;

$\mathbf{Z_1}$ and $\mathbf{Z_2}$ are elevations at position 1 and 2;

$\mathbf{v_1}$ and $\mathbf{v_2}$ are fluid of velocities at position 1 and 2; and

$\mathbf{P_1}$ and $\mathbf{P_2}$ are pressures at position 1 and 2 respectively.

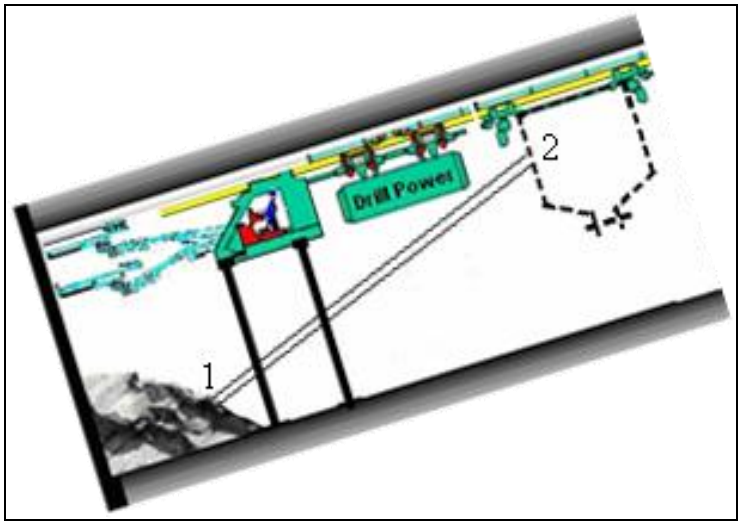

Figure 4.27: Monorail loading system total head determination

Since the velocity of solids in the suction pipe is constant throughout the fluid flow, the total head is determined as indicated in Equation 4.9:

$$H_T = \frac{\Delta P}{\rho g} + \Delta Z + h_f \qquad 4.9$$

where:

ΔZ is vertical height difference between point 1 and 2 (i.e., static head); and

ΔP is the change in pressure.

4.7.2.1 Static head

Static head is the total elevation change that the solids must undergo during conveyance. In effect, static head represents the net change in height that the pump must overcome. For the pneumatic loading system, the static head is the total elevation change from decline floor to the hopper, i.e., the vertical distance from the muck pile to the hopper as shown in Figure 4.28. Since the pipe length and pipe inclination from the horizontal are known, the static head was determined as 11.4m using trigonometry.

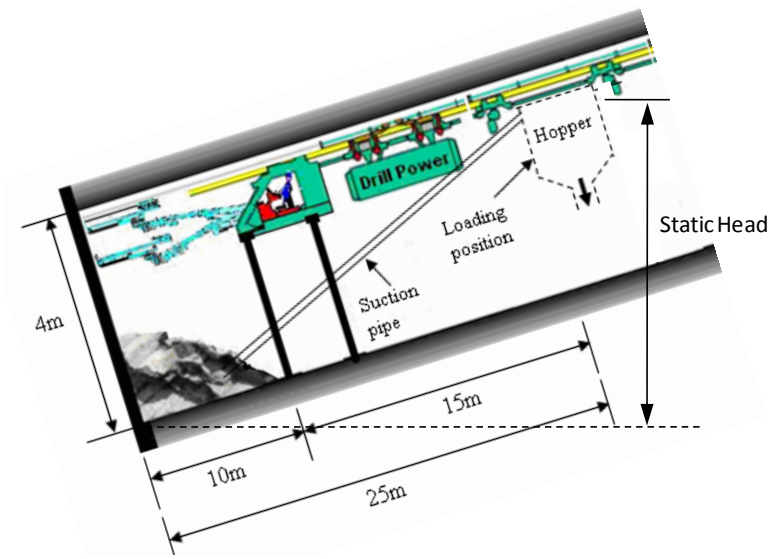

Figure 4.28: Static head for the monorail loading system

4.7.2.2 Friction head

Friction head (h_f) is the head necessary to overcome the friction losses in the suction pipe for the system in which the pump operates. This is the amount of pressure (or head) required to 'force' fluid through the suction pipe. When an incompressible fluid flows in a suction pipe and the flow is turbulent, the friction head loss is a function of the pipe length, diameter of pipe, surface roughness of the pipe wall, the velocity of the fluid in the pipe, the density of the fluid, and the viscosity of the air. Darcy-Weisbach equation (expressed in terms of friction head losses), Equation 4.10, is generally used to calculate the frictional head losses in pipes.

$$h_f = f \frac{L}{D} \frac{v^2}{2g} \qquad 4.10$$

where:

h_f is friction head;

f is friction factor;

L is length of suction pipe;

D is diameter of suction pipe;

v is the velocity of fluid; and

g is acceleration due to gravity.

The friction factor is determined for the turbulent flow regime, using the relationship between the relative roughness of pipe and the Reynolds Number, i.e., using Colebrook equation or the Moody chart. Therefore, friction head loss for monorail pneumatic loading system was determined using Equation 4.10 whilst the friction factor is determined using Equation 3.15.

4.7.2.3 Pressure head

The pressure head is the head required to overcome a pressure or vacuum in the system upstream or downstream of the pump. For the monorail pneumatic loading system, pressure head is determined using Equation 4.11:

$$H_p = \frac{\Delta P}{\rho g} \qquad 4.11$$

Table 4.2 shows the determined pressure head, static head, friction head as well as the total head for the monorail loading system at maximum negative pressure i.e., ΔP.

Table 4.2: Pressure head, static head, friction head and total head at maximum negative pressure (ρ=2400kg/m^3)

Conveying Air Vel. (m/s)	Particle diameter (m)	Particle velocity (m/s)	Pressure Head (Hp) – (m)	Static Head (ΔZ) – (m)	Friction Head (h_f) - (m)	Total Head (H_T) – (m)
132.0	0.05	2.56	2.6	11.4	10.6	24.6
147.0	0.05	2.27	2.6	11.4	10.6	24.6
263.0	0.20	5.09	2.6	11.4	10.6	24.6
293.0	0.20	4.53	2.6	11.4	10.6	24.6

4.7.3 Pump performance curve

Pump's performance is shown in its characteristic performance curve, where its capacity, i.e., mass flow rate, is plotted against its total head. The pump performance curve also shows the Best Efficiency Point (BEP), required input Brake-Horsepower (BHP), Net Positive Suction Head (NPSH), speed in

Revolutions Per Minute (RPM), and other information such as pump size and type, impeller size, etc. This curve is plotted for a constant speed and for a given impeller diameter. Typical performance curve is shown in Figure 4.29.

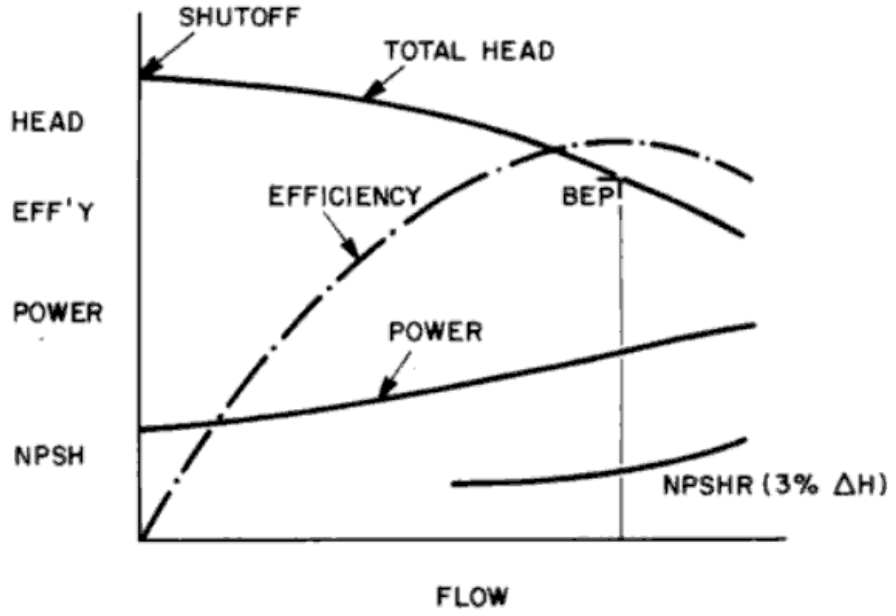

Figure 4.29: Typical pump performance curve (Klinzing et al., 1997)

4.7.4 Brake-horsepower and pump efficiency

The brake horsepower refers to the amount of energy (or actual amount of power) that must be supplied to operate a pump so as to obtain a particular flow and head. It is the input power to the pump or the required output power from the driver. Brake horsepower is determined using Equation 4.12:

$$\mathrm{BHP} = \frac{\mathrm{Q} \times \mathrm{H} \times \mathrm{s.g}}{3960 \times \eta} \qquad 4.12$$

where:

BHP is brake-horsepower;

Q is volume flow rate;

H is the total head;

s.g is specific gravity; and

η is the pump efficiency.

Expressing brake-horsepower in SI units, Equation 4.12 can be written as shown in Equation 4.13:

$$\text{Power(kW)} = 0.746 \times \text{BHP}$$

$$\text{Power(kW)} = 0.746 \times \frac{Q \times H \times s.g}{3960 \times \eta} \qquad 4.13$$

The BHP required to operate a pump at a given point can also be obtained from the pump performance curve. On the pump performance curve, the brake horsepower curve runs below the total head (see Figure 4.29). There is a brake horsepower curve for each different impeller trim and is usually provided by the manufacturer of the pump. The efficiency of the pump can also be obtained from the pump performance curve. The pump efficiency normally measures the degree of its hydraulic and mechanical perfection. On the pump performance curve, the efficiency curve intersects with the head-capacity curve. Thus, each pump will have its own maximum efficiency point. The pump efficiency and brake-horsepower for monorail pneumatic loading system was determined using a 3540rpm pump characteristic curve. This was based on the maximum pump capacity of 23t/h (7.4m^3/h for 3000kg/m^3 rock fragments) and maximum total head of 24.6m. The maximum capacity and total head of the pneumatic loading system were plotted on the 3540rpm pump characteristic curve, to give the pump operating point shown as **OP** in Figure 4.30.

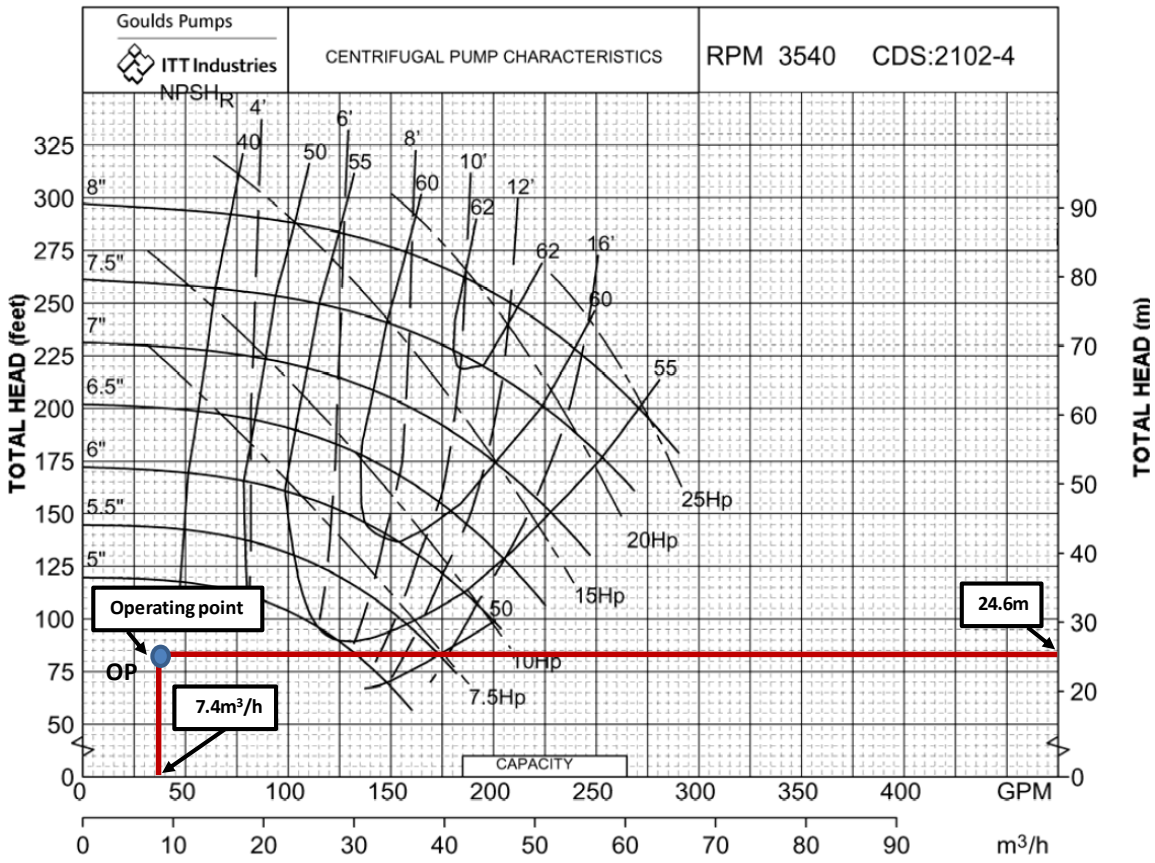

Figure 4.30: Performance curve showing operating point (OP) for the monorail loading system pump

According to Figure 4.30, the pump characteristics for the pneumatic loading system are indicated in Table 4.3.

Table 4.3: Pump characteristics for monorail pneumatic loading system

Parameter	Value
Pump horsepower	7.5HP (5.6kW)
Pump efficiency	40%
Impeller diameters or trims	5”

4.8 Monorail system surface infrastructure

Planning and arrangement of the monorail system surface infrastructure (i.e., for ore and waste handling, workshops, loading bays, etc) is an important phase while considering monorail system. Proper planning and arrangement of surface monorail / rail network system has an impact on the ease with which the

material is handled on surface as well as on the speed with which the monorail loading system dumps and returns underground. Therefore, installation and arrangement of monorail surface infrastructure should allow easy material handling and rapid dumping and return of monorail loading system underground. In this Section, arrangement of monorail system surface infrastructure is described.

4.8.1 Surface infrastructure arrangement

Figure 4.31 shows the schematic arrangement of the monorail system surface infrastructure. The infrastructure consists of the monorail / rail network system to and from underground, surface ore and waste handling system and the monorail system workshops. As shown in Figure 4.31, from the decline portal, the monorail is connected to the surface ore and waste handling system with another bypass loop to the monorail system workshops. Surface ore/waste handling system bins that serve as storage locations for ore and waste transported from underground. From the bins, ore/waste is loaded into trucks for further processing.

The monorail return loop connected from the ore/waste handling system serves as underground return way by the system. There is also a provision for a turning loop on the return way that enables the monorail system change direction as it goes back underground. From the ore/waste handling system, there is another loop to the workshop where monorail systems are repaired and maintained. This is also where suspension (hanging) of the monorail system onto the rail network is to be done. Other sections, such as, loading bays for both material and personnel can also be linked to the network.

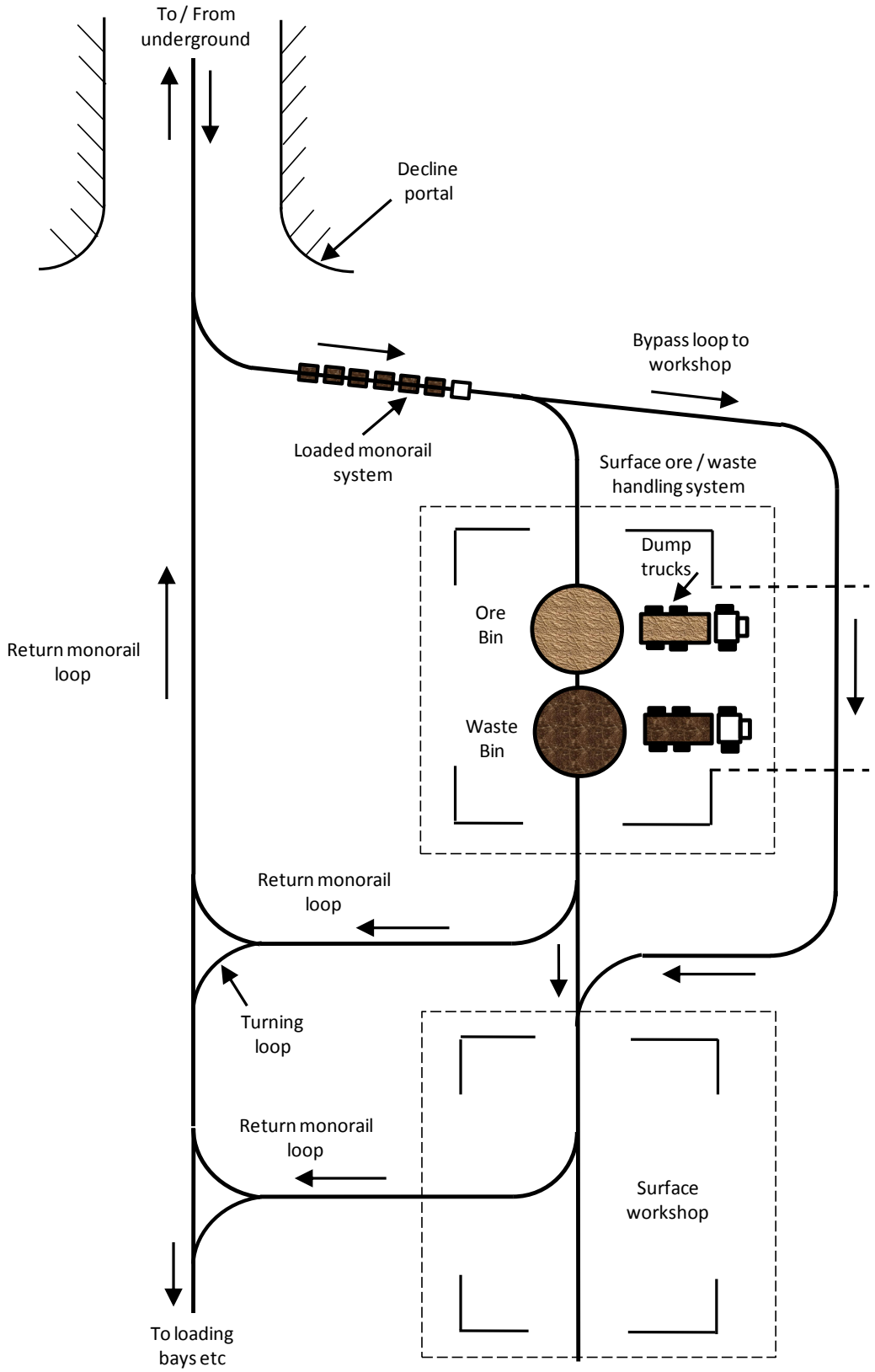

Figure 4.31: Schematic diagram showing monorail surface infrastructure arrangement

4.8.2 Surface material handling system

Figure 4.32 shows schematic diagram for monorail system surface ore and waste handling system.

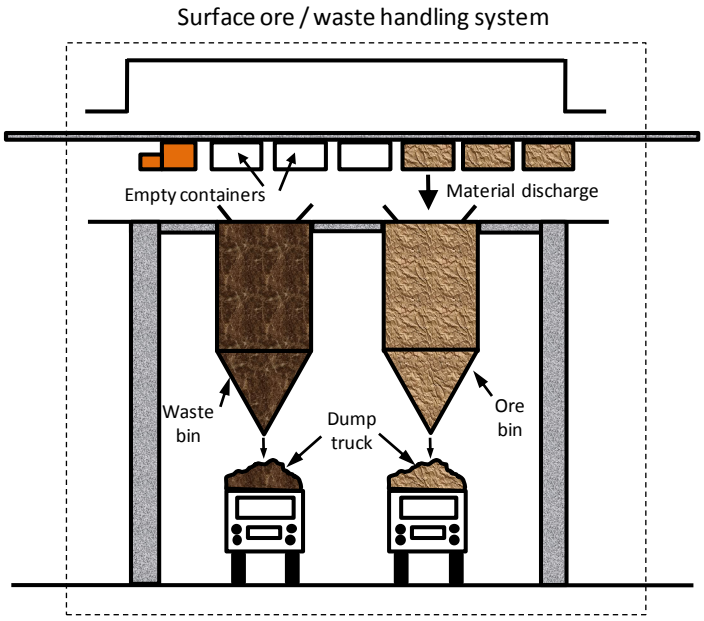

Figure 4.32: Schematic diagram showing ore and waste handling systems

As indicated in the Figure 4.32, surface materials handling system is composed of ore and waste bins which are dumping points for the monorail loading system.

Figure 4.33: Monorail system bottom dumping container (Scharf, 2007)

During dumping operations, monorail containers are positioned below the bin where discharge of material takes place. Discharge of material by the monorail system is done automatically by opening of monorail containers from the bottom as indicated in Figure 4.33.

4.9 Summary

From this study, it has been determined that transportation of rock fragments from development face into monorail containers is possible with the use of pneumatic loading system. Results have shown that the solid loading ratio determines the amount of solids in the suction pipe. Thus, the higher the solid loading ratio, the higher the mass flow rate of solids in the pipe. Results also indicate that the mass flow rate of solids depends on the conveying air velocity, density of the rock fragments as well as rock fragmentation. At maximum negative pressure, larger rock fragments results in higher mass flow rate than more fragmented rock particles. In terms of pressure loss, the study has revealed that the pressure loss of the system depends on the rock fragmentation and conveying air velocity. It was observed that more fragmented rocks would result in more pressure loss due to their higher superficial velocity in the suction pipe than larger particles. Also due to higher velocity that is required to convey larger rock fragments, results show that more power is required to convey larger particles. Therefore, as a result of this high velocity, the loading time of larger rock fragments is lower than more fragmented particles. In Chapter 5, the conceptual monorail drilling system working in conjunction with the pneumatic loading system at the development face is described.

Chapter 5

5.0 Design of monorail drilling system

5.1 Introduction

This Chapter outlines the conceptual design of the drilling system that uses monorail technology. The concept involves mounting twin-boom drilling jumbo onto the monorail train/driver's cabin and using horizontal and vertical hydraulic props to stabilise the system during drilling process. This Chapter focuses on stabilising the monorail drilling system by determining the required balancing forces in each hydraulic stabiliser that will oppose drilling forces.

5.2 Configuration of monorail drilling system

The configuration of the conceptual monorail drilling system is shown in Figure 5.1. The system has its own power supply attached with two horizontal and two vertical hydraulic stabilisers (props) to act as supports during drilling operations. The operation of the monorail drilling system is such that drilling the top part of the development face would commence immediately after the face is blasted and made safe, as the monorail pneumatic loading system continues cleaning the blasted material at the development face. The advantage of this operation is that drilling of the face continues whilst monorail loading system cleans the face, i.e., the drilling system does not wait for the face to be completely cleaned before drilling commences. It is hoped that this process would reduce the drilling cycle time that would eventually result in an increase in the daily advance of decline development.

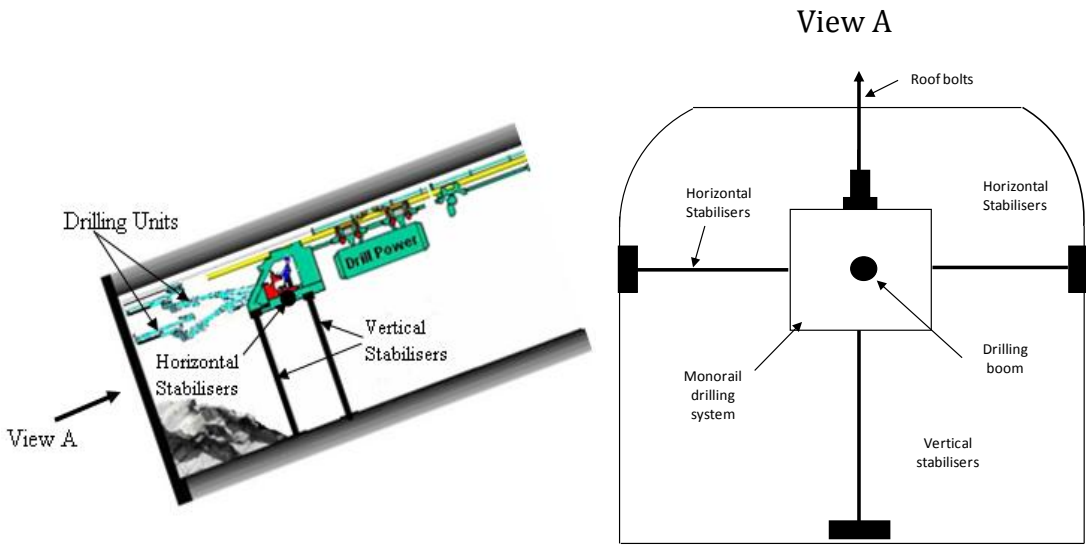

Figure 5.1: Configuration of conceptual monorail drilling system

5.3 Components of the monorail drilling unit

A wide and varied range of drilling units is available for underground tunnelling and many factors influence their choice in development projects. The drilling unit, loading and rock removal equipment must be selected so that its combined efficiency is optimised (Atlas Copco Manual, 1982). The choice of drilling unit to be mounted onto the monorail train is therefore, worth attention. Figure 5.2 shows the type of drilling unit (drilling boom) with its components to be mounted onto the monorail train.

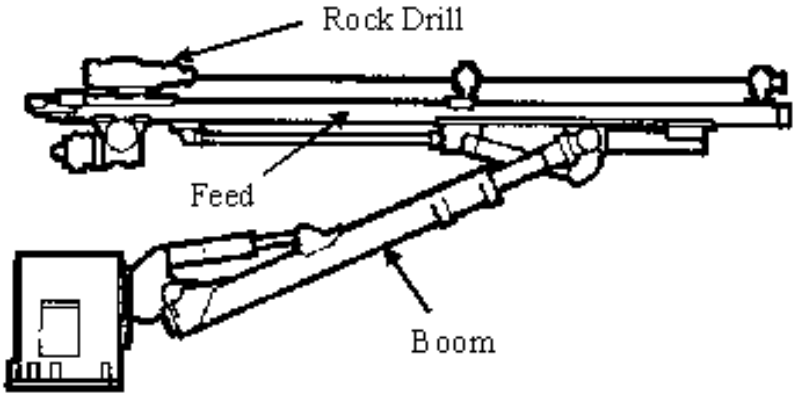

Figure 5.2: Drilling boom with components (Atlas Copco Manual, 1982)

5.3.1 Rock drill

A rock drill is a machine or device used for penetrating the rock (i.e., used for drilling holes in a rock) so that the hole may be blasted. Figure 5.3 shows an example of a rock drill machine.

Length	1008mm
Width	251mm
Height	223mm
Impact power, max	16kW
Input power to rock drill, max	26kW

Figure 5.3: COP 1638 Rock drill (Atlas Copco Manual, 1982)

The rock drill is usually driven by compressed air although it may also be driven by electricity. In most underground tunnelling machines, the rock drill is mounted onto the feed. Therefore, the feed should be equipped with extremely fast rock drill with advanced drilling controls. This is in order to drill out the face quickly, accurately and efficiently. Thus, the reliability and productivity of the drilling equipment depend on the rock drill used. Additionally, high efficiency rock drill gives lower cost per meter drilled. Therefore, the monorail drilling system should be equipped with high performance pneumatic rock drills with ergonomic controls and automated drilling control system. Table 5.1 shows the types of rock drills available with their technical specifications.

Table 5.1: Rock drill parameters (Sandvik Mining and Construction, 2007; Atlas Copco Manual, 1982)

Supplier	Rock Drill Type	Power (kW)	Weight (kg)	Max Pressure (bars)		Hole Size (mm)
				Percussion	Rotation	
Sandvik	HLX5	20	210	225	175	43 – 64
	HLX5T	22	218	245	175	43 – 64
	HL 510 S	16	130	175	175	43 – 51
	Hydrastar 200	6 - 10	115	200	210	30 - 45
Atlas	COP 1638	16	170	200	310	33 - 76
Copco	COP 1838 ME-07	20	171	230	240rpm	45 - 64
	COP 1838ME-05	20	171	230	300rpm	45 - 64
	COP 3038	30	165	200	380	43 - 64

5.3.2 Feed

Feed is a metal channel on which a rock drill is mounted and fed forward as drilling progresses (Figure 5.4). In percussive drilling, as much as possible of the impact energy from the rock drill has to be transmitted to the rock in order to do the drilling. In top-hammer drilling, the drill is mounted on a cradle, which runs on a feed. Feeding can take place mechanically, utilising a chain, screw or hydraulically.

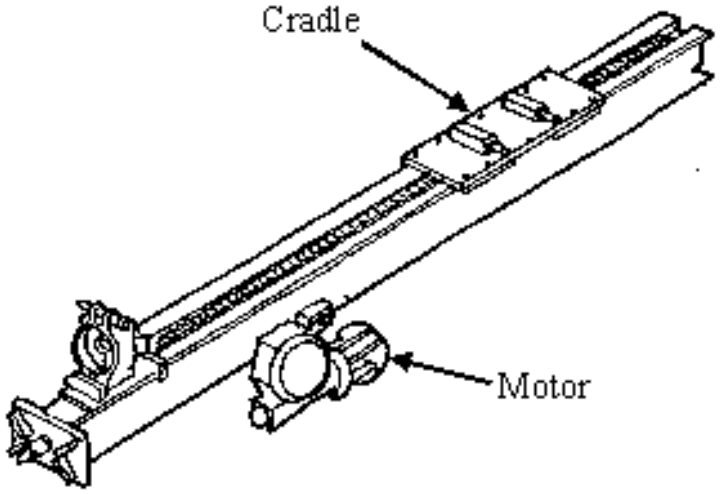

Figure 5.4: Feed with feed motor and cradle (Atlas Copco Manual, 1982)

The feed force varies according to the nature of the rock to be drilled and the mass of the drill rig and the drill steel. When drilling is done by the rotary crushing method the feed force is utilised to drive the buttons of the roller bit

into rock and a very high feed force will be required. Thus, the life of the bit depends on the feed force, the properties of the rock being drilled and the type of bit. The use of the new Super Material Abrasive Resistant Tools (SMART) or SMART*CUT® diamond composite bits being developed by Australian Commonwealth Scientific and Industrial Research Organisation (CSIRO) could revolutionise the drilling, i.e., higher drilling rates and longer lasting bit. Table 5.2 shows feed parameters for different types of feeds.

Table 5.2: Feed types and technical parameters (Sandvik Mining and Construction, 2007; Atlas Copco Manual, 1982)

Supplier	Feed Type	Maximum Feed Force (kN)	Net Weight (kg)	Feed Length (m)
Sandvik	TF 500 – 10'	25	470	4.66
	TF 500 – 12'	25	500	5.27
	TF 500 – 14'	25	530	5.88
	TF 500 – 16'	25	560	6.49
Atlas	BMH 2831	15	474	4.68
Copco	BMH 2833	15	494	5.29
	BMH 2840	15	514	5.59
	BMH 2843	15	524	5.90
	BMH 2849	15	541	6.51
	BMH 6812	20	601	5.29
	BMH 6814	20	631	5.88
	BMH 6816	20	665	6.50
	BMH 6818	20	696	7.10

As can be seen from Table 5.2, all the feed lengths are greater than the minimum required decline opening for monorail system application, i.e., 3m x 3m. This means that, if any of the feed shown in Figure 5.2 is used on the monorail system, installation of ground support will not be possible because the feed cannot fit within the cross-section area of the decline. Thus, a tailor-made feed (e.g., extendable feed) that is able to fit within the cross-section area of the decline should be mounted on the monorail drilling system to enable installation of the ground support by the system.

It is also essential for the rig to be firmly erected, to secure the feed and provide sufficient force to ensure that the bit is constantly in contact with the rock. Insufficient thrust produces several undesirable effects including reduced speed,

damage to the drill caused by the piston shrinking the front head and heating of the drill rod and bits due to conversion of unabsorbed energy to heat. With increase in thrust, penetration speed improves progressively until an optimum level is attained (Atlas Copco Manual, 1982). Further increase gives rise to interference in the operation of the percussive mechanism because the bit is no longer able to rotate freely and the length of the piston stroke and thereby the power of the impact is reduced (Figure 5.5). The percussive drill can only produce its full stroke if the rods are allowed to rotate because the two movements are coupled. Therefore, optimum thrust can be considered as the maximum level conducive with satisfactory results and that at which any increase of thrust brings undesirable consequences.

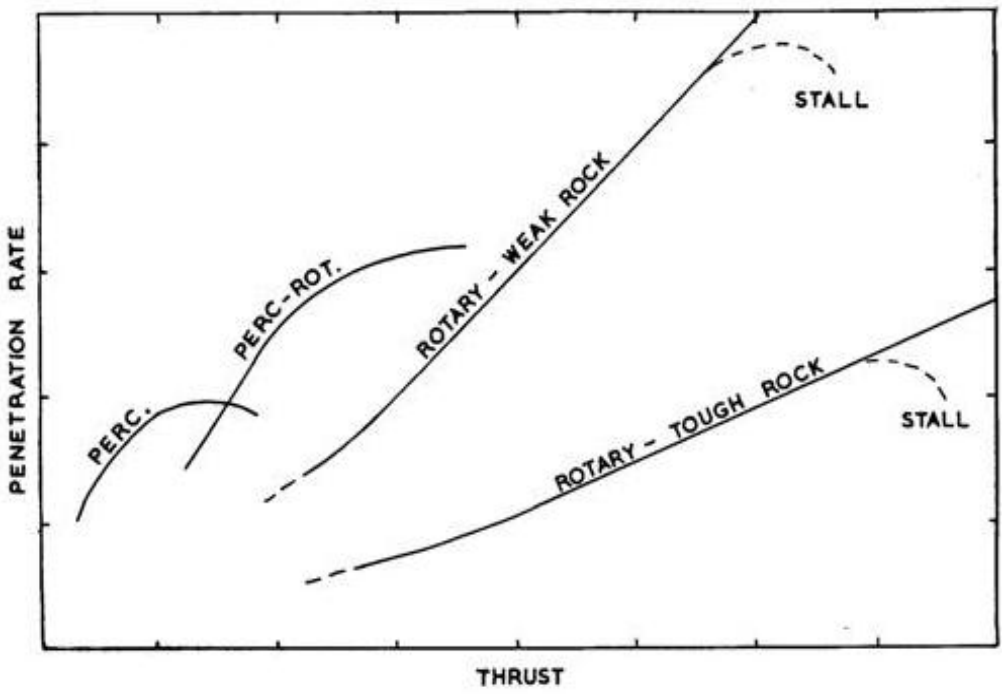

Figure 5.5: Effects of thrust on penetration rate (McGregor, 1967)

5.3.3 Drill boom

A drill boom is a telescoping, hydraulically adjustable powered steel arm projecting from the drill carriage to carry a drill and hold it in selected positions (AusIMM, 2007). Figure 5.6 shows an example of the drill boom.

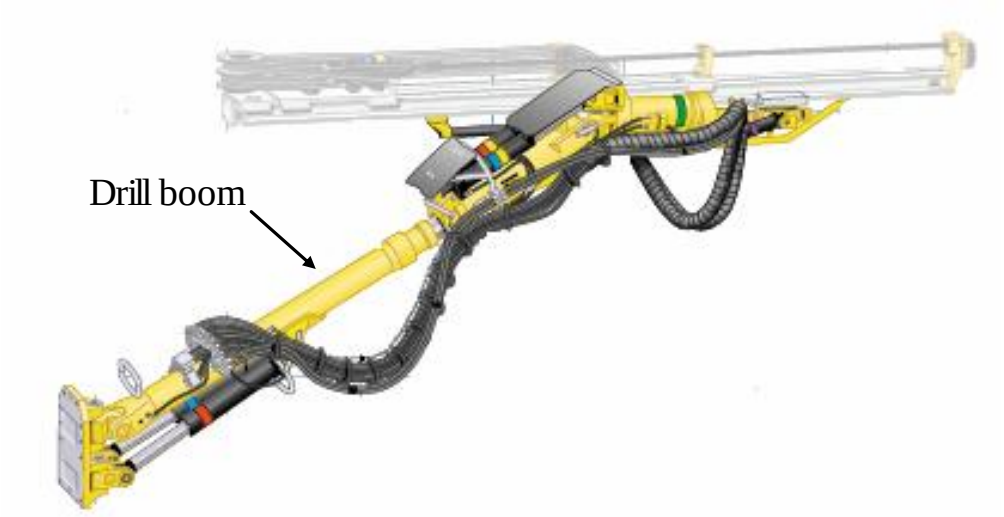

Figure 5.6: BUT 28 drill boom (Atlas Copco Manual, 1982)

Most of the drill booms have automatic parallel holding of the feed, which results in easy positioning of the boom and maximises the advance per round. The boom consists of two hydraulic cylinders coupled between the support plate and the boom. The cylinders are located on each side of the drill boom so that they are both loaded by the weight of the boom, which makes the boom very stable in all positions. With the monorail drilling system, the drill boom carries the feed beam for rock drill and is universally pivoted to the monorail train. Table 5.3 shows various types of drill booms with their respective technical parameters.

Table 5.3: Drill boom types with respective technical parameters (Sandvik Mining and Construction, 2007; Atlas Copco Manual, 1982)

Supplier	Drill boom type	Boom Wt (kg)	Boom Length (m)	Telescopic Boom Ext. (m)	Feed roll-over	Coverage area (m^2)	Maximum Lifting angle		Max. Swing angle
Sandvik	TB 60	2250	-	1.2	358^0	54	55^0	-25^0	$\pm45^0$
	TB 40	1850	-	1.05	358^0	44.5	55^0	-30^0	$\pm40^0$
	B 26XL F	1960	-	1.7	360^0	41.4	54^0	-16^0	$\pm50^0$
	B 26 F	1850	-	1.2	360^0	38.9	45^0	-16^0	$\pm45^0$
Atlas Copco	BUT 4B	1100	1.50	0.90	360^0	23	$+55^0$	-45^0	±30
	BUT 28	1750	1.25	1.25	360^0	48	$+65^0$	-30^0	$\pm45^0$
	BUT 32	2075	1.80	1.25	360^0	41	$+65^0$	-30^0	$\pm45^0$
	BUT 35G	2860	1.80	1.60	360^0	92	$+65^0$	-30^0	$\pm45^0$

5.4 Forces acting on the monorail drilling system

In hard rock drilling, the economical blast hole drilling requires drilling equipment that is capable of both rotation and percussion. The tools used in drilling, i.e., whether percussive or rotary, handheld or mounted are subjected to great strains during drilling operations. Thrust describes the force which must be applied by the drilling system to hold a bit to the rock, make it penetrate and feed it forward as chippings are removed during drilling. Therefore, the drilling efficiency of the monorail drilling system depends on its thrust as well as its resistance to forces from the drilling unit. The stability of the monorail drilling system during drilling operations is of paramount importance in achieving high drilling performance. Therefore, both the analysis and the design of a monorail drilling system involve determining reaction forces that stabilise the monorail drilling system during drilling operations. Figures 5.7 and 5.8 summarise the forces acting on the monorail drilling system during drilling operations.

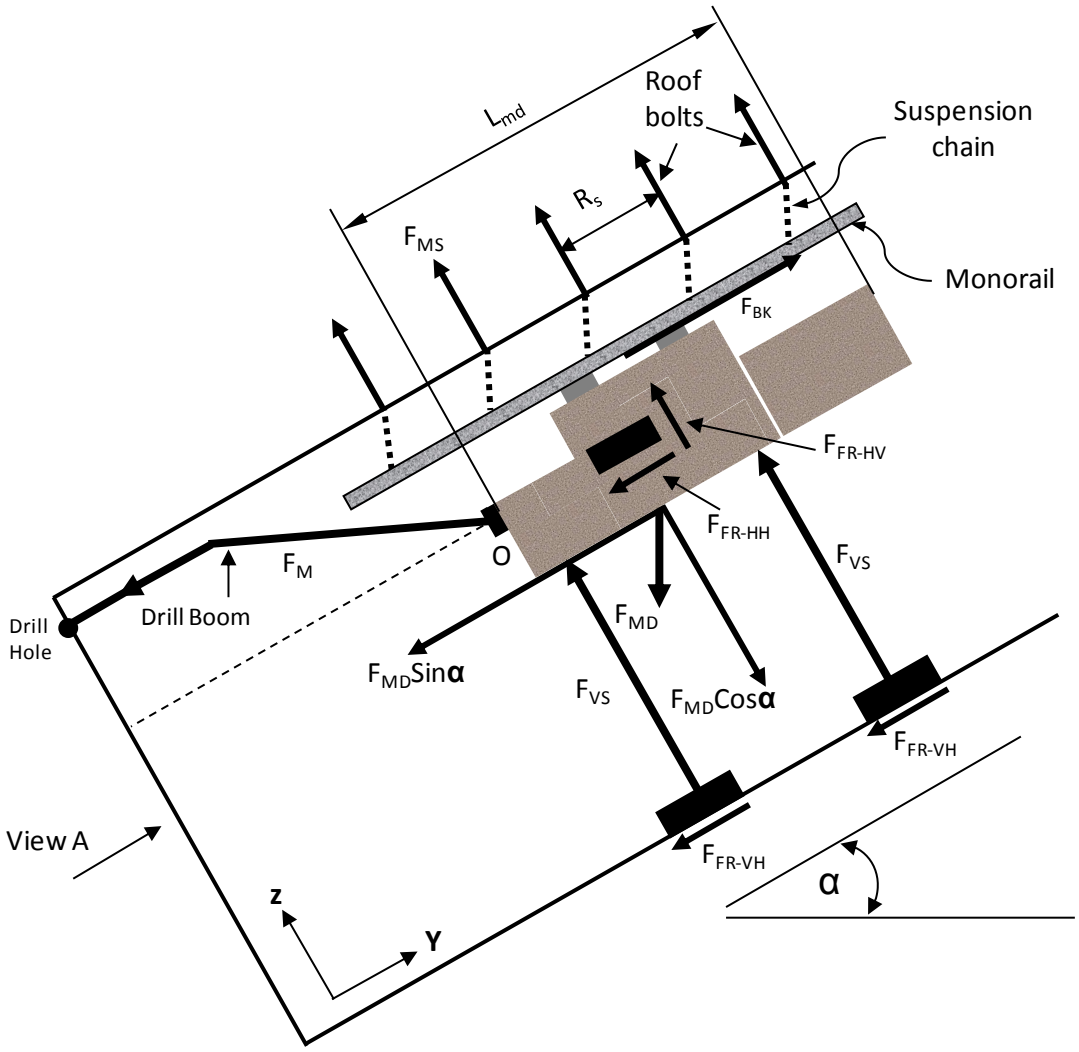

F_M = Drilling or feed force from the monorail drilling system
F_{MS} = Force suspending monorail train
F_{MD} = Force due to weight of monorail drilling system (plus weight of two drilling booms)
F_{VS} = Force in vertical stabilisers
F_{FR-VH} = Longitudinal frictional forces at base of vertical stabilisers (frictional forces in y-direction)
F_{FR-HH} = Longitudinal frictional forces at base of horizontal stabilisers (frictional forces in y-direction)
F_{FR-HV} = Vertical frictional forces at base of horizontal stabilisers
F_{BK} = Braking force
α = Decline gradient (degrees)
L_{md} = Length / span of monorail drilling system
R_s = Roof bolt spacing

Figure 5.7: Longitudinal section showing forces on the monorail drilling system

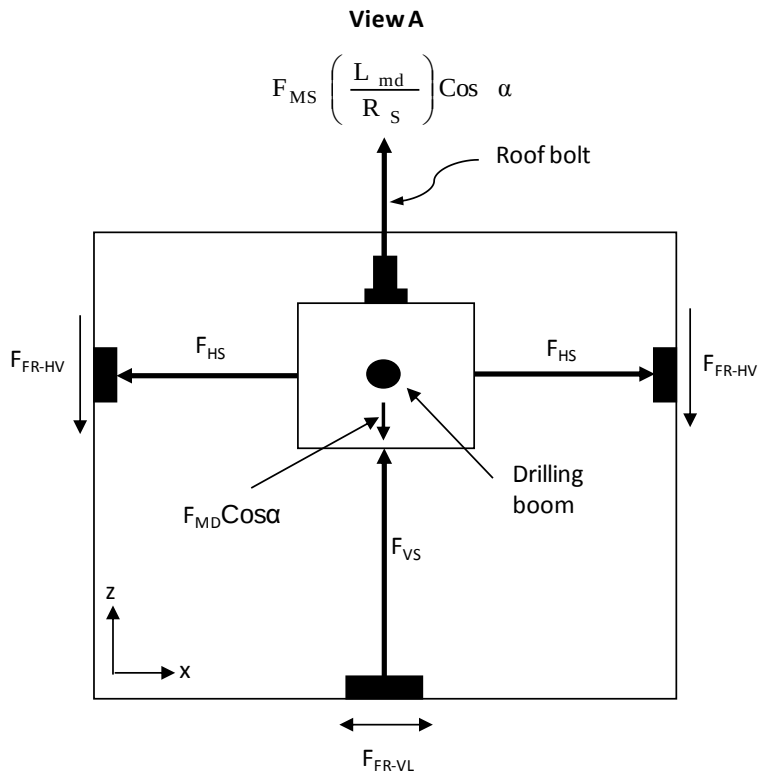

F_{MS}	=	Force suspending monorail train
F_{MD}	=	Force due to weight of monorail drilling system (plus weight of two drilling booms)
F_{VS}	=	Force in vertical stabilisers
$F_{FR\text{-}HV}$	=	Vertical frictional forces at base of horizontal stabilisers (frictional forces in z-direction)
F_{HS}	=	Forces in horizontal stabilisers
$F_{FR\text{-}HL}$	=	Lateral frictional forces at base of vertical stabilisers (frictional forces in x-direction)
α	=	Decline gradient (degrees)
L_{md}	=	Length / span of monorail drilling system
R_s	=	Roof bolt spacing

Figure 5.8: Cross- section showing forces on the monorail drilling system

The monorail drilling system will be acted upon by forces in lateral (X), longitudinal (Y) and vertical (Z) direction depending on the drilling direction of the two drilling booms. Therefore, whether the monorail drilling system remains stable during drilling operations depend on the reaction forces in horizontal and vertical stabilisers, the frictional forces at the base of the two horizontal stabilisers and the brake forces of the monorail drilling system. Reaction forces in horizontal stabilisers act on lateral forces from the two drilling units; vertical stabilisers oppose vertical forces from the drilling units while frictional forces at the base of the two horizontal stabilisers and brake forces resist longitudinal forces (i.e., resists movement of the system in Y-direction during drilling process).

5.5 Reaction forces from the monorail drilling system

As indicated in Section 5.4, three force components result from the drilling unit in X, Y and Z-directions. The magnitude of these forces varies depending on the magnitude and direction of the two drilling booms. Thus, the reaction forces from the monorail drilling system also vary according to the magnitude and direction of the three force components. In this Section, details of the three reaction force components from the monorail drilling system are presented.

5.5.1 Forces in y-direction (longitudinal forces)

As can be seen from Figure 5.7, three forces result from the monorail drilling system in y-direction. The forces include those that are due to weight of monorail drilling system, brake forces and frictional forces at the base of horizontal stabilisers. In this sub-section these forces are described in detail.

5.5.1.1 Forces due to weight of monorail drilling system

Since the monorail drilling system is inclined at decline gradient $\boldsymbol{\alpha}$, the weight of the monorail drilling system exerts forces in y-direction on the drilling unit equal to $\mathbf{F_{MD}Sin\alpha}$ (see Figure 5.7). This force is fixed and opposes forces in y-direction from the drilling unit.

5.5.1.2 Brake force

Brake force (F_{BK}) is a fixed force that results from applied brakes during monorail drilling process. These forces prevent longitudinal movements of the monorail drilling system during drilling operation. According to Scharf (2007), the braking force is calculated as follows:

$$\text{Monorail system braking Force} = 1.5 \times \text{Pulling force} \qquad 5.1$$

However, the braking force differs depending on the type of monorail system, the number of drive units and the number of brakes the system has. The EMTS with four drive units, six brakes with pulling force of 64kN has braking force equal to 96kN.

5.5.1.3 Longitudinal frictional forces at base of horizontal stabilisers

Friction results from the two surfaces being pressed together closely causing intermolecular attractive forces between molecules of different surfaces (Meriam and Kraige, 1993). As such, friction depends upon the nature of the two surfaces and the degree to which they are pressed together. Friction force opposes the motion of an object and it balances the net force tending to cause motion. When the force tending to cause motion is zero, equilibrium requires that there be no friction. According to Figure 5.9, as the opposing force (F) is increased, the friction must be equal and opposite to force tending to cause motion (P) as long as equilibrium exits.

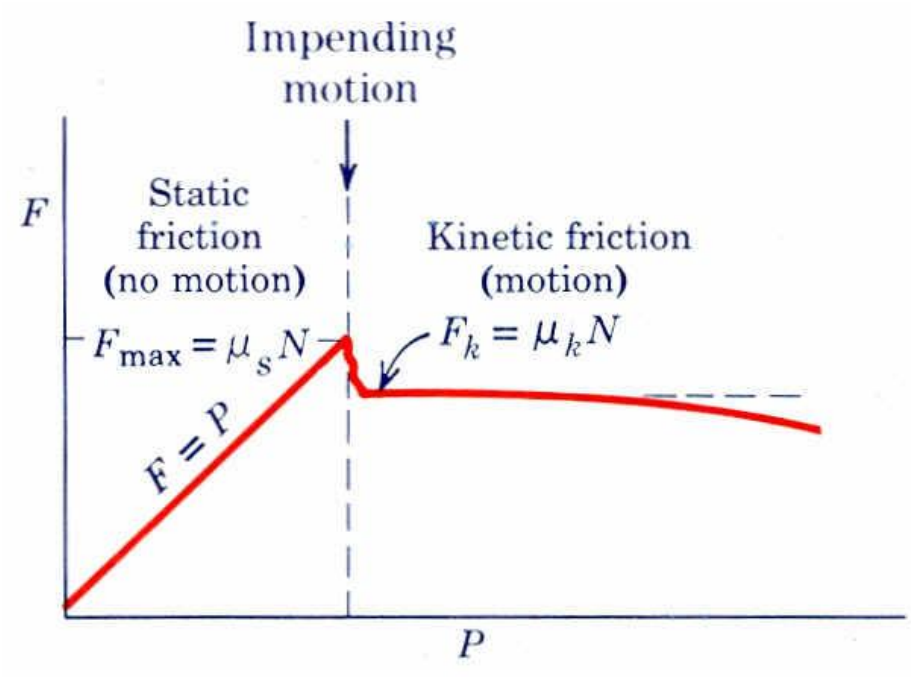

μ_s and μ_k are coefficient of static and kinetic friction

Figure 5.9: Static and kinetic frictional forces (Meriam and Kraige, 1993)

However, friction force reaches maximum value which causes the system to slip and to move in the direction of applied force. At the same time, frictional force drops slightly and rather abruptly to a lower value. Here it remains constant for an interval but then drops. After slippage occurs, a condition of kinetic friction accompanies the ensuing motion. With monorail drilling system, longitudinal friction forces ($F_{FR\text{-}HH}$) exist at the contact point between the base of the two horizontal stabilisers and the decline surface (Figure 5.7). This means, $F_{FR\text{-}HH}$ depends on normal forces in horizontal stabilisers. The maximum amount of friction force which a surface can exert upon an object just before sliding can be calculated using Coulomb friction formula as indicated in Equation 5.2 (Nisture, 2006; Meriam and Kraige, 1993). Therefore, maximum longitudinal frictional force on the monorail drilling system is determined using Equation 5.2:

$$F_{FR\text{-}HH} = \mu_s F_{HS} \qquad 5.2$$

where:

$F_{FR\text{-}HH}$ is longitudinal frictional forces at base of horizontal stabilisers;

μ_s is coefficient of static friction; and

F_{HS} is normal force in horizontal stabilisers.

Therefore, for a condition of static equilibrium, when motion is not impending, the static friction force is:

$$F_{FR\text{-}HH} < \mu_s F_{HS} \qquad 5.3$$

5.5.2 Forces in z-direction (vertical forces)

According to Figures 5.7 and 5.8, vertical forces which include forces due to weight of monorail drilling system, forces in roof bolts within L_{mb}, vertical forces at base of horizontal stabilisers and forces in vertical stabilisers results from the drilling system. Detailed description of the vertical forces is presented in this sub-section.

5.5.2.1 Forces due to weight of monorail drilling system

According to Figures 5.7 and 5.8, the monorail drilling system exerts downward forces (in Z-direction) equal to $\mathbf{F_{MD}Cos\alpha}$ due to its weight. This force opposes vertical forces from the two drilling units. It is also fixed and does not change during drilling operations.

5.5.2.2 Total force in roof bolts within span L_{md}

Figure 5.7 also indicates that the total force required to suspend the monorail drilling system is the sum of individual force in the roof bolt installed within the span L_{md}. The total force is necessary for suspending the monorail drilling system before releasing the hydraulic stabilisers. This force, therefore, depends on the force in each roof bolt within the span L_{md}. To suspend the monorail drilling system, the total force in the roof bolts within L_{md} should be larger than the total weight of the monorail drilling system. According to Figure 5.7, the total force in the roof bolts installed within L_{md} is determined by first determining the total number of roof bolts installed within L_{md}. Since the roof bolt spacing (R_s) is known, the total number of roof bolts is determined as follows:

$$\text{Total number of roof bolts within } L_{md} = \left(\frac{L_{md}}{R_s}\right) \qquad 5.4$$

Thus, the total force from installed roof bolts within the span L_{md} is the product of the total number of roof bolts (Equation 5.4) and the force in each roof bolt (F_{MS}) as indicated below:

$$\text{Total force in roof bolts within } L_{md} = F_{MS}\left(\frac{L_{md}}{R_s}\right)$$

$$\text{Total force in roof bolts in Z-direction within } L_{md} = F_{MS}\left(\frac{L_{md}}{R_s}\right)Cos\alpha \qquad 5.5$$

5.5.2.3 Vertical frictional forces at base of horizontal stabilisers

Vertical frictional forces ($F_{FR\text{-}HV}$) in the two horizontal stabilisers tend to oppose the vertical movement of the monorail drilling system. These forces depend on the normal forces in vertical stabilisers and the coefficient of static friction between the base of the two horizontal stabilisers and the decline surface. However, the monorail drilling system is well supported by vertical stabilisers in the vertical direction during drilling, hence $F_{FR\text{-}HV}$ components are ignored (i.e., $F_{FR\text{-}HV}$ =0).

5.5.2.4 Forces in vertical stabilisers

To stabilise the monorail drilling system in vertical direction, two vertical stabilisers are used. The forces in vertical stabilisers oppose resultant vertical forces from the two drilling units. Thus, whether or not the monorail drilling system would fail under any given load depends on the ability of the two vertical stabilisers to withstand drilling forces.

5.5.3 Forces in x-direction (lateral forces)

According to Figures 5.7 and 5.8, lateral forces, which include forces in horizontal stabilisers and frictional forces at the base of vertical stabilisers, result from the drilling system. Detailed description of the lateral forces is presented in this sub-section.

5.5.3.1 Lateral forces in horizontal stabilisers

Lateral stabilisation of the monorail drilling system is achieved by means of forces in horizontal stabilisers (F_{HS}) as shown in Figure 5.8. The forces in horizontal stabilisers oppose drilling forces tending to cause motion of the drilling system in lateral direction. Thus, to counteract lateral forces resulting from the two drilling units, there should be equal and opposite forces from the monorail drilling system in a lateral direction from the horizontal stabilisers.

5.5.3.2 Lateral frictional forces at base of vertical stabilisers

As indicated in Figure 5.8, during drilling operations, lateral frictional forces (F_{FR-VL}) results between the base of the two vertical stabilisers and the decline floor. The direction of action of the frictional forces always opposes the motion or impending motion. These forces also depend on the position of the two drilling booms with respect to the Z-axis, the normal forces in vertical stabilisers and the coefficient of static friction. Since the monorail is well-supported in x-direction by horizontal stabilisers, F_{FR-VL} components are ignored (i.e., $F_{FR-VL}=0$).

5.6 Forces from the monorail drilling unit

Since the drilling boom can be defined as a directed line segment in space, it can be represented as a vector **OV** in 3D space as indicated in Figure 5.10.

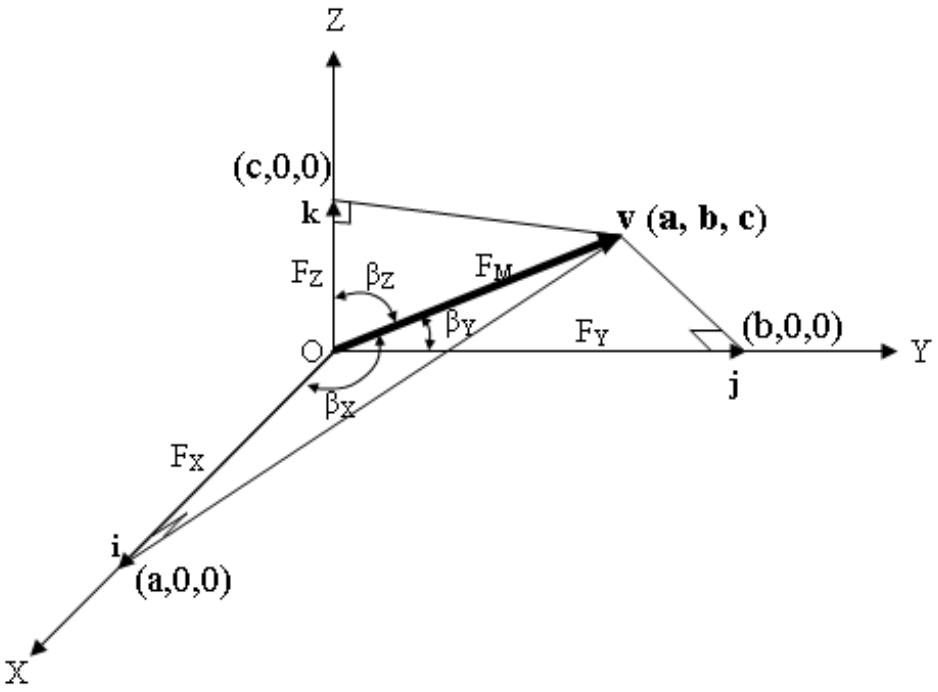

Figure 5.10: Drilling boom represented as line segment in 3D space

Therefore, during drilling with maximum drill force F_M, three force components (i.e., F_X, F_Y and F_Z) results from the drilling unit in X, Y and Z direction respectively. In mechanics involving 3D forces, it is often necessary to resolve a

force into its three mutually perpendicular components during the analysis (Meriam and Kraige, 1993; Hall et al., 1999).

5.6.1 Resolution of drilling force (F_M) into its components

In Figure 5.10, ***v*** (representing a drill boom) can be represented as a vector in 3D positioned so that its initial point is at the origin, **O** (representing pivoting point of drill boom on the monorail train) of the rectangular coordinate system. The coordinates (***a, b, c***) of the terminal point of ***v*** can be written as ***v*** = (***a, b, c***) with vector, ***v*** = ***a*****i** + ***b*****j** + ***c*****k** and direction angles[1] β_X, β_Y and β_Z (Meriam and Kraige, 1993; Hall et al., 1999). The length of the vector ***v***, denoted by $\|v\|$, is the distance from the origin (**O**) to the point (***a, b, c***) and can be found as:

$$\|v\| = \sqrt{\left(a^2 + b^2 + c^2\right)} \qquad 5.6$$

With the monorail drilling system, the components of drilling force (F_M) depend on the direction angles of the drilling boom (i.e., position in space of the drilling boom) and the coordinates in 3D of the terminal point ***v,*** i.e., the length of drilling boom. Therefore, to determine the direction angles of the drilling boom, direction cosines of the vector ***v*** = ***a*****i** + ***b*****j** + ***c*****k** are used as follows:

$$\mathrm{Cos}\beta_X = \frac{\mathrm{a}}{\|\mathrm{v}\|} \qquad 5.7$$

$$\mathrm{Cos}\beta_Y = \frac{\mathrm{b}}{\|\mathrm{v}\|} \qquad 5.8$$

$$\mathrm{Cos}\beta_Z = \frac{\mathrm{c}}{\|\mathrm{v}\|} \qquad 5.9$$

Given F_M as the maximum drilling force of the drilling system through origin O, the line of action of the drilling boom is inclined to three mutually perpendicular axes O_X, O_Y, and O_Z with direction angles β_X, β_Y, and β_Z respectively. Therefore, to determine the component of the drilling force (F_M) acting on the monorail

[1] Direction angles β_X, β_Y and β_Z are angles the vector ***v*** makes with the positive x, y and z-axis

drilling system, the drilling force (F_M) is regarded as the diagonal of a rectangular parallelepiped whose sides are ***a, b*** and ***c*** in the direction $\boldsymbol{v} = \boldsymbol{a}\mathbf{i} + \boldsymbol{b}\mathbf{j} + \boldsymbol{c}\mathbf{k}$. As depicted in Figure 5.10 the triangle XOV is right angled with X-axis and $\mathbf{F_X = F_M Cos\beta_X}$. Similarly, for triangle YOP and ZOP we see that $\mathbf{F_Y = F_M Cos\beta_Y}$ and $\mathbf{F_Z = F_M Cos\beta_Z}$ respectively. Therefore, the magnitudes of the three force components depend on the drilling force (F_M), the coordinates ***a, b, c*** and the boom length $\|v\|$. The three force components of F_M in X, Y and Z-direction are summarised in Figure 5.11.

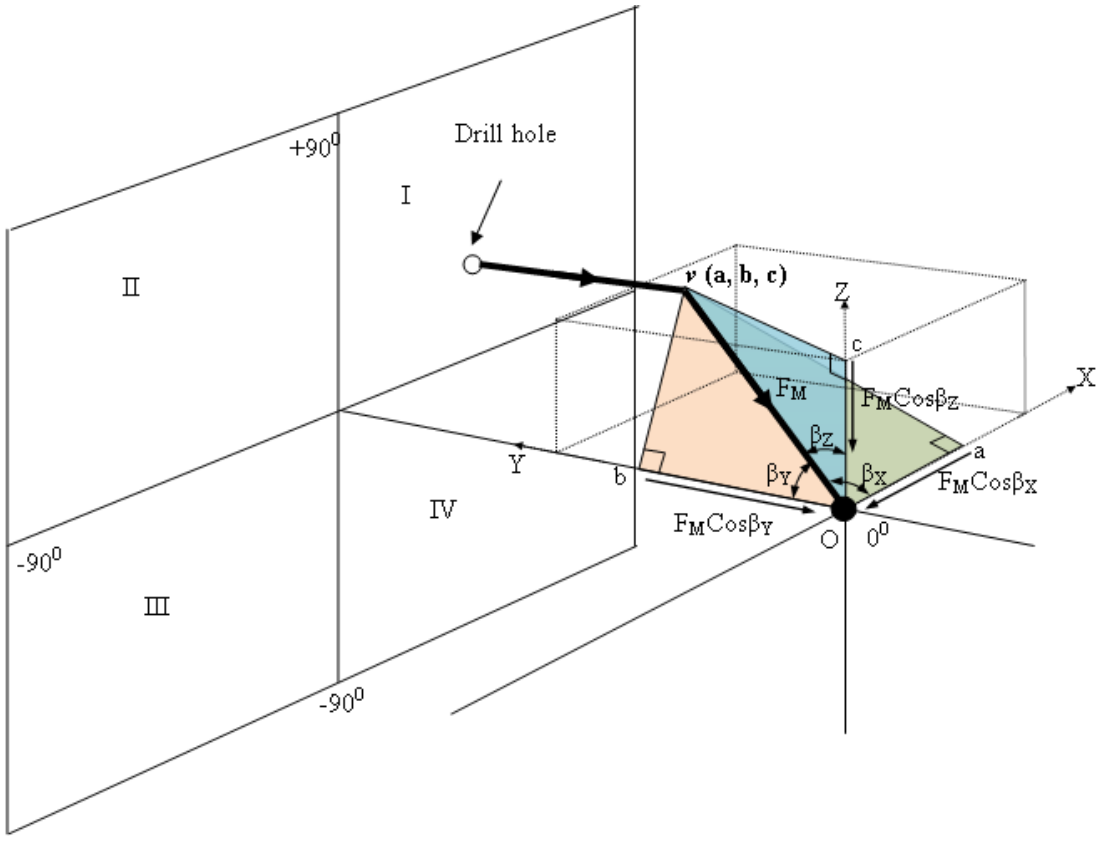

Figure 5.11: Forces acting on the monorail drilling system from the drilling unit

Two drilling booms will be mounted onto the monorail train and the force components from the second drilling boom are given as follows:

$$F_X = F_M{}^1 Cos\beta^1{}_X \qquad 5.10$$

$$F_Y = F_M{}^1 Cos\beta^1{}_Y \qquad 5.11$$

$$F_Z = F_M{}^1 Cos\beta^1{}_Z \qquad 5.12$$

where:

$F_M{}^1$ is the drilling force from the second drilling boom; and

$\beta^1{}_X$, $\beta^1{}_Y$, $\beta^1{}_Z$ are direction angles of the second drilling boom to three mutually perpendicular axes O_X, O_Y, and O_Z respectively.

Therefore, for two drilling booms mounted on the monorail train, at least two forces from the two drilling booms act on the monorail drilling system in each of the X, Y and Z directions. The forces acting in each direction are indicated below:

$$F_X = F_M Cos\beta_X + F_M{}^1 Cos\beta^1{}_X \text{ (Lateral)} \quad 5.13$$

$$F_Y = F_M Cos\beta_Y + F_M{}^1 Cos\beta^1{}_Y \text{ (Longitudinal)} \quad 5.14$$

$$F_Z = F_M Cos\beta_Z + F_M{}^1 Cos\beta^1{}_Z \text{ (Vertical)} \quad 5.15$$

5.6.2 Drilling boom vector definition

As indicated in Section 5.6.1, the forces acting on the monorail drilling system depend on the position in space of the two drilling booms with respect to the X, Y and Z-axes. Therefore, to determine the components of drilling force, the boom length $\|v\|$ and direction of the two drilling booms are critical. Hence, the reaction forces from the monorail drilling system will also depend on the length and direction of the two drilling booms as well.

Considering the origin, **O** (i.e., the pivoting point) as the starting point, the vectors $\boldsymbol{v}$ and $\boldsymbol{v^1}$ (i.e., positions of two drilling booms) can be described by specifying their end points in Cartesian coordinates $\boldsymbol{(a, b, c)}$ and $\boldsymbol{(a^1, b^1, c^1)}$ respectively. This means that the two drilling booms can be described in vector form with coordinates $\boldsymbol{(a, b, c)}$ and $\boldsymbol{(a^1, b^1, c^1)}$ in 3D where $\boldsymbol{a, b, c}$ and $\boldsymbol{a^1, b^1, c^1}$ are real numbers. Therefore, the position vectors $\boldsymbol{v}$ and $\boldsymbol{v^1}$ of the two drilling booms at any point are the vectors represented by two line segments from the origin O, to end points $\boldsymbol{v}$ and $\boldsymbol{v^1}$.

In development face drilling, the coordinates **(*a, c*)** and **(a^1, c^1)** depend on the size of the development face being drilled, i.e., the coordinate ***a*** represents the distance from the origin **O** to the side walls of the decline while **c** represents distance from origin, **O** to the roof or floor of the decline. In defining the two drilling booms as vectors, the minimum decline opening requirements (dimensions) for monorail system installation are used as shown in Figure 5.12.

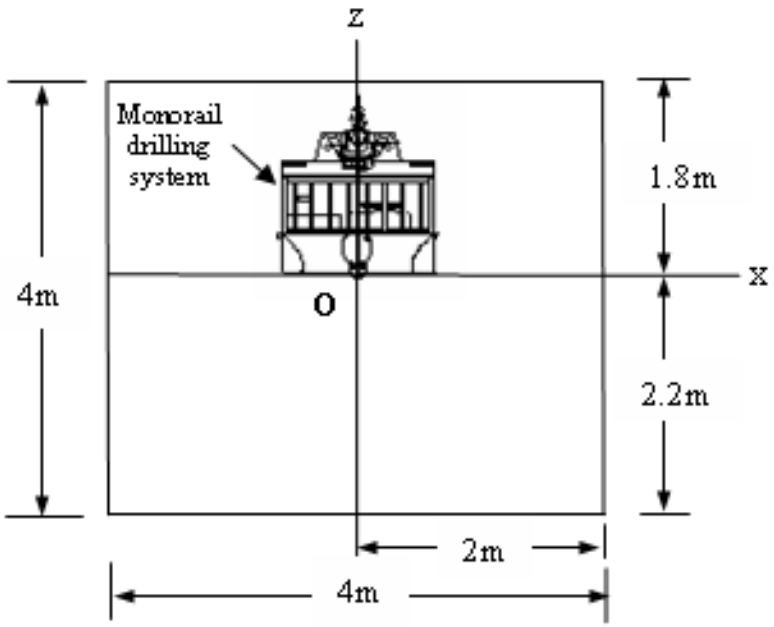

Figure 5.12: Dimensions of decline opening showing position of monorail system for vector definition

The dimensions shown in Figure 5.12 give the exact position of the origin O, (i.e., pivoting position of drilling booms) relative to the development face being drilled. Dimension of 4m x 4m is used as minimum decline opening instead of 3m x 3m as recommended by the manufacturers of the train because this is the size of decline opening which will be used during mine design case study (Chapter 10). According to Figure 5.10 and Figure 5.11, the two drilling booms can be represented as vectors with end point having coordinates **(a, b, c)** and **(a^1, b^1, c^1)** respectively as follows:

$$\boldsymbol{v} = a\mathbf{i} + b\mathbf{j} + c\mathbf{k} \qquad 5.16$$

$$\boldsymbol{v}^1 = a^1\mathbf{i} + b^1\mathbf{j} + c^1\mathbf{k} \qquad 5.17$$

The vector components **bj** and **b¹j** represents the longitudinal (y-axis), i.e., from the origin **O**, to the development face. According to Figure 2.20 (Chapter 2), it was assumed that the monorail drilling system drills from a distance of ≤10m from the development face. Therefore, the total distance of the drilling boom from the joint **O** to the drill face is 10m. This means the total boom length (i.e., feed length plus boom length) of the system is 10m. In this study, it is assumed that the monorail drilling system has a fixed boom segment of 2.5m. Therefore, the values of vector **b** and **b¹** have a minimum value of 2.5m and maximum value of 10m. The range of values for ***a, b*** and **c** is summarised below:

$$-2\text{m} \le \text{a} \le 2\text{m} \qquad -2\text{m} \le \text{a}^1 \le 2\text{m}$$
$$2.5\text{m} \le \text{b} \le 10\text{m} \qquad 2.5\text{m} \le \text{b}^1 \le 10\text{m}$$
$$-2.2\text{m} \le \text{c} \le 1.8\text{m} \qquad -2.2\text{m} \le \text{c}^1 \le 1.8\text{m}$$

5.7 Stabilisation of the monorail drilling system

In this Section, models that are used to determine balancing forces (i.e., stabilisation forces in X, Y and Z directions) from the monorail drilling system are developed.

5.7.1 Stabilisation in y-direction

According to Figures 5.7 and 5.8, the monorail drilling system remains stable in longitudinal or y-direction during drilling operations when the sum of all action and reaction forces in y-direction on the system are equal to zero i.e.:

$$\sum \text{F}_\text{Y} = 0 \qquad 5.18$$

where:

$\sum \text{F}_\text{Y}$ is the sum of action and reaction forces in y-direction on the system.

However, forces in y-direction acting on the monorail drilling system are:

1) Forces from two drilling units, i.e., $F_M Cos\beta_Y + F^1{}_M Cos\beta^1{}_Y$
2) Braking forces, i.e., F_{BK}

Reaction forces in y-direction from monorail drilling system are:

1) Forces due to weight of monorail drilling system, i.e., $F_{MD} Sin\alpha$
2) Frictional forces in y-direction in the two vertical stabilisers, i.e., $2F_{FR-VH}$
3) Frictional forces in y-direction in the two horizontal stabilisers, i.e., $2F_{FR-HH}$

In equilibrium, action and reaction forces in y-direction on the monorail drilling system are equal. Therefore:

$$F_{MD} Sin\alpha + 2F_{FR-VH} + 2F_{FR-HH} = F_M Cos\beta_Y + F^1{}_M Cos\beta^1{}_Y + F_{BK} \qquad 5.19$$

Assumption

In this study, it is assumed that all the longitudinal action forces from the two drilling units are opposed by longitudinal friction forces in the two horizontal stabilisers and brake forces. This means that frictional forces at the base of the two vertical stabilisers are negligible (i.e., $F_{FR-VH} = 0$) making vertical stabilisers stationary during drilling operations. Therefore, with this assumption, F_{FR-HH} can be determined as indicated in Equation 5.20:

$$F_{FR-HH} = \frac{1}{2}\left[F_M Cos\beta_Y + F_M^1 Cos\beta_Y^1 + F_{BK} - F_{MD} Sin\alpha\right] \qquad 5.20$$

However, from Equation 5.8, $Cos\beta_Y = \frac{b}{\|v\|}$ and $Cos\beta^1{}_Y = \frac{b^1}{\|v^1\|}$, hence Equation 5.20 can be written as follows:

$$F_{FR-HH} = \frac{1}{2}\left[F_M \times \frac{b}{\|v\|} + F_M^1 \times \frac{b^1}{\|v^1\|} + F_{BK} - F_{MD}\,\mathrm{Sin}\alpha \right] \qquad 5.21$$

5.7.1.1 Minimum frictional forces in y-direction

Minimum frictional forces in horizontal stabilisers result when the monorail drilling system is drilling holes at extreme points on the face along the X-axis, i.e., at maximum values of $\boldsymbol{a}$ and $\boldsymbol{a^1}$. However, as vectors $\boldsymbol{a}$ and $\boldsymbol{a^1}$ approach maximum, i.e., 2m, the vectors $\boldsymbol{c}$ and $\boldsymbol{c^1}$ approach maximum value, i.e., $\boldsymbol{c}$ and $\boldsymbol{c^1}\rightarrow$ 1.8m. From Section 5.6.2, it was assumed that the minimum boom length in 2.5m, thus the minimum value of vectors $\boldsymbol{b}$ and $\boldsymbol{b^1}$ is 2.5m. This means also that the minimum longitudinal force is determined when $\boldsymbol{b} = \boldsymbol{b^1} \rightarrow$ 2.5m, $\boldsymbol{a} = \boldsymbol{a^1}\rightarrow$2m and as $\boldsymbol{c} = \boldsymbol{c^1}\rightarrow$ 1.8m. Therefore, to determine the minimum longitudinal force, the two drilling booms will have vectors $\boldsymbol{v}$ = **2i** + **2.5j** + **1.8k** and $\boldsymbol{v^1}$ = **2i** + **2.5j** + **1.8k** with minimum boom length $\|v\|$ of 3.67m. Thus, with this minimum boom length, as $\boldsymbol{a}$, $\boldsymbol{a^1}$, **c** and $\boldsymbol{c^1}$ approach maximum, the maximum swing angle (in lateral direction) of the drilling booms will be 33^0 (calculated from trigonometry).

5.7.1.2 Maximum frictional forces in y-direction

Maximum longitudinal frictional force on the drilling system results when the two drilling booms are drilling longitudinally, i.e., the values of $\boldsymbol{a} = \boldsymbol{a^1}\rightarrow 0$ and $\boldsymbol{c} = \boldsymbol{c^1}\rightarrow 0$. Therefore, as $\boldsymbol{a} = \boldsymbol{a^1}\rightarrow 0$ and $\boldsymbol{c} = \boldsymbol{c^1}\rightarrow 0$, the values of $\boldsymbol{b} = \boldsymbol{b^1}$ approach maximum or minimum value, i.e., 2.5m or 10m making the two drilling booms horizontal.

5.7.2 Stabilisation in z-direction

According to Figure 5.7 and Figure 5.8, the monorail drilling system will remain in vertical equilibrium (i.e., z-direction) when the sum of action and reaction vertical forces on the system is equal to zero:

$$\sum F_Z = 0 \qquad 5.22$$

where:

$\sum F_Z$ is the sum of action and reaction forces in z-direction acting on monorail drilling system.

Thus,

$$\sum \text{Upward forces} = \sum \text{Downward forces} \qquad 5.23$$

For two drilling units and two vertical stabilisers, Figures 5.7 and 5.8 give the following upward and downward forces:

$$\sum \text{Upward forces} = 2F_{VS} + F_{MS}\left(\frac{L_{md}}{R_s}\right) + 2F_{FR\text{-}HV} \qquad 5.24$$

$$\sum \text{Downward forces} = F_{MD}\,\text{Cos}\,\alpha + F_M \text{Cos}\beta_Z + F^1{}_M \text{Cos}\beta^1{}_Z \qquad 5.25$$

However, for the monorail drilling system to be in vertical equilibrium, the upward forces must be equal to the downward forces. Therefore, equating Equations 5.24 and 5.25 gives:

$$2F_{FV} + F_{MS}\left(\frac{L_{md}}{R_s}\right) + 2F_{FR\text{-}HV} = F_{MD}\text{Cos}\alpha + F_M \text{Cos}\beta_z + F_M^1 \text{Cos}\beta_z^1 \qquad 5.26$$

Assumption

It is assumed that vertical reaction from the drilling system is through vertical stabilisers only. As given in Section 5.5.2.3, this means that the frictional force ($F_{FR\text{-}HV}$) in z-direction in horizontal stabilisers is ignored (i.e., $F_{FR\text{-}HV} = 0$). Therefore, using this assumption and Equation 5.26, the force in each vertical stabiliser, when the drilling system is drilling up holes, can be determined as follows:

$$F_{VS} = \frac{1}{2}\left(F_{MD}\text{Cos}\,\alpha + F_M\text{Cos}\beta_Z + F_M^1\text{Cos}\beta_Z^1 - F_{MS}\frac{L_{md}}{R_s}\text{Cos}\alpha \right) \qquad 5.27$$

However, when the drilling system is drilling down holes, the two drilling units will exert upward forces on the drilling system, i.e., all drilling forces will be directed upwards. In this situation, the weight of the monorail is cardinal in ensuring the stability of the drilling system, i.e., the weight of system should resist drilling forces. Therefore, from Equation 5.27, when the drilling system is drilling down holes the forces in vertical stabiliser can be written as indicated in Equation 5.28:

$$F_{VS} = \frac{1}{2}\left(F_{MD}\text{Cos}\,\alpha - F_M\text{Cos}\beta_Z - F_M^1\text{Cos}\beta_Z^1 - F_{MS}\frac{L_{md}}{R_s}\text{Cos}\alpha \right) \qquad 5.28$$

It was further assumed that the forces in z-direction from the drilling unit will be opposed by the vertical stabilisers only. This means that the forces in z-direction will not affect the monorail support system, i.e., roof bolts. With this assumption, the change in forces in roof bolts is ignored during drilling operation, i.e., $\Delta F_{MS}\left(\frac{L_{md}}{R_s}\right)\text{Cos}\alpha = 0$. Therefore, Equation 5.27 and 5.28 can be written as:

$$F_{VS} = \frac{1}{2}\left(F_{MD}\text{Cos}\,\alpha + F_M\text{Cos}\beta_Z + F_M^1\text{Cos}\beta_Z^1 \right) \qquad 5.29$$

$$F_{VS} = \frac{1}{2}\left(F_{MD}\text{Cos}\,\alpha - F_M\text{Cos}\beta_Z - F_M^1\text{Cos}\beta_Z^1 \right) \qquad 5.30$$

Thus, whether or not the monorail drilling system will resist vertical drilling forces depends on the force from vertical stabilisers F_{VS} as well as the position of the holes being drilled, i.e., up or down holes. Using Equation 5.9, i.e., $\text{Cos}\beta_Z = \frac{c}{\|v\|}$ and $\text{Cos}\beta_Z^1 = \frac{c^1}{\|v^1\|}$, Equations 5.29 and 5.30 can be written as follows:

$$F_{VS} = \frac{1}{2}\left(F_M \frac{c}{\|v\|} + F_M^1 \frac{c^1}{\|v^1\|} + F_{MD} Cos\alpha \right) \quad 5.31$$

$$F_{VS} = \frac{1}{2}\left(F_M \frac{c}{\|v\|} - F_M^1 \frac{c^1}{\|v^1\|} - F_{MD} Cos\alpha \right) \quad 5.32$$

5.7.2.1 Minimum force in vertical stabilisers

The minimum force in vertical stabilisers results when the system is drilling extreme down holes on the development face. Since the monorail drilling system is suspended on the monorail (in the decline roof), drilling of down holes at the development face will exert upward vertical forces on the monorail drilling system. This means that the maximum downward lifting angle of the system should be enough to enable the drilling system to drill all the holes at the lowest point (bottom) of the drill face, i.e., the drilling system should be able to cover the whole drill face during drilling operations. Thus, as ***c*** and ***c¹*** approach minimum of -2.2m and as ***a*** and ***a¹*** approach minimum of 0, ***b*** approaches minimum value of 2.5m. Also, the vectors ***v*** = **0i** + **2.5j** - **2.2k** and ***v¹*** = **0i** + **2.5j** - **2.2k,** will have minimum boom length of 3.33m. The resultant force is negative meaning that the force acts upwards, i.e., it pushes the monorail drilling system upwards. Therefore, computing the swing angle of the two vectors using trigonometry gives the maximum downward swing angle of 41^0. However, for the monorail drilling system to be vertically stable, the weight of the system in Z-direction ($F_{MD}Cos\alpha$) must be more than the upward force from the drilling unit (i.e., $F_MCos\beta_Z + F^1{}_MCos\beta^1{}_Z < F_{MD}Cos\alpha$).

5.7.2.2 Maximum force in vertical stabilisers

According to Equation 5.31, the maximum force in vertical stabilisers results when the monorail drilling system is drilling extreme up holes along the Z-axis on the development face, i.e., as **c** = ***c¹*** approaches maximum (***c = c¹*** →1.8m), ***a*** and ***a¹*** →***0*** and ***b = b¹*** approaches minimum of 2.5m. Therefore, the vectors ***v*** = **0i**

+ **2.5j** + **1.8k** and $\mathbf{v^1}$ = **0i** + **2.5j** + **1.8k** have maximum length (i.e., boom length) of 3.1m. Computing the maximum upward lifting angle using trigonometry gives 35^0.

5.7.3 Stabilisation in x-direction

For the monorail drilling system to remain in equilibrium in x-direction during drilling operations, the sum of all lateral forces (along X-axis), i.e., the sum of action forces from the drilling unit and reaction forces from the monorail drilling system must be equal to zero:

$$\sum F_X = 0 \qquad 5.33$$

where:

$\mathbf{\sum F_X}$ is the sum of action and reaction forces in x-direction on monorail drilling system.

Thus,

∑Lateral forces from drilling units = ∑Lateral forces from monorail drilling system 5.34

The maximum lateral reaction force on the monorail drilling system is exerted when the two drilling units are drilling on the same side of the Z-axis with drilling booms in horizontal position (along the X-axis). Therefore, all the lateral forces from the drilling unit are opposed by one horizontal stabiliser opposite to the direction of force. From Figures 5.7 and 5.8, for two drilling units and two horizontal stabilisers, the following lateral forces exist:

$$\sum \text{Lateral forces from the drilling unit} = F_M Cos\beta_x + F_M^1 Cos\beta_x^1 \qquad 5.35$$

$$\sum \text{Lateral Forces from monorail drilling system} = F_{HS} + 2F_{FR-VL} \qquad 5.36$$

Equating Equations 5.35 and 5.36 gives:

$$F_{HS} + 2F_{FR-VL} = F_M Cos\beta_x + F_M^1 Cos\beta_x^1 \qquad 5.37$$

Assumption

All action forces in x-direction from the two drilling units are opposed by reaction forces in horizontal stabilisers. As indicated in Section 5.5.3.2, the frictional forces in x-direction at the base of the vertical stabilisers are ignored, i.e., $F_{FR-VL} = 0$. With this assumption, determining the minimum force in each horizontal stabiliser (F_{HS}) from Equation 5.37 gives the following:

$$F_{HS} = F_M Cos\beta_X + F_M^1 Cos\beta_X^1 \qquad 5.38$$

From Equation 5.7, i.e., $Cos\beta_Z = \frac{a}{\|v\|}$ and $Cos\beta_Z = \frac{a^1}{\|v\|}$, Equation 5.38 can be written as:

$$F_{HS} = F_M \frac{a}{\|v\|} + F_M^1 \frac{a^1}{\|v\|} \qquad 5.39$$

5.7.3.1 Minimum force in horizontal stabilisers

The minimum force in horizontal stabilisers results when the system is drilling horizontal holes along the Y-axis, i.e., when $\boldsymbol{a}$ and $\boldsymbol{a^1}$ approach zero ($\boldsymbol{a} = \boldsymbol{a^1} \rightarrow 0$) and $\boldsymbol{c}$ and $\boldsymbol{c^1}$ approach 0 ($\boldsymbol{c}$ and $\boldsymbol{c^1} \rightarrow 0$). Therefore, as $\boldsymbol{a}$, $\boldsymbol{a^1}$, $\boldsymbol{c}$ and $\boldsymbol{c^1}$ tend to zero, $\boldsymbol{b}$ and $\boldsymbol{b^1}$ approach minimum or maximum value of 2.5m or 10m, respectively. This also means that the drilling boom will have vector $\boldsymbol{v}$ = **0i** + **2.5j** + **0k** (or $\boldsymbol{v}$ = **0i** + **10j** + **0k**) and $\boldsymbol{v^1}$ = **0i** + **2.5j** + **0k** (or $\boldsymbol{v^1}$ = **0i** + **10j** + **0k**) with drilling boom length varying from minimum 2.5m to maximum 10m along Y-axis.

5.7.3.2 Maximum force in horizontal stabilisers

The maximum force in horizontal stabilisers is exerted on the system when drilling extreme holes along the X-axis, i.e., when $\boldsymbol{a}$ and $\boldsymbol{a^1}$ approach maximum (as $\boldsymbol{a}$ and $\boldsymbol{a^1} \rightarrow$ 2m) and $\boldsymbol{c}$ and $\boldsymbol{c^1}$ approach minimum (as $\boldsymbol{c}$ and $\boldsymbol{c^1} \rightarrow$ 0). From Section 5.7.1.1, it was determined that the maximum swing angle was 33^0. Therefore, as $\boldsymbol{a}$ and $\boldsymbol{a^1} \rightarrow$ 2m and $\boldsymbol{c}$ and $\boldsymbol{c^1} \rightarrow$ 0, the boom length approaches 3.67m and $\boldsymbol{b}$ and $\boldsymbol{b^1}$ approach 2.5m. This means that the two drilling booms have vectors $\boldsymbol{v} = \mathbf{2i} + \mathbf{2.5j} + \mathbf{0k}$ and $\boldsymbol{v^1} = \mathbf{2i} + \mathbf{2.5j} + \mathbf{0k}$, with maximum boom length of 3.67m.

5.8 Stabilisation of monorail drilling system

Section 5.6.1 has shown that the monorail drilling system is acted upon by forces from the drilling unit in vertical, longitudinal and lateral directions. These forces make the monorail drilling system unstable during drilling process. Therefore, to stabilise the monorail drilling system, it is necessary to determine the magnitude of reaction forces in longitudinal, vertical and lateral directions of the monorail drilling system. These reaction forces will oppose action forces resulting from the drilling unit and by so doing making the system stable.

5.8.1 Method

To determine reaction forces in horizontal and vertical stabilisers of the monorail drilling system, models developed in Section 5.7 were used. Using maximum feed force of 25kN as highlighted in Table 5.2, maximum and minimum possible reaction forces in horizontal and vertical stabilisers have been determined. Additionally, using the models developed, minimum and maximum frictional forces in y-direction at the base of horizontal stabilisers have also been determined.

5.8.2 System assumptions

The following assumptions were made during the analysis:

1) The monorail drilling system has a braking force (F_{BK}) of 96kN;
2) Decline gradient (α) of 20^0 was used;
3) According to Scharf (2007), the monorail system with four drive units weighs 92kN. However, the two drilling booms that will be mounted onto the drilling system would increase the weight of the drilling system. Therefore, in this study, the total weight of the two drilling booms is assumed to be half the weight of the monorail train. Thus, the total weight of the two drilling booms is 46kN giving the train a total weight of 138kN;
4) Frictional forces in y-direction at the base of the two vertical stabilisers are ignored (i.e., $F_{FR\text{-}VH} = 0$);
5) Frictional forces in z-direction at the base of horizontal stabilisers are ignored (i.e., $F_{FR\text{-}HV} = 0$);
6) Frictional forces x-direction at the base of the vertical stabilisers are ignored (i.e., $F_{FR\text{-}VL} = 0$); and
7) The drilling boom has a lifting angle of -41^0 and $+35^0$ and swing angle of 33^0.

5.8.3 Stabilisation forces in y-direction

In this Section, the magnitude of minimum and maximum stabilisation forces in y-direction is determined using the models developed.

5.8.3.1 Minimum frictional forces

The magnitude of minimum frictional forces in y-direction at the base of horizontal stabilisers is determined using Equation 5.21 under the following conditions:

$F_{FR\text{-}HH}$		$F_{FR\text{-}HH}$	
	$\boldsymbol{a} \rightarrow 2\text{m}; \boldsymbol{b} \rightarrow 2.5\text{m};$ $\boldsymbol{c} \rightarrow 1.8\text{m}; \lVert v \rVert \rightarrow 3.67m$		$\boldsymbol{a^1} \rightarrow 2\text{m}; \boldsymbol{b^1} \rightarrow 2.5\text{m};$ $\boldsymbol{c^1} \rightarrow 1.8\text{m}; \lVert v^1 \rVert \rightarrow 3.67m$

Using the maximum feed force of 25kN and decline gradient ($\boldsymbol{\alpha}$) of 20^0, minimum frictional force in horizontal stabilisers was determined as indicated in Table 5.4. Table 5.4 shows that the minimum frictional force ($F_{FR\text{-}HH} = F_Y$) at the base of horizontal stabilisers is 82kN.

Table 5.4: Minimum frictional force in y-direction at base of horizontal stabilisers

Max. feed force (F_M)	**Vector coordinates**			***b = b¹*** **(m)**	$\lVert v \rVert$ **(m)**	$\lVert v^1 \rVert$ **(m)**	**F_Y (kN)**	**$F_{FR\text{-}HH\ (min)}$ (kN)**
	a = a¹	***b = b¹***	***c = c¹***					
25	2	2.5	1.8	2.5	3.67	3.67	82	82

5.8.3.2 Maximum frictional forces

Maximum frictional force in y-direction at the base of horizontal stabilisers was also determined using Equation 5.21 under the following conditions:

$F_{FR\text{-}HH}$		$F_{FR\text{-}HH}$	
	$2.5\text{m} \leq \boldsymbol{b} \leq 10\text{m};$ $\boldsymbol{a} = \boldsymbol{c} = 0;\ 2.5\text{m} \leq \lVert v \rVert \leq 10\text{m}$		$2.5\text{m} \leq \boldsymbol{b^1} \leq 10\text{m};$ $\boldsymbol{a^1} = \boldsymbol{c^1} = 0;\ 2.5\text{m} \leq \lVert v^1 \rVert \leq 10\text{m}$

Using the maximum feed force of 25kN, maximum frictional forces in y-direction was determined as indicated in Table 5.5.

Table 5.5: Maximum frictional forces in y-direction at base of horizontal stabilisers

Max. feed force (F_M)	**Vector coordinates**			***b = b¹*** **(m)**	$\lVert v \rVert$ **(m)**	$\lVert v^1 \rVert$ **(m)**	**F_Y**	**$F_{FR\text{-}HH\ (max)}$ (kN)**
	a = a¹	***b = b¹***	***c = c¹***					
25	0	2.5	0	2.5	2.5	2.5	25	99
25	0	10	0	10	10	10	25	99

According to Table 5.5, at maximum feed force, the maximum longitudinal friction force of 99kN results from drilling operations. This means that any normal force in horizontal stabilisers less than 99kN will cause the system to slide since $\mu_s > 1$. Therefore, to stabilise the system, i.e., to avoid slippage, a normal force greater than 99kN is required in horizontal stabilisers.

5.8.4 Stabilisation of forces in z-direction

In this Section, the magnitude of minimum and maximum stabilisation forces in z-direction is determined using the models developed.

5.8.4.1 Minimum force in vertical stabilisers

The minimum force in vertical stabilisers is determined using Equation 5.29 under the following conditions:

$$F_{VS} \left| \begin{array}{l} \boldsymbol{c = c^1} \rightarrow -2.2;\ \boldsymbol{a = a^1} \rightarrow 0 \\ 2.5\text{m} \leq b \leq 10\text{m};\ 2.5\text{m} \leq \|v\| \leq 10m \end{array} \right. \qquad F_{VS} \left| \begin{array}{l} \boldsymbol{c = c^1} \rightarrow -2.2;\ \boldsymbol{a = a^1} \rightarrow 0 \\ 2.5\text{m} \leq b^1 \leq 10\text{m};\ 2.5\text{m} \leq \|v^1\| \leq 10m \end{array} \right.$$

With maximum feed force of 25kN, minimum force in vertical stabilisers was determined as indicated in Table 5.6.

Table 5.6: Minimum force in vertical stabilisers

Max. drill force (F_M)	Vector coordinates			$c = c^1$ (m)	$\|v\|$ (m)	$\|v^1\|$ (m)	F_Z (kN)	F_{VS} (kN)
	$a = a^1$	$b = b^1$	$c = c^1$					
25	0	2.5	0	0	2.5	2.5	64	64
25	0	10	0	0	10	10	64	64
25	0	2.5	-2.2	-2.2	3.33	3.33	48	48.3

Table 5.6 shows that minimum forces in vertical stabilisers ($F_{VS} = F_Z$) occur when the monorail drilling system is drilling horizontal holes (i.e., $\boldsymbol{a = a^1} \rightarrow 0$) along Z-axis. This is because as $\boldsymbol{a = a^1} \rightarrow 0$ and $\boldsymbol{c = c^1} \rightarrow 0$, all the forces concentrate along the horizontal plane. However, when the system is drilling down holes

(with maximum boom lifting angle of -41^0 with $\boldsymbol{c} = \boldsymbol{c^1} \rightarrow$ -2.2), the vertical force from the drilling units will be 48.3kN acting upwards and against the weight of the monorail drilling system.

5.8.4.2 Maximum force in vertical stabilisers

According to Section 5.7.2.2, maximum force in vertical stabilisers ($F_{VS} = F_Z$) in z-direction was determined under the following conditions:

F_{VS} | $\boldsymbol{c = c^1} \rightarrow 1.8$; $\boldsymbol{a = a^1} \rightarrow 0$; $\boldsymbol{b = b^1} \rightarrow 2.5$m; $\|v\| \rightarrow 3.1$m

F_{VS} | $\boldsymbol{c = c^1} \rightarrow 1.8$; $\boldsymbol{a} = \boldsymbol{a^1} \rightarrow 0$; $\boldsymbol{b = b^1} \rightarrow 2.5$m; $\|v^1\| \rightarrow 3.1$m

Using Equation 5.31, the maximum force in vertical stabilisers was determined as indicated in Table 5.7. Table 5.7 shows that the maximum drilling force in each vertical stabiliser should be 87.3kN.

Table 5.7: Maximum force in vertical stabilisers

Max. drill force (F_M)	Vector coordinates			$c = c^1$ (m)	$\|v\|$ (m)	$\|v^1\|$ (m)	F_Z (kN)	F_{VS} (kN)
	$a = a^1$	$b = b^1$	$c = c^1$					
25	0	2.5	1.8	1.8	3.1	3.1	87.3	87.3

5.8.5 Stabilisation of forces in x-direction

This Section determines the magnitude of minimum and maximum stabilisation forces in x-direction using the models developed.

5.8.5.1 Minimum force in horizontal stabilisers

Minimum lateral force ($F_{HS} = F_X$), i.e., minimum force in horizontal stabilisers, was determined using Equation 5.38 under the following conditions:

$$F_{HS} \left| \begin{array}{l} \boldsymbol{a = a^1} \rightarrow 0;\ 2.5\text{m} \le \boldsymbol{b} \le 10\text{m}; \\ \boldsymbol{c = c^1} = 0;\ 2.5\text{m} \le \|v\| \le 10\text{m} \end{array} \right. \qquad F_{HS} \left| \begin{array}{l} \boldsymbol{a = a^1} \rightarrow 0;\ 2.5\text{m} \le \boldsymbol{b^1} \le 10\text{m}; \\ \boldsymbol{c = c^1} = 0;\ 2.5\text{m} \le \|v^1\| \le 10\text{m} \end{array} \right.$$

Table 5.8 shows the determined values.

Table 5.8: Minimum force in horizontal stabilisers

Max. drill force (F_M)	Vector coordinates			$a = a^1$ (m)	$\|v\|$ (m)	$\|v^1\|$ (m)	F_X (kN)	F_Y (kN)	F_Z (kN)	F_{HS} (kN)
	$a = a^1$	$b = b^1$	$c = c^1$							
25	0	2.5	0	0	2.5	2.5	0	50	0	0
25	0	10	0	0	10	10	0	50	0	0

As shown in Table 5.8, the minimum force in horizontal stabilisers is 0kN and is obtained when the monorail drilling system is drilling holes with coordinates (**a,c**) equal to (**0,0**). The minimum lateral force is 0kN indicating that vectors $\boldsymbol{v}$ = **0i** + **2.5j** + **0k** (or $\boldsymbol{v}$ = **0i** + **10j** + **0k**) and $\boldsymbol{v^1}$ = **0i** + **2.5j** + **0k** (or $\boldsymbol{v^1}$ = **0i** + **10j** + **0k**) will have all the forces directed along the Y-axis.

5.8.5.2 Maximum force in horizontal stabilisers

According to Section 5.7.3.2, the maximum lateral force ($F_{HS} = F_X$), i.e., the maximum force in horizontal stabilisers, was determined using Equation 5.38 under the following conditions:

$$F_{HS} \left| \begin{array}{l} \boldsymbol{a = a^1} \rightarrow 2;\ \boldsymbol{b = b^1} \rightarrow 2.5\text{m}; \\ \boldsymbol{c = c^1} \rightarrow 0;\ \|v\| = 3.67\text{m} \end{array} \right. \qquad F_{HS} \left| \begin{array}{l} \boldsymbol{a = a^1} \rightarrow 2;\ \boldsymbol{b} = \boldsymbol{b^1} \rightarrow 2.5\text{m}; \\ \boldsymbol{c = c^1} = 0;\ \|v^1\| = 3.67\text{m} \end{array} \right.$$

Table 5.9 shows the maximum force in horizontal stabilisers of the drilling system.

Table 5.9: Maximum force in horizontal stabilisers

Max. drill force (F_M)	Vector coordinates			$a = a^1$ (m)	$\|v\|$ (m)	$\|v^1\|$ (m)	F_X (kN)	F_{HS} (kN)
	$a = a^1$	$b = b^1$	$c = c^1$					
25	2	2.5	0	2	3.67	3.67	27.2	27.2

Table 5.9 shows that the maximum lateral force in horizontal stabilisers should be 27.2kN. Thus, with the two drilling booms drilling in the same quadrant, i.e., either I, II, III or IV (see Figure 5.11), all the forces in x-direction from the two drilling units are opposed by one horizontal stabiliser opposite to the direction of force. Therefore, the maximum force in each stabiliser is equal to the total lateral force from the two drilling units.

5.8.6 Coefficient of static friction at base of horizontal stabilisers

The coefficient of static friction (μ_s) depends on the normal forces in the two horizontal stabilisers (F_{HS}) and the maximum frictional forces in horizontal stabilisers ($F_{FR\text{-}HH}$). In the absence of any pre-compression in the horizontal stabilisers, the results obtained in Section 5.8.3.2 show that the maximum frictional force at the base of horizontal stabilisers will be larger than the normal forces in horizontal stabilisers, i.e., $F_{FR\text{-}HH}$ = 99kN > F_{HS} =27.2kN. Also according to Equation 5.2, the maximum possible friction force between the two surfaces before sliding begins is the product of the coefficient of static friction and the normal force. Thus, from the results obtained, unless there is a pre-compression supporting the horizontal stabilisers, the coefficient of static friction is larger than unit (i.e., $1<\mu_s$) indicating that the system will slide during drilling operations. Therefore, the normal forces in horizontal stabilisers should be large enough to avoid sliding. Just before sliding takes place, $F_{FR\text{-}HH} = \mu_s F_{HS}$, thus $\mu_s F_{HS}$ should have a value of 99kN. Also, according to Equation 5.3, for the system to remain static, $\mu_s F_{HS}$ should be larger than 99kN.

Assumptions

In this study, it is assumed that the normal force in horizontal stabilisers (F_{HS}) is twice the maximum frictional force at the base of horizontal stabilisers ($F_{FR\text{-}HH}$). This is because to overcome slippage, the applied normal force must exceed 99kN. Therefore, F_{HS} will have a value of 198kN. When this force is applied in horizontal stabilisers, the normal force will be larger than the frictional force in

y-direction at the base making the system stable (no slippage) during operation since $\mu_s<1$.

5.9 Factor of Safety

The Factor of Safety (FoS) also known as Safety Factor is used to provide a design margin over the theoretical design capacity. This allows for uncertainty in the design process (Ferdinand et al., 2002). The FoS is a multiplier applied to the maximum expected load to which a component or assembly is subjected to. The uncertainty could be any one of a number of the components of the design process including calculations, material strengths, manufacture quality, and others. The selection of the appropriate FoS to be used in design of components is essentially a compromise between the associated additional cost and weight and the benefit of increased safety and/or reliability. An appropriate FoS is chosen based on several considerations. The prime consideration is safety while secondary considerations include the accuracy of load and wear estimates, the consequences of failure and the cost of over-engineering the component to achieve that FoS. For example, components whose failure could result in health and safety (serious injury or death) and substantial financial loss, usually use a FoS of four or higher (often ten). Non-critical components generally have a safety factor of two.

5.9.1 Factor of safety for monorail drilling system stabilisers

The Factor of Safety for the monorail drilling system is applied to minimum and maximum forces in horizontal and vertical stabilisers. The maximum load that these stabilisers are allowed to carry under normal conditions of utilisation is considerably smaller than the ultimate load. The smaller load is referred to as the allowable load. Thus, only a fraction of the ultimate load capacity in the hydraulic stabilisers is utilised when the allowable load is applied. The remaining portion of the load carrying capacity of the member is kept in reserve to ensure its safe performance. Thus, the FoS of the hydraulic stabilisers is the ratio of the ultimate load to the allowable load and is calculated as:

$$\text{Factor of Safety} = \frac{\text{Ultimate load}}{\text{Allowable load}} \quad 5.40$$

Assumption

Since hydraulic stabilizers will be made with known certified materials and will be operated in reasonably constant environmental conditions with subjected loads and stresses that can be determined using qualified design procedures, a Factor of Safety of 2.0 is assumed in the design.

Regular inspection and maintenance of the hydraulic stabilisers is required to achieve maximum and safe performance. Additionally, there is also a possibility of failure of horizontal and vertical stabilizers when they are subjected to compressive stresses due to buckling. Therefore, there is need to check the stabiliser for buckling during the design or selection stage. Table 5.10 shows maximum and minimum reaction forces in horizontal and vertical stabilisers of the monorail drilling system after applying a factor of safety of 2.0.

Table 5.10: Maximum and minimum reaction forces in hydraulic stabilisers

Parameter	Design parameters without FoS		Factor of Safety	Design parameters with FoS	
	Minimum Force (kN)	Maximum Force (kN)		Minimum Force (kN)	Maximum Force (kN)
Force in vertical stabiliser (F_{VS})	48	87.3	2	96	174.4
Forces in horizontal stabilisers (F_{HS})	0	198	2	0	396

Based on the maximum normal force and longitudinal frictional forces in horizontal stabiliser, the coefficient of static friction between the decline wall and the base of horizontal stabilisers is determined as follows:

$$\mu_s = \frac{F_{FR-HH(max)}}{F_{HS(max)}} \quad 5.41$$

$$\mu_s = \frac{99}{396} = 0.25$$

Since the coefficient of static friction is less than unit (μ_s<1), the monorail drilling system will be stable and will not slide during drilling operations.

5.10 Summary

It has been determined that the stability of the monorail drilling system is critical in ensuring safe and high performance of the system. Stabilisation of the system requires determination of the longitudinal, vertical and lateral forces of the drilling system. According to the findings, these forces depend on the vector position of the two drilling booms with respect to the origin (pivoting point). Due to configuration and positioning of the monorail drilling system, the swing angles and lifting angles need to be determined accurately for the system to cover the entire drill face. In order for horizontal and vertical stabilisers not to slide against the decline wall, the coefficient of static friction is also critical. Coefficient of static friction in horizontal stabilisers less than a unit (μ_s<1) will make the monorail drilling system stable during drilling process. Table 5.11 summarises the design parameters for the monorail drilling system.

Table 5.11: Summary of design parameters for monorail drilling system

Parameter	Value	
	Minimum	**Maximum**
Force in vertical stabiliser (F_{VS})	96	174.4
Forces in horizontal stabilisers (F_{HS})	0	396
Factor of safety	2	-

Chapter 6

6.0 Monorail installation and support system

6.1 Introduction

This Chapter looks at monorail installation and support system requirements for the monorail drilling and loading systems. The two systems move on the rail installed in the roof of the decline and supported by roof bolts, suspension chains and steel supports. However, due to the weight of the components of the two systems, it is imperative that the force in each roof bolt, suspension chain and steel support capable of suspending the weight of the heaviest component is determined. This is in order to avoid failure of the two systems from their support systems as well as to overcome dynamic effects. Hence, the aim of this Chapter is to develop numerical models that relate the weight of the monorail drilling and loading systems components to the required strength in the support system. Using these models, numerical values of the forces required in each roof bolt, suspension chain and steel support to suspend the weight of the heaviest component of the monorail system are determined. The Chapter begins by highlighting the installation procedure of the monorail system in the decline.

6.2 Decline support system for monorail installation

Declines are a means of accessing mineral resources in underground mining operations. Their design lifetime is generally in the order of a century or at least few decades (Hartman, 1992). Since decline openings are continuously used throughout the life of the mine, their design considerations must be more conservative. Additionally, because decline openings are supposed to remain

open and stable for the entire life of the mine, their support system must be adequate. In general, decline support system involves the use (individually or in combination) of roof bolts, wire mesh, shotcrete as well as steel sets. According to Monsees and Hansmire (1992), the aim of the support is to provide the following characteristics:

- Absence of rock falls;
- Control of stress-induced local instability;
- Restriction of loosening; and
- Absence of mass instability by 'reinforcing' the rock, i.e., encourage the rock to support itself.

In underground mining operations accessed by means of declines and where monorail system is to be used as a means of underground transport system, support system (for the decline and monorail installation) is vital due to additional stresses resulting from the weight of the monorail system.

Generally, the decline opening support for a monorail system application is the same as in conventional truck haulage method, i.e., use of roof bolts, wire mesh, shotcrete as well as steel sets. However, the support system for monorail installations must be adequate to prevent hangingwall/roof bolt, suspension chain and steel support failure due to the weight of the monorail system as well as dynamic effects. Therefore, high strength roof bolts, suspension chains and steel supports in combination with wire mesh are used as monorail supports system in relatively competent grounds. However, steel arc sets in combination with shotcrete are used to support the monorail installations in weak ground. Figure 6.1 shows an example of monorail installation support system in the haulage.

Figure 6.1: Decline support system for monorail installation (Scharf, 2007)

6.3 Monorail installation

The monorail consist of a specially designed I-beam rail that is suspended from the haulage or decline roof by means of suspension chains or steel supports attached to the roof bolts or steel arc sets (Figure 6.2).

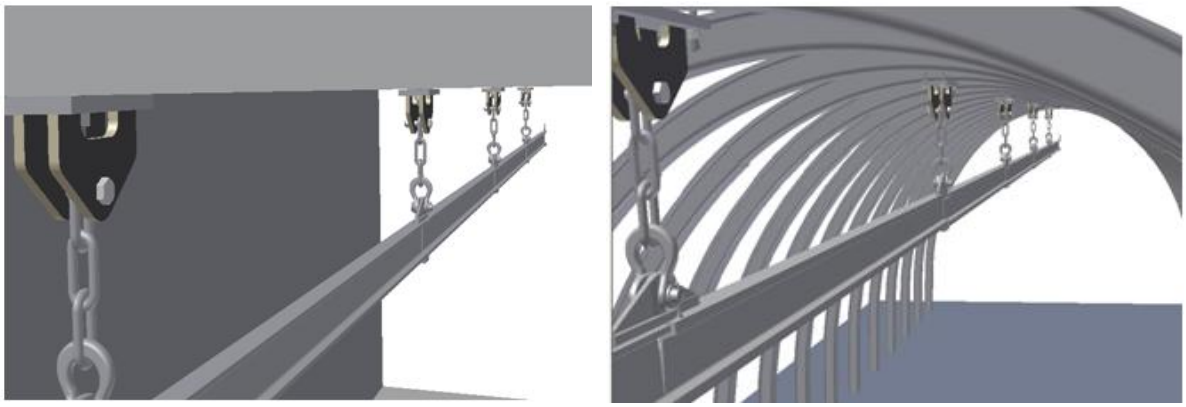

Figure 6.2: Monorail installation (Scharf, 2007)

The monorail can also be suspended directly from the hanging wall by a suitable suspension bracket. During operations, the monorail system runs on the reinforced lower flange of the I-beam guided by rollers on the web. This design

has an advantage of preventing any derailment, which is a major safety concern. The free-hanging sections of the monorail reduce the likelihood of developing excessive bending stresses in the roof bolts.

The monorail I-beam section has an average length of 3.0m and weighs approximately 114kg for ease handling, mounting and transportation. Monorail systems suspended from roof bolts have proven to be cost-effective and safe in difficult mining operations throughout the world (Scharf, 2007). To achieve higher travelling speeds and for long term rail installations, the fixed rail system 'Universal Flange Rail (UFR)' (Figure 6.3) has been developed by Scharf. These rails are bolted to a suspension bracket which itself is bolted to the hanging wall.

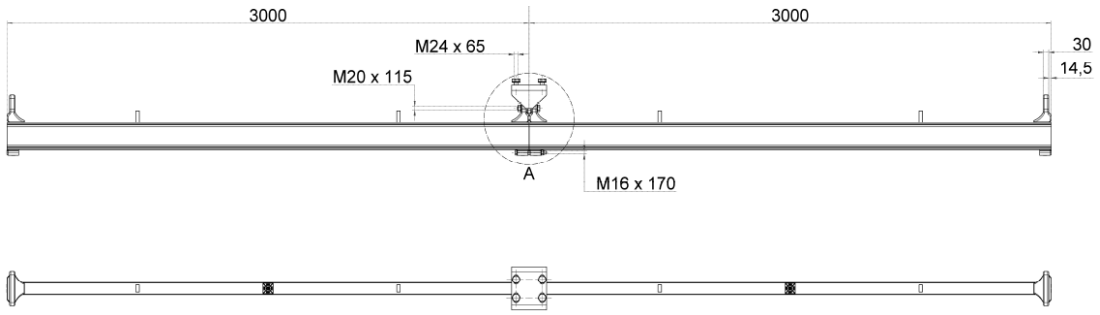

Figure 6.3: "Universal Flange Rail" type (Scharf, 2007)

According to Scharf (2007), monorail sections are available in two different profiles, i.e., either I140E or I140V (Figure 6.4). The high performance profile I140V is a strengthened profile providing higher bending moments to allow for higher total train weights. The life of I140V profile is usually four to five times longer than the I140E profile.

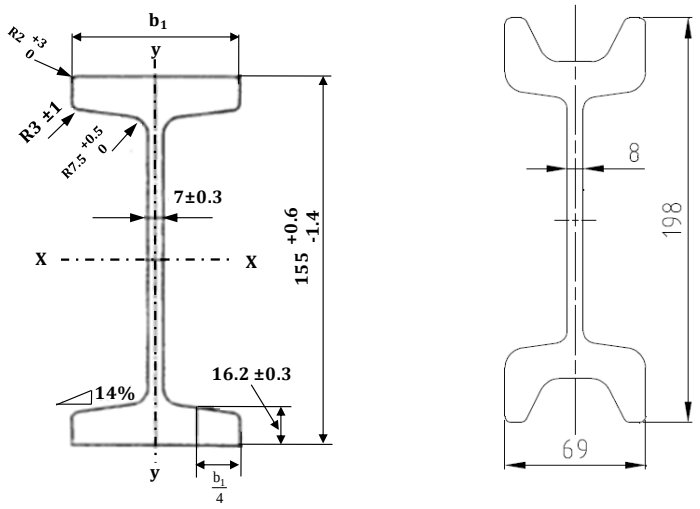

(a) (b)

Figure 6.4: Monorail profiles (a) I140E (b) I140V (Scharf, 2007)

Generally, installation of a monorail is a combination of three major activities:

- Drilling of roof bolt support holes;
- Roof bolt installation; and
- Rail placement and alignment.

6.3.1 Drilling of roof bolt support holes

During monorail installation, roof bolt support holes are drilled to a depth of 2m at 3m interval perpendicular to the decline roof surface (Figure 6.5). Preparatory activities, such as, lining and marking the hole, setting up the stoper and collaring the hole are important phases during drilling process (Oguz and Stefanko, 1971). Improper drilling of support holes reduces the lifetime of the roof bolts. The monorail drilling system itself can be used for the development drilling as well as drilling of support holes for roof bolt installation.

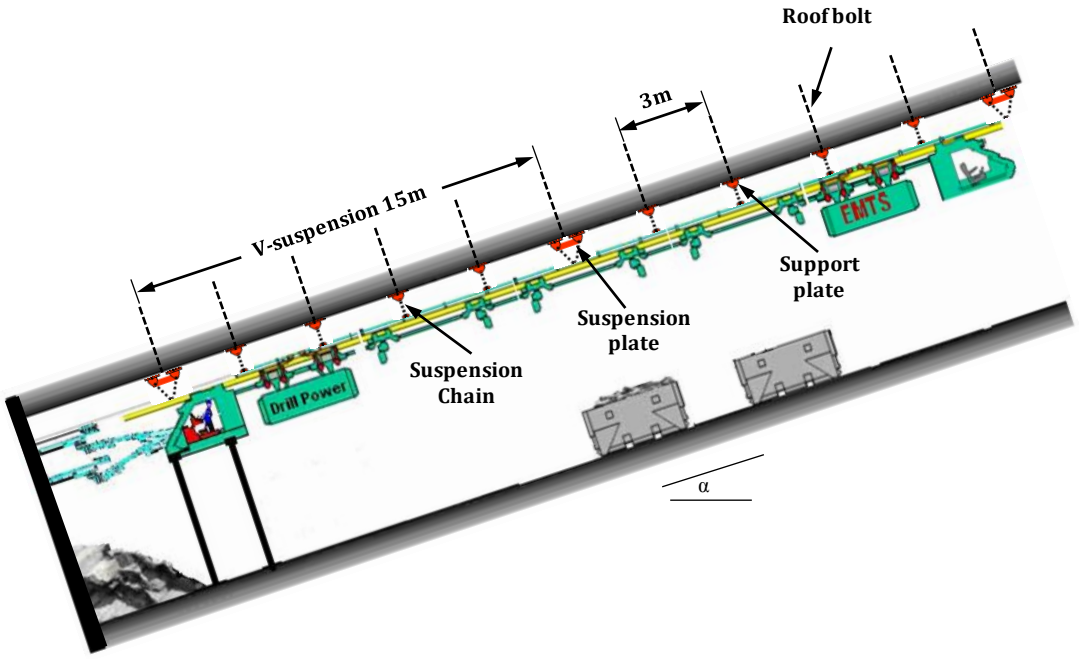

Figure 6.5: Drilling of roof bolt support holes for monorail installation (Scharf, 2007)

According to Oguz and Stefanko (1971), drilling time (manual drilling) per support hole, including all kinds of work and delays, is approximately 16 minutes. Net drilling time excluding delays takes approximately 6 minutes per hole. However, since drilling of support holes for the conceptual monorail drill-load-haul system will be done using the monorail drilling system, drilling time per support hole is likely to decreases.

6.3.2 Roof bolt installation and load transmission

Drilling of support holes is followed by installation of roof bolts. According to Oguz and Stefanko (1971), roof bolt installation requires one operator and can be installed in less than a minute after drilling the support hole. Hilti OneStep® roof bolts are used as the suspension bolts (Figure 6.6). These bolts have an ultimate force of 320kN, a diameter of 38.5mm, length of 2m and require a 41mm diameter hole. Each bolt requires the purchase of a dispenser and an intensifier for the installation. Resin containing rapid-curing adhesive is contained within the bolt.

Figure 6.6: Hilti OneStep® anchor bolt (Hilti Corporation, 2004)

Since a roof bolt for monorail installation must take static and dynamic load, load transmission in line with roof bolts is ideal (Figure 6.7). However, dynamic load with angular transmission is not recommended since it causes deflection of roof bolts. This reduces the lifetime of the roof bolts by a factor of 10 or more (Scharf, 2007). Therefore, to improve the life of roof bolts, a bracket with preloaded roof bolt is used.

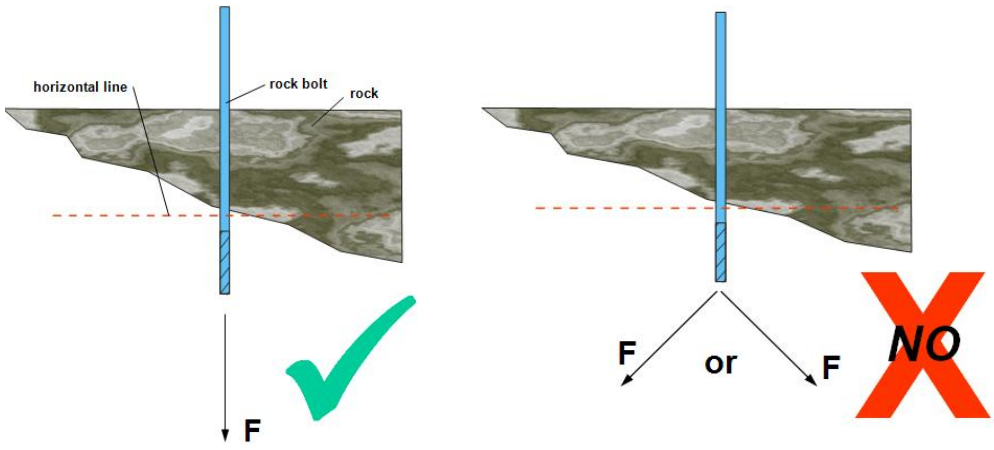

Figure 6.7: Load transmission in roof bolts (Scharf, 2007)

6.3.3 Rail placement

Rail/monorail placement begins by inserting a bracket (bottom plate) with dome ball (dome nut) at the bottom (Figure 6.8).

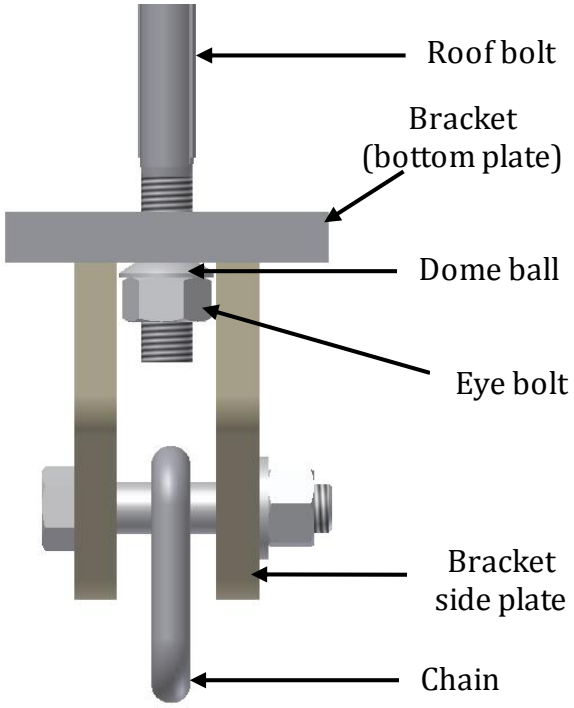

Figure 6.8: Details of roof bolt and bracket (Scharf, 2007)

A dome ball is used to avoid bending of the roof bolt. This is followed by attachment of a special eyebolt on the threaded end of the bolt. The bracket must have full contact with the roof to avoid roof bolt failure. Irregular roof conditions must be levelled or adjusted with concrete as indicated in Figure 6.9.

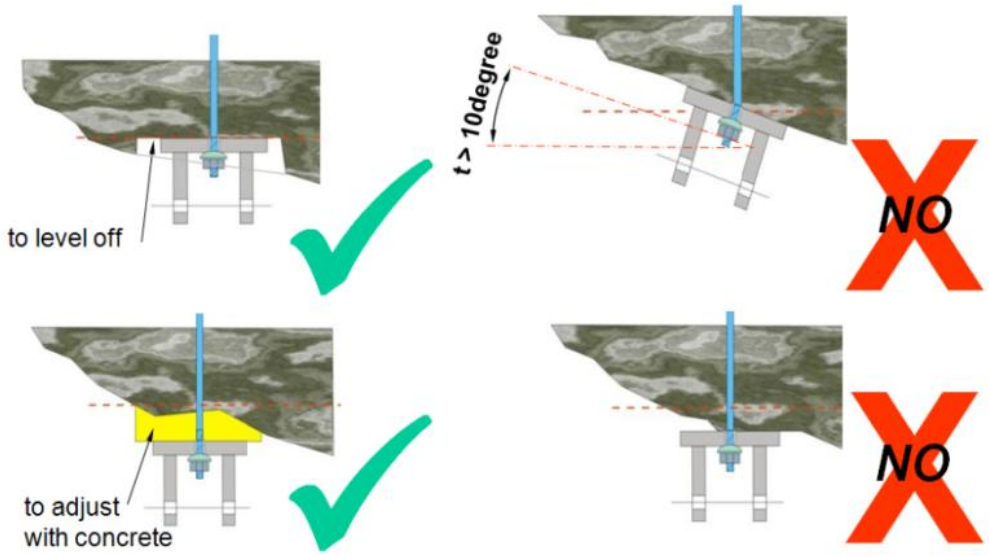

Figure 6.9: Levelling of irregular roof conditions (Scharf, 2007)

From the bracket side plate, a chain is connected to a shackle which provides connections to the rail. The distance from the shackle down to the position of the monorail should be carefully measured to obtain the correct length of the chain. Measurement of the chain is done by connecting a new rail section to the one which is already installed permanently. The front end of the new rail section is lifted until it is in line with the others. While one man holds the rail in this position, another man takes the measurement from the shackle to the hook on the top flange of the rail. Measured lengths of the chain are then cut using oxygen burner.

6.3.4 Rail alignment

Alignment of the rail is also critical in ensuring smooth movement of the monorail system as well as to avoid derailments. According to Scharf (2007), a badly installed monorail track develops unnecessary tensions in the system and leads to high power consumption. Figures 6.10 to 6.13 show rail alignment in various directions.

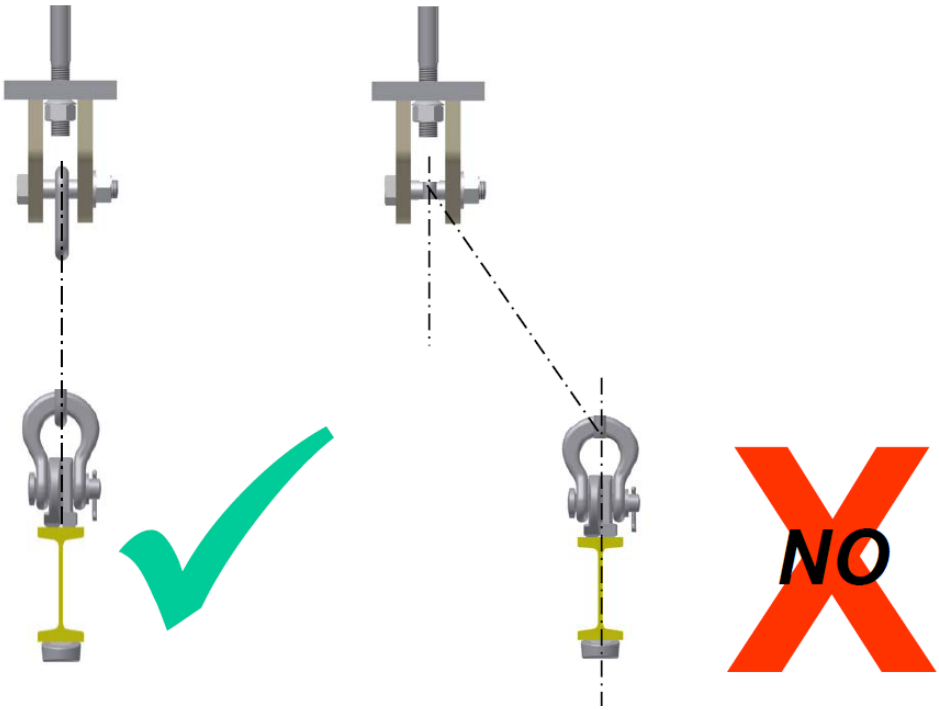

Figure 6.10: Chain angle cross to rail direction must be 0^0 (Scharf, 2007)

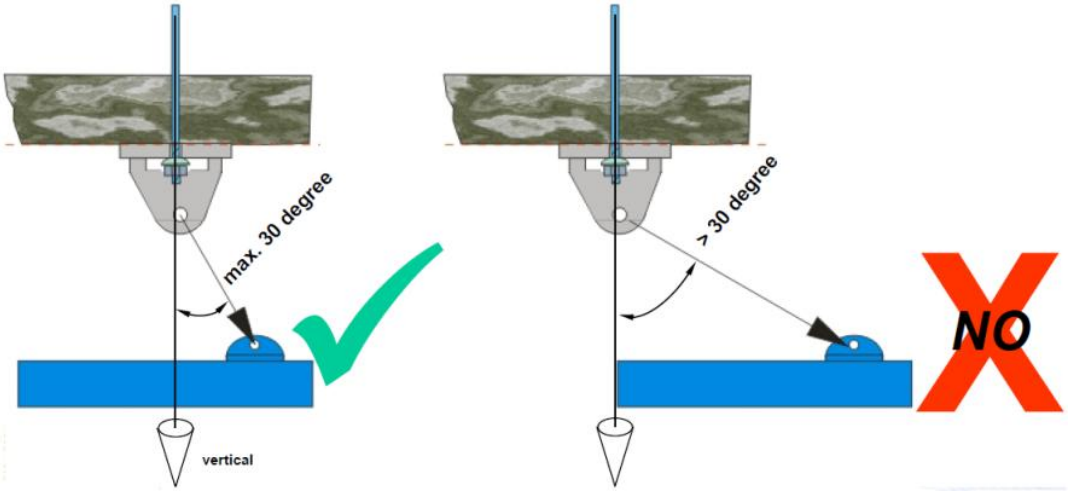

Figure 6.11: Chain angle in rail direction must be maximum 30^0 (Scharf, 2007)

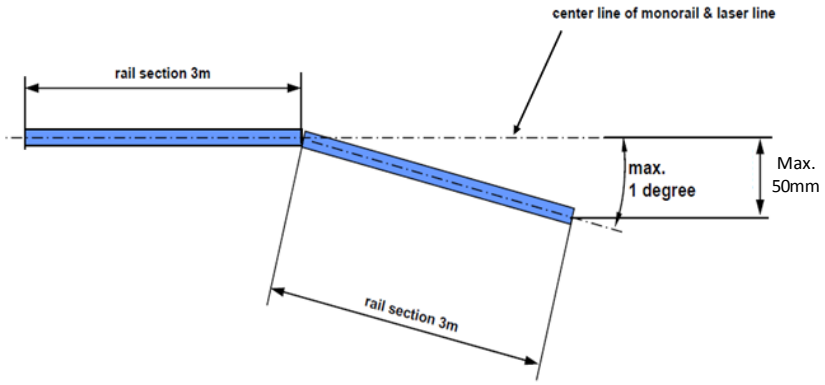

Figure 6.12: Horizontal angle between two rails must be maximum 1^0 (Scharf, 2007)

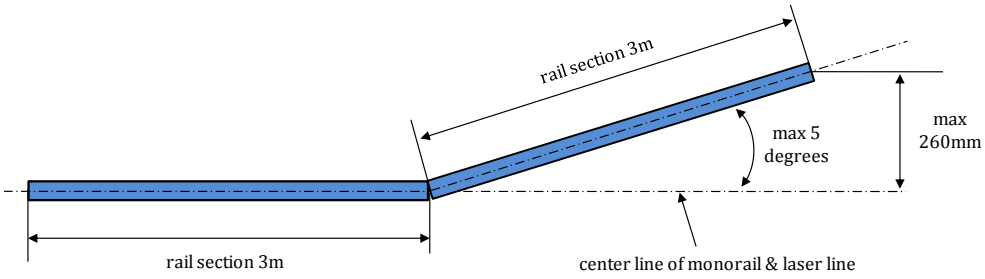

Figure 6.13: Vertical angle between two rails must be maximum 5^0 (Scharf, 2007)

6.4 Weight of monorail system components in an incline versus required support system

The proper design and selection of each roof bolt and suspension chain to support and suspend the monorail drilling and loading system components in an incline is significant in ensuring the components of the two systems remain suspended under load. To avoid failure of roof bolts and/or suspension chains due to the weight of monorail system components, high strength roof bolts and suspension chains must be installed. It is, therefore, important that the minimum required force in each support system necessary to suspend the weight of monorail drilling and loading system components is determined. In this Section, models that determine the required axial force in each roof bolt and suspension chain in an incline based on the heaviest monorail loading and drilling system components are established.

6.4.1 Weight of monorail loading system components versus required support system

The relationship between the weight of monorail loading system components and the required axial force in each roof bolt and suspension chain in an incline is shown in Figure 6.14.

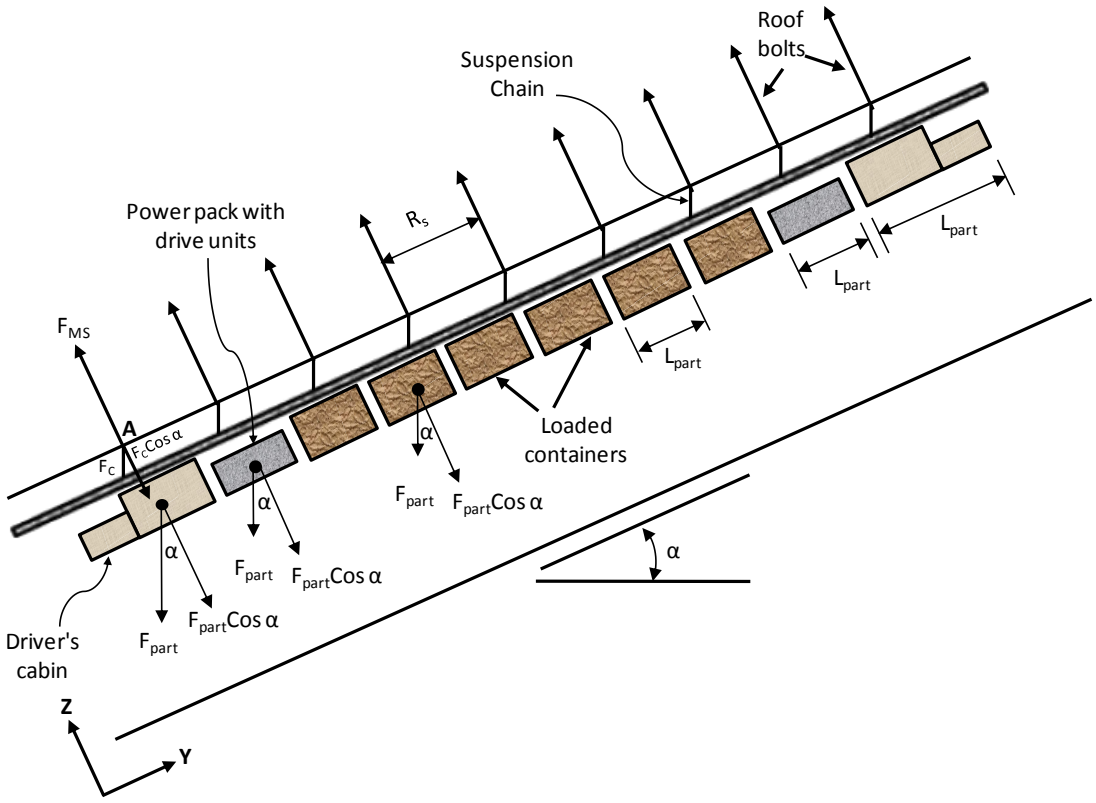

L_{part} is length of monorail loading system component
F_{part} is weight of monorail loading system component
R_s is roof bolt spacing
F_{MS} is axial force in each roof bolt (forces suspending monorail system)
F_C is force in each suspension chain
α is decline gradient

Figure 6.14: Axial forces in roof bolts and suspension chains for the monorail loading system components in an incline

Taking equilibrium of forces in Z-direction at point **A**, the following equation that relates the axial force in each roof bolt and suspension chain is established:

$$F_{MS} = F_C \cos\alpha \qquad 6.1$$

However, the monorail loading system component remains in equilibrium (in Z-direction) if the total upward force (i.e., total forces in suspension chains installed within length L_{part} occupying the system component is equal to the total downward force (i.e., weight of the heaviest monorail loading system component). In these calculations, the weight of the rail, suspension chains and bolts is neglected.

6.4.1.1 Total force in suspension chains within L_{part}

The total force in suspension chains depends on the number of suspension chains installed within the span L_{part} and the force in each chain. Since the roof bolt spacing (R_s) is known (which is also equal to suspension chain spacing), the number of suspension chains installed within L_{part} is determined as follows:

$$\text{Total number of suspension chains within } L_{part} = \left(\frac{L_{part}}{R_s}\right) \qquad 6.2$$

Thus, the total force in suspension chains within the span L_{part} is the product of the total number of suspension chains installed and the force in each chain (F_C) as indicated below:

$$\text{Total force in suspension chains within } L_{part} = F_C\left(\frac{L_{part}}{R_s}\right) \qquad 6.3$$

$$Z\text{-component of the total force in suspension chains} = F_C\left(\frac{L_{part}}{R_s}\right)\cos\alpha \qquad 6.4$$

6.4.1.2 Weight of monorail loading system component

In determining the weight of the heaviest monorail loading system component (F_{part}) of length L_{part}, the weight of the driver's cabin/train, loaded containers and the power pack (with drive units) and their respective lengths are considered in this analysis. Figure 6.15 shows the monorail loading system components with respective lengths and weights.

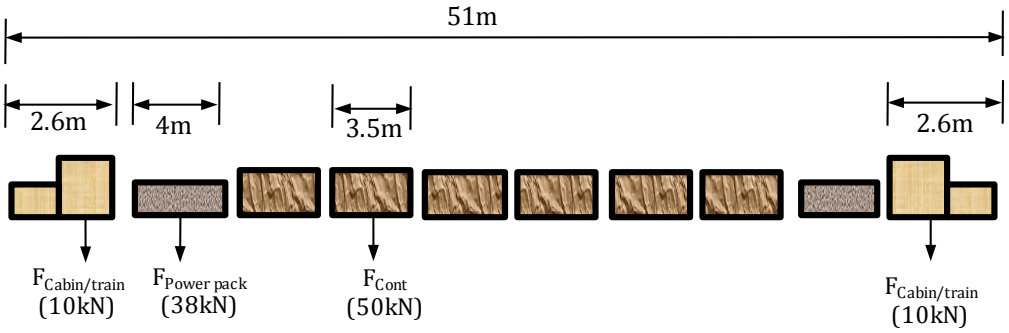

F_{Cont} is weight of loaded monorail container
$F_{Power\ pack}$ is weight of one power pack (with drive unit)
$F_{Cabin/train}$ is weight of driver's cabin or train

Figure 6.15: Schematic diagram showing lengths and weights of monorail loading system components

As indicated in Figure 6.15, the monorail loading system consists of components of different lengths and weights. The heaviest component is the loaded monorail container, which has a total weight of 50kN. Therefore, the length (L_{part}) and weight (F_{part}) of the heaviest component of the monorail loading system used in the analysis is 3.5m and 50kN, respectively. The weight of the heaviest component of the monorail loading system can be written as:

$$\text{Weight of heaviest component of monorail loading system} = F_{part} \qquad 6.5$$

$$\text{Z-component of the heaviest monorail loading system} = F_{part}\text{Cos}\alpha \qquad 6.6$$

6.4.1.3 Required strength of suspension chains

As indicated in Figures 6.14 and 6.15, the heaviest monorail loading system component remains in equilibrium (in Z-direction) if its weight and total force in the suspension chains are equal. Therefore, the relationship between the weight of the heaviest monorail loading system component and the required maximum force in each suspension chain is determined by equating Equations 6.4 and 6.6 to yield:

$$F_C = \frac{R_s}{L_{part}} F_{part} \qquad 6.7$$

Since the allowable maximum load in suspension chains is known (using Equation 6.7), the strength of the suspension chain should be more than the allowable load. It should also be noted that suspension chain failure occurs if the weight of the heaviest monorail loading system component (allowable load) is more than the capacity (ultimate load) of the suspension chains within L_{part} occupying the heaviest component. The classical approach used in designing engineering structures is to increase the capacity (ultimate load) of the system in comparison with the allowable load. A factor of safety is applied to increase the loading capacity of the chains. In this study, a factor of safety of 2.0 is assumed. Therefore, applying a factor of safety to Equation 6.7 yields the following:

$$F_{C,\,max} = \frac{2R_s}{L_{part}} F_{part} \qquad 6.8$$

Since R_S and L_{part} are constants, the required strength of suspension chains depends on the weight of the loaded monorail containers. Alternatively, R_s can be determined if the strength of the suspension chain is known.

6.4.1.4 Required strength of roof bolts

The required strength of installed roof bolts within the span occupying the heaviest monorail loading system component L_{part} is determined using the relationship given in Equation 6.1. Therefore, substituting Equation 6.8 into Equation 6.1 gives the maximum required strength in each roof bolt:

$$F_{MS,\,max} = \frac{2R_s}{L_{part}} F_{part} Cos\alpha \qquad 6.9$$

6.4.2 Weight of monorail drilling system components versus required support system

The minimum strength required in each roof bolt and suspension chain to suspend the monorail drilling system components depends on the weight of the drilling system components (i.e., the weight of monorail train together with the

two drilling booms and the weight of power pack with drive units). Figure 6.16 is used to determine the required strength in each roof bolt and suspension chains based on the weight of monorail drilling system components. It should also be noted that this analysis is limited to the case of drilling system in transit. The system is further supported when drilling a face.

6.4.2.1 Total forces in suspension chains within L_{dpart}

An analysis similar to that shown in Section 6.4.1 yields:

$$Z\text{-component of total force in suspension chain} = F_C\left(\frac{L_{dpart}}{R_s}\right)\cos\alpha \qquad 6.10$$

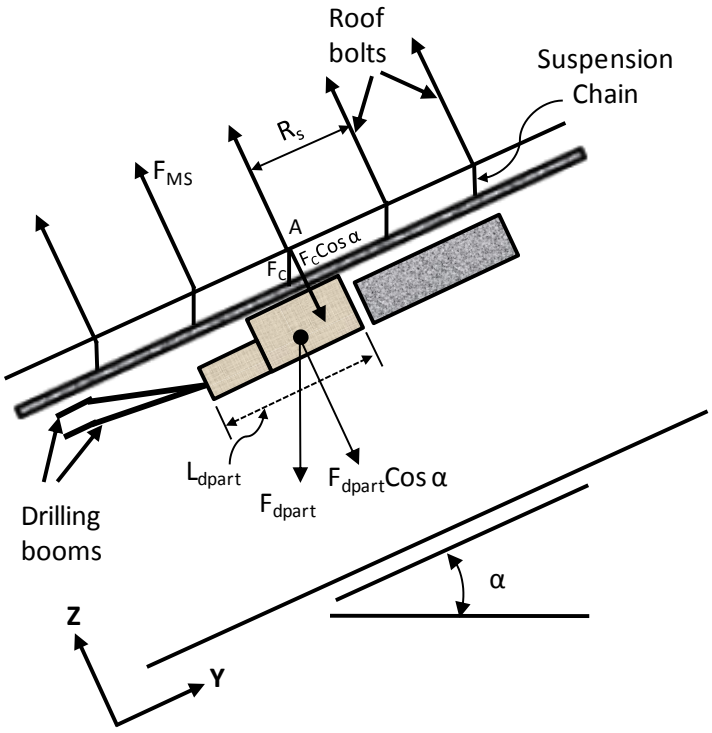

L_{dpart} is length of monorail drilling system component
F_{dpart} is weight of monorail drilling system component
R_s is roof bolt spacing
F_{MS} is axial force in each roof bolts (forces suspending monorail system)
F_C is force in each suspension chain
α is decline gradient

Figure 6.16: Axial forces in roof bolts and suspension chains for the monorail drilling system components in an incline

6.4.2.2 Weight of monorail drilling system component

Figure 6.17, which shows monorail drilling system components with respective lengths and weights, is used to determine the weight of the heaviest component to be used in the analysis.

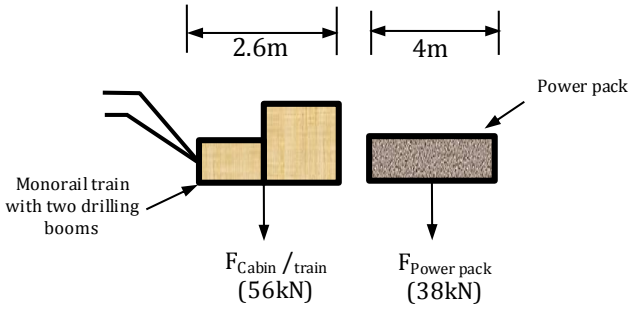

$F_{power\ pack}$ is weight of power pack with drive unit
$F_{cabin\ /\ train}$ is weight of driver's cabin together with two drilling booms

Figure 6.17: Schematic diagram showing lengths and weights of monorail drilling system components

Figure 6.17 shows that the monorail drilling system consisting of two components, i.e., the driver's cabin/train with two drilling booms and the power pack each with different length and weight. Thus, to determine the strength of the roof bolts and suspension chains the heaviest component of the drilling system is used in the analysis. According to Figure 6.17, the heaviest component is the driver's cabin/train together with the two drilling booms which has a weight of 56kN (i.e., weight of driver's cabin is 10kN and the two booms were assumed to weigh 46kN (see Section 4.8.2)). Therefore, the length (L_{dpart}) and the weight (F_{dpart}) of the heaviest monorail drilling system component used in the analysis are 2.6m (suspended length only) and 56kN respectively. The heaviest drilling system component in Z-direction can be written as indicated in Equation 6.11:

$$Z\text{-component of the heaviest drilling system component} = F_{dpart}\,Cos\alpha \qquad 6.11$$

6.4.2.3 Required strength of suspension chains

The maximum required strength (with factor of safety of 2.0) in each suspension chain is determined by equating Equations 6.10 and 6.11:

$$F_{C,\,max} = \frac{2R_s}{L_{dpart}} F_{dpart} \qquad 6.12$$

6.4.2.4 Required strength of roof bolts

The required strength in each roof bolt is determined by substituting Equation 6.12 into Equation 6.1:

$$F_{MS,\,max} = \frac{2R_s}{L_{dpart}} F_{dpart} Cos\alpha \qquad 6.13$$

6.5 Strength of support system at horizontal and vertical curves

During monorail installation at vertical and horizontal curves, the required support system must be adequate to overcome the dynamic effects and to avoid system failure. Also, it should be noted that during monorail installation process, the monorail components are rigidly fixed using steel supports at vertical curves while suspension chains are used at horizontal curves. It is thus necessary to determine the strength of the required support systems that are used to suspend the monorail components at vertical and horizontal curves. As highlighted in Section 2.2.2, the monorail system can negotiate horizontal and vertical curve radii of 4m and 10m respectively. However, the curve lengths that result from these radii are small to accommodate the whole length of the monorail drilling and loading systems. Therefore, the weight of heaviest monorail drilling and loading systems component passing the vertical and horizontal curve is used. In this Section, models that determine the strength of roof bolts, steel supports and suspension chains at vertical and horizontal curves based on the dynamic forces of the heaviest monorail drilling and loading system components are presented.

6.5.1 Strength of steel supports at vertical curves based on weight of monorail loading system components

This Section determines the required strength of roof bolts and steel supports at vertical curves based on the weight of the heaviest monorail loading system components. Figure 6.18 is used during the determination.

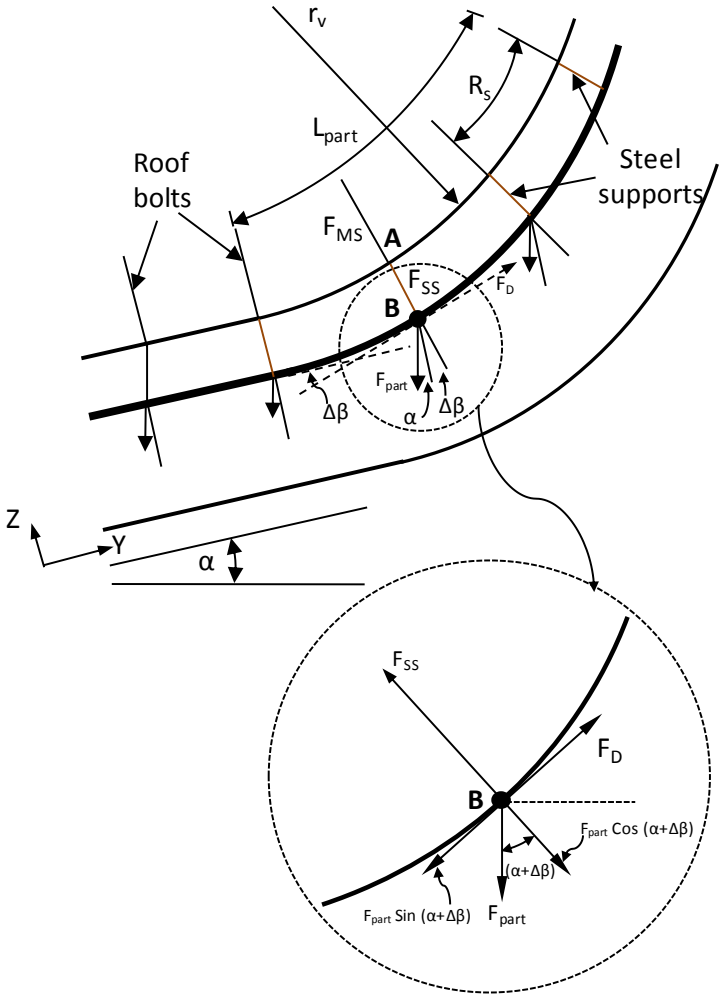

L_{part} is length of monorail loading system component
R_s is roof bolt spacing
F_{MS} is axial force required in each roof bolts (forces suspending monorail system)
F_{part} is weight of monorail loading system component
F_{SS} is axial force in each steel support
F_D is net driving (propulsion) force
α is decline gradient
Δβ is angle change at vertical curve
r_v is vertical curve radius

Figure 6.18: Schematic longitudinal-section view of required support system at vertical curve based on the weight of monorail loading system components

Taking equilibrium of forces at point **A** (Figure 6.18), the following equation that relates the axial force in each roof bolt and steel support is established:

$$F_{MS} = F_{SS} \qquad 6.14$$

During motion of the monorail loading system at a curve a centrifugal force, F_S, (given in Equation 6.15) directed towards the centre of the curve is needed to make the monorail train or any component attached to it undergo motion at a vertical curve (Alan, 2003; Lawrence, 1997):

$$F_S = \frac{m_{part} v^2}{r_v} \qquad 6.15$$

where:

F_S is the centrifugal force needed to make the monorail train or its components undergo uniform motion at a curve;

v is velocity of the monorail train or its component as it moves along the curve;

r_v is vertical radius of the curve around which the monorail loading system or its components is moving; and

m_{part} is mass of the monorail loading system component negotiating the curve.

6.5.1.1 Total axial force in steel supports at vertical curve

The total axial force in steel supports at vertical curves depends on the number of steel supports installed within the length, L_{part}, occupying the monorail loading system component and the axial force in each steel support. Since the roof bolt spacing, R_s, is known (also equal to steel support spacing), the number of steel supports occupying the monorail loading system component of length L_{part}, at a vertical curve is determined as follows:

$$\text{Total number of steel supports within } L_{part} = \left(\frac{L_{part}}{R_s} \right) \qquad 6.16$$

where:

L_{part} is the length of monorail loading system component.

Thus, the total axial force in steel supports within the length L_{part} at a vertical curve is the product of the total number of steel supports installed within the length L_{part} and the axial force in each steel support (F_{SS}):

$$\text{Total axial force in steel support within } L_{part} = F_{SS}\left(\frac{L_{part}}{R_s}\right) \qquad 6.17$$

It is assumed that the support distance L_{part} is small and the variation of angle can be ignored. Using Equation 6.15 and taking equilibrium of forces in Z-direction at point **B** (Figure 6.18), the resultant force of the monorail loading system component at a curve is determined as follows:

$$F_{SS}\left(\frac{L_{part}}{R_s}\right) - F_{part}\text{Cos}(\alpha + \Delta\beta) = \frac{m_{part}v^2}{r_v} \qquad 6.18$$

where:

$$0^0 \le \Delta\beta \le 70^0$$

Similarly, the net propulsion (pushing) force (F_D) of the monorail train at a curve is determined as indicated in Equation 6.19:

$$F_D = F_{part}\text{Sin}(\alpha + \Delta\beta) \qquad 6.19$$

Using Equation 6.18, the maximum strength in each steel support (with a factor of safety of 2.0) is determined as indicated below:

$$F_{SS,\,max} = \frac{2R_s}{L_{part}} \times \left(\frac{m_{part}v^2}{r_v} + F_{part}\text{Cos}(\alpha + \Delta\beta)\right) \qquad 6.20$$

The maximum strength of steel supports at vertical curves is determined based on the heaviest component of the monorail loading system as discussed in Section 6.4.1.2.

6.5.1.2 Required strength of steel supports at vertical curves

The required strength of each steel support at a vertical curve is determined using Equations 6.20. It should also be noted that the maximum axial force in steel supports occurs when $\Delta\beta = 0$. Therefore, with this condition, Equation 6.20 can be written as indicated be below:

$$F_{SS,\,max} = \frac{2R_s}{L_{part}} \times \left(\frac{m_{part} v^2}{r_v} + F_{part} \cos\alpha \right) \qquad 6.21$$

6.5.1.3 Required strength of roof bolts at vertical curves

According to Equation 6.14, the axial force in each roof bolt at vertical curve is equal to the axial force in each steel support. Therefore, using Equations 6.14 and 6.21, the maximum required strength in each roof bolt is determined as follows:

$$F_{MS,\,max} = \frac{2R_s}{L_{part}} \times \left(\frac{m_{part} v^2}{r_v} + F_{part} \cos\alpha \right) \qquad 6.22$$

6.5.2 Strength of steel supports at vertical curves based on weight of monorail drilling system component

The strength of required roof bolts and steel supports at vertical curves based on the weight of the monorail drilling system components is determined using Figure 6.19 (configuration is the same as for the monorail loading system in Figure 6.18).

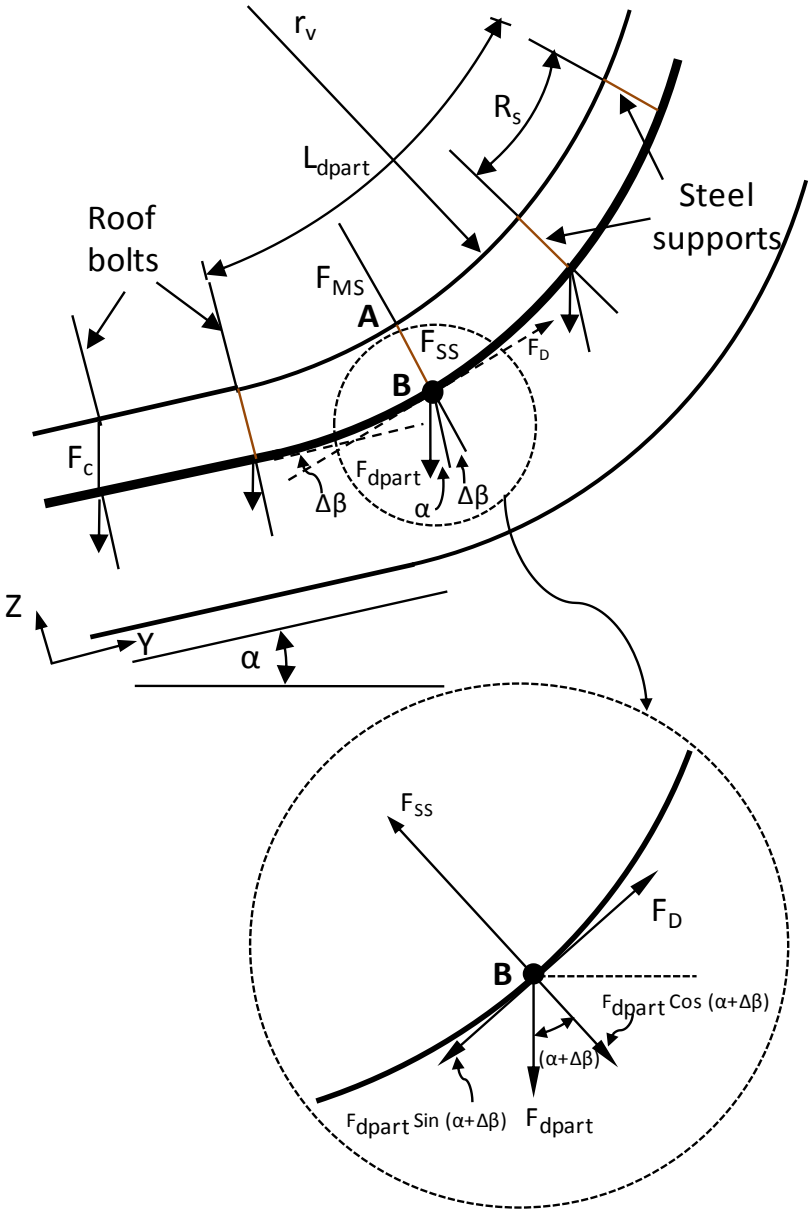

L_{part} is length of monorail drilling system component
R_s is roof bolt spacing
F_{MS} is axial force required in each roof bolts (forces suspending monorail system)
F_{dpart} is weight of any monorail drilling system component
F_{SS} is axial force in each steel support
α is decline gradient
Δβ is angle change at vertical curve
r_v is vertical curve radius

Figure 6.19: Schematic longitudinal-section view of required support system at vertical curve based on weight of monorail drilling system components

6.5.2.1 Total axial force in steel supports at vertical curves

Using similar analysis as for the monorail loading system yields:

$$\text{Total force in steel supports within curve } L_{dpart} = F_{SS}\left(\frac{L_{dpart}}{R_s}\right) \qquad 6.23$$

The net propulsion (pushing) force (F_D) of the monorail drilling system at vertical curve is determined as:

$$F_D = F_{dpart}\,\text{Sin}\,(\alpha + \Delta\beta) \qquad 6.24$$

The axial force in each steel support (with a factor of safety of 2.0) is also determined as:

$$F_{SS,\,max} = \frac{2R_s}{L_{dpart}} \times \left(\frac{m_{dpart}\,v^2}{r_v} + F_{dpart}\,\text{Cos}\,(\alpha + \Delta\beta)\right) \qquad 6.25$$

6.5.2.2 Weight of monorail drilling system component

The weight of the heaviest monorail drilling system component (F_{dpart}) of length L_{dpart} is determined as outlined in Section 6.4.2.2.

6.5.2.3 Required strength of steel supports at vertical curve

Since the maximum axial force in steel supports occurs when $\Delta\beta = 0$, the ultimate axial force in steel supports at a vertical curve is determined using Equation 6.26:

$$F_{SS,\,max} = \frac{2R_s}{L_{dpart}} \times \left(\frac{m_{dpart}\,v^2}{r_v} + F_{dpart}\,\text{Cos}\,\alpha\right) \qquad 6.26$$

6.5.2.4 Required strength in roof bolts at vertical curve

Using Equations 6.14 and 6.26, the ultimate axial force in each roof bolt is determined as follows:

$$F_{MS,\,max} = \frac{2R_s}{L_{dpart}} \times \left(\frac{m_{dpart} v^2}{r_v} + F_{dpart} \mathrm{Cos}\,\alpha \right) \qquad 6.27$$

6.5.3 Strength of suspension chains at horizontal curves based on monorail loading system

6.5.3.1 Force and displacement of suspension chains at horizontal curves

As the monorail loading system negotiates a horizontal curve, suspension chains are displaced from the vertical position due to dynamic forces resulting from the motion of the system. Figures 6.20 and 6.21 show the forces and displacement of suspension chain at a horizontal curve.

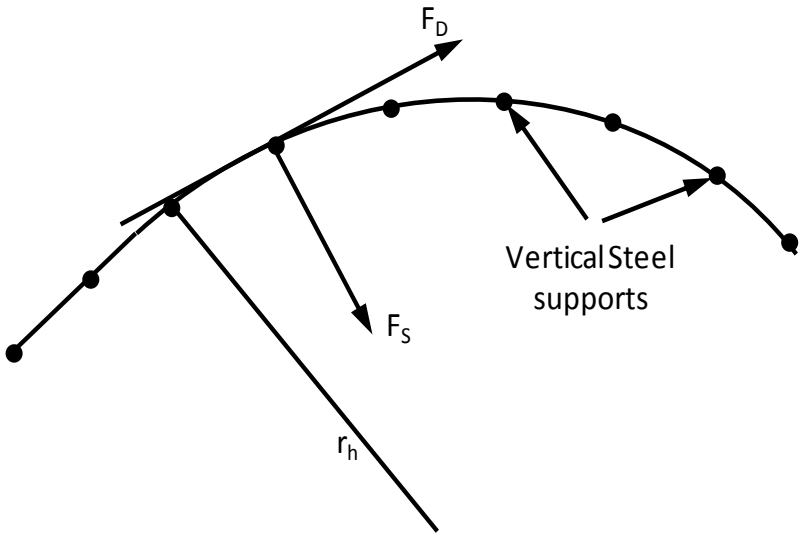

F_S is centrifugal force exerted on moving monorail loading system
F_D is net driving (propulsion) force
r_h is horizontal curve radius

Figure 6.20: Plan view of forces at the horizontal curve

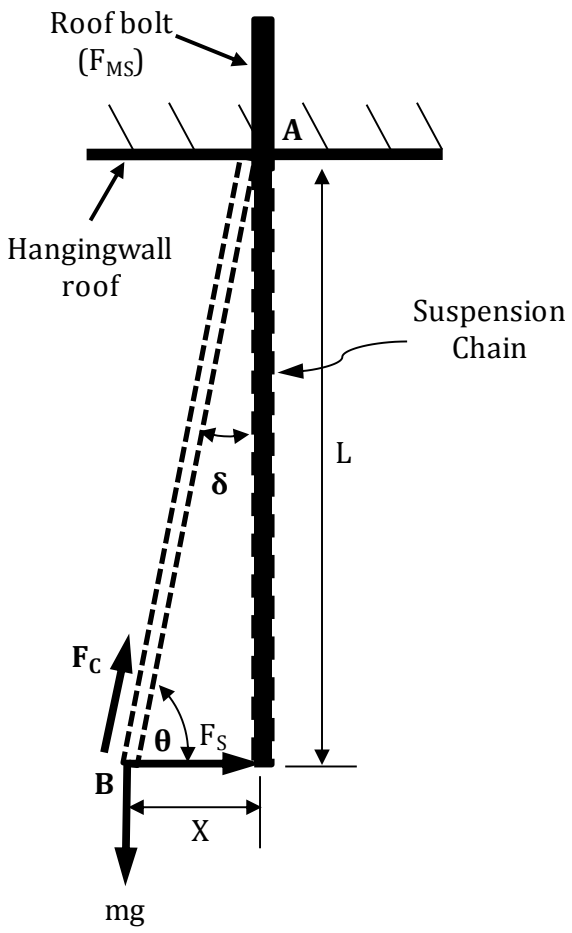

Figure 6.21: Displacement of suspension chain from vertical position at horizontal curve

As can be seen from Figures 6.20 and 6.21, centrifugal force, F_S, results as the monorail loading system moves along the curve as given in Equation 6.28:

$$F_S = \frac{m_{part} v^2}{r_h} \qquad 6.28$$

where:

$\mathbf{r_h}$ is horizontal radius of the curve around which the monorail loading system or its components is moving.

According to Figure 6.21, as the monorail drilling and loading systems negotiate the horizontal curve, the suspension chains are displaced from vertical positions by the angle **δ** and horizontal distance **X**. It is important to determine these two

parameters and the force carried by the suspension chains so as to determine whether the chains will fail or the systems will hit (as the chain is displaced) into the sidewall of the underground opening at a horizontal curve. This is why control measures are put in place.

From Figure 6.21, the following equation that relates the axial force in each roof bolt and the force in suspension chains at horizontal curve is established.

$$F_{MS} = F_C \mathrm{Sin}\theta \qquad 6.29$$

6.5.3.2 Angular displacement (δ) of suspension chains due to monorail loading system

The angular displacement of suspension chains from the vertical position is determined by resolving forces at point **B** to yield:

$$\text{Horizontal force balance:} \quad F_C \mathrm{Cos}\theta = F_S = \frac{m_{part} v^2}{r_h} \qquad 6.30$$

$$\text{Vertical force balance:} \quad F_C \mathrm{Sin}\theta = m_{part} g \qquad 6.31$$

Dividing Equation 6.31 by Equation 6.30 gives the following:

$$\mathrm{Tan}\theta = \left(\frac{g \times r_h}{v^2} \right) \qquad 6.32$$

Therefore, the angular displacement of suspension chains is determined as:

$$\delta = 90 - \mathrm{Tan}^{-1}\left(\frac{g \times r_h}{v^2} \right) \qquad 6.33$$

Equation 6.33 indicates that the maximum angular displacement of suspension chains depends on the radius of curvature of the horizontal curve and velocity of

the monorail system component at the curve. Thus, an increase in the radius of the horizontal curve results in smaller angular displacement and vice versa. Equation 6.33 also reveals that an increase in the velocity of the monorail system component at a curve results in an increase in angular displacement of suspension chains and vice versa.

6.5.3.3 Horizontal displacement (X) of suspension chains due to monorail loading system

Using trigonometry, the horizontal displacement by which suspension chains are displaced from the vertical position due to dynamic forces is found using Equation 6.34:

$$X = \frac{L \times v^2}{r_h \times g} \qquad 6.34$$

Equation 6.34 shows that horizontal displacement depends on the length of suspension chains, velocity of the monorail loading system components and the radius of curvature of the horizontal curve. The length of suspension chains and square of the velocity of the monorail loading system component varies directly with the horizontal displacement while the radius of curvature is inversely related with **X.**

6.5.3.4 Force in suspension chains at horizontal curves

Having found θ as per Equation 6.32, Equations 6.30 gives the value of the force (with a factor of safety of 2.0) in suspension chains, F_C, due to dynamic force of the system as:

$$F_{C,\,max} = \frac{2m_{part}v^2}{r_h} \times \frac{1}{Cos\theta} \qquad 6.35$$

Using trigonometry:

$$\text{Cos}\,\theta = \frac{v^2}{\sqrt{v^4 + g^2 r_h^2}} \qquad 6.36$$

Replacing Equation 6.36 into Equation 6.35 gives:

$$F_{C,\,max} = \frac{2m_{part}}{r_h} \times \sqrt{v^4 + g^2 r_h^2} \qquad 6.37$$

6.5.3.5 Axial force in roof bolts at horizontal curves

The maximum axial force in roof bolts at horizontal curves is obtained by using Equations 6.29 and 6.37 to yield:

$$F_{MS,\,max} = 2m_{part}g \qquad 6.38$$

6.5.4 Strength of suspension chains at horizontal curves based on monorail drilling system

6.5.4.1 Force and displacement of suspension chains at horizontal curves

Using the similar analysis as in Section 6.5.3, centrifugal force, F_S, which results as the monorail drilling system moves along the curve is given in Equation 6.39:

$$F_S = \frac{m_{dpart} v^2}{r_h} \qquad 6.39$$

Using Figure 6.21, the angular displacement of suspension chains from the vertical position is given as follows:

$$\text{Horizontal force balance:} \quad F_C \text{Cos}\theta = F_S = \frac{m_{dpart} v^2}{r_h} \qquad 6.40$$

$$\text{Vertical force balance:} \quad F_C \text{Sin}\theta = m_{dpart} g \qquad 6.41$$

6.5.4.2 Required strength of suspension chains at horizontal curves

The required strength of suspension chains (with a factor of safety of 2.0) at horizontal curves for the monorail drilling system is given by Equation 6.42:

$$F_{C,\,max} = \frac{2m_{dpart}}{r_h} \times \sqrt{v^4 + g^2 r_h^2} \qquad 6.42$$

6.5.4.3 Axial force in roof bolts at horizontal curves

The axial force in roof bolts at horizontal curves is obtained by using Equations 6.29 and 6.42 to yield:

$$F_{MS,\,max} = 2m_{dpart} g \qquad 6.43$$

6.5.5 Summary of models to determine required support at curves

Table 6.1 summarises the models developed for determining the required strength of support system (i.e., roof bolts, suspension chains and steel supports) in an incline as well as at vertical and horizontal curves.

Table 6.1: Models for determining required support system

Parameter	Monorail loading system	Monorail drilling System
Strength of support system in an incline		
Required strength of suspension chains (**F_C**)	$F_{C,\,max} = \frac{2R_s}{L_{part}} F_{part}$	$F_{C,\,max} = \frac{2R_s}{L_{dpart}} F_{dpart}$
Required strength of roof bolts (**F_{MS}**)	$F_{MS,\,max} = \frac{2R_s}{L_{part}} F_{part} Cos\alpha$	$F_{MS,\,max} = \frac{2R_s}{L_{dpart}} F_{dpart} Cos\alpha$
Strength of support at vertical curves		
Required strength of steel supports (**F_{SS}**)	$F_{SS,\,max} = \frac{2R_s}{L_{part}} \times \left(\frac{m_{part} v^2}{r_v} + F_{part} Cos\,\alpha \right)$	$F_{SS,\,max} = \frac{2R_s}{L_{dpart}} \times \left(\frac{m_{dpart} v^2}{r_v} + F_{dpart} Cos\,\alpha \right)$
Required strength of roof bolts (**F_{MS}**)	$F_{MS,\,max} = \frac{2R_s}{L_{part}} \times \left(\frac{m_{part} v^2}{r_v} + F_{part} Cos\,\alpha \right)$	$F_{MS,\,max} = \frac{2R_s}{L_{dpart}} \times \left(\frac{m_{dpart} v^2}{r_v} + F_{dpart} Cos\,\alpha \right)$
Strength of support at horizontal curves		
Required strength of suspension chains (**F_C**)	$F_{C,\,max} = \frac{2m_{part}}{r_h} \times \sqrt{v^4 + g^2 r_h^2}$	$F_{C,\,max} = \frac{2m_{dpart}}{r_h} \times \sqrt{v^4 + g^2 r_h^2}$
Required strength of roof bolts (**F_{MS}**)	$F_{MS,\,max} = 2m_{part} g$	$F_{MS,\,max} = 2m_{dpart} g$
Displacement of suspension chains at horizontal curves		
Angular displacement (**δ**)	$\delta = 90 - Tan^{-1}\left(\frac{g \times r_h}{v^2} \right)$	$\delta = 90 - Tan^{-1}\left(\frac{g \times r_h}{v^2} \right)$
Horizontal displacement (**X**)	$X = \frac{L \times v^2}{r_h \times g}$	$X = \frac{L \times v^2}{r_h \times g}$

6.5.6 Variation of support system strength with change in decline gradient

In this Section, the variation of support system strength with changes in decline gradient is established. As the decline gradient changes, there is a corresponding change in the required strength of each support system. The developed models, as shown in Table 6.1, are used to establish this variation. Table 6.2 shows the data used during the determination. The data is based on information from manufacturers of the monorail train (Scharf, 2007) and assumptions made in Chapters 4 and 5.

Table 6.2: Parameters of the monorail system

Parameter	Unit	Value	Comment
L_{part}	m	3.5	Manufacturer supplied
L_{dpart}	m	2.6	Manufacturer supplied
m_{part}	kg	5.1	Manufacturer supplied
m_{dpart}	kg	5.7	Manufacturer supplied
F_{part}	kN	50	Manufacturer supplied
F_{dpart}	kN	56	Manufacturer supplied
R_s	m	3	Manufacturer supplied
α	degrees	20	Assumed
r_v	m	10	Manufacturer supplied
r_h	m	4	Manufacturer supplied
v	m/s	3.5	Manufacturer supplied
L	m	0.6	Manufacturer supplied
g	m/s^2	9.81	Constant

6.5.6.1 Numerical values of support system strength

Using the developed models, the strength of the required support system with changes in decline gradient for the monorail drilling and loading systems is determined as indicated in Figures 6.22 and 6.23.

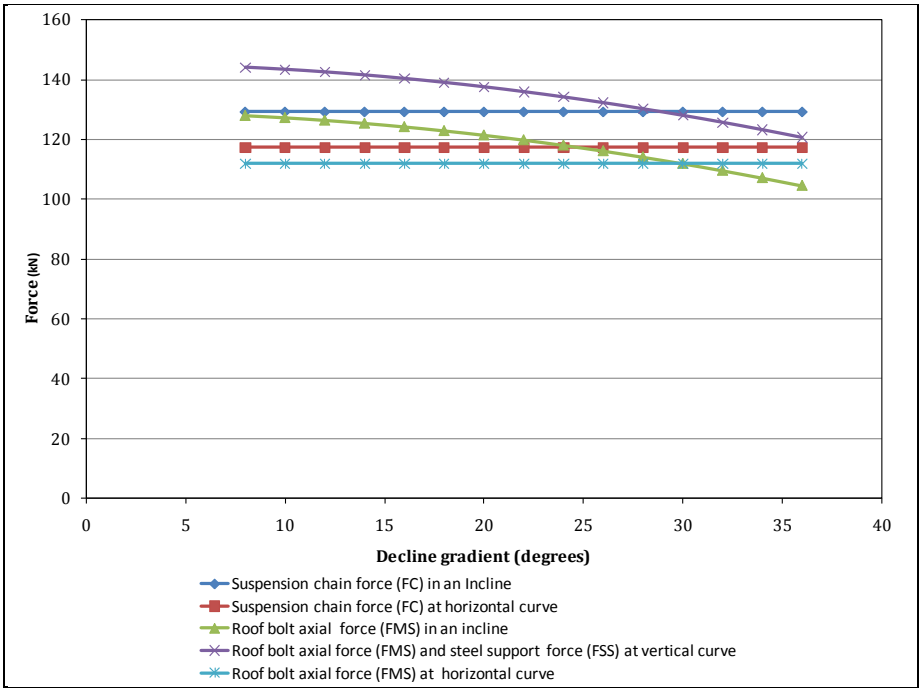

Figure 6.22: Variation of force in support system with change in decline gradient for the monorail drilling system

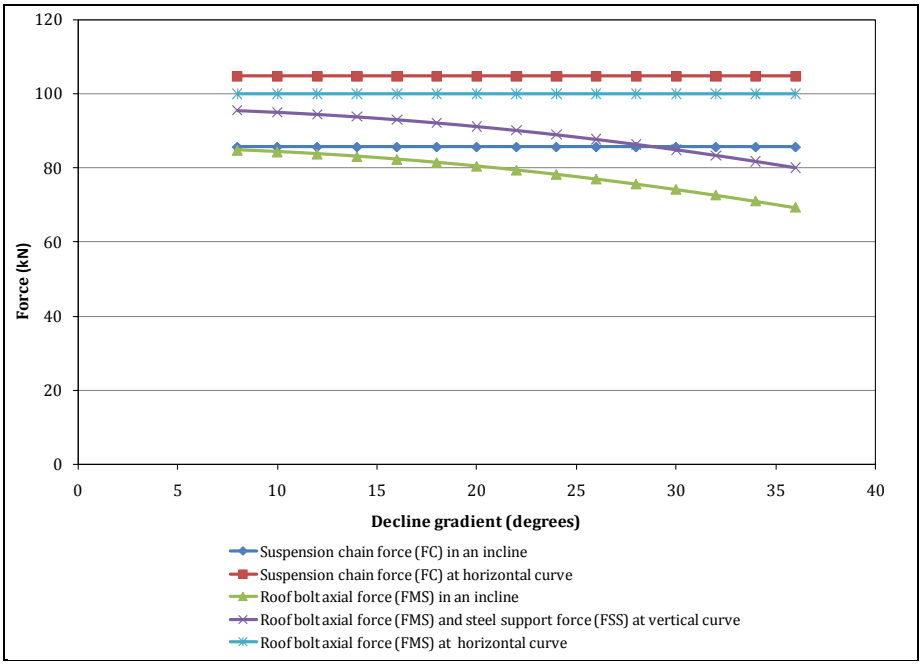

Figure 6.23: Variation of force in support system with change in decline gradient for the monorail loading system

Results shown in Figure 6.22 and Figure 6.23 indicate that the force required to suspend the monorail drilling system components is higher than that needed to

suspend the loading system components. According to the results, the strength of suspension chains in an incline, horizontal curves and in roof bolts at horizontal curves remains constant with changes in decline gradient. However, in an incline and at vertical curves, the axial strength of the roof bolts varies inversely with change in decline gradient, i.e., as the decline gradient increases the required axial strength of the roof bolts reduces. Roof bolts are strong enough to carry the additional bearing force that they are subjected to in this application. Similarly, the axial strength of steel supports at vertical curves varies inversely with decline gradient.

6.5.6.2 Strength of support system at 20^0 decline gradient

In Chapter 10, a mine design case study is presented in which the decline is designed with gradient of 20^0. Therefore, numerical values of the required support system strength at 20^0 decline gradient are determined. Figure 6.24 shows the numerical values for each system while Table 6.3 shows the displacements of suspension chains at horizontal curves for 20^0 decline gradient.

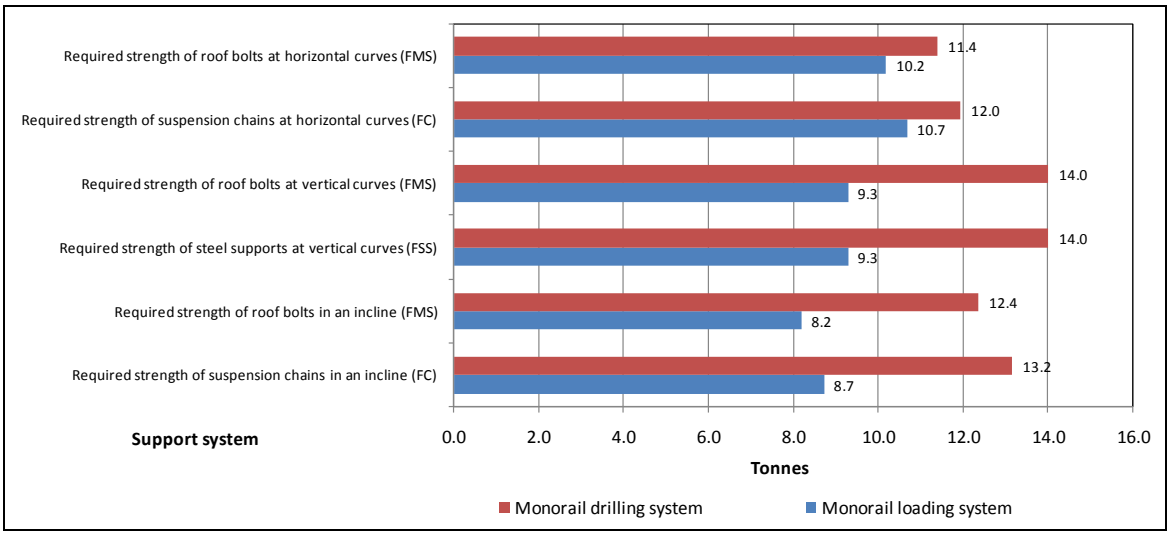

Figure 6.24: Strength of support system at 20^0 decline gradient

Table 6.3: Displacement of suspension chains at horizontal curves

Parameter	Unit	Monorail loading system	Monorail drilling System
Angular displacement (**δ**)	degrees	17.3	17.3
Horizontal displacement (**X**)	cm	18.7	18.7

According to the results, high strength roof bolts, suspension chains and steel supports are required to suspend and support the monorail drilling system components more than that required for the monorail loading system. In comparison with the roof bolts and suspension chains currently being used (namely Hilti OneStep® roof bolts), which have an ultimate strength of 320kN (32 tonnes) and 250kN (25 tonnes), respectively, it is clear that the roof bolts and suspension chains have adequate strength to suspend and support the components of the two systems. Analysis of variation of decline gradient with strength of support system shows that the higher the decline gradient, the lower is the axial force in the support system. In terms of suspension chain displacements at horizontal curves, results have shown that both systems would give the same angular and horizontal displacement of 17.3^0 and 18.7cm, respectively. These displacements can be minimized by reducing the velocity of the monorail systems at horizontal curves or increasing the radius of the curve. Since both systems move on the same rail Table 6.4 shows the recommended minimum numerical values. It should be noted that the recommended strength of support system at vertical and horizontal curves shown in Table 6.4 corresponds to minimum vertical and horizontal radii, i.e., $(r_v)_{min}$ = 10m and $(r_h)_{min}$ = 4m respectively

Table 6.4: Required strength of the support system

Parameter	Recommended value	
	kN	Tonnes
Suspension chains in an incline (F_C)	129.2	13.1
Roof bolts in an incline (F_{MS})	121.4	12.3
Steel supports at vertical curves (F_{SS})	137.6	14.0
Roof bolts at vertical curves (F_{MS})	137.6	14.0
Suspension chains at horizontal curves (F_C)	117.3	12.0
Roof bolts at horizontal curves (F_{MS})	112.0	11.4

6.6 Summary

This Chapter has revealed that correct installation of the roof bolts play a key role in ensuring smooth operations of the monorail system. The study has revealed that wrongly installed roof bolts result in shorter life of the support system. It is also apparent that improperly aligned rail/monorail develops unnecessary stresses in the system and leads to high power consumption and may result in derailments posing a safety hazard to the system and underground personnel. This Chapter has also demonstrated that to avoid roof bolt, suspension chain and steel support failure due to additional stresses from weight of the monorail drilling and loading systems components, high strength roof bolts, suspension chains and steel supports to support the components of two systems must be installed. In comparison with the roof bolts currently in use, the models developed have demonstrated that the support system has adequate strength to support and suspend the two systems. It has also been established that the required axial strength of roof bolts varies inversely with the decline gradient. However, the strength of suspension chains in the decline and at horizontal curves as well as the strength of roof bolts at horizontal curves remains constant but changes with horizontal radius (r_h). To reduce or minimise displacements of suspension chains, it is recommended that the velocity of the monorail system at horizontal curves be reduced during motion.

Chapter 7

7.0 Automation design for monorail system processes

7.1 Introduction

In Chapters 4 and 5, the conceptual monorail drilling and loading systems were developed. However, to improve the efficiency of the two systems, critical processes performed by the two systems during mining operations must be automated. Automation increases safety and productivity, reduces operator fatigue and also reduces the labour costs of the system. The aim of this Chapter is, therefore, to describe automation designs of major processes performed by the monorail drilling and loading systems during operations. During automation design, critical processes performed by the two systems and control requirements necessary to allow the two systems execute such processes automatically have also been identified. This Chapter begins by highlighting fundamental literature on the aspects of system automation and control engineering.

7.2 Process control engineering

Control engineering has evolved over time. In the past, humans were the main method for controlling a system (Olaf, 1979). More recently, electricity has been used for system control and early electrical control was based on relays. According to Ozdimir and Hanna (1995), these relays allow power to be switched on and off without a mechanical switch. It is also common to use relays to make simple logical control decisions. The development of low cost computer brought

the most recent revolution, the Programmable Logic Controller (PLC). The advent of the PLC began in the 1970s, and has become the most common choice for manufacturing controls. Also, operation of today's modern mining machines is carried out with PLC system (Gunnar et al., 1993). The PLC controls all processes with direct connection to the machines. Based on the logic implemented in the program, PLC determines which actions need to be executed with output instruments. Thus, many complex operational tasks have been solved by connecting PLC and possibly a central computer (Ozdimir and Hanna, 1995). Beside connections with instruments like operating panels, sensors, switches, valves etc, possibilities for communication among instruments are so great that they allow high level of process coordination as well as greater flexibility in realizing any process control system. PLC has the following advantages:

- Cost effective for controlling complex systems;
- Flexible and can be reapplied to control other systems quickly and easily;
- Trouble shooting aids make programming easier and reduce downtime;
- Computational abilities allow more sophisticated control; and
- Reliable components make PLC likely to operate for years before failure.

7.3 What is automation?

Dorf and Kusiak (1994) defined automation as a technology in which a process or procedure is accomplished by means of programmed instructions, usually combined with automatic feedback control to ensure the proper execution of the instructions. The effectiveness of any automation system depends entirely on the quality of its underlying electrical, mechanical and control engineering. This means that all systems that qualify as being automated must include the following three components (see also Figure 7.1):

- Power to accomplish the process;
- System program; and
- Feedback control.

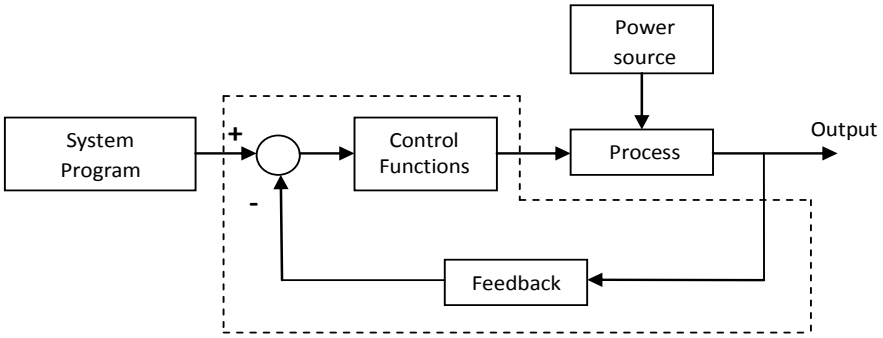

Figure 7.1: Components of an automated system (Dorf and Kusiak, 1994)

(i) Power to accomplish the process

The action performed by the automated system to accomplish its functions requires power. According to Dorf and Kusiak (1994), most power sources used in automated system are based on electrical energy.

(ii) System program

System program refers to the architecture and design of the application and services that make up an operating system or other control program. The actions performed by an automated system are determined by a program of instructions normally without human intervention. The instructions contained in the program specify the details of each action that must be accomplished and the sequence in which the actions must be performed.

(iii) Feedback control

Feedback controls can be defined as the use of different signals, determined by comparing the actual values of system variables to their desired values, as a means of controlling a system or process (Hellerstein et al., 2004). These controls are widely used in automated systems to ensure that the programmed commands have been properly executed. Feedback control is, therefore, a basic mechanism by which systems, whether mechanical, electrical, or biological, maintain their equilibrium or homeostasis (Dorf and Kusiak, 1994). Feedback control system consists of the following components:

- Input signal;
- Process;
- Output;
- Feedback sensing elements; and
- Controllers and actuators.

The input signal represents the desired value of the process output while the output is some variable that is being measured and compared with the input, e.g., pressure, temperature, others. Generally, the output value is a function of the process. Sensing elements close the loop between output and input while controllers and actuators compare the output with the desired input and make adjustments in the process. Since the system output is used to regulate its input, such a device is said to be a closed-loop control system (Dorf and Kusiak, 1994). Thus, feedback control in this case is used in closed-loop control systems.

7.4 Reasons for system automation

In many mining situations, manual operation requires that several repetitive operations be executed by the operator, thus, reducing the efficiency of the system. Therefore, the most obvious advantages of automating the system are its ability to increase the safety (i.e., removal of workers from dangerous and hazardous environment), efficiency (i.e., increase in effective working hours) as well as reduction in labour costs. According to Dorf and Kusiak (1994), the following arguments can also be raised in support of automation in designed systems:

- The system is safe since automation tends to remove humans from direct participation in the operations;
- Human errors in operations are minimised using automation;
- Automation also increases system reliability; and
- In industrialised nations where there is a shortage of labour, automation of systems is an alternative to increase in production with lower labour force.

7.5 Fundamentals of open and closed-loop control system

To maintain a physical quantity, such as pressure, flow-rate or temperature at a desired level during a technical process, the physical quantity can be controlled either by means of open-loop or closed-loop control system. This Section outlines the fundamental literature regarding the two control systems as they are applied to control engineering.

7.5.1 Open-loop control system

An open-loop controller is also called a non-feedback controller. According to Kuo (1991), an open-loop control system is a type of controller that does not use feedback to determine if its input has achieved the desired goal. This means that the system does not observe the output of the processes that it is controlling. Thus, an open-loop control system cannot correct any errors that it could make. The distinguishing feature of open-loop control is the open nature of its action, i.e., the output variable does not have any influence on the input variable. An open-loop controller is often used in simple processes because of its simplicity and low-cost, especially, in systems where feedback is not critical. Figure 7.2 shows an example of an open-loop control system.

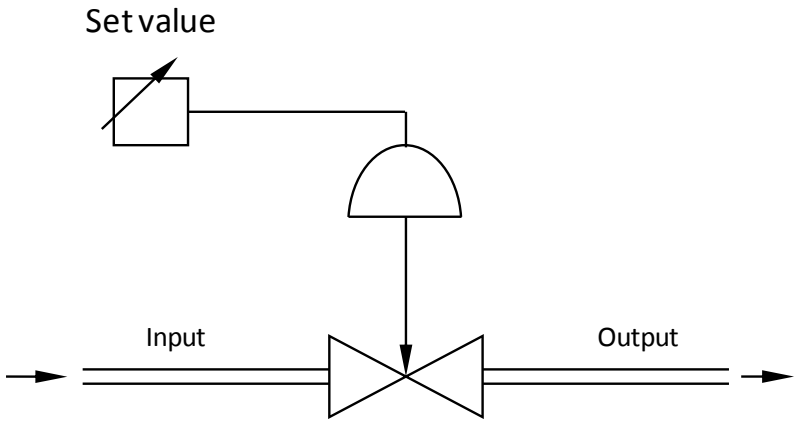

Figure 7.2: Open-loop control system (Samson, 2003)

7.5.2 Closed-loop control system

Kuo (1991) defined a closed-loop control system as a system in which the variable to be controlled is continuously measured and then compared with a predetermined value through the feedback system (Figure 7.3). If there is a difference between these two variables (i.e., error or system deviation), adjustments are made until the measured difference is eliminated and the controlled variable equal to the reference variable. Hence, feedback is an essential attribute of a closed-loop control system.

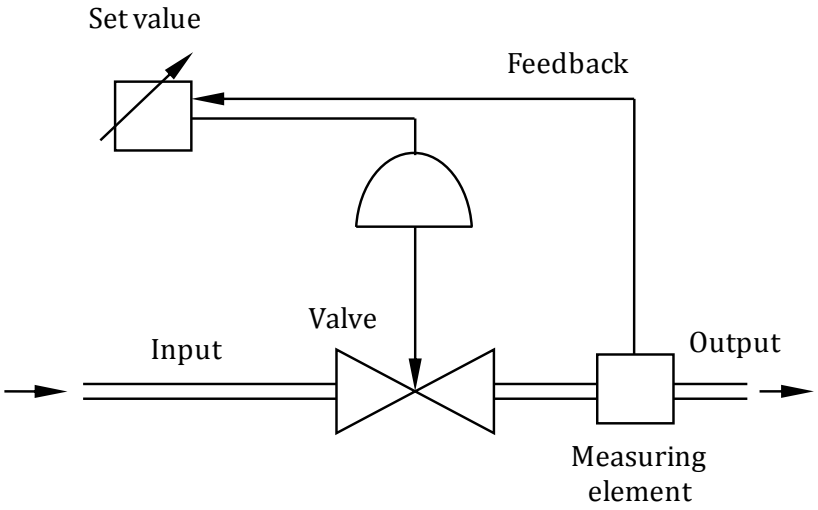

Figure 7.3: Closed-loop control system (Samson, 2003)

A closed-loop control system consists of a controller, actuator, plant and measurement device as indicated Figure 7.4.

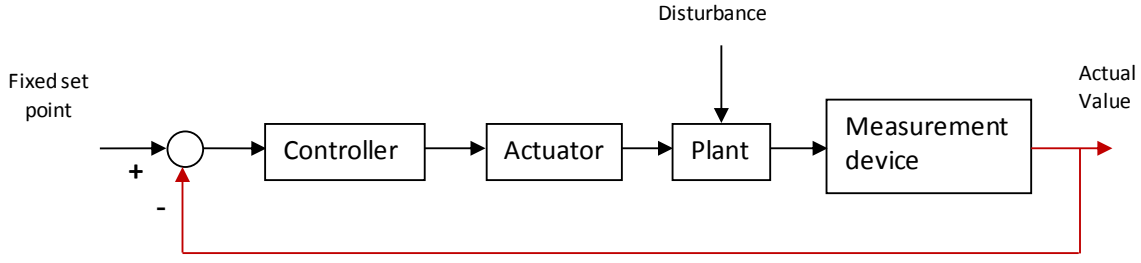

Figure 7.4: Components of a closed-loop control system (Schmid, 2005)

The signals in the closed loop are denoted by symbols as (see also Figure 7.5):

- y = controlled variable (actual value);
- w = Fixed set point;
- e = control error;
- u = manipulated variable; and
- z = disturbance.

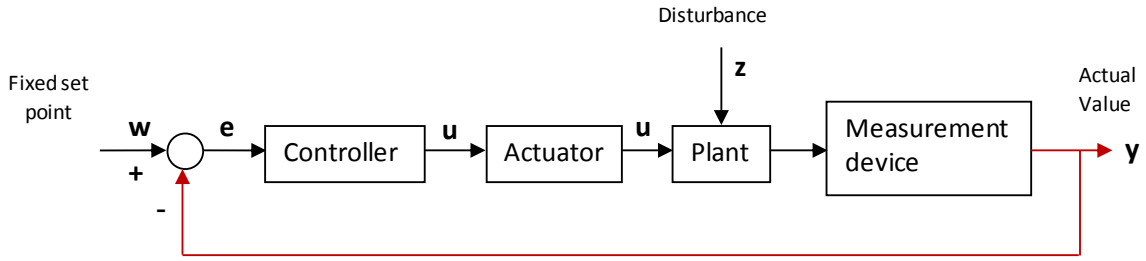

Figure 7.5: Signals of a closed-loop control system (Schmid, 2005)

As shown in Figure 7.5, the task of controlling a process (plant) consists of holding the controlled value y (t) acquired by the measurement device, either on a constant set point, i.e., w(t) = constant or tracking a time-varying reference variable w(t) ≠ constant, independent of external disturbances z(t). This function is performed by a controller. Thus, the controller has the task of holding the controlled variable as near as possible to the reference variable. The controller processes the control error e(t) = w(t) – y(t), i.e., the difference between the set point w(t) and the actual value y(t) of the controlled variable. Thus, it becomes obvious that the comparison of the set-point value **w** and the actual value **y** of the controlled variable for generating the control error **e** will become possible just through the negative feedback of the controlled variable **y**. The control signal $u_c(t)$ generated by the controller acts via the actuator as the manipulated variable u(t) on the plant, such that it counteracts in the case of fixed command control against the disturbance z(t).

The common closed-loop controller architecture is the Proportional-Integral-Derivative (PID) controller. According to Liptak (1995), a PID controller attempts to correct the error between a measured process variable and a desired

set point by calculating and then outputting a corrective action that can adjust the process accordingly. The PID controller calculation (algorithm) involves three separate parameters: Proportional, Integral and Derivative values as shown in Figure 7.6.

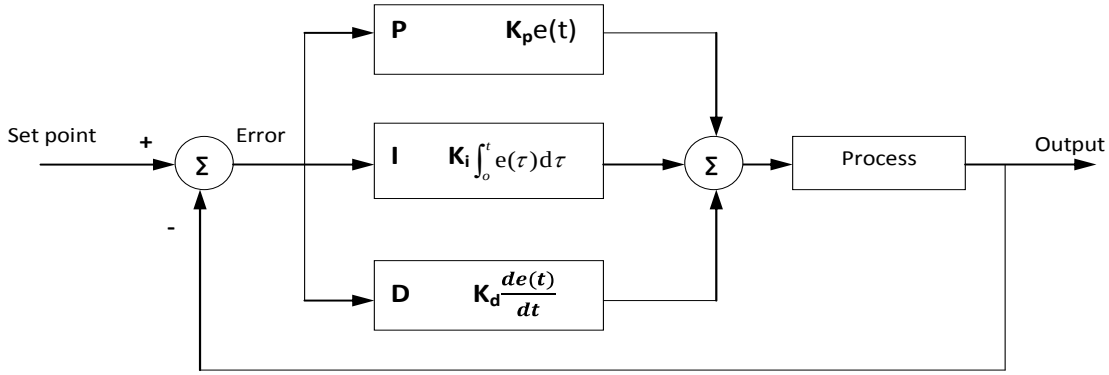

K_p	=	Proportional gain
K_i	=	Integral gain
K_d	=	Derivative gain
τ	=	Time in the past contributing to the integral response
t	=	Time or instantaneous time (the present)

Figure 7.6: PID controller (Samson, 2003)

The Proportional term determines the reaction to the current error, the Integral term determines the reaction based on the sum of recent errors and the Derivative term determines the reaction to the rate at which the error has been changing. The weighted sum of these three actions is used to adjust the process via a control element such as the position of a control valve or the power supply. The signal (u) from the controller is determined as shown in Equation 7.1:

$$u = K_P e(t) + K_i \int_0^t e(\tau)d\tau + K_d \frac{de(t)}{dt} \qquad 7.1$$

(a) Proportional term

The proportional term makes a change to the output that is proportional to the current error value. The proportional response can be adjusted by multiplying the error by the proportional gain. The proportional term is given by Equation 7.2:

$$P_{out} = K_P e(t) \qquad 7.2$$

where:

P_{out} = Proportional output; and

e = w(t) – y(t)

A high proportional gain results in a large change in the output for a given change in the error. Larger K_p typically means faster response since the larger the error, the larger the proportional term compensation (Figure 7.7). An excessively large proportional gain may lead to process instability and oscillation. In contrast, a small gain results in a small output response to a large input error and a less responsive (or sensitive) controller. If the proportional gain is too low, the control action may be too small when responding to system disturbances.

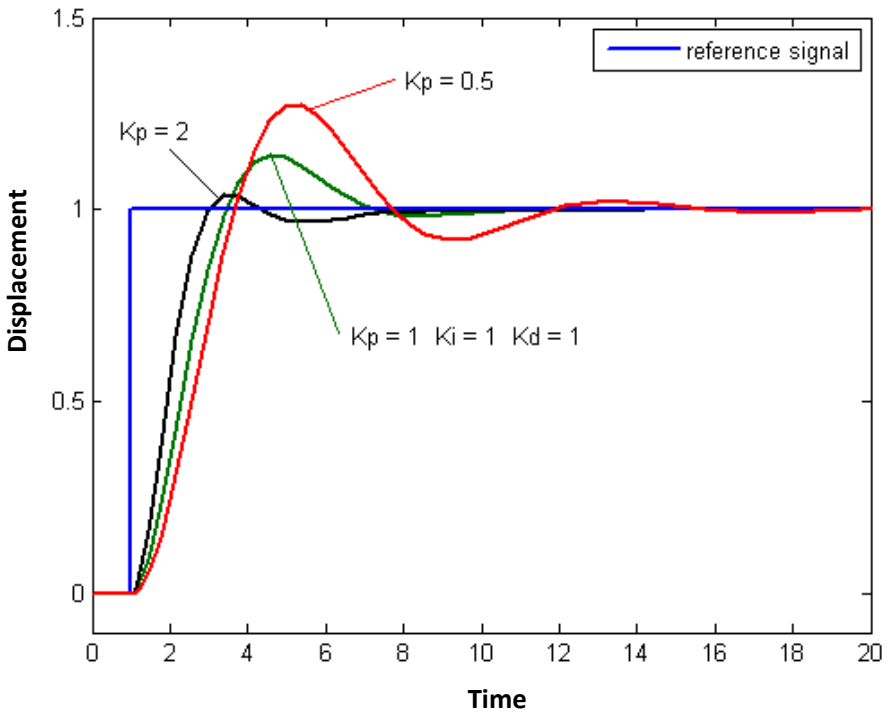

Figure 7.7: Process variables versus time for three values of K_p with K_i and K_d held constant (Source: http://www.wikipedia.org, 2007)

(b) Integral term

The contribution from the integral term is proportional to both the magnitude of the error and the duration of the error. Summing the instantaneous error over time (integrating the error) gives the accumulated offset that should have been corrected previously. The accumulated error is then multiplied by the integral gain and added to the controller output. The magnitude of the contribution of the integral term to the overall control action is determined by the integral gain, K_i. Larger K_i implies steady state errors are eliminated quicker. The integral term is given by Equation 7.3:

$$I_{out} = K_i \int_0^t e(\tau) d\tau \qquad 7.3$$

where:

$\mathbf{I_{out}}$ = Integral output

The integral term accelerates the movement of the process towards a set point and eliminates the residual steady-state error that occurs with a proportional only controller (Figure 7.8).

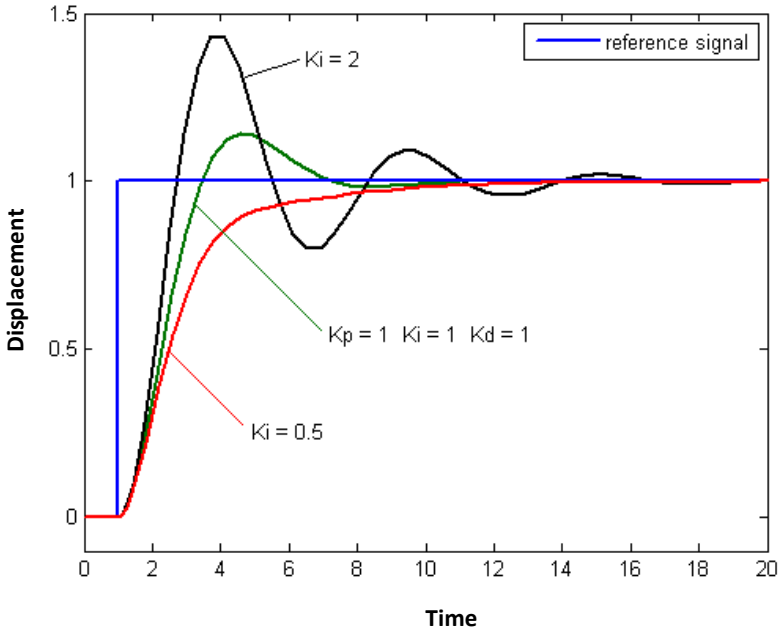

Figure 7.8: Process variable versus time for three values of K_i with Kp and K_d held constant (Source: http://www.wikipedia.org, 2007)

(c) Derivative term

The rate of change of the process error is calculated by determining the slope of the error over time and multiplying this rate of change by the derivative gain K_d. The magnitude of the contribution of the derivative term to the overall control action is termed the derivative gain, K_d. The derivative term is given by Equation 7.4:

$$D_{out} = K_d \frac{de(t)}{dt} \qquad 7.4$$

where:

$\mathbf{D_{out}}$ = Derivative output

The derivative term shows the rate of change of the controller output and this effect is most noticeable close to the controller set point. Hence, derivative control is used to reduce the magnitude of the overshoot produced by the integral component and improve the combined controller-process stability (Figure 7.9).

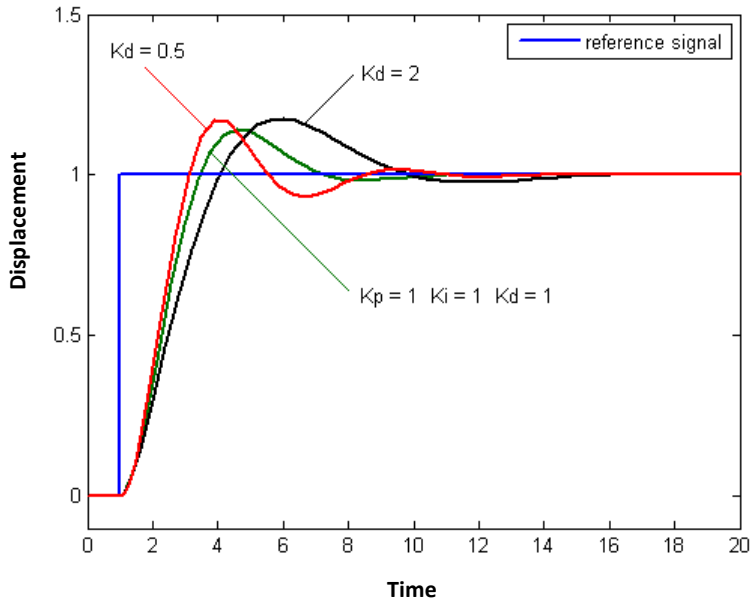

Figure 7.9: Process variable versus time for three values of K_d with K_p and K_i held constant (Source: http://www.wikipedia.org, 2007)

7.6 Automation design for monorail system processes

Using the Theory in Section 7.5, the description of automation design for the monorail drilling and loading systems processes is conducted. Automation design for monorail drilling and loading systems begins by identifying and describing critical processes performed by the two systems. This Section is intended to provide details of the automated processes performed by the two systems.

7.6.1 Overview of monorail system processes

Details of processes performed by the two systems, i.e., monorail loading and drilling systems are:

- Monorail loading system processes; and
- Monorail drilling system process.

(a) Monorail loading system processes

There are two critical processes performed by the monorail loading system that are automated: pneumatic loading and material discharge processes.

(i) Pneumatic loading process

This process involves automatic loading (suction) of rock fragments from the development face into the hopper. Automation of this process is such that, once the suction pipe is connected to the hopper, upon pressing a loading button on the control panel (located in the driver's cabin) the high pressure fan/pump is activated that creates negative pressure inside the hopper. The negative pressure enables automatic loading of material in the hopper. Since the negative pressure created inside the hopper should be monitored and controlled, to ensure that the pressure inside the hopper is correct, closed-loop control system is used during the process.

(ii) Material discharge from the hopper

Once the hopper is fully loaded, the loading process is stopped automatically when the required tonnage is loaded after which the suction pipe is disconnected from the hopper. The hopper is connected to the monorail train, which pulls the loaded hopper to the position of an empty monorail container where automatic discharge of rock fragments takes place. Therefore, automation involves automatic discharge of material from the hopper into an empty container. This means that when the discharge button is pressed on the control panel, material is discharged under gravity from the hopper into an empty container. The hopper will have an open and close mechanism at the bottom that will allow discharge of material to take place. Hydraulic system will be used for opening and closing mechanism of the hopper. Since there is no direct connection between the output (material discharge) and the input (hydraulic pressure needed for the open/close mechanism), open loop control system is used during automation design of this process.

(a) Monorail drilling system process

Automation of the monorail drilling system consists of the process of automatic face marking using laser beams projected onto the development face. In conventional mining, once cleaning of the development face is completed, face marking is done manually using paint. Manual face marking normally takes longer (than face marking using laser technology) and increases the total drill-blast-load-haul cycle time. Therefore, to reduce the mark-up time and the total drill-blast-load-haul cycle time, it is suggested that the monorail drilling system be equipped with drilling pattern laser projection technology (Graves and O'Brien (1998). This technology will enable the monorail drilling system project laser spots of the desired drilling pattern onto the development face. The projected laser spots will indicate precisely the location of drill holes on the development face. Therefore, automation of the monorail drilling system process involves automatic face marking by projecting desired drilling pattern onto the face. Because the projected drill pattern needs to be aligned properly on the drill

face, i.e., the input signal (desired drill pattern) is related to the output signal (position of drill holes on the face), closed-loop control system is used during the design of the automation system.

7.6.2 Description of automation design for monorail loading process

Figure 7.10 shows the description of automation design for the monorail loading process. The main components of the automation design are:

- Control panel;
- Feedback display monitor; and
- Surface control.

Since the control panel of the monorail loading system is an interactive and menu driven device, once the loading process is selected on the control panel, the process being executed is displayed on the feedback display monitor located in the driver's cabin as well as on surface monitoring control unit. All operations of the loading system are monitored on the feedback display monitor.

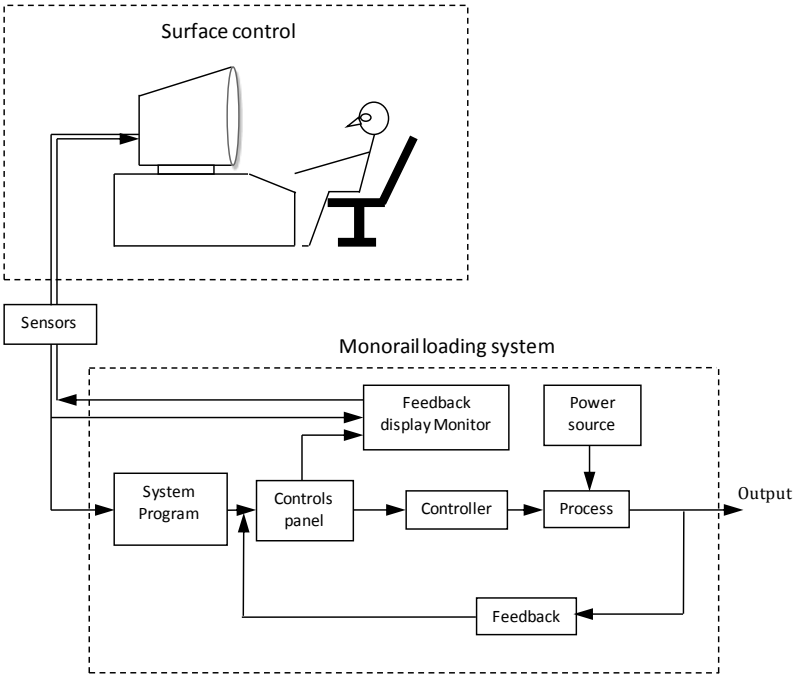

Figure 7.10: Schematic description of automation design for the loading process

(a) Control panel

The control panel is located in the driver's cabin of the monorail train. The operation of the system is done from the control panel. It is also used as an interactive input device by the operator to select processes to be accomplished by the system. The control panel is also linked to the feedback display monitor for the purpose of monitoring whether the processes currently being executed by the system are being done correctly.

(b) Feedback display monitor

The most basic tool of control engineering is the feedback loop. For the monorail loading system, the output signal (i.e., the actual negative pressure in the hopper) during the loading process is displayed and viewed on the feedback display monitor. The output signal is compared with the input signal (i.e., the desired negative pressure in the hopper) and adjustments are made via the PID controller if the output signal deviates from the desired input signal. The feedback monitor is used to monitor and control the dynamic behaviour of the loading process. Other advantages of feedback monitoring include:

- Indication whether the system is functioning properly or not; and
- Showing the current operation being executed by the system.

(c) Surface Controls

The monorail system is also linked to surface control unit where all operations and processes being executed by the drilling system are monitored and may be controlled. This means that all signals resulting from the operator's instructions as well as feedback from system process are viewed on the feedback display monitor (in driver's cabin) as well as on surface control monitors. The following are some of the benefits and/or advantages of having monorail system surface control units:

- Monitoring, controlling and recording of operations of the monorail drilling and loading systems, thus increasing the safety of the system;
- Acquiring and recording of production data (e.g. drilled metres, number of holes drilled, tonnes loaded etc.);
- Serving as a communication centre for monorail system operations; and
- Automatic transfer of production data to the mine management network.

7.6.3 Description of automation design for the monorail drilling system

As highlighted in Section 7.6.1, automation design for the monorail drilling system involves automating face marking using laser technology. The description of the layout (Figure 7.11) is similar to the loading system but with addition of components 4 and 5, i.e., drilling pattern and laser projection with video sensor, respectively.

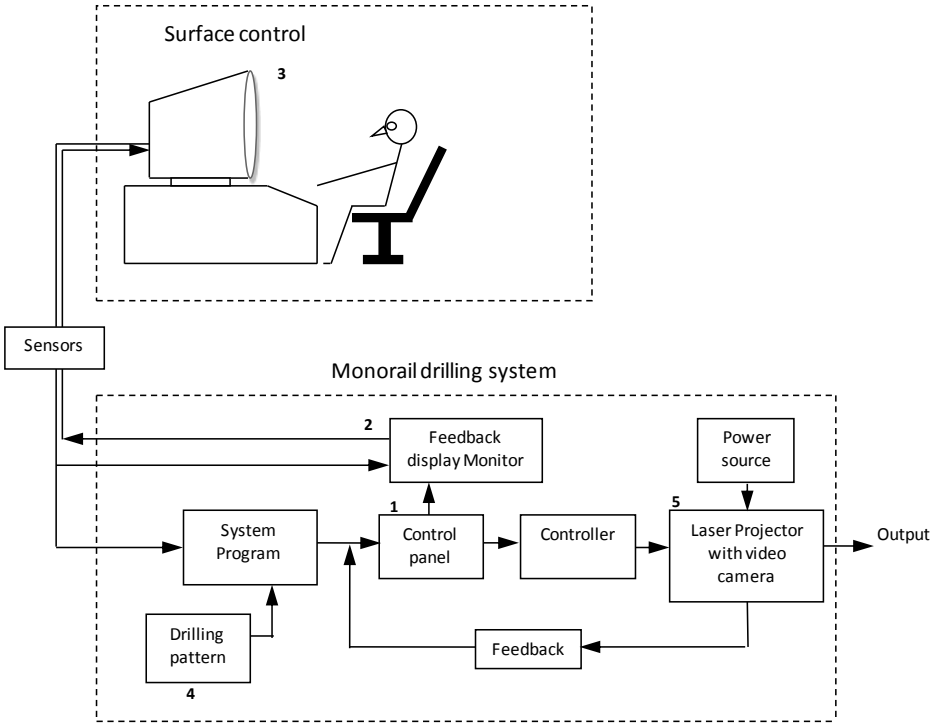

Figure 7.11: Schematic description of automation system for face marking

The drilling pattern component (4) includes programming of different drilling patterns for the operator to choose from. Thus, before face drilling commences,

the system operator will select the required drilling pattern from the drilling pattern database depending on the size of the face being drilled. Alternatively, drilling patterns can be saved on the USB flash drive from which the operator can select the desired pattern. The selected drilling pattern can be viewed on the feedback display monitor as well as on surface control system. Alignment of the drill pattern on the drill face is done using the controller. The system is also equipped with drill pattern laser projection technology with video sensor. The technology allows the selected drilling pattern to be projected onto the development face using laser beams. Thus, the exact position of drill holes on the drill face is indicated by laser spots from the projector.

7.7 Process control flow diagrams for monorail system

In this Section, process control flow diagrams for monorail system automated processes are developed.

7.7.1 Process control flow diagram for monorail loading process

Based on Figure 7.10, the process control flow diagram for monorail loading process is described and shown in Figure 7.12. Closed-loop control system is used during the design.

For the loading process, the output being controlled is the negative pressure inside the plant (hopper) while the control variable is the fan/pump speed which influences output negative pressure. According to the process control flow diagram, the required negative pressure in the hopper is set using the pressure gauge knob in the driver's cabin. Using the servo-valve or valve actuator, the speed of the high pressure fan/pump that gives the required negative pressure in the hopper is set. The PID controller has the task of controlling the pressure in the hopper and to keep it as close as possible to the value of the set pressure, i.e., it compares the actual pressure in the hopper with the set pressure and try and keep the error (difference between set value and actual value) to a minimum.

The operations of the monorail loading process are also monitored on surface control system through sensors.

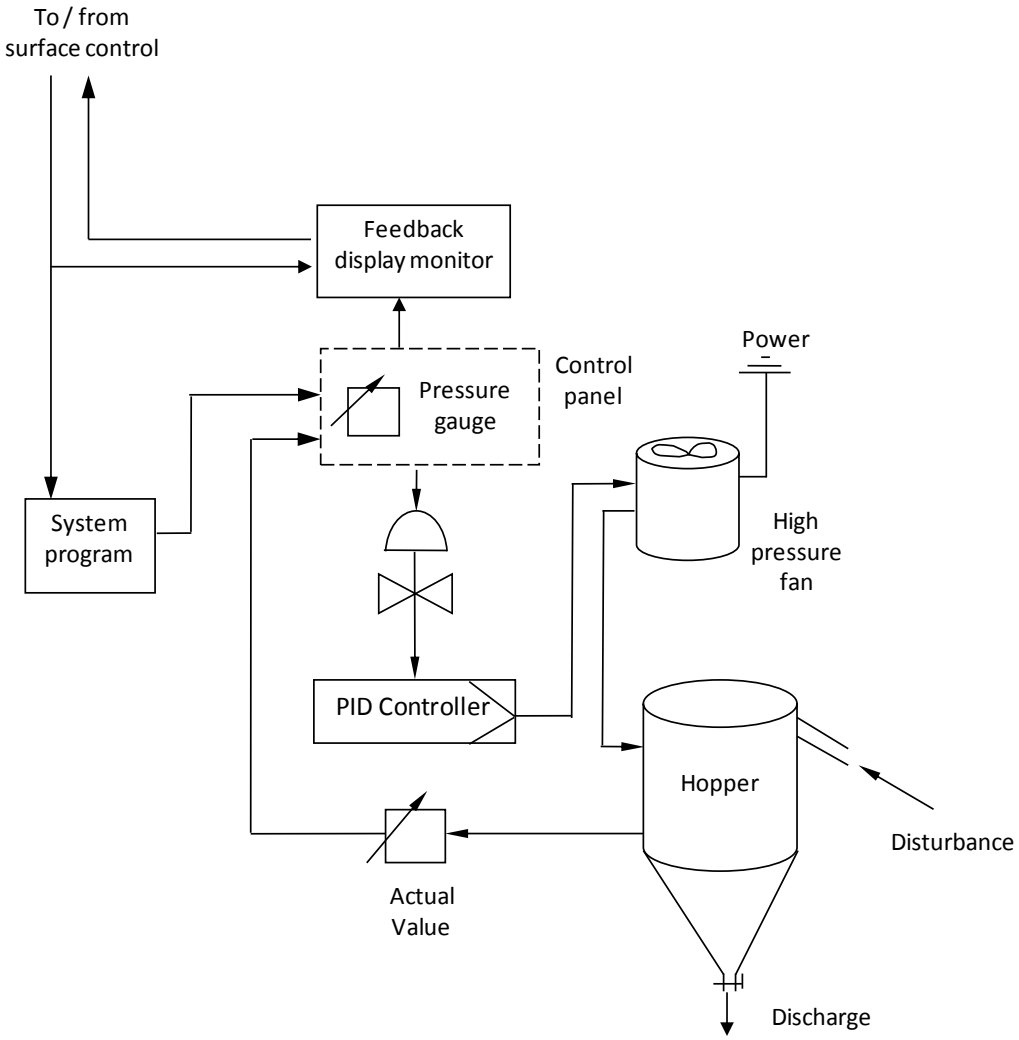

Figure 7.12: Process control flow diagram for monorail loading process

7.7.2 Process control flow diagram for material discharge process

Figure 7.13 shows the process control flow diagram for material discharge process for the monorail loading system. The open and close mechanism of the hopper is spring loaded and is connected to the hydraulic system.

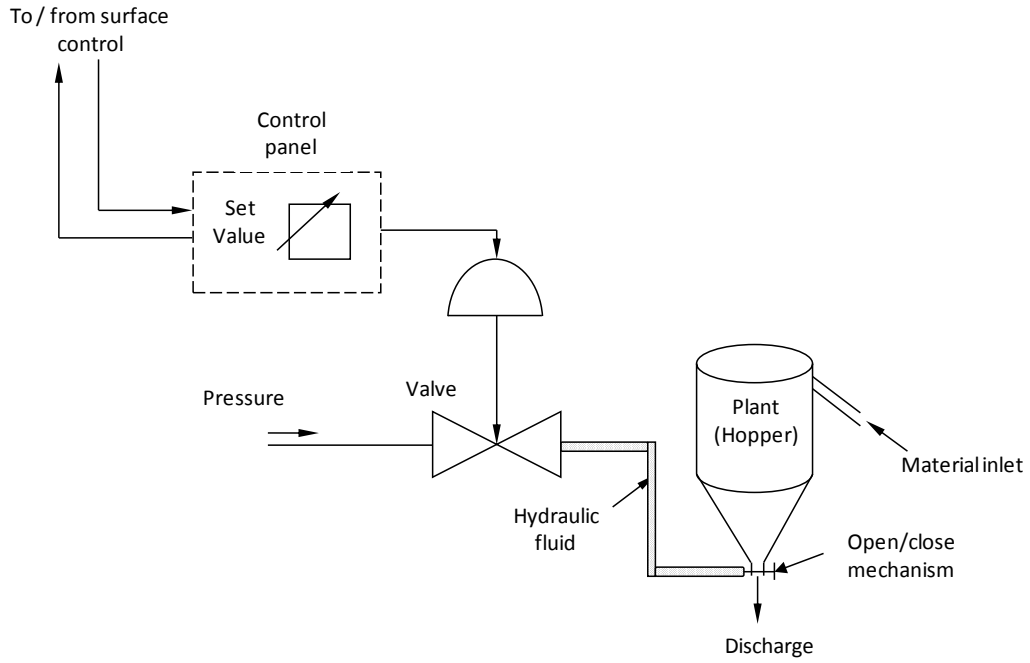

Figure 7.13: Process control flow diagram for monorail discharge process

Control of opening and closing of the hydraulic discharge mechanism at the bottom of the hopper is by means of a control valve along the pressure line. The opening mechanism is such that when the pressure valve is open, the hydraulic fluid is forced to open the open/close mechanism at the bottom of the hopper. Since the mechanism is spring loaded, once material is discharged, closing of the hopper is accomplished by cutting out the pressure supply to the hydraulic system, i.e., by closing the pressure valve and the spring forces the mechanism to close. A hydraulic pressure gauge is used to indicate the pressure in the hydraulic system during the open mode. However, this automated control action is capable of manual override by the operator. This provision gives the monorail system some flexibility in case of a problem with an automation system. Figure 7.14 shows process control flow automation diagram for the monorail loading process and material discharge.

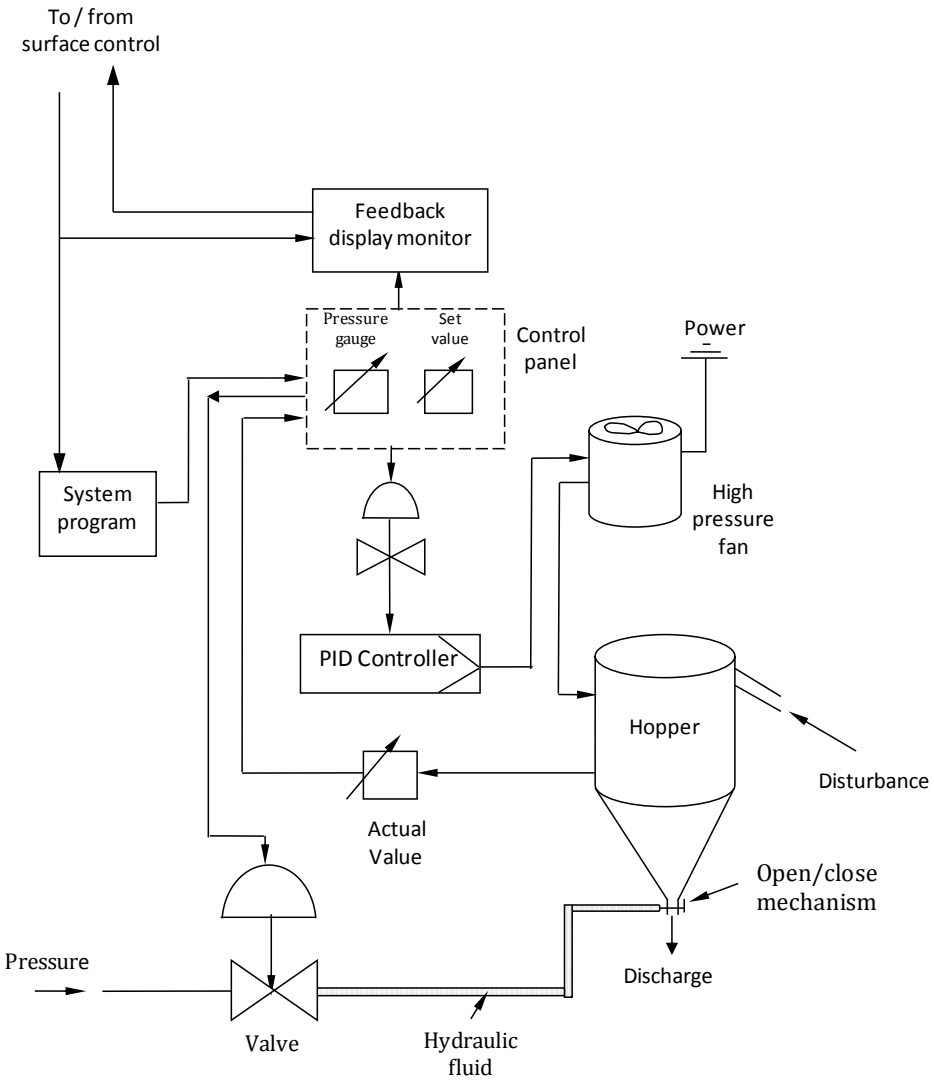

Figure 7.14: Process control flow diagram for monorail loading and discharge processes

7.7.3 Process control flow diagram for face marking process

Since the feedback is required to ensure that the projected drill pattern is aligned properly onto the drill face, closed-loop control system is used to design the automation system for laser projection face marking. Figure 7.15 shows the process control flow automation diagram for face marking using laser projection technology.

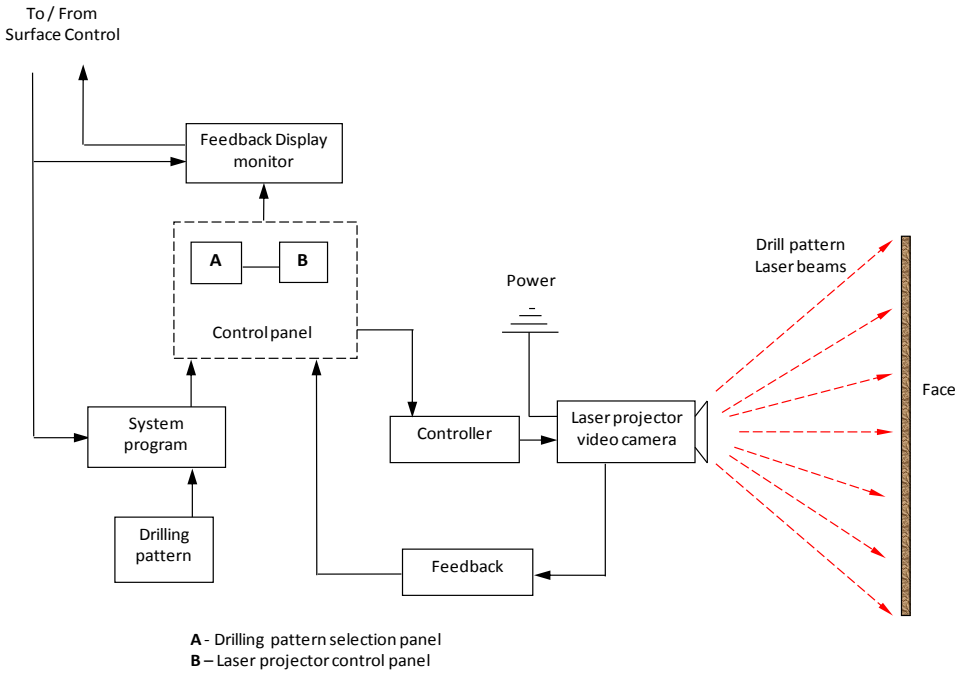

Figure 7.15: Process control flow automation diagram for face marking

As shown in Figure 7.15, the required drilling pattern is selected using the drill pattern selection panel (A) on the control panel. The selected drill pattern is displayed on the display monitor in the driver's cabin as well as on surface control system. Once the laser projector and video camera are switched on using control panel (B), the selected drill pattern is projected on the drilling face. Laser spot would indicate the precise location of drill holes on the development face. The video camera located within the laser projector is used to send images of the projected drill pattern onto the feedback display monitor and surface control unit through video sensors.

7.8 Summary

This Chapter has demonstrated that automation of monorail loading and drilling systems processes is possible. The ultimate aim of automation design is to increase the safety and improve the efficiency of the two systems. The proposed automation system increases productivity by improving operator performance through control of the system processes. Automation of the monorail drilling and loading systems will reduce the total drill-load-haul cycle time hence improving

the efficiency of the systems. It is also envisaged that monorail surface controls will have the following advantages:

- Monitoring, controlling and recording of operations of the monorail drilling and loading systems, thus increasing the safety of the system;
- Acquiring and recording of production data (e.g., drilled metres, number of holes drilled, tonnes loaded, etc.);
- Automatic transfer of production data to the mine management network; and
- Serving as a communication centre for monorail system operations.

Chapter 8

8.0 Simulation of monorail system

8.1 Introduction

In Chapters 4 and 5, theoretical models of the monorail drilling and loading systems were developed. It is, however, necessary to determine the performance of the two systems in terms of advance rates per day using time and motion studies. The aim of this Chapter is to model the conceptual monorail drilling and loading systems and use computer simulation to determine the performance of the two systems against which operational performance could be measured. GPSS/H simulation software and PROOF animation software are used to simulate and animate the drilling and loading systems, respectively. During the simulation process, the performance of the two systems to variation in loading time of the pneumatic loading system is also explored.

8.2 Discrete-event simulation

Simulation is defined as 'the process of designing a computerised model of the system (or process) and conducting experiments with this model for the purpose of either understanding the behaviour of the system or of evaluating various strategies for operations of the system' (Udo and James, 1993). The act of simulating generally entails representing certain key characteristics or behaviour of a selected physical or abstract system in order to identify and understand the factors which control the system and/or to predict the future behaviour of the system. The purpose of simulation is, therefore, to shed light on the underlying mechanisms that control the behaviour of a system. More

practically, simulation can be used to predict (forecast) the future behaviour of a system and determine what can be done to influence that future behaviour. This means that simulation can be used to predict the way in which the system might evolve and respond to its surroundings. Therefore, during the simulation process one can identify any necessary changes that will help make the system perform the way that is desired. It is a powerful and important tool because it provides a way in which alternative designs, plans and/or policies can be evaluated without having to experiment on a real system, which may be prohibitively costly, time-consuming or simply impractical to do.

Because simulation is such a powerful tool to assist in understanding complex systems and to support decision-making, a wide variety of approaches and simulation tools exist (Fishman, 2001). Modelling complex systems, especially, in engineering, health, management, mathematics, military, telecommunications, and in transportation science uses discrete-event as a simulation tool. This tool provides a relatively low-cost way of gathering information for decision making. Fishman (2001) described discrete-event system as a system in which one or more phenomenon of interest changes value or state at discrete points in time, rather than continuously with time. Thus, in discrete-event systems, the number of actions taking place can be counted at any one instant in time (Sturgul, 2000).

Discrete-event simulation has long been an integral part of the design process of complex engineering systems and modelling of natural phenomena (Carl, 2002). Many of the systems which we seek to understand or control can be modelled as digital systems. In digital model, the system is viewed at discrete instants of time in effect taking snapshots of the system at these instants. In designing, analysing and operating such complex systems, one is normally interested not only in performance evaluation but also in sensitivity analysis and optimization. Since the performance of the monorail drilling and loading systems will be viewed at discrete instants of time, discrete-event simulation is used during simulation of the two systems.

8.3 Simulation model development

Fishman (2001) defined a simulation model as an abstract logical and mathematical representation of a system that describes the relationship among objects in a system. Thus, to model a system, such as, the monorail drilling and loading systems, one must first understand its working principles. Acquiring sufficient understanding of the system to develop an appropriate conceptual, logical and then simulation models, is one of the most difficult tasks in simulation analysis. Clear understanding of all working principles and processes of the monorail system is fundamental in developing a valid model. Figure 8.1 shows the model development cycle whilst Figure 8.2 offers an elaboration of the phases within each of the periods shown in Figure 8.1. Figures 8.1 and 8.2 also depict the processes by which a modelling study transitions from one phase to another.

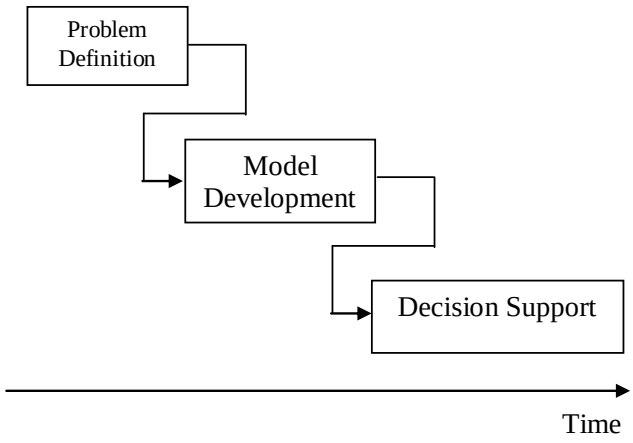

Figure 8.1: Chronological periods of the model life cycle (Nance, 1984)

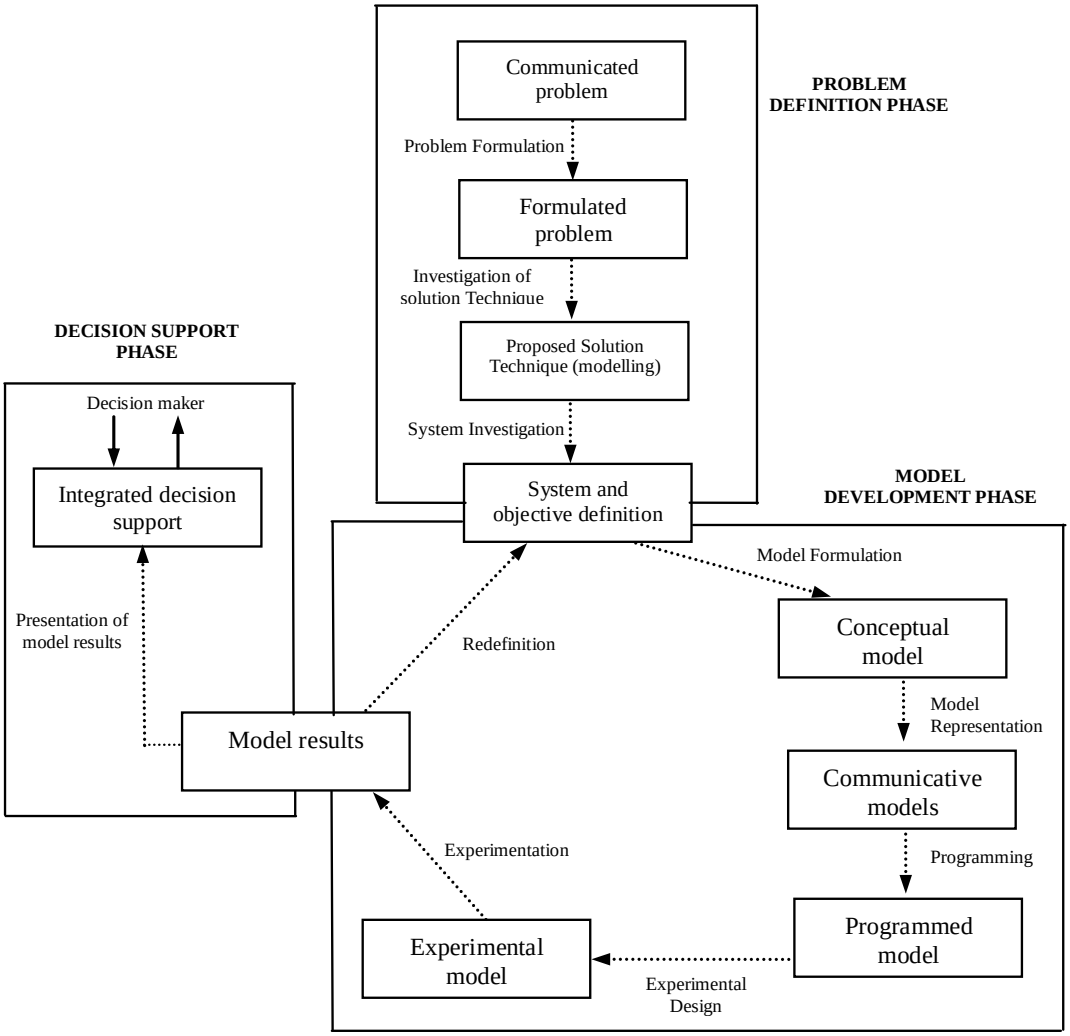

Figure 8.2: Phases in chronological periods of the model life cycle (Nance, 1984)

In general, having a definitive approach for conducting a simulation study is critical to the study's success and to developing a valid model in particular. This Section describes the approach that is followed during simulation of the monorail system.

8.3.1 Problem formulation

The first step in conducting a significant simulation project is to ensure that adequate attention is directed towards understanding what is to be accomplished by performing the study. During problem formulation, the problem of interest should be stated. According to Law (2005), the problem may

not be stated precisely or in quantitative terms. Thus, during this stage, an iterative process is often necessary. Chung (2003) also reveals that during problem formulation stage, the simulation practitioner can firmly establish the practicality of using simulation to analyse the system. Thus, at this stage the overall objectives as well as the specific questions to be answered by the study are highlighted.

8.3.2 Validity of conceptual model

To obtain best results from the simulation model, it is necessary to ensure that the conceptual model is valid. It is often necessary to perform a structured walk-through of the conceptual model to check its validity. If errors or omissions are discovered, the conceptual model must then be corrected before programming commences.

8.3.3 Model programming

This stage involves programming of the model using simulation software. Selection of simulation software to be used during programming is critical at this stage. Software selection for simulation modelling is invariably a more complex process. It requires a careful and thoughtful approach to fully address the issues and impacts related to decisions.

After the model has been programmed into simulation software, verification and debugging of the programme follows. In general, verification focuses on the internal consistency of a model, while validation is concerned with the correspondence between the model and the reality. The term validation is applied to those processes which seek to determine whether or not a simulation is correct with respect to the 'real' system. More prosaically, validation is concerned with the question 'Are we building the right system?' Verification, on the other hand, seeks to answer the question 'Are we building the system right?' Verification checks that the implementation of the simulation model (program) corresponds to the model.

There are currently no algorithms or procedures available to identify specific validation techniques, statistical tests, or other mechanism to use in the validation process (Sargent, 1991). Various authors, such as, Shannon (1975), suggest that, as a minimum, the three steps: face validity, testing of the model assumptions and testing of input-output transformations are taken. Therefore, during monorail system model development, it was prudent to validate and verify the model to achieve accurate (but not 100%) results from the model. Verification was performed by testing the model, which enable error identification and correctable made to the underlying model.

8.3.4 Model performance measure

The simulation models are often subject to errors caused by the estimated parameter(s) of underlying input distribution functions. 'What-if' analysis is needed to establish confidence with respect to small changes in the parameters of the input distributions. Performance measure is used to develop measurable performance indicators of the system. However, estimating system performance for several scenarios via simulation, generally, requires a separate simulation run for each scenario. Thus, a system performance measure is normally estimated by a value or series of values quantifying system behaviour as captured by the model and simulation (Standridge and Tsai, 1992). In simulating the monorail system, the system tasks and processes were reviewed, analysed and interpreted and thus performance requirements were revised.

8.3.4.1 System performance measure

The overall performance value of the monorail system depends on its operational speed, i.e., the efficiency with which the system completes the scheduled job. Thus, the performance of the monorail system will be measured by the speed with which it completes drilling and cleaning the development face. This is measured by the number of development faces drilled and cleaned during a specified period of time (shift or day). The numbers of faces drilled and cleaned per shift are determined using Equations 8.1 and 8.2:

$$\text{No. of faces drilled/ shift} = \frac{\text{Total hours in a shift}}{\text{Time to drill one face (plus delay time)}} \qquad 8.1$$

$$\text{No. of faces cleaned/ shift} = \frac{\text{Total hours in a shift}}{\text{Time to clean one face (plus delay time)}} \qquad 8.2$$

The system also needs targets against which the above performance can be judged. These targets determine the true capabilities of the system. The need for targets emphasises the point that operational performance can only be meaningful if measured against the system capabilities. Therefore, for the monorail system, the advance rate was determined at minimum loading time and is used as target to evaluate the system capability.

8.3.4.2 Process performance measure

Process performance measure relates to time interval that a process is delayed by the system. This means that the more time the process takes to be completed, the more inefficient will be the system and vice versa. During simulation of the monorail system, the following process performance measures were of interest:

- Drilling of support holes;
- Drilling of development face holes;
- Connecting / disconnecting suction pipe;
- Loading (sucking) of rock fragments from the development face into the hopper;
- Discharge of material from hopper into monorail containers;
- Lifting of loaded monorail containers by monorail train;
- Transportation of loaded monorail containers to the surface for dumping;
- Dumping time on surface;
- Return of monorail system underground; and
- Lowering of empty monorail system container underground.

The performance of the monorail system is judged by its effectiveness and efficiency with which the above processes are fulfilled. This means also that the faster the system achieves the above processes, the more efficient is the system and vice versa.

8.4 Simulation of monorail drilling and loading systems

8.4.1 Description of monorail system simulation processes

In this Section, monorail drilling and loading system's major processes that are modelled during simulation are described. Figure 8.3 shows the process flow chart for the monorail drilling and loading systems.

As shown in Figure 8.3, the monorail system consists of three processes: drilling, loading and material haulage (including dumping) on surface. The processes shown in Figure 8.3 are interdependent and affect the total drill-blast-load-haul cycle time and eventually the performance of the system. Because the monorail drilling system depends on the performance of the monorail loading system, sensitivity analysis of the pneumatic loading time on the total drill-blast-load-haul cycle time was performed during simulation studies, to determine the optimal drill-blast-load-haul cycle time of the system.

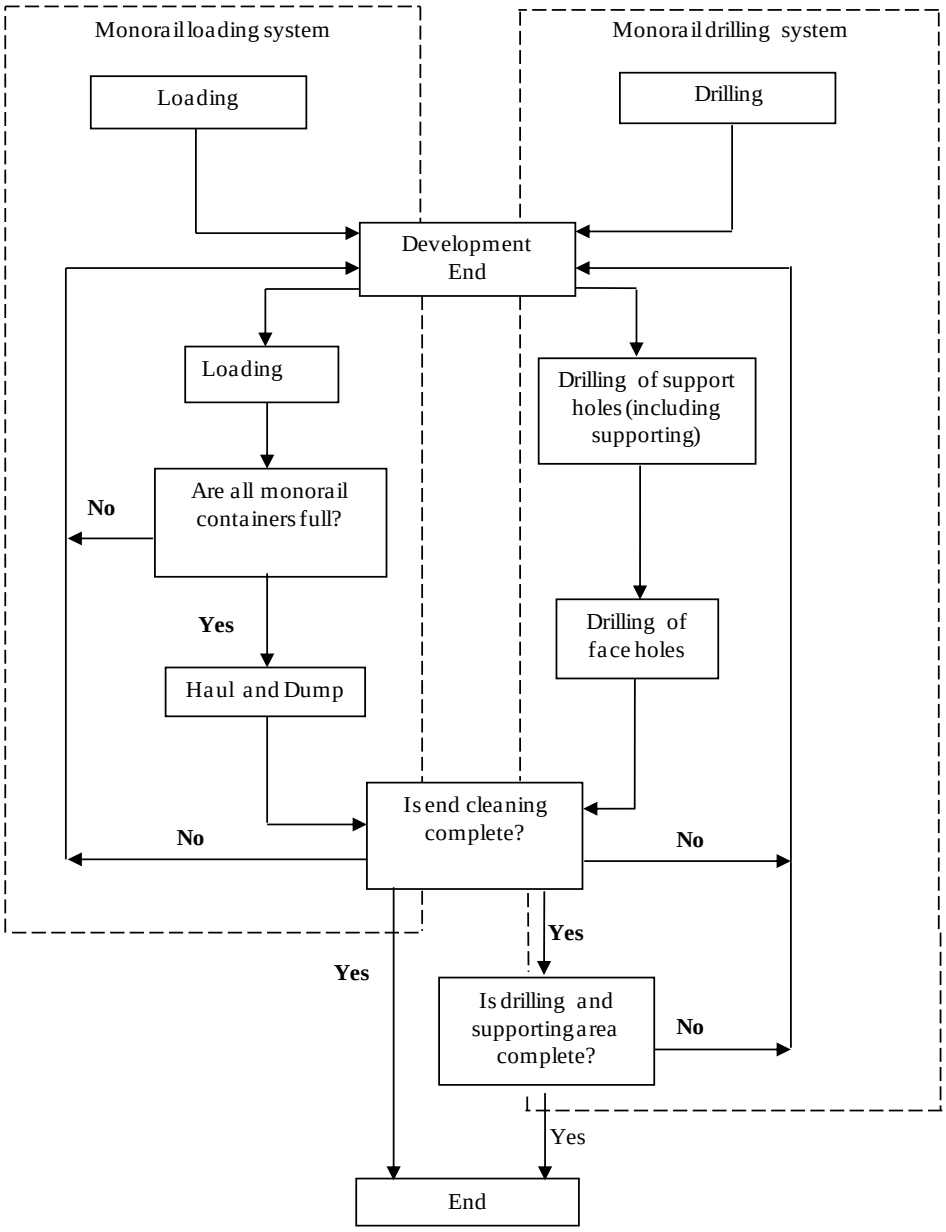

Figure 8.3: Process flow chart for monorail drill-load-haul system

(a) Drilling process

Figure 8.3 shows that drilling of the development face (including face support) commences at the same time as face cleaning process. The operation of the drilling system is such that drilling the top part of the face commences immediately after the development face is blasted and made safe as the loading system continues cleaning the development face. Therefore, drilling is not

completed as long as the development face is being cleaned. Drilling will also continue for some time after cleaning the face has been completed to allow drilling of down holes to take place. This means that the cycle time for the monorail drilling depends on the efficiency of the loading system, the number of holes being drilled as well as the time to drill one hole.

(b) Loading process

As shown in Figure 8.3, the operations of the monorail pneumatic loading system are such that when the development face is blasted and ready to be cleaned, the pneumatic loading system immediately begins loading rock fragments into the hopper via the suction pipe. When the hopper is fully loaded, the suction pipe is disconnected from the hopper. The hopper is then connected to the monorail train, which pulls the hopper to the position of an empty container where automatic discharge of rock fragments takes place. After material discharge, the monorail train pushes the hopper back to the loading position where the suction pipe is reconnected to the hopper to begin the loading process. The process is repeated until all the material from the face is loaded, i.e., until the face is completely cleaned. Figure 8.4 summarizes the loading process of the monorail loading system.

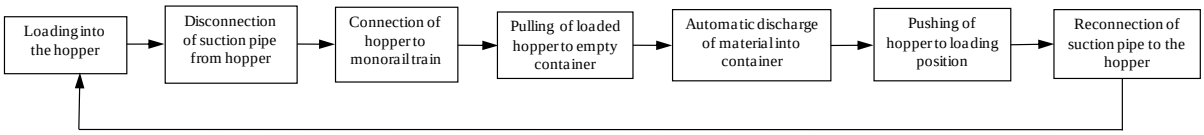

Figure 8.4: Process flow chart for monorail loading operation

The above processes are modelled during programming of monorail loading system model. Since the objective of the loading system is to clean the development face as fast as possible, the sensitivity of the loading process (loading time) on the total drill-blast-load-haul cycle time is investigated. Additionally, during model simulation, the performance of the loading system was examined by optimising the loading time.

(c) Hauling and dumping

When all the monorail containers are fully loaded, the hopper is disconnected from the monorail train and the train is moved to the container's lifting position where lifting of loaded containers take place. Loaded containers are then transported to the surface by the monorail train for material dumping. After material is dumped, the monorail system returns underground with empty monorail containers. Upon lowering the empty containers to the loading position, the hopper is reconnected to the monorail train and face cleaning resumes. This process is repeated until the whole face is completely cleaned. Figure 8.5 shows the hauling and dumping process of the monorail system.

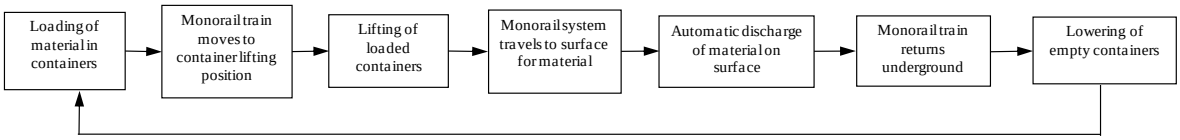

Figure 8.5: Process flow chart for material haulage to surface

Hauling and dumping operations are also affected by the length of the decline. This means that the longer the decline length, the longer the monorail system takes to haul and dump the material to the surface and return underground. This will eventually affect the drill-blast-load-haul cycle time of the system. However, drilling operation will not be affected since the monorail drilling system will continue drilling the development face when the material is being hauled to surface.

8.4.2 Model assumptions

Tables 8.1 and 8.2 show the assumptions used during simulation of the monorail system. Since the monorail is a new system, time estimates used in the model are based on the information from the manufacturers (Scharf, 2007) of the monorail train as well as on the author's engineering judgement.

Table 8.1: Time estimates for monorail system model simulation

Process	Time (Sec)
Time to lower monorail container	10±0.5
Time to connect / disconnect pipe	20±10
Time to discharge material into containers	5±0.1
Waiting time before Monorail lifts containers (Connection of chains)	8±0.1
Time to lift containers	10±0.5
Dumping time on surface	120±30
Time to drill one hole	360±10
Time to drill and support one hole	360±10

Table 8.2: Parameters for monorail system model simulation

Description	Unit	Value
Number of holes (48 face holes, 32 support holes and 6 monorail support holes)	-	86
Decline end size	m	4 x 4
Density factor	t/m^3	2.8
Total tonnage from the development face	t	136
charging/blasting/fume dissipation and monorail extension	minutes	90±10

8.4.3 Model programming

GPSS/H programming software is selected for simulating the monorail system. The software is designed for studying systems represented by discrete-events. According to literature, GPSS/H can solve variety of mining problems rapidly and accurately (Sturgul, 2000). GPSS/H has been proved to be extremely versatile for modelling mining and mining-related operations and can also easily be coupled with PROOF animation software for making animations (Sturgul, 2000). The monorail system model was programmed using GPSS/H software while PROOF animation software was used to animate the system. Appendix 1 gives a listing of the GPSS/H model programme while Appendix 2 shows PROOF animation screen-shots of monorail system model during simulation study.

8.5 Results of monorail system simulation model

In this Section, results of the monorail system simulation study are presented. The model was simulated for different loading times during the 12-hour shift.

8.5.1 Effect of loading time on lashing speed

In this study, the 'loading time' means the time the pneumatic suction system takes to suck rock fragments from the development face to fill the hopper. On the other hand, the 'lashing speed' is the time the suction system takes to completely clean the development face (i.e., time to suck all rock fragments from the face), which requires a number of hopper loads.

To determine the effects of the loading time on the lashing speed, the loading time of the pneumatic loading model was varied while examining the time it would take to clean the development face. According to Section 4.5.3, the minimum and maximum loading times of the pneumatic loading system are 11 minutes and 24 minutes, respectively. Therefore, the model was simulated from 10 minutes (600 seconds) to 24 minutes (1440 seconds) with 60 seconds being the interval time. For each loading time, the lashing speed of the pneumatic loading system was determined. Figure 8.6 shows the simulation results obtained.

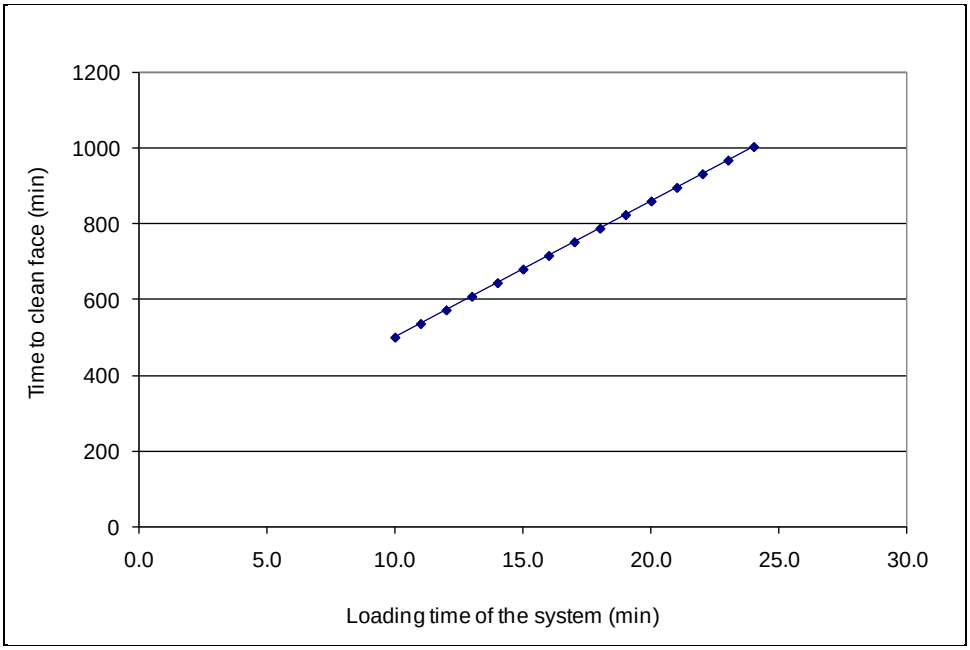

Figure 8.6: Effect of loading time on the lashing speed

According to Figure 8.6, the loading time of the pneumatic loading system is directly proportional to the lashing speed. Results indicate that an increase in the loading time of the pneumatic loading system (i.e., decrease in loading speed) results in an increase in time to clean the development face and vice versa. As an example, Figure 8.6 reveals that at minimum loading time (i.e., 11 minutes) the system would take approximately 537 minutes (8.9 hours) to clean the development face (i.e., to load, haul and dump 136 tonnes) whilst at maximum loading time (i.e., 24 minutes) it would take approximately 1005 minutes (16.7 hours) for the system to clean the same face. It is evident from the results that an increase in loading time of the pneumatic loading system results in a steady increase in the time to clean the development face and vice versa.

8.5.2 Effect of loading time on drilling speed

In this study, drilling time or drilling speed is defined as the time it takes for the monorail drilling system to completely drilling all the holes on the development face. During simulation process, the effects of loading time of the pneumatic loading system on the drilling speed were examined. This was done by varying the loading time of the pneumatic system and examining the time it would take to drill the face. Figure 8.7 shows the results obtained.

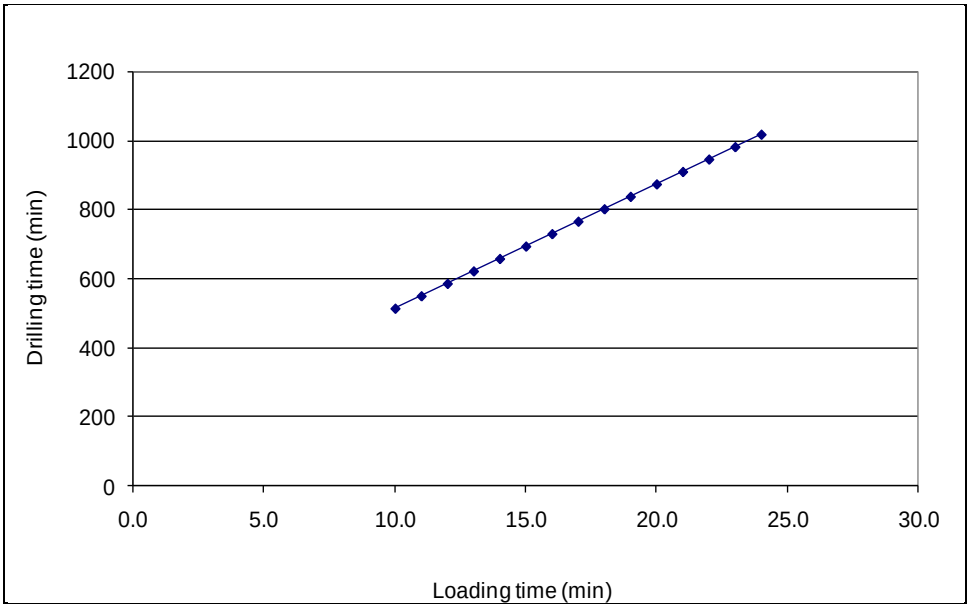

Figure 8.7: Effect of loading time on the drilling speed

The results shown in Figure 8.7 indicate that the loading time of the pneumatic system is directly proportional to the drilling speed of the monorail drilling system. According to Figure 8.7, an increase in the loading time of the pneumatic loading system results in an increase in the drilling time of the drilling system and vice versa. From the results obtained, we can conclude that the efficiency of the monorail drilling system depends on the efficiency and performance of the pneumatic loading system.

Also, as can be seen from Figure 8.8 below, drilling of the development face always takes relatively longer time to complete than face cleaning.

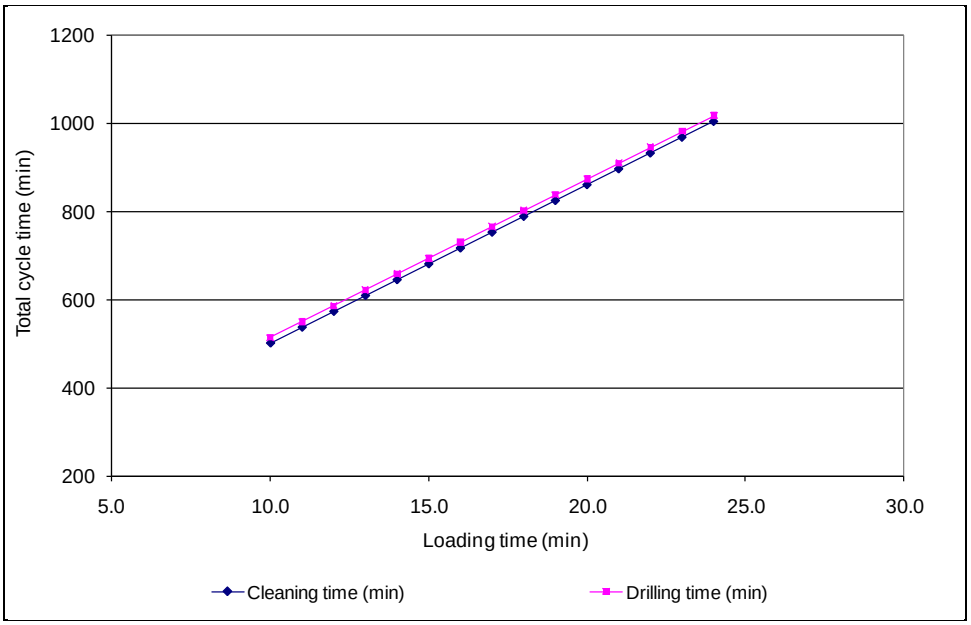

Figure 8.8: Effect of loading time on face drilling and cleaning cycle time

The drilling time will always be longer than the cleaning time because cleaning of the development face should be completed before face drilling is completed. This gives an extra time to allow for completion of drilling of all holes at the face. Thus, drilling of the development face is not completed while the development face is being cleaned. This is because the drilling time includes time to clean the face. This also means that the total cycle time to drill, blast, load and haul rock fragments from the development face depends on the efficiency of the pneumatic loading system.

8.5.3 Effect of loading time on total drill-blast-load-haul cycle time

The effect of loading time on the total drill-blast-load-haul cycle time was investigated during model simulation. The total drill-blast-load-haul cycle time is the total time to drill, blast, clean and haul the material from the development face to the surface (Equation 8.3). Results of the investigations are shown in Figure 8.9.

$$\text{Total drill}-\text{blast}-\text{load}-\text{haul cycle time} = \text{drilling time} + \text{blasting time} + \text{cleaning time} + \text{haulage time (including dumping)} + \text{return time} \quad 8.3$$

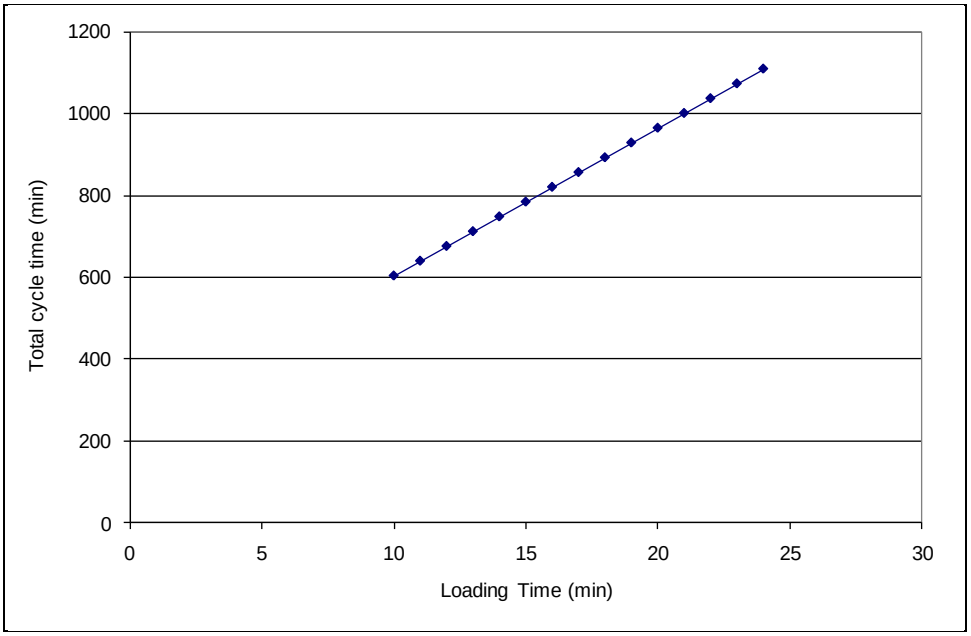

Figure 8.9: Effects of loading time on total drill-blast-load-haul cycle time

Figure 8.9 reveals that an increase in loading time of the pneumatic loading system results in an increase in the total drill-blast-load-haul cycle time and vice versa. The increase in total cycle time is as a result of the longer time it takes to clean the development face at longer loading time. This also results in delaying drilling, charging and blasting operations. As can be seen from Figure 8.9, at minimum loading time (i.e., 11 minutes), the total drill-blast-load-haul cycle time is 641 minutes (10.7 hours) whilst at maximum loading time (i.e., 24 minutes) the total cycle time would be 1106 minutes (18.5 hours).

8.5.4 Effect of lashing time on the number of blasts per shift

The productivity of the monorail system in terms of number of blasts it can achieve per shift was evaluated during simulation studies. During the analysis a restriction that prohibits blasting between shifts was considered, although in some Western Australian situations of isolated development, independent firing (i.e., blasting at times dependent of shift change) is allowed. This means that development blasting cannot be done during or just before shift change. This is to allow the incoming shift to start exactly on schedule. Figure 8.10 shows the simulation results in terms of the number of blasts per shift to be achieved by the monorail system. The number of blasts per shift was obtained using Equation 8.4.

$$\text{Number of blasts} = \frac{\text{Hours in a shift}}{\text{Total drill-blast-load-haul (including dumping)}} \qquad 8.4$$

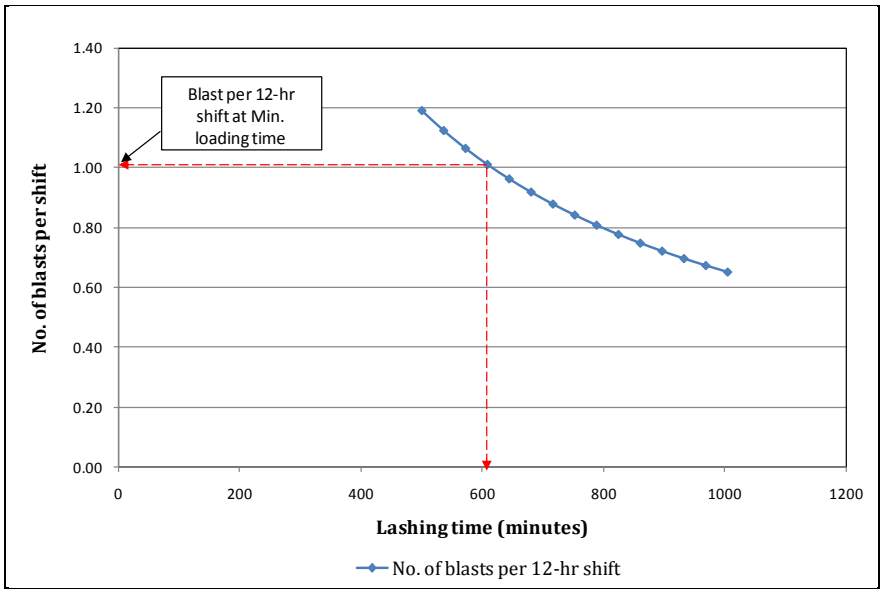

Figure 8.10: Effects of lashing time on the number of blasts per shift

As shown in Figure 8.10, the lashing time of the pneumatic system is inversely proportional to the number of blasts per shift. This means that the shorter the lashing time, the more blasts will be achieved by the system per shift and vice versa. According to the results, lashing times of 600 minutes or less will result in

one blast per shift whilst lashing times greater than 600 minutes will result in no blast per shift.

8.5.5 Effect of lashing time on face advance rates

Figure 8.11 shows the effect of lashing time of the pneumatic system on face advance rates (i.e., m/shift). Face advance rates were determined at 90% face advance recovery, which is the ratio of the actual development meters obtained after face blasting to target development meters. Target development meters are equal to the length of the drill steel used to drill holes at the face. Face advance rates were determined using Equation 8.5.

$$\text{Face advance} = \text{Target development meters} \times 90\% \qquad 8.5$$

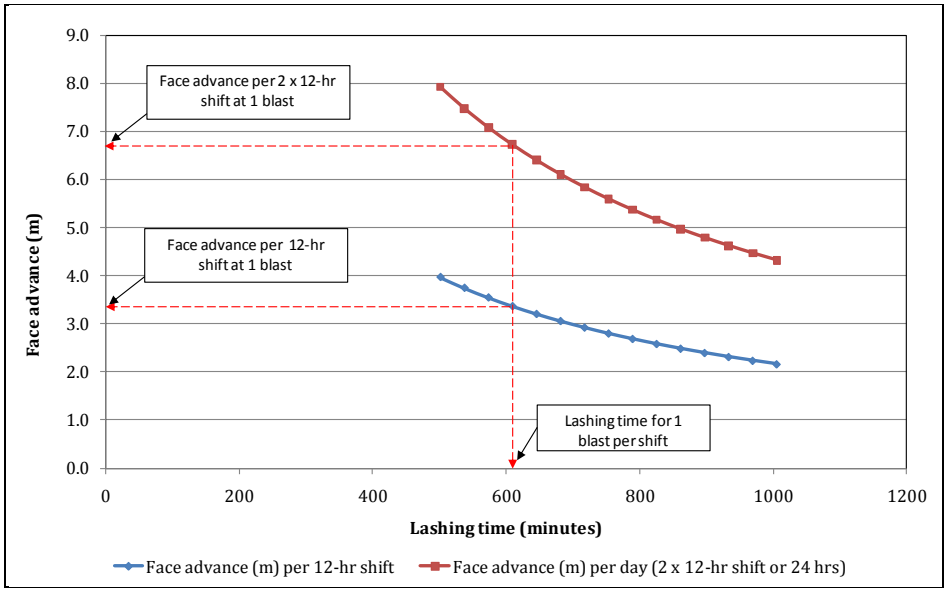

Figure 8.11: Effect of lashing time on advance rates

Results show that the lashing time is inversely proportional to the face advance rates. It can be seen from Figure 8.11 that the face advance rates decrease with increase in lashing time and vice versa. According to the results, lashing times of 600 minutes or less result in 3.33m advance per 12-hour shift (or 6.6 per 2 x 12-hour shift) at 90% face advance recovery. However, lashing time more than 600 minutes will not give any advance during the 12-hour shift since there will be no

blast. However, an advance of 3.33m results per day (i.e., 2 x 12-hour shift) since there will be only one blast during the two shifts.

8.5.6 Effect of loading time on productivity of monorail system

The productivity of the monorail system in terms of the total tonnage it can transport from underground to surface per shift was examined during simulation. From the simulation study, the total cycle time (i.e., the total time the monorail system takes to transport all the material from the development face to surface) was determined for each loading time. Since the total tonnage from the development face and the total time to clean the development face are known for each loading time, the productivity of the system per hour can be determined (i.e., by diving the total tonnage from face by the total time to clean face). Thus, for a 12-hour shift, the productivity of the system was determined as indicated Equation 8.6. Figure 8.12 shows the relationship between the productivity of the system per shift with the loading time of the pneumatic system.

$$\text{Productivity (tonnes/shift)} = \frac{\text{Tonnage from development face (t)}}{\text{Total cycle time to clean face (hrs)}} \times 12 \frac{\text{hrs}}{\text{shift}} \qquad 8.6$$

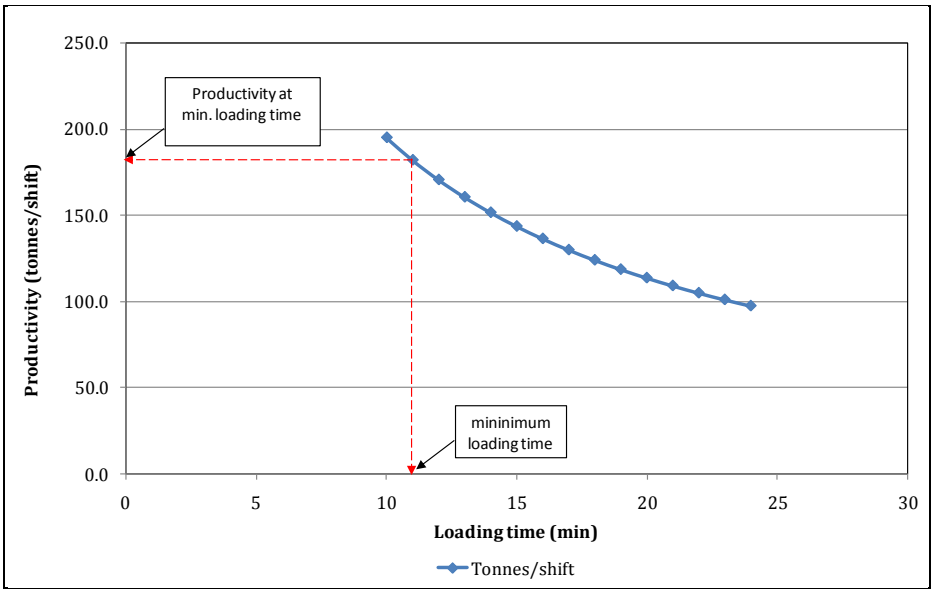

Figure 8.12: Effect of loading time on productivity of monorail system

Figure 8.12 show that the loading time is inversely proportional to the productivity of the monorail system. According to results, smaller loading times give higher productivity than larger loading time. As can be seen from Figure 8.12, at minimum loading time (i.e., 11 minutes) the productivity of the monorail system is 182.2 tonnes per 12-hour shift while at maximum loading time (i.e., 24 minutes) the productivity is 97.4 tonnes per 12-hour shift. The higher productivity at lower loading time is attributed to the reduced cycle time the monorail system has to make per shift i.e., the number of cycles the monorail system will make per shift will increase.

8.6 Summary of monorail system simulation results

Table 8.3 shows the summary of the simulation results for the monorail system at minimum and maximum loading time.

Table 8.3: Summary of monorail system simulation results

Description	Unit	Results	
		For minimum loading time	For maximum loading time
Time to clean the decline face per shift	hrs	8.95	16.75
Time to drilling and support decline face per shift	hrs	9.2	17.0
Total drill-blast-load-haul cycle time per shift	hrs	10.7	18.5
No. of blasts per shift	-	1	0
No. of blasts per day	-	2	1
Productivity of monorail system	t/shift	182.2	97.4
Face advance rate per shift (for 3.7m cut @ 90% face advance recovery)	M	3.33	0
Face advance rate per day (for 3.7m cut @ 90% face advance recovery)	M	6.66	3.33

8.7 Conventional decline development versus monorail system

A comparison was also made between the performance of the monorail system and that of the conventional truck haulage method. The comparison was performed on the time to clean and drill the development face, drill-blast-load-haul cycle times and advance rates per shift. To effectively compare the above parameters for the two systems, the monorail system model was simulated with

exactly the same parameters (shown in Table 8.4) as that used during studies on conventional truck haulage method in Western Australia as highlighted by Leppkes (2005).

Table 8.4: Parameters used for model simulation

Description	Unit	Value
Total tonnage	T	93.2
Decline length	M	2000
Size of face	M	3 x 3
Density of rock	kg/m^3	2.8

8.7.1 Time to drill and clean the development face

Figure 8.13 shows a comparison of the cleaning and drilling time of the development face for conventional and monorail systems using the parameters defined in Table 8.4.

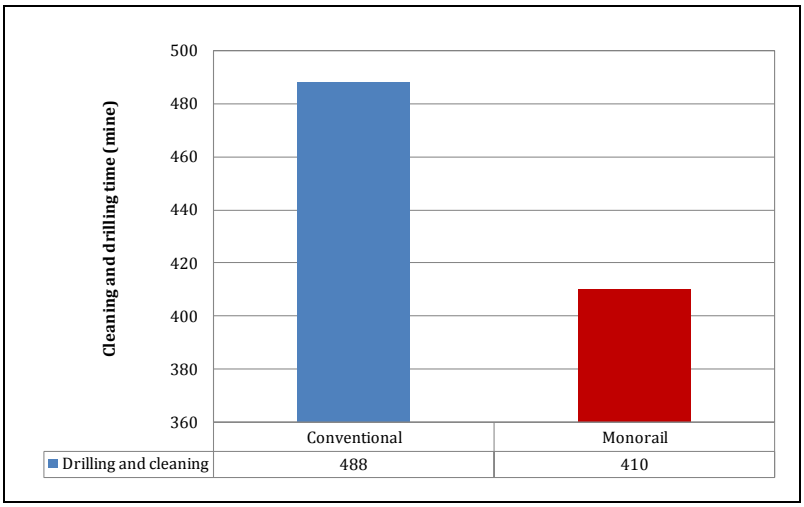

Figure 8.13: Cleaning and drilling time of the development face

Figure 8.13 shows that the total cycle time of cleaning and drilling the face, using the monorail system, is less than the conventional method. According to the results, at minimum loading time, the monorail system takes 410 minutes (6.83 hours) to clean and drill the face whilst a total of 488 minutes (8.13 hours) is spent to clean the same face using conventional method. The reduction in total

cycle time is attributed to the simultaneous drilling and cleaning of the development face by the monorail system. Additionally, since the conceptual monorail drilling system has been designed with automatic face marking using laser technology, it is anticipated that this technology will result in a reduction of the face mark up time thereby reducing the total drilling cycle time.

8.7.2 Charging, blasting and re-entry cycle time

Figure 8.14 shows a comparison of total time to charge/blast/re-entry time of the development face for conventional and monorail systems.

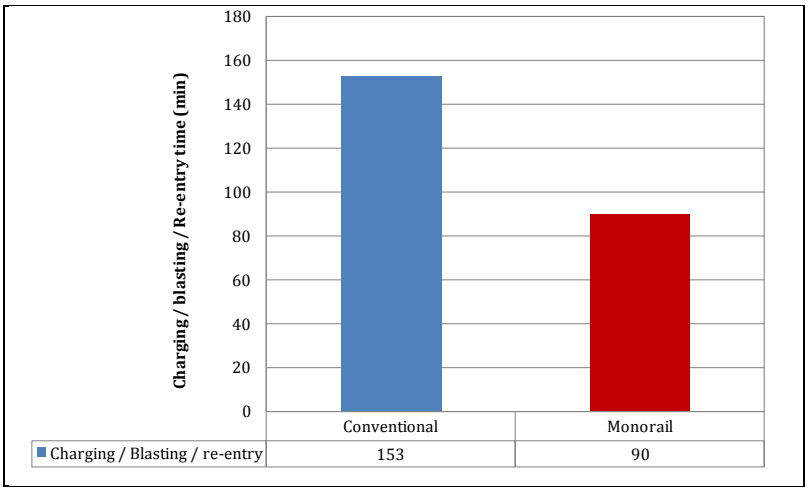

Figure 8.14: Charging, blasting and re-entry time for the two systems

As can be seen in Figure 8.14, the total time to charge/blast/re-entry time for the monorail system is lower than in conventional method. The anticipated reduction in charging/blasting/re-entry time is attributed to the following:

- Reduced size of development, i.e., from the conventional 5.5m x 5.5m to 3m x 3m with monorail system application as less volume of air is required to ventilate the face after blasting. This gives a considerable saving in the re-entry time;
- Since the monorail system uses electricity, there will be less diesel fumes in the decline as well as underground environment during operations. Less diesel fumes in underground mining operations will improve

underground environment by reducing the amount of toxic gases generated underground. This will help reduce the amount of time required to ventilate the area and make it safe after blasting hence reducing the total charge/blast/re-entry cycle time;

- Diesel engine efficiency is generally estimated at 33% (Payne and Mitra, 2008). The remaining two-thirds of the heat load are released as heat into the underground environment. Therefore, with the use of the electric monorail system in underground mining operations, significant time is saved from cooling the underground environment; and
- Reduced size of development also means that less heat from the development face as well as from the decline surface will be released. Thus, less time is required to ventilate and cool the area. In addition, as suggested by Payne and Mitra (2008), at the design stage, mines should plan on having mining excavations that are only as large as required to accommodate the equipment. The transfer of heat from the rock mass into the air will be reduced through a reduction in the area available for heat transfer.

8.7.3 Total drill-blast-load-haul cycle time

Figure 8.15 shows the comparison of the total drill-blast-load and haul cycle time for the monorail and conventional systems using the parameters defined in Table 8.4. According to the results, the drill-blast-load-haul cycle times for conventional method is approximately 10.7 hours while simulation results indicate that the monorail system would take approximately 8.33 hours. This represents 22.1% reduction (or approximately 2.4 hours) in total drill-blast-load-haul cycle time.

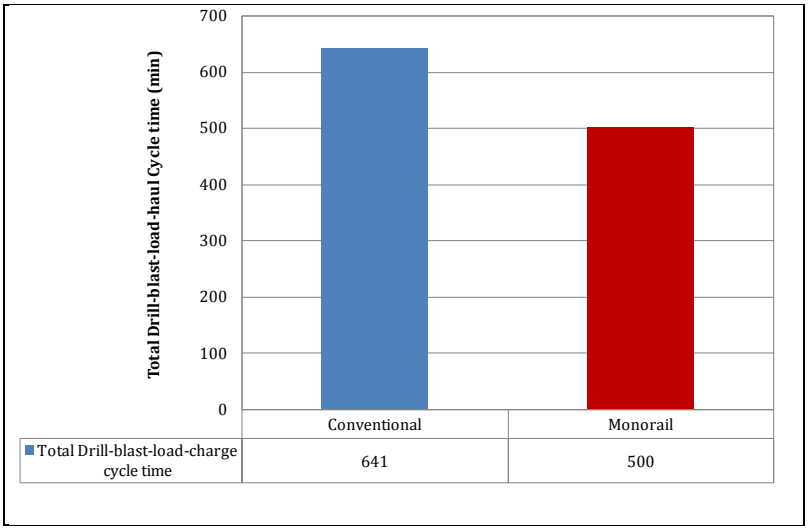

Figure 8.15: Drill-blast-load-haul cycle time

8.7.4 Advance rate per shift

Advance rates achieved by the two systems were also compared using the parameters defined in Table 8.4. Figure 8.16 shows the results of the comparison.

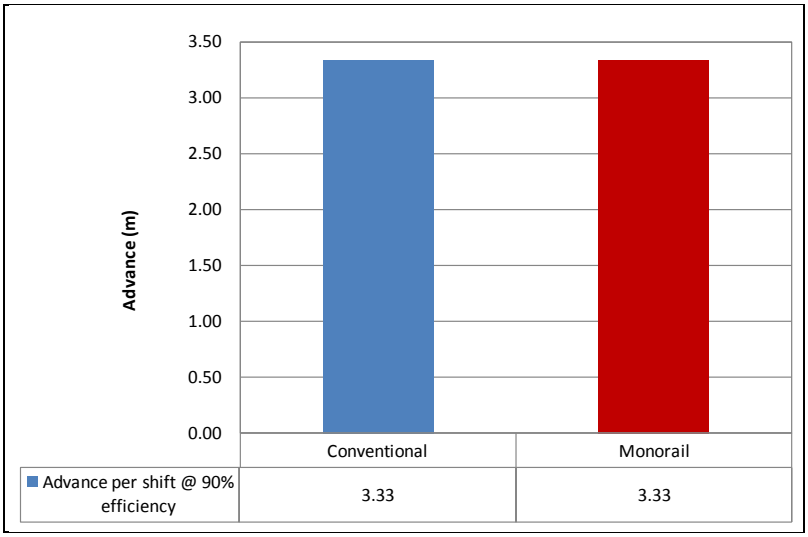

Figure 8.16: Advance rates for conventional and monorail systems

According to simulation results, the two systems will have the same advance rate per shift. This is because each system has one blast per shift resulting in the same advance rates.

8.8 Summary

From the simulation results, it has been established that the monorail and conventional system will have the same advance rate, as both systems have one blast per shift. However, the total mining cycle is lower for the monorail system, allowing for a further drill and blast cycle. Thus, if blasting between shifts were considered, the number of blasts as well as advance would increase. The decrease in total cycle time is attributed to the simultaneous drilling and cleaning of the decline face. Hence, there is no waiting time for the development face to be cleaned before drilling commences. The speed with which the material is removed from the development face at minimum loading time also contributed to the reduction of the cycle time for the monorail system.

Chapter 9

9.0 Monorail system risk analysis and hazard control

9.1 Introduction

In Chapters 4 and 5, the conceptual monorail drill-load-haul system is described based on theoretical principles. Since the monorail systems will be operated and driven by people in an underground mine environment where ground conditions are dynamic, the system is prone to risks that would affect its safe operations. Additionally, the whole monorail system has hazards that have the potential to create significant risks during operations. Hence, to improve the health and safety aspects of the monorail system in underground mining operations, the hazards and risks associated with the monorail system operations require identification and controlling.

The purpose of this Chapter is to identify potential hazards associated with the monorail system operations and evaluate the associated risks by carrying out risk analysis to assist in risk management. The Chapter begins by discussing risk and hazard and their dimensions, background theory to risk assessment processes and fundamental analytical tools necessary for this purpose. This Chapter also examines the potential hazards resulting from the use and operations of the monorail system in underground mining operations. Monorail system risk analysis as well as risk management are also discussed in this Chapter.

9.2 Risk and hazard definitions

In this Section, definitions of terminologies for performing risk analysis and management that are frequently used in the Chapter are presented.

(a) Risk

Many definitions of 'risk' exist that vary by specific application and situational context (Kelman, 2002; Thywissen, 2006). According to Mohammed (2006), the term risk conveys not only the occurrence of an undesirable consequence, but also how likely (or probable) such consequence will occur. Risk is also defined by the Risk Management Standard AS/NZS 4360 (2004) as 'the chance of something happening that will have an impact on objective.'

Other definitions of risk are:

- A threat to life or health (Fischhoff et al., 1981);
- The possibility of some adverse effects resulting from a hazard (Lawrence, 1976);
- The probability of either financial or physical damage (Starr and Whipple, 1980); and
- The events that, if they occur, will cause unwanted change in the cost, schedule or technical performance of an engineering system (Garvey, 2009).

A risk is often specified in terms of an event or circumstance and the consequences that may flow from it. Risk is measured in terms of a combination of the likelihood and consequences of an event. 'Likelihood' describes how often a hazard is likely to occur and is commonly referred to as the probability or frequency of an event. 'Consequence' describes the effect or impact of a hazard on people, economic loss or on the environment. Likelihood and consequence may be expressed using either descriptive words (i.e., qualitative measures) or numerical values (i.e., quantitative measures) to communicate the magnitude of

the potential impact (AS/NZS 4360, 2004). Thus, a risk can be viewed to be a multidimensional quantity that includes event occurrence probability, event occurrence consequences and the population at risk. Figure 9.1 shows the components of risk.

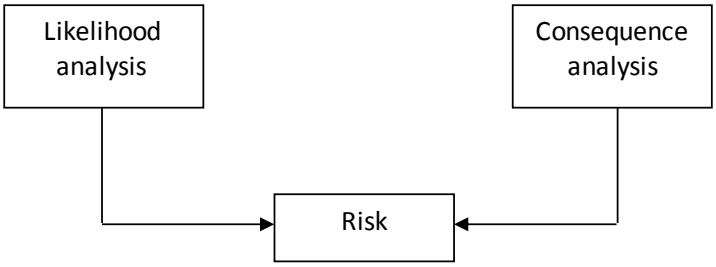

Figure 9.1: Components of risk (CCPS, 2000)

According to Mohammad (2006), risk is commonly evaluated as the product of frequency (likelihood) of occurrence and the magnitude (consequence) of severity of occurrence of the event as indicated in Equation 9.1:

$$\text{Risk}\left(\frac{\text{Consequence}}{\text{Time}}\right) = \text{Frequency}\left(\frac{\text{Event}}{\text{Time}}\right) \times \text{Magnitude}\left(\frac{\text{Consequence}}{\text{Event}}\right) \qquad 9.1$$

(b) Hazard

Mohammad (2006) defined 'hazard' as anything that has the potential of producing an undesired consequences (loss) without regard to the frequency or probability of the loss. Hazards are normally sources of danger that could result in an accident. They can either be natural or human-made and can endanger people and their environment if precautions to control them are not taken. Hazard identification is normally done early in safety life cycle of a system, otherwise an unsafe system may be put into use, or costly modifications may be needed to make the system acceptably safe. Thus, potential hazards must be identified and considered during system analysis in regard to the threats they pose that could lead to system failure.

System failures are the result of the existence of challenges and conditions occurring in a particular scenario. Most systems have the inherent capacity to withstand or endure such challenges. However, capacities may be reduced by specific internal or external conditions over time or cycle of application. Thus when challenges surpass the capacity of the system, failure may occur.

9.3 Risk assessment methodology – a theoretical approach

Ayyub (2003) defined risk assessment as a formal and systematic analysis to identify or quantify frequencies or probabilities and magnitudes of loss to recipients due to exposure to hazards from failures. Also, as highlighted by Mohammad (2006) risk assessment provides the process for identifying hazards, event-probability assessment and consequence assessment. Therefore, risk assessment provides both qualitative and quantitative data to decision makers for use in risk management. According to Kaplan and Garrick (1981), risk assessment amounts to addressing the following three basic questions:

1. What can go wrong?
2. What is the likelihood that it will go wrong?
3. What are the consequences (losses) if it does go wrong?

The answer to the first question leads to identification of the set of undesirable scenarios (such as accidents). The second question requires estimating the probabilities (or frequencies) of these scenarios, while the third estimates the magnitude of potential loss. Thus, answering these questions require the utilisation of various risk methods. Risk assessment requires the use of analytical methods at the systems level that takes into considerations subsystems and components when assessing their failure probabilities and consequences. According to Vincent and Miley (1993), the methodology should account for the various sources and types of uncertainty involved in decision-making process.

9.3.1 Hazard identification

Hazard identification is the first step performed in risk analysis. Hazard identification provides the scenarios that can be assessed for likelihood and consequences. The list of scenarios must cover all of the potential hazards and initiating events on the site. Hazard identification is often described as the most important step in a risk assessment, since what has not been identified will not be evaluated and cannot be managed (CCPS, 2000). From hazard identification, an operator should gain a comprehensive understanding of what hazards exist, the range of accidents that these hazards could lead to and what outcomes these accidents have the potential of causing. Thus, risk identification is concerned with determining potential risks and it starts with the source of problems, or with the problem itself.

In risk assessment, a survey of the processes under analysis should be performed to identify the likely hazards. Conceptualization of the different possible hazards for the system is an important part of risk identification. One should first take into account as many types of hazards as possible. The aim of hazard identification is therefore, to produce a comprehensive list of all possible hazards. The initial list can then be reduced by eliminating those types of hazards considered implausible. Hazard and risk identification is based on the information available concerning the system. Another way to identify hazards and risks is to ask the question 'What if?' Having a structured approach to identifying hazards improves the chances of identifying all hazards at workplaces. A person can ask himself: 'Is this activity safe? What if this or that occurs - then - what will happen?' When identifying a hazard a person should also ask: 'Is it possible that . . .?', or 'What would happen if . . .?' This is the 'What if' approach to what could happen.

9.3.2 System barrier identification

In an engineering system, each of the hazards must be examined to determine all barriers that contain, prevent or mitigate undesirable exposures or occurrence of

such hazards. These barriers may physically surround and isolate the hazards. These barriers may provide direct shielding of the recipient from hazards or they may mitigate the condition to minimize exposure to the hazard.

9.3.3 Risk analysis

According to AS/NZS 4360 (2004), risk analysis is 'the systematic process to understand the nature of and to deduce the level of risk.' Whereas hazard identification obtains information about what can go wrong, the purpose of risk analysis is to determine how likely accidents are to occur and to determine the magnitude and effects of these accidents on people, plant and the environment. Therefore, the objectives of risk analysis are to:

- Enhance site personnel understanding of hazards and risks;
- Identify major risk contributors;
- Enable decisions on risk reduction measures to be made using appropriate criteria and justification;
- Identify areas of concern for critical safety management;
- System controls and emergency plans; and
- Achieve an acceptable level of on-site and off-site risk.

Thus, as described by Ayyub (2003), risk analysis is the process that is concerned about estimating the potential and magnitude of any loss and ways of controlling it from or to a system. According to AS/NZS 4360 (2004) risk analysis may be undertaken to varying degrees of detail depending upon the risk, the purpose of analysis and the information and resources available. Generally, three types of risk analysis are available as outlined below:

(a) Qualitative risk analysis

Qualitative risk analysis is a quicker and easier way to perform risk analysis due to its simplicity and also does not require gathering precise data. According to

Mohammad (2006), in this type of analysis, the potential loss is qualitatively estimated using linguistic scales such as 'low', 'medium' and 'high'. Thus, the techniques for analysing qualitative data are ranking methods (Gibbons et al., 1977). Ayyub (2003) further elaborates that in this type of analysis, a matrix is formed which characterises risk in the form of the frequency of the loss versus potential magnitudes of the loss in qualitative scales. Ranked-ordered approximations of probability and consequence can yield useful approximations of risk. Therefore, qualitative approaches are useful and they illustrate the minimum data necessary to understand risk. An example of a qualitative risk assessment matrix is shown in Table 9.1.

Table 9.1: Example of qualitative risk analysis matrix (AS/NZS 4360, 2004)

	Consequence				
	Insignificant	Minor	Moderate	Major	Catastrophic
Likelihood	1	2	3	4	5
Almost certain	H	H	E	E	E
Likely	M	H	H	E	E
Moderate	L	M	H	E	E
Unlikely	L	L	M	H	E
Rare	L	L	M	H	H

Legend:

E – Extreme risk (immediate action required, e.g. do not proceed with activity until the level of risk is reduced);
H – High risk (senior management attention required);
M – Moderate risk; and
L – Low risk (manage by routine procedures).

(b) Quantitative risk analysis

Quantitative risk analysis attempts to estimate the risk in the form of the probability of loss and evaluates such probabilities to make decisions and communicate results. In this analysis, the uncertainty associated with the estimation of the frequency of occurrence of the undesirable events and the

magnitude of loss are characterised by using the probability concepts. Quantitative risk analysis is clearly the preferred approach when adequate field data, test data and other evidence exist to estimate the probability and magnitude of the loss.

(c) Mixed qualitative – quantitative analysis

Risk analysis may also be a mix of qualitative and quantitative analyses. According to Mohammad (2006) the mix can happen in two ways: the frequency or potential for loss is measured qualitatively, but the magnitude of the loss is measured quantitatively or vice versa; it is also possible that both the frequency and magnitude of the loss are measured quantitatively, but the policy setting and decision making part of the analysis relies on qualitative methods.

9.3.4 Evaluation of failure consequence

According to Ayyub (2003), failure consequence can be described as the degree of damage or loss from some failure. The failure of an engineering system could lead to consequences that create a need to assess potential failure consequences and severities. The losses produced by exposure to a hazard may harm the recipient (injury or death), cause damage to an asset or may cause loss of production. These losses are evaluated from knowledge of the behaviour of the particular hazard when recipients are exposed to them and the amount of such exposure for each scenario. Table 9.2 shows an example of consequence failure categories.

Table 9.2: Consequence failure categories

Consequence	Severity
Fatal	Death
Major injuries	Normally irreversible injury
Minor injuries	Typically reversible injury
Negligible injuries	Requires first aid

9.3.5 Risk management and control

Risk management is a practice involving coordinated activities to prevent, control and minimize losses incurred due to a risk exposure. Adding risk control to risk assessment produces risk management. Risk management involves using information from the previously described risk assessment stage to make educated decisions about system safety. Risk control on the other hand includes failure prevention and consequence mitigation. The goals of risk management are to reduce risk to an acceptable Level. Risk reduction is normally accomplished by preventing an unfavourable scenario, reducing the frequency, and/or reducing the consequences. The broad steps involved in the risk management process are shown in Figure 9.2.

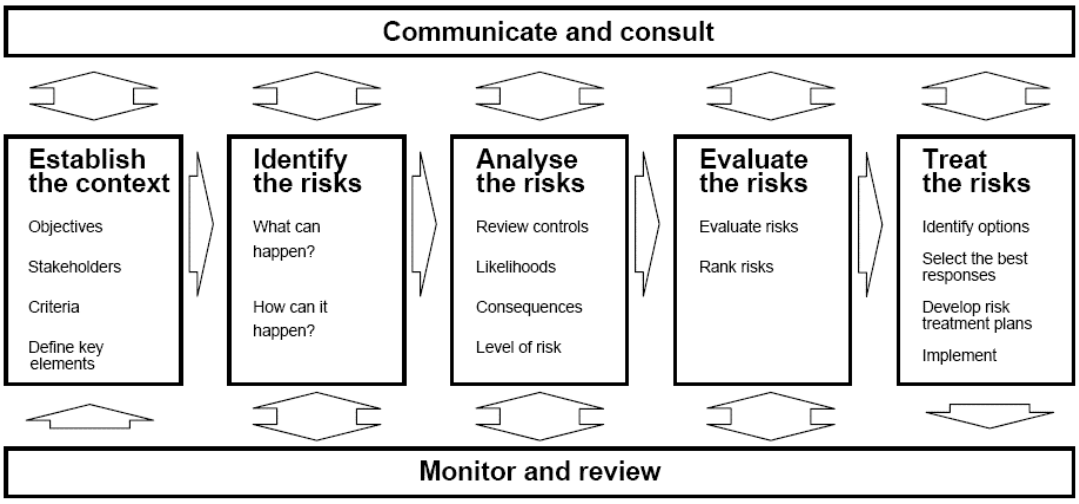

Figure 9.2: Framework for managing risk (AS/NZS 4360, 2004)

9.3.6 Risk communication

Risk communication is the activity of transferring, exchanging or sharing data, information and knowledge about risk, risk assessment results and risk management approach between decision makers, analysts and the rest of stakeholders (Mohammad, 2006). The information can relate to the existence, form, likelihood, frequency, severity acceptability, controllability or other aspects of risk. The basic reason for risk communication is to inform all those with an

interest in decision making about the possible risk scenarios and consequences of various risk management. According to Ayyub (2003), risk communication also provides vital links between the risk assessors, risk managers and the public for understanding risk.

9.4 Risk assessment for monorail system

The conceptual monorail drilling and loading systems have the potential to cause significant risks that require assessment, management and possibly regulating. In this respect, risk assessment was conducted for the two systems in order to determine whether there is any likelihood of a potentially hazardous situation that can cause death or injury during operations. The severity of monorail system risks was also evaluated in order to determine how urgently they need to be controlled to minimise their impacts. Assessing or evaluating monorail system risks would help determine the most serious hazards so that action plans to prevent or mitigate them are put in place before risk and hazard failure.

9.4.1 Risk assessment procedure

Since the monorail system is in its conceptual stage, risk assessment was undertaken through a careful analysis of its anticipated operation and use in underground mining. Due to lack of actual data on monorail system operations for probabilistic treatment of such data, qualitative risk analysis approach was used during the assessment. Risk assessment began by indentifying possible hazards that could occur during monorail system operations. The task of identifying monorail system hazards was broken down into three categories as indicated below:

- Identification of hazards that can cause the monorail system fail from the support system;
- Identification of hazards that can cause the monorail system run out of control or moving inadvertently during operations; and

- Identification of hazards related to operations and maintenance of the monorail system.

Hazard identification was followed by identification of available and in-built monorail system controls that would prevent or mitigate undesirable exposures to such hazards during operations. Challenges of some available controls were also highlighted during this stage. Risk assessment matrix was used to estimate the levels of risk for monorail system hazard. With this method, opposing scales for severity of occurrence and likelihood of occurrence was developed. The consequences of each hazard were divided into three categories, i.e., effects on people, on monorail system and on underground environment. Each category was assigned a weight, with the impact on people having a weighted factor of 3; impact on monorail system was given a weight of 2 and the impact on underground environment had a weighted factor of 1. The weighted average impact was determined by multiplying the weight factor for each category with the consequence level. The consequence level varied from 1 to 5 with level 1 having insignificant impacts while level 5 had catastrophic impacts. As illustrated in Section 9.4.6, the calculated weighted average impact had a range which varied from 6 to 30 with 6 having 'insignificant' impacts and 30 with 'catastrophic' impacts. Due to lack of actual data on monorail system operations, the likelihood range was determined based on consultations and on author's judgement on the likelihood of occurrence of monorail system hazards. The likelihood range also varied from 1 to 5 with 1 being 'rare' and 5 as 'almost certain'.

The use of risk assessment matrix enabled monorail system risks to be ranked relative to each other although it was not able to provide indication whether the calculated risk is acceptable, tolerable or unacceptable. This assessment enabled the risks for identified hazards to be ranked to give a guide to the order in which the risks should be addressed. The risk levels were determined using risk score numbers from the risk assessment matrix. The level of risk for each hazard was determined by multiplying the likelihood of occurrence and the weighted average impact of each hazard. The level of risk was represented by a risk score

number with the lowest and highest risk levels having score numbers of 6 and 150 respectively. This means that the higher the risk score number, the higher the risk for the hazard to occur and vice versa.

Risk management and control was the last stage performed. During this stage, possible measures that are likely to eliminate, prevent, reduce or mitigate monorail system risks were suggested. The initial step during this stage involved carrying out fault-tree analysis on the monorail system hazards so as to determine the potential root causes of undesirable events. This method is used because it addresses fundamental causes of the problem as opposed to merely addressing the immediate obvious symptoms. By directing corrective measures at root causes of the problem, it is hoped that the likelihood of a problem will be minimized. After conducting fault-tree analysis for the monorail system hazards, potential root causes of undesirable events were determined and corrective measures suggested.

9.4.2 Identification of monorail system hazards

Identification of monorail system hazards or 'what can go wrong' during monorail system operations was the first step performed in assessing its risk. This process involved identifying tasks, activities, situations, events and scenarios that have the potential to harm or injure a person or cause damage to the system or the environment as a result of hazard release. Different monorail system tasks, activities, situations, events and scenarios that are considered hazardous and risky were identified and documented during the assessment process. The monorail system risks were categorised into three as highlighted in Section 9.4.1. In this Section, details of identified monorail system hazards and their characteristics are presented.

(a) Monorail system falling from support system

Since the monorail system moves on the single rail/monorail track suspended in the decline roof using roof bolts, suspension chains and steel supports, there is a

possibility that the system may fall from the support system due to one of the following hazards:

- Failure of the hanging wall or roof due to the weight of the monorail system;
- Failure of roof bolts, suspension chains and steel supports under static and dynamic loads;
- Derailments due to breaking or disconnection of rail tracks and rail track connections;
- Monorail system driving off the end of the open rail track; and
- Switch failing under the load of the monorail train, or due to the switch being operated while the monorail train is travelling through the switch or due to the switch being switched in the wrong direction causing the monorail train to drive off the end of the open rail track.

(b) Monorail system running out of control or moving inadvertently

During monorail system operations, there is a likelihood that the system may run out of control down the decline as a result of one of the following hazards:

- Lack of traction by the drive unit to the rail track. For the fully loaded monorail system to be able to negotiate steep gradients, it depends on the traction by the drive unit to the rail tracks. Thus, if traction by the drive units is not enough, there is a likelihood that the system may run out of control down the decline;
- Drive unit or operator allowing it to exceed a safe speed. Should the monorail system operator excessively over speeds the system down the decline, it is likely that the system may run out of control and cause harm or injure the people along the way;
- Brakes failing to stop the running monorail train or the brakes failing to hold the standing monorail train static, or the operator failing to apply the brakes correctly;

- Any part of the monorail train becoming disconnected from the drive unit or braking unit and running out of control; and
- Monorail train running out of control or being set in motion by an unauthorised person.

(c) Operational and maintenance hazards

There are also other monorail system hazards which results from operational and maintenance issues as indicated below:

- Objects falling on persons from the monorail overhead system;
- Persons in close proximity to the monorail system being bumped, crushed or caught by the monorail train whenever it is in motion;
- Because of the high voltage in conductor bars, there is a possibility that a person maybe electrocuted from the electric conductor bars during train operations as well as during maintenance of monorail installations;
- Collisions with any dangerous object or conditions ahead;
- Hazards due to misinterpretation of signals;
- Accidents due to failure or malfunctioning of any part of the monorail system;
- Brake or other failures due to overloading;
- Person being hit or crushed by monorail container during lifting or lowering; and
- Material falling on person when lifting containers.

9.4.3 Existing hazard control measures and challenges

The monorail system consists of in-built safety features that contain, prevent or mitigate undesirable exposure to hazards. The safety features are incorporated into the PLC software and provides safety to the monorail system. The PLC software also incorporates a fault-finding facility and records all operational details of the system. This data is downloadable and facilitates accurate record

keeping. Therefore, for each threat, one or more control measures are specified to prevent or minimize the likelihood of hazard release. Identification of control measure was therefore, followed by outlining the challenges of each control measure to ensure the functionality of the control measure is maintained. For the monorail system, this stage involved identifying the scenarios in which all the control measures may be breached and the hazard may reach the recipient. Table 9.3 provides details of identified monorail system hazards, available controls measures and the challenges of some of the control measures.

Table 9.3: Existing control measure for identified hazards

Specific hazard	Available controls / Barriers	Challenges of available control measures
• Failure of the hanging wall or roof due to the weight of the monorail system.	• Where ground conditions are weaker, the monorail / rail tracks are suspended on steel arch sets.	• Nil
• Failure of roof bolts, bolts, shackles, chains and steel supports under static and dynamic loads.	• Use of standard or manufacturer approved roof bolts, bolts, shackles, suspension chains and steel supports. • Use of new Universal Flange Rail (UFR) rail type which is connected by flanges suspended from the hanging wall. The rail type has no shackles and suspension chains and has a FoS greater than 5.	• Peeling of hanging wall and weakening the flanges thus affecting the monorail connection.
• Derailment due to breaking or disconnection of rail tracks and rail track connections.	• Nil - According to the manufacturers of the train (Scharf), the train is tightly coupled together and there is no way of declutching.	• Since the monorail / tracks are connected by connectors, the rail connectors gets loosened with time due to swinging movement and may cause disconnection or breaking at joints.
• Monorail driving off the end of the open rail track.	• Use of rail end stop blocks mounted at the end of the rail track. There are also simple mechanic stop blocks available as well as more sophisticated spring-loaded bumpers.	• What is the maximum force and train speed can the stop blocks withstand?
• Monorail switch failure due to; ➢ the load of the monorail train; ➢ the switch being operated while the monorail train is travelling through the switch; and ➢ the switch being switched in the wrong direction.	• The switch entry and exit rails are also secured by an automatically set rail end stop block. These stop blocks are opened and closed automatically when the switch is changing from one track to the other. Due to a safety switch, the operation of the rail switch is impossible while a train is passing it.	• What happens when the switch stops functioning when the monorail system is already in motion? • What happens in case of power failure and the monorail system is still in motion?
• Lack of traction by the drive unit to the rail track.	• When traction is lost, brakes are automatically released.	• What happens in case of break failure?
• Drive unit or operator allowing it to exceed a safe speed.	• Use of overspeed governor incorporated in the monorail train which activates the brakes once the train exceeds the maximum applicable speed.	• Overspeed governor malfunctions or stops working when the train is already in motion.
• Brakes failing to stop the running monorail train, or brakes failing to hold the standing monorail train static, or operator failing to apply the brakes correctly.	• The monorail system brakes are spring loaded. Hence when the brake shoes are in a good condition the train's total brake system provides more than 1.5 times the running down force. This means that there is 50% more brake-force available to hold and stop the train. • The EMTS is equipped with two types of braking systems, soft and emergency braking system. The emergency brakes are released within a millisecond. Braking is managed by the PLC and should a preset speed be reached and the operator fails to brake, brakes are automatically applied by a command from the PLC.	• Nil

• Any part of the monorail train becoming disconnected from the drive unit or braking unit and running out of control.	• Nil	• Brakes can only be applied from the monorail driver's cabin. What happens if one component (e.g. container) disconnects from the main system?
• Monorail train running out of control or being set in motion by an unauthorised person.	• When the monorail train is stationary or being worked on, it is fixed by a chain secured around the train and a fixed point which is only removed by authorised persons. The system also provides a bugle to warn people by the driver. • Use of an overspeed governor and emergency brakes incorporated in the train which trips and activates the brakes once the train exceeds the maximum applicable speed.	• Nil
• Objects falling on persons from the monorail overhead system.	• The system is provided with a bugle to warn people during motion. This clears off the people along the way.	• What happens when the bugle has a malfunction during motion?
• Persons in close proximity to the monorail system being bumped, crushed or caught by the monorail train whenever it is in motion.	• The monorail can be equipped with bumper acting on the emergency brakes. There is also an emergency stop button in every driver's cabin to stop the train in emergency. The system also provides a bugle to warn people by the driver as it moves.	• Nil
• Person being electrocuted from the electric conductor bars;	• Placement of danger signs that warns the people about the high voltage in conductor bars.	• Nil
• Collision with any dangerous object or conditions ahead.	• The train is equipped with enough lighting system to improve the visibility. However, the train must not travel if it has no sufficient lighting or in areas with little visibility unless there is an additional system (e.g. radar) providing the driver some information on the way of travelling.	• Nil
• Hazards due to misinterpretation of signals.	• The signals need to be clearly identified, visible and known by everyone working in the vicinity of a monorail train.	• Nil
• Accidents due to failure or malfunctioning of any part of the monorail system.	• Manuals are provided on each train which give detailed information on all possible dangers and risks. • Certain procedures are also recommended for the maintenance and repair of the train.	• Nil
• Brake or other failures due to overloading.	• When train is overloaded, the PLC automatically prevents the train from moving.	• Nil
• Person being hit or crushed by monorail container during lifting or lowering.	• The system is provided with a bugle to warn the people of the danger.	• Nil
• Material falling on person when lifting containers.	• Full automation (removal of personnel from hazardous underground environment).	• Nil

9.4.4 Likelihood and consequence risk factors

The likelihood of an event occurring during monorail system operations depends on the frequency of exposure to a hazard. There are also a number of risk factors that can influence the likelihood of an event occurring during monorail system operations. The following risk factors were identified as having an effect on the likelihood of occurrence of the monorail system hazards:

- Conditions of the monorail system;
- Skills and competence of persons operating the monorail system;
- The environmental conditions in which the system operates;
- The effectiveness of the existing control measures; and
- Duration of the exposure.

The severity or potential consequences that would result from an incident during monorail system operations also depend on several factors. The following were identified as the main risk factors on which the severity or potential consequences that results from monorail system hazard release depend.

- The number of people that are exposed to the risk;
- The extent of harm the hazard could do;
- Whether the harm could be short or long term; and
- Position of workers relative to the hazard.

9.4.5 Likelihood analysis

The likelihood of occurrence of a hazard event provides an estimation of how often the event occurs. This is generally based on the past hazard events that have occurred in the area. However, since the monorail system is in its conceptual stage, i.e., there is lack of actual data on monorail system hazard events for probabilistic treatment of such data, the likelihood of occurrence was estimated based on consultations and on author's judgment of the likelihood of

occurrence of such hazards. The likelihood range for the system was assigned, for each hazard, as 'almost certain', 'likely', 'possible', 'unlikely' or 'rare' (Table 9.5). Numerical values of 1 to 5 were assigned to each category with 1 being 'rare' and 5 being 'almost certain'. The numerical value assigned to each category was used to determine the risk rating of each hazard. Table 9.4 shows the likelihood range that was used to nominate the likelihood of an incident or event occurring during monorail system operation. Figure 9.3 show the likelihood ranking for monorail system hazards.

Table 9.4: Likelihood range for monorail system hazards

Level	Likelihood	Description
5	Almost certain	Expected in most circumstances
4	Likely	Will possibly occur in most circumstances
3	Possible	Could occur at some time
2	Unlikely	Not likely to occur in normal circumstances
1	Rare	May occur only in exceptional circumstances

Table 9.5: Likelihood ranking for monorail system hazards

Specific hazard	Likelihood	
	Description	Value (Range 1-5)
• Failure of the hanging wall or roof due to weight of monorail system.	Possible	3
• Failure of roof bolts, bolts, shackles, suspension chains and steel supports under static and dynamic loads.	Possible	3
• Derailment due to breaking or disconnection of rail tracks and rail track connections.	Possible	3
• Monorail driving off the end of the open rail track due to failure or derailing of rail tracks;	Possible	3
• Monorail system switch failure.	Rare	1
• Lack of traction by the drive unit to the rail track.	Unlikely	2
• Drive unit or operator allowing it to exceed a safe speed.	Possible	3
• Brakes failing to stop the running monorail train, or brakes failing to hold the standing monorail train static, or operator failing to apply the brakes correctly.	Possible	3
• Any part of the monorail train becoming disconnected from the drive unit or braking unit and running out of control.	Rare	1
• Monorail train running out of control or being set in motion by an unauthorised person.	Rare	1
• Objects falling on persons from the monorail overhead system.	Possible	3
• Persons in close proximity to the monorail system being bumped, crushed or caught by the monorail train whenever it is in motion.	Possible	3
• Person getting electrocuted from the electric conductor bars	Possible	3
• Collision with any dangerous object or conditions ahead occurring due to a lack of visibility in the direction of travel.	Unlikely	2
• Hazards due to misinterpretation of signals.	Rare	1
• Failure or malfunctioning of any part of the monorail system.	Possible	3
• Brake or other failures due to overloading.	Unlikely	2
• Person being hit or crushed by monorail container during lifting or lowering.	Possible	3
• Material falling on person when lifting containers.	Possible	3

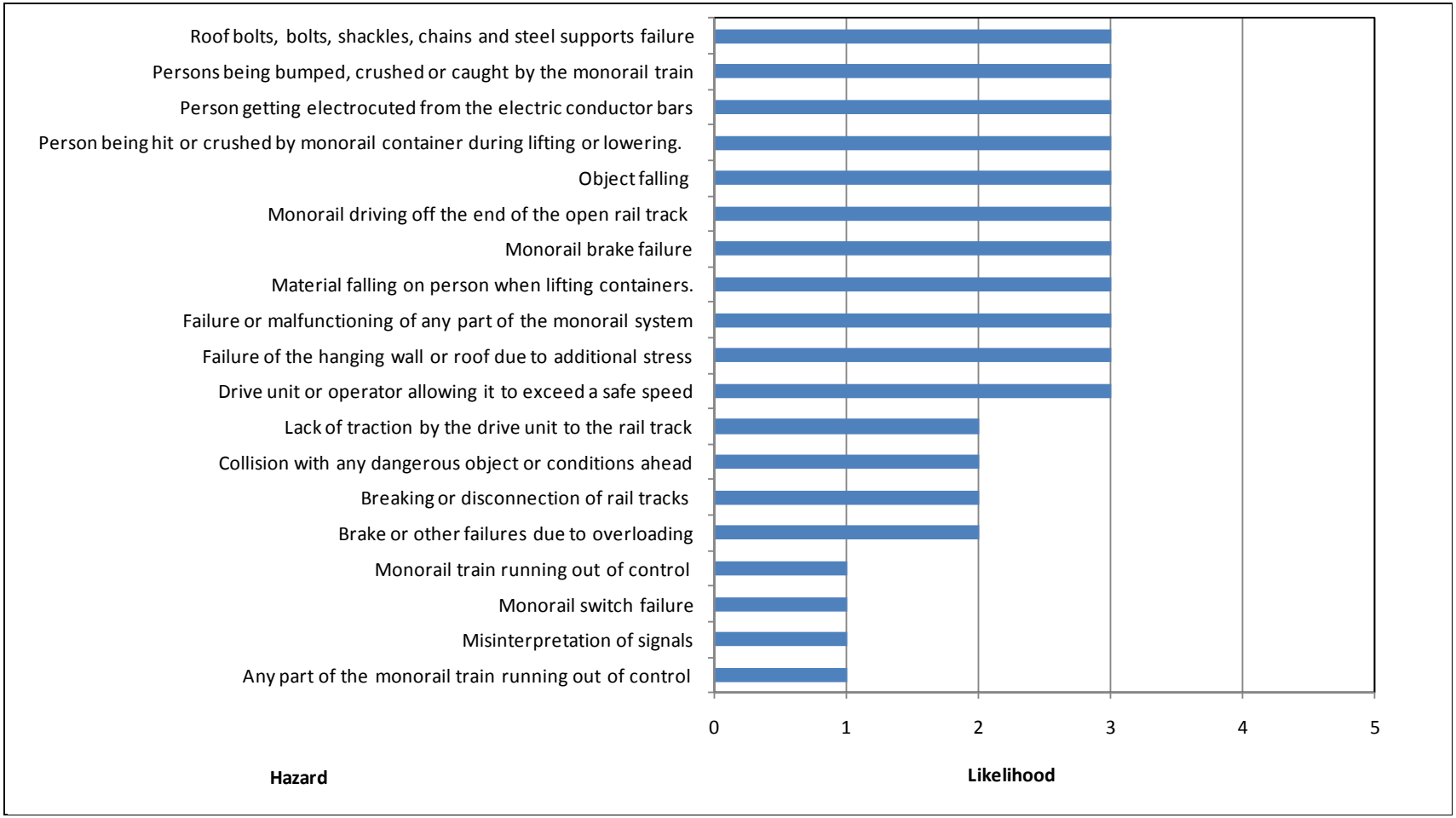

Figure 9.3: Monorail system hazard likelihood ranking

9.4.6 Consequence analysis

Consequence analysis of the monorail system hazards involves quantification of the potential of accidents resulting from hazard failure to cause undesirable events. During the analysis, consequences of each hazard were divided into three categories, i.e., effects on people, monorail system and on the underground environment. The three categories were each assigned weighted values as follows: the impact on people was given a weighted factor of 3; impact on monorail system was given a weight of 2 and the impact on the underground environment had a weighted factor of 1. The impact values on monorail system represent the property (monorail system) loss from each hazard using the value of the property. The values for underground environment impact represent estimates of what the loss would be from the major event of each hazard. The consequence category was assigned, for each hazard, as 'catastrophe', 'major', 'moderate', 'minor' or 'insignificant'. Table 9.6 shows the impact or consequences level/impact for each category that was used to nominate the consequences of an incidence or event occurring during monorail system operations and considered to be the weight in each category.

Table 9.6: Consequences range for monorail system risks

Level /weight	Consequence	Description
5	Catastrophic	Death or permanent disability; Huge financial loss
4	Major	Extensive injuries; Loss of production; Extensive damage to monorail system
3	Moderate	Require medical treatment
2	Minor	First aid treatment; medium financial loss
1	Insignificant	No injuries; Low financial loss

The weighted average was calculated using Equation 9.2. Results of the analysis are shown in Table 9.7 and Figure 9.4.

$$\text{Weighted average impact} = (\text{People} \times \text{weight} + \text{System} \times \text{weight} + \text{Env} \times \text{weight}) \qquad 9.2$$

Table 9.7: Monorail system hazard consequences ranking

Specific hazard	Consequence						Consequence (Weighted average)			Weighted Impact
	People		Monorail System		Underground Environment		People	Monorail System	Underground Environment	
• Failure of the hanging wall or roof due to the weight of monorail system.	Catastrophic	5	Catastrophic	5	Catastrophic	5	3	2	1	30
• Failure of roof bolts, bolts, shackles, chains and steel supports under static and dynamic loads.	Catastrophic	5	Catastrophic	5	Major	4	3	2	1	29
• Derailment due to breaking or disconnection of rail tracks and rail track connections.	Major	4	Major	4	Moderate	3	3	2	1	23
• Monorail driving off the end of the open rail track.	Catastrophic	5	Catastrophic	5	Major	4	3	2	1	29
• Monorail system switch failure.	Moderate	3	Moderate	3	Minor	2	3	2	1	17
• Lack of traction by the drive unit to the rail track.	Moderate	3	Minor	2	Minor	2	3	2	1	15
• Drive unit or operator allowing it to exceed a safe speed.	Major	4	Minor	2	Minor	2	3	2	1	18
• Brakes failing to stop the running monorail train, or brakes failing to hold the standing monorail train static, or operator failing to apply the brakes correctly.	Major	4	Minor	2	Minor	2	3	2	1	18
• Any part of the monorail train becoming disconnected from the drive unit or braking unit and running out of control.	Major	4	Major	3	Minor	2	3	2	1	20
• Monorail train running out of control or being set in motion by an unauthorised person.	Major	4	Major	4	Minor	2	3	2	1	22
• Objects falling on persons from the monorail overhead system.	Catastrophic	5	Insignificant	1	Minor	2	3	2	1	19
• Persons in close proximity to the monorail system being bumped, crushed or caught by the monorail train whenever it is in motion.	Catastrophic	5	Insignificant	1	Insignificant	1	3	2	1	18
• Collision with any dangerous object or conditions ahead occurring due to a lack of visibility in the direction of travel.	Major	4	Catastrophic	5	Major	1	3	2	1	23
• Hazards due to misinterpretation of signals.	Moderate	3	Moderate	3	Insignificant	1	3	2	1	16
• Failure or malfunctioning of any part of the monorail system.	Minor	2	Moderate	3	Insignificant	1	3	2	1	13
• Brake or other failures due to overloading.	Major	4	Major	4	Moderate	3	3	2	1	23
• Person being hit or crushed by monorail container during lifting or lowering.	Major	4	Insignificant	1	Insignificant	1	3	2	1	15
• Material falling on person when lifting containers.	Major	4	Insignificant	1	Insignificant	1	3	2	1	15
• Person getting electrocuted from the electric conductor bars	Catastrophic	5	Major	4	Insignificant	1	3	2	1	24

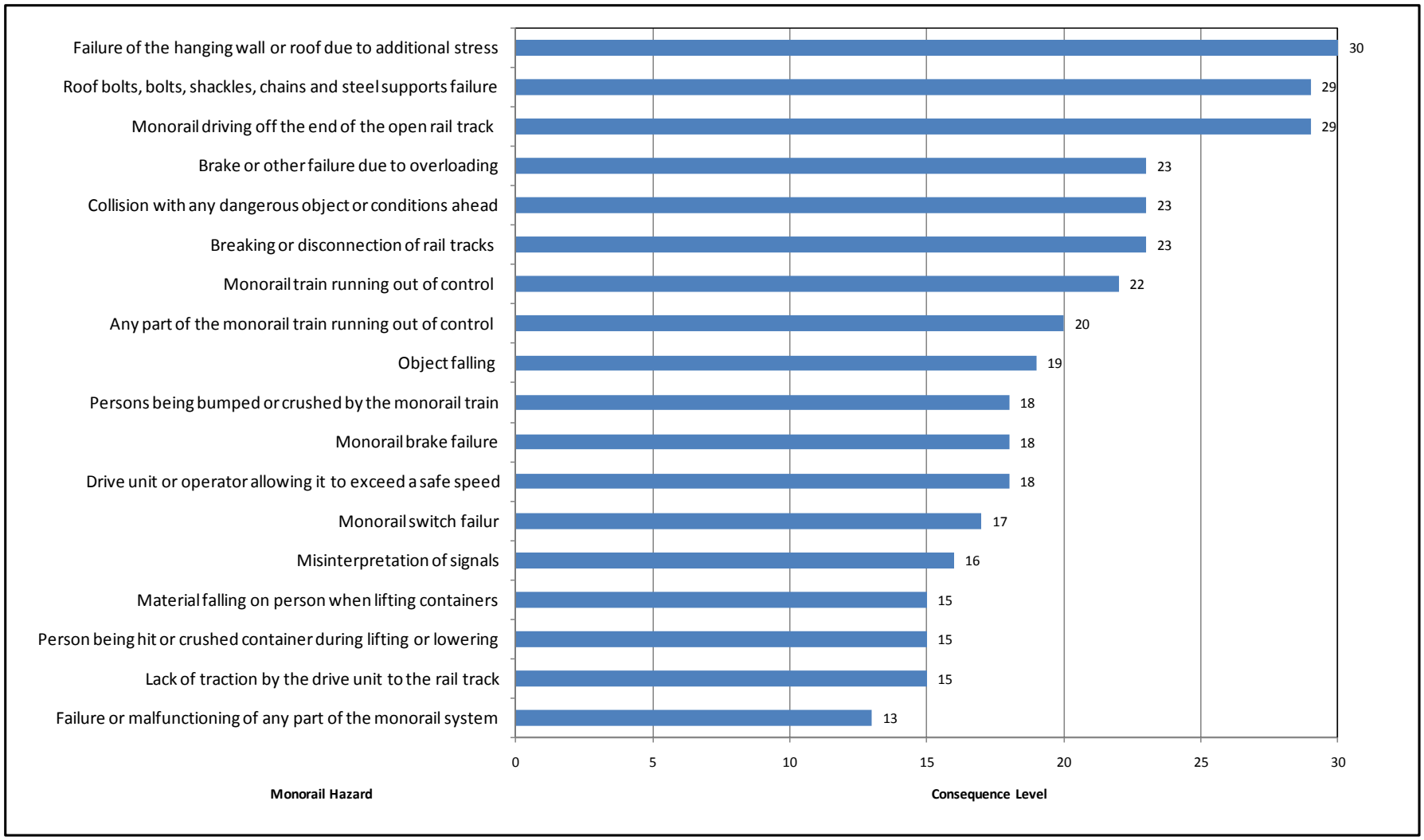

Figure 9.4: Monorail system hazard weighted consequence ranking

As a result of the assigned weights to each category, the weighted average consequence range was determined as indicated in Table 9.8. Equation 9.2 was used to calculate the weighted average impact for each category. As can be seen from Table 9.8, the weighted impact range varied from 6 to 30 with 6 having 'insignificant' impacts and 30 with 'catastrophic' impacts.

Table 9.8: Weighted consequences range for monorail system risks

Level / impact	Impact	Weights			Weighted impact	Description
		People	System	U/G Env		
5	Catastrophic	3	2	1	30	Death or permanent disability; Huge financial loss
4	Major	3	2	1	24	Extensive injuries; Loss of production; Extensive damage to monorail system.
3	Moderate	3	2	1	18	Require medical treatment
2	Minor	3	2	1	12	First aid treatment;, medium financial loss
1	Insignificant	3	2	1	6	No injuries ; Low financial loss

9.4.7 Risk ranking

Risk ranking is a method of identifying and classifying risks through application of likelihood of an event and its consequences. Potential monorail system risks were ranked based on their likelihood and anticipated consequences that may result from their release. The purpose of risk ranking is to describe the likelihood of each of these hazards to occur and also to describe the consequence or severity of each hazard on people, monorail system and on the underground environment.

The risk ranking for the monorail system is divided into four categories, i.e., 'very high', 'high', 'medium' and 'low'. A risk ranking matrix showing the risk levels was constructed. The risk matrix has rows representing increasing severity of consequences of a released hazard and columns representing increasing likelihood of these consequences. The risk ranking matrix and the recommended actions are shown in Tables 9.9 and 9.10 respectively. The risk ranking for each hazard was determined by multiplying the assigned numerical value for likelihood to the numerical value of the consequence using Equation 9.1.

Table 9.9: Risk ranking matrix

Likelihood	Consequence				
	Insignificant (6)	**Minor (12)**	**Moderate (18)**	**Major (24)**	**Catastrophic (30)**
Almost certain (5)	Medium (30)	High (60)	Very High (90)	Very High (120)	Very High (150
Likely (4)	Medium (24)	High (48)	Very High (72)	Very High (96)	Very High (120)
Possible (3)	Low (18)	Medium (36)	High (54)	Very High (72)	Very High (90)
Unlikely (2)	Low (12)	Low (24)	Medium (36)	High (48)	High (60)
Rare (1)	Low (6)	Low (12)	Low (18)	Medium (24)	Medium (30)

Table 9.10: Risk recommended action

Risk level / score	Recommended action
Very High (72 -150)	**Act Now:** Steps must be taken to lower the risk level to as low as reasonably practicable using the hierarchy of risk controls.
High (48 -71)	**Act Today:** Highest management decision is required urgently
Medium (24 – 47)	**Follow management instructions:** The supervisor must review and document the effectiveness of the implemented risk controls.
Low (6 – 23)	**OK for now:** Record and review if any equipment/ people/ materials/ work processes or procedures change. Managed by local documented routine procedures which must include application of the hierarchy of controls.

9.4.8 Risk level evaluation

Monorail system risks were computed using risk ranking matrix shown in Table 9.9. Risk level for each hazard was computed and ranked according to the risk score number. The results of the risk ranking for the system are indicated in Table 9.11 and Figure 9.5. The risk ranking results provide a first order prioritisation of the system risk before application of risk reduction action. This ranking also serves as a guide to the order in which these risks should be addressed.

Table 9.11: Risk assessment levels for monorail system hazards

Specific hazard	Likelihood (Range 1- 5)	Consequence (Range 6- 30)	Risk score (Range 6-150)	Risk Level/score
• Failure of the hanging wall or roof due to the weight of the monorail system.	3	30	90	Very High
• Failure of roof bolts, bolts, shackles, suspension chains and steel supports under static and dynamic loads.	3	29	87	Very High
• Monorail driving off the end of the open rail track due to failure or derailing of rail tracks.	3	29	87	Very High
• Person getting electrocuted from the electric conductor bars	3	24	72	Very High
• Derailment due to breaking or disconnection of rail tracks and rail track connections.	3	23	69	High
• Objects falling on persons from the monorail overhead system.	3	19	57	High
• Drive unit or operator allowing it to exceed a safe speed.	3	18	54	High
• Brakes failing to stop the running monorail train, or brakes failing to hold the standing monorail train static, or operator failing to apply the brakes correctly.	3	18	54	High
• Persons in close proximity to the monorail system being bumped, crushed or caught by the monorail train whenever it is in motion.	3	18	54	High
• Collision with any dangerous object or conditions ahead occurring due to a lack of visibility in the direction of travel.	2	23	46	Medium
• Brake or other failures due to overloading.	2	23	46	Medium
• Person being hit or crushed by monorail container during lifting or lowering.	3	15	45	Medium
• Material falling on person when lifting containers.	3	15	45	Medium
• Failure or malfunctioning of any part of the monorail system.	3	13	39	Medium
• Lack of traction by the drive unit to the rail track.	2	15	30	Medium
• Monorail train running out of control or being set in motion by an unauthorised person.	1	22	22	Low
• Any part of the monorail train becoming disconnected from the drive unit or braking unit and running out of control.	1	20	20	Low
• Monorail switch failure.	1	17	17	Low
• Hazards due to misinterpretation of signals.	1	16	16	Low

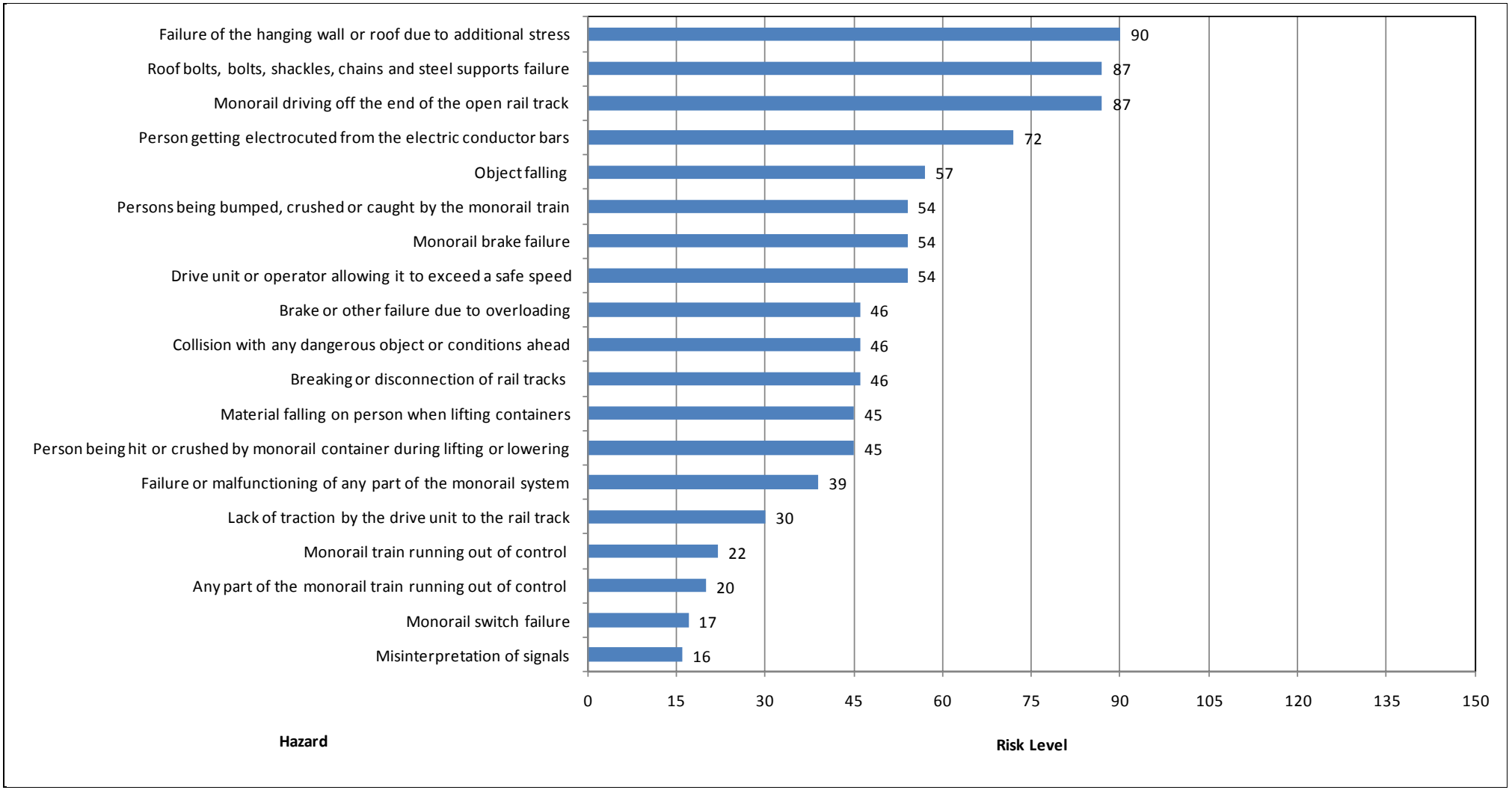

Figure 9.5: Monorail system risk ranking

9.4.9 Risk management and hazard control

Risk management and hazard control began by conducting fault-tree analysis on monorail system risks. The aim of the analysis was to identify potential root causes and contributory factors to monorail system risks. After the analysis the most fundamental reasons for risk and hazard failure were identified. This stage was followed by suggesting risk and hazard control measures that could mitigate or eliminate the identified potential root causes of risk and hazard failure. In this Section, fault-tree analysis process and risk and hazard control strategies are presented.

9.4.9.1 Fault-tree analysis

As highlighted earlier, fault-tree analysis for the monorail system involved identification of potential and fundamental causes of system risks that initiate the occurrence of undesirable events. The undesirable monorail system events were divided into three categories as highlighted in Section 9.4.1. Results of the analysis are shown in Figures 9.6, 9.7 and 9.8.

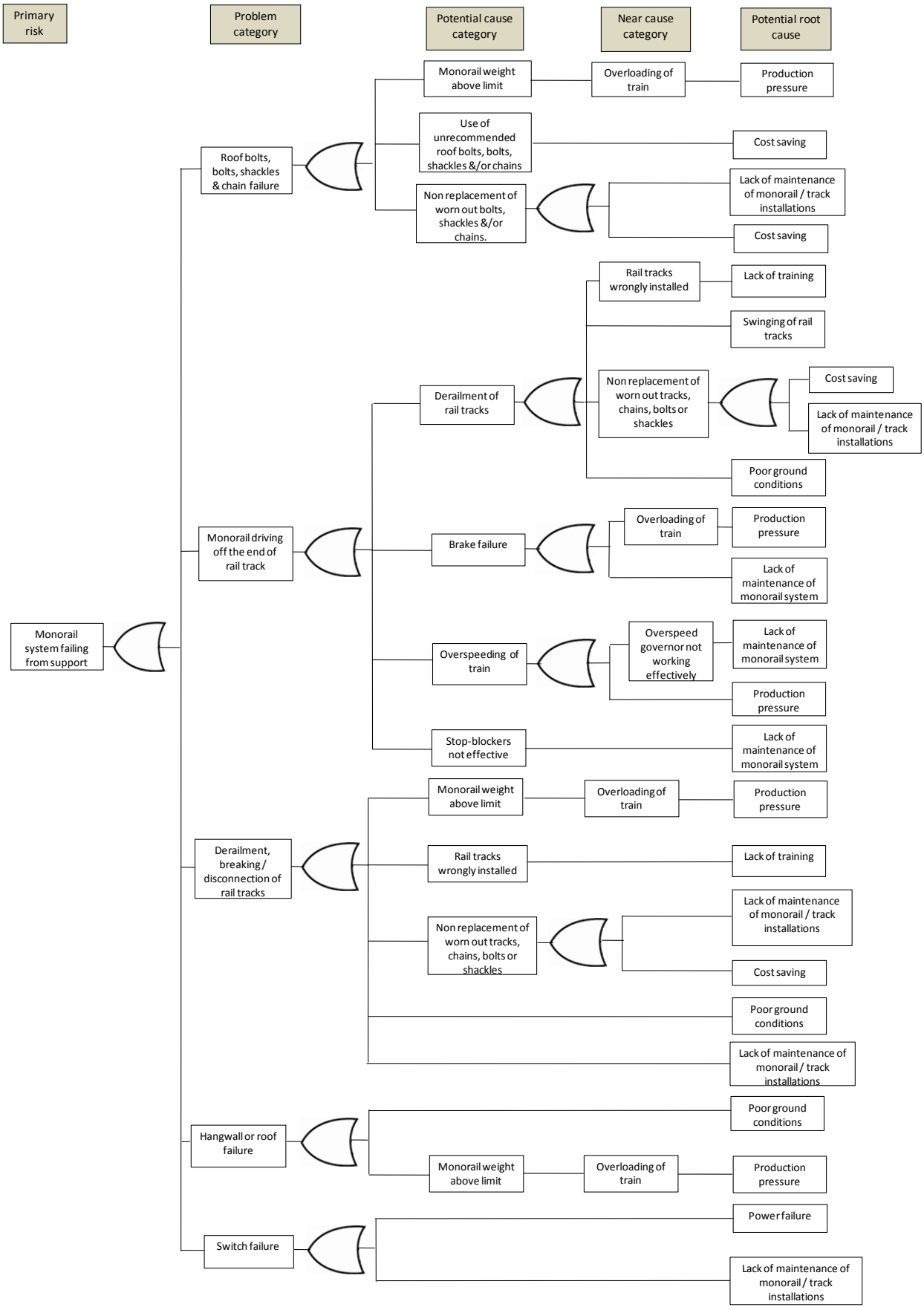

Figure 9.6: Fault-tree diagram for monorail system failing from supports

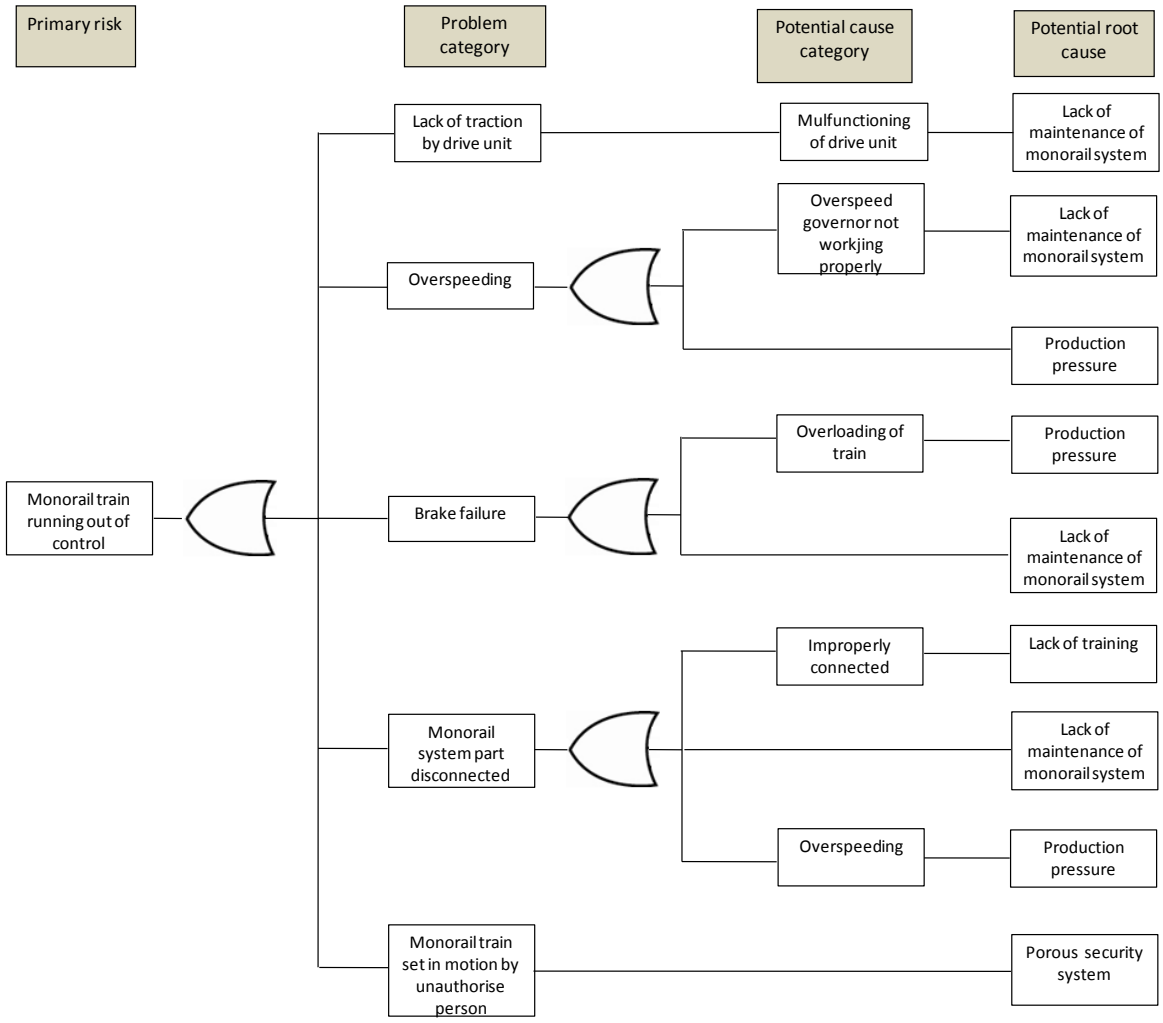

Figure 9.7: Fault-tree diagram for monorail system running out of control

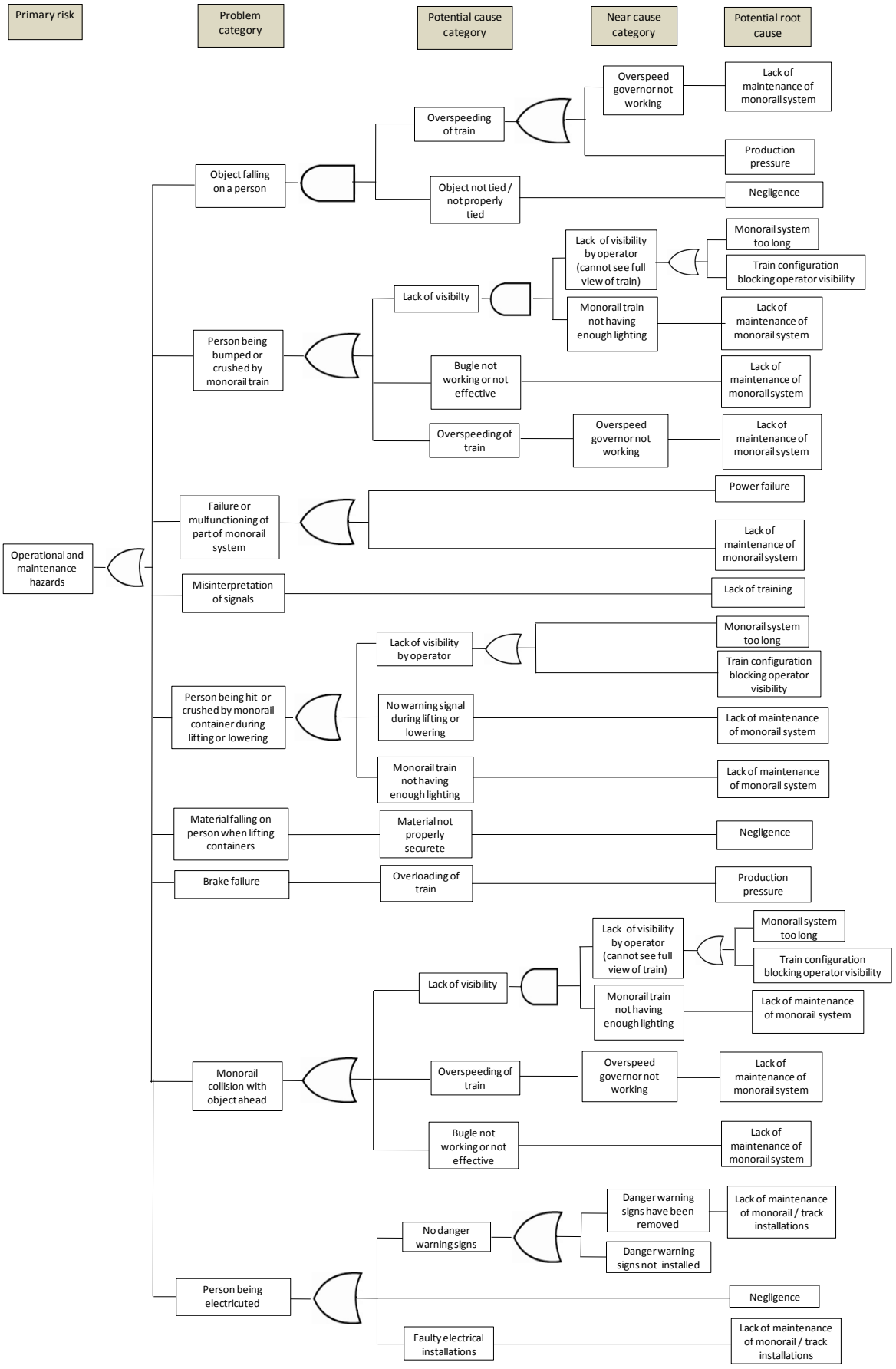

Figure 9.8: Fault-tree diagram for operational and maintenance hazards

9.4.9.2 Analysis of fault-tree results

According to the fault-tree diagrams shown in Figures 9.6, 9.7 and 9.8, it can be seen that there are several factors that have the potential to cause monorail system risk failure. Table 9.12 and Figure 9.9 shows percent contribution of potential root causes to monorail system risk failure.

Table 9.12: Percent contribution of potential root causes to monorail system risk failure

Potential root cause	Contribution to system risk failure (%)			Total contribution to system risk failure (%)
	Monorail falling from support	Monorail running out of control	Hazards causing personal injury	
Porous security system	0.0	1.7	0.0	1.7
Swinging of rail trucks	1.7	0.0	0.0	1.7
Person being electrocuted from conductor bars	0.0	0.0	1.7	1.7
Power failure	1.7	0.0	1.7	3.3
Poor ground conditions	5.0	0.0	0.0	5.0
Monorail system too long	0.0	0.0	5.0	5.0
Train configuration blocking operator visibility	0.0	0.0	5.0	5.0
Negligence	0.0	0.0	6.7	6.7
Cost saving	6.7	0.0	0.0	6.7
Lack of training	3.3	1.7	1.7	6.7
Lack of maintenance of Track / Monorail Installation	8.3	0.0	3.3	11.7
Production pressure	8.3	5.0	3.3	16.7
Lack of maintenance of Monorail system	5.0	6.7	16.7	28.3

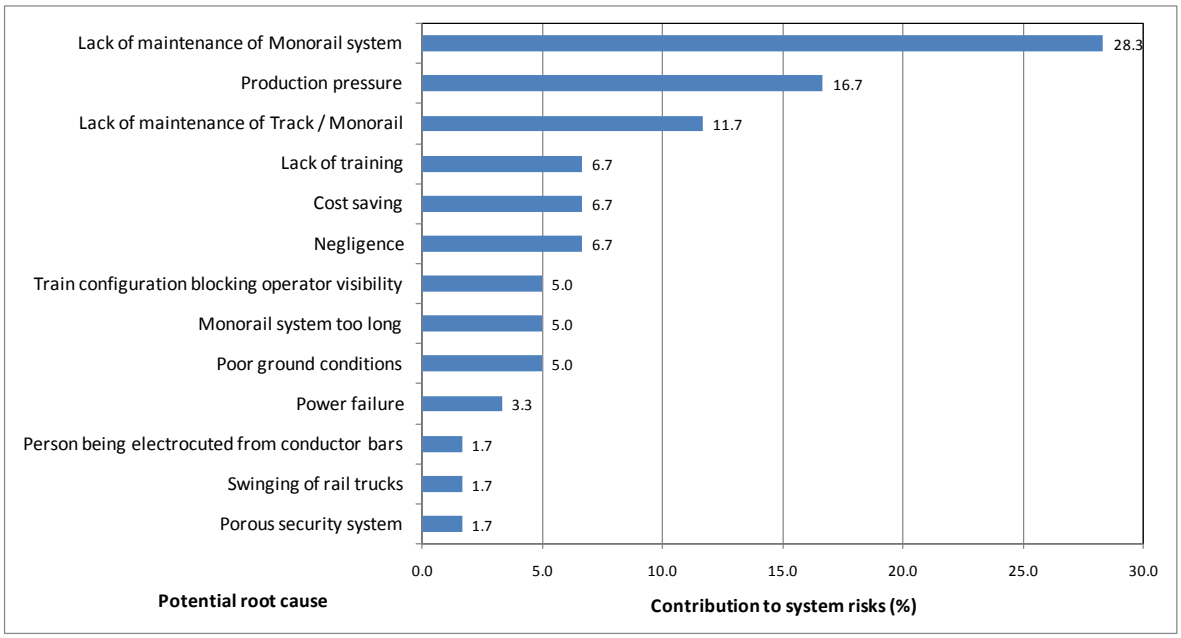

Figure 9.9: Percent contribution of potential root causes to monorail system risk failure

In this Section, detailed description of the fault-tree analysis findings are presented in order of priority.

1. According to the fault-tree analysis results shown in Table 9.12 and Figure 9.9, lack of maintenance of the monorail system has the potential to cause approximately 28.3% of the total risks. As indicated in the fault-tree diagrams shown in Figures 9.6, 9.7 and 9.8, the following risks are associated with lack of maintenance of the monorail system:

    - Risk of brake failure would lead to the monorail system running out of control or driving off the end of the rail tracks causing it to fall from the support system;
    - Over-speeding of the monorail train resulting from non-functioning or ineffective over-speed governor can also cause the monorail system to run out of control or driving off the end of the rail tracks causing the system to fall from the support system;

- Stop blockers not working effectively can pose a danger by making the monorail system driving off the end of the rail track causing the system to fall from support system;
- Lack of traction due to malfunctioning of the drive unit can make the monorail system running out of control;
- Part of the monorail system being disconnected and running out of control during operations; and
- Person being bumped or crushed due to lack of visibility (i.e., poor lighting system from monorail train), bugle not working properly and over-speeding of the train. This may also result in collision of the train with objects ahead.

2. Production pressure has also been identified as having the potential to initiate approximately 16.7% of the total monorail system risks. The following are the likely risks resulting from production pressure:

    - Overloading of the monorail train so as to meet targets thus increasing its weight above limit. This will cause failure of roof bolts, suspension chains and steel supports due to additional stress;
    - Over-speeding of the train to meet targets would result in the disconnection of monorail system parts as well as object falling from the system; and
    - Overloading of the monorail system might also result in system brake failure.

3. As indicated in Table 9.12 and Figure 9.9, lack of maintenance of track/monorail installations would result in 11.7% of the total risks. The following risks are associated with lack or poor maintenance of the monorail installations.

    - Roof bolt, suspension chain and steel support failure due to non-replacement of the same. This will result in derailments due to breaking or disconnections of the rail tracks; and

- Monorail switch failure under load causing the system to run out of control and falling at the end of rail tracks.

4. Lack of training on the use and operations of the monorail system as well as insufficient knowledge on proper installation of the monorail/tracks has also been recognized as a contributing factor to increased monorail system risks. As indicated in Table 9.12 and Figure 9.9, this deficiency may cause 6.7% of the total monorail system risks. According to the fault-tree diagrams, lack of training and insufficient knowledge has the following potential risks:

    - Misinterpretation of monorail system signals;
    - Monorail system switch being operated in wrong direction;
    - Derailment of rail tracks due to wrong or improperly installed rail tracks; and
    - Monorail system part getting disconnected.

5. Cost saving has the potential to contribute 6.7% to the total monorail system risks. Below are the risks that are associated with cost saving measures:

    - Roof bolt, suspension chain and steel support failure due to the use of poor or unrecommended material; and
    - Non-replacement of roof bolt, bolts, shackles, chain and steel supports due to cost saving measures.

6. Negligence can also contribute approximately 6.7% of monorail system risks. As indicated in Figure 9.8, an object may fall on the person during monorail system operation or during lifting of monorail containers if the object or material is not well secured in the containers due to negligence. Also a person can get electrocuted if safety / danger signs are not observed during operations or maintenance of the monorail installations.

7. Configuration of the monorail system (in terms of its design) has also been identified as one of the potential root causes of the system risks. The configuration of the system poses a risk by blocking operator's visibility during operations. According to Table 9.12 and Figure 9.9, this risk is likely to contribute 5.0% to the total monorail system risks. The following risks are associated with lack of visibility and train configurations:

    - Blocking operator visibility resulting in persons being hit or crushed during operations;
    - Lack of visibility by the operator can cause a person being hit or crushed during lifting and lowering of monorail containers; and
    - Poor visibility by the monorail system (no enough lighting) and limited visibility by the operator can lead to collision of the monorail system with objects ahead or behind.

8. The length of the monorail system is likely to cause 5.0% of the total monorail system risks. The following risks are associated with the length of the monorail system:

    - Blocking operator visibility since the operator is not able to see full view of the system resulting in persons being hit or crushed during operations; and
    - As a result of the operator not able to see full view of the monorail system, a person maybe hit or crushed during lifting and lowering of monorail containers.

9. Poor ground conditions would also pose a number of risks during monorail system operations. As can be seen from Table 9.12 and Figure 9.9, 5.0% of the total risks would result from poor ground conditions. The following risks are associated with poor ground conditions:

- Derailment due to breaking and disconnection of the rail tracks as a result of ground failure. This may cause the monorail system to drive off the end of open rail tracks or fall from support system; and
- Hanging wall and roof bolt failure resulting in monorail system falling from support system.

10. According to Table 9.12 and Figure 9.9, 3.3% of the total risks may also result from power failure during monorail system operations. The following risk is associated with power failure during monorail system operations:

    - Switch failure causing the monorail system driving off the end of the rail tracks.

11. Because the monorail system is electrically driven, approximately 1.7% of the total risk would be caused from being electrocuted from monorail electric conductor bars. The risk would occur when the monorail train is in operation or during maintenance of the monorail installations if safety precautions are not taken.

12. Approximately 1.7% of the monorail system risks would be initiated by the swinging of rail tracks during monorail system movements. This would result in derailment due to breaking and disconnection of rail tracks causing the monorail train to drive off the end of the rail track. This would cause the system to fall from its support.

13. Lack of adequate security system for monorail train would instigate approximately 1.7% of the total risks, i.e., there is likelihood that the system can be set into motion by an unauthorised person should the security system for monorail train be inadequate or porous.

9.4.9.3 Monorail system risk and hazard control strategies

To prevent or minimise undesirable events as a result of risk and hazard failure during monorail system operations, it is imperative that the risks and hazards be managed and controlled before failure occurs. Results from fault-tree analysis were used to come up with suggestions on appropriate control measures of potential root causes of undesirable events. The goal of control measures is to reduce the level of risk by directing corrective measures at potential root causes of risk and hazard failure. In this Section, strategies for managing and controlling potential root causes of risk and hazard failure during monorail system operations are presented. Table 9.13 shows suggested risk and hazard control measures.

Table 9.13: Recommended risk and hazard control strategies

Root cause	Recommended action	Type of action (Eliminate or control)
1	**Lack of maintenance of monorail system**	
	• To avoid risks and hazard failure resulting from lack of maintenance of the monorail system, an effective maintenance program is recommended. In this program, system components and parts should be thoroughly checked for any possible malfunctions. Additionally, monorail system daily checklist should be developed to determine the functionality of the following components before system use: o Monorail system brakes; o Over-speed governor; o Drive unit; o Lighting system; o Bugle; and o Stop-blockers. For each of the above components, the following should be included in the checklist: o Person(s) who conducted the check; o Time and date of check; o Description of defect(s), if any; o Severity of effect(s); and o Counter measures taken or to be taken.	Control

Root cause	Recommended action	Type of action (Eliminate or control)
	• In addition, regular servicing and condition monitoring and inspection of the monorail system must be done by a competent person to reduce maintenance risks. In this study, it is suggested that the system be regularly serviced and inspected every 100 hours of service. • To prevent the monorail system driving off the end of an open rail track, it is suggested that the monorail system be equipped with sensors that warns or alerts the operator (in form of signal light or alarm) when the train reaches 25 - 30m before the end of the track. This will allow the operator take necessary precautions before the system reaches the end of rail track.	
2	**Production pressure**	
	• Setting of realistic and manageable targets for the monorail system will prevent risk and hazard failure due to production pressure. Reasonable targets will avoid overloading and over-speeding of the monorail train. This will also prevent brake failure resulting from overloading of the monorail system.	Control
3	**Lack of maintenance of track / monorail installations**	
	• Track/monorail installations also require a planned maintenance program to ensure that the roof bolts, bolts, shackles, suspension chains, steel supports and switches do not pose a danger during monorail operations. During maintenance, each rail/monorail section, roof bolt, bolt, shackle, steel support, suspension chain and switch point should be thoroughly inspected for possible defects at least twice a week. Defective components should be immediately replaced with new ones and no recycling (reuse) of components is to be allowed.	Control
4	**Lack of training**	
	• Training of employees on the use, operations and health and safety aspects of the monorail system is cardinal in reducing system risks. It is, therefore, suggested that operators of the monorail system undergo training on the use, operations and health and safety aspects of the system before being allowed to operate the system. Additionally, easy to understand operating, health and safety manuals must be placed in each driver's cabin for reference. Similarly, monorail installation crew should undergo training on the correct installation of the monorail. This will prevent risks and hazard failure as a result of wrong monorail installation. The maintenance crew should also be trained properly.	Control

Root cause	Recommended action	Type of action (Eliminate or control)
5	**Cost saving**	
	• Cost saving on essential material (i.e., roof bolts, bolts, shackles, suspension chains and steel supports) can cause undesirable effects on the safety of the personnel and monorail system. To avoid risk and hazard failure due to cost saving measures on material, it is suggested that only manufacturer approved material be used during monorail installation. During maintenance of the monorail, all worn out parts should be immediately replaced with new ones and no recycling (reuse) of material should be allowed.	Control
6	**Negligence**	
	• To reduce the risk and hazard failure due to negligence by employees, it is suggested that safety communications and awareness campaigns on the importance of taking safety measures during monorail operations be made.	Eliminate
7	**Configuration and length of monorail system**	
	• To prevent risks associated with operator visibility due to configuration and length of monorail system, it is suggested that a computer monitor/panel that gives the operator clear view of the whole monorail system operations be installed in the driver's cabin. Additionally, the monorail system should have good communication network between the driver/operator and the crew operating on the same system. Thus, signals should be developed to be used as communication tools between the operator and system crew. It is also suggested that a radar system be installed in the driver's cabin to detect any incoming object within the vicinity of the monorail system. This will also reduce risks due to poor visibility.	Eliminate
8	**Poor ground conditions**	
	• To avoid risk and hazard failure due to poor ground conditions, it is suggested that an assessment of the ground conditions be done prior to monorail installation. Weak grounds must be fully supported and steel arches used to suspend the monorail installation. Suspension of monorail on steel arches will prevent roof bolt failure resulting from ground falls due to poor ground conditions as well as the weight of the monorail system.	Control

Root cause	Recommended action	Type of action (Eliminate or control)
9	**Power failure**	
	• To avoid undesirable events due to power failure during monorail operations, a secondary power source is suggested. The secondary power source should supply power to the monorail system instantaneously in case of primary power source failure. Secondary power will prevent the risk and hazard failure associated with switch failure.	Eliminate
10	**Person being electrocuted**	
	• To avoid the risks that may result from monorail electric conductor bars, the following measure have been suggested; o A schedule should be formulated for routine maintenance of electric installations. All faulty electrical installations must be replaced immediately; o Danger warning signs must be installed to constantly remind the personnel of the high voltage in the conductor bars. o When personnel are maintaining the rail/monorail installations, electricity must be switched off and proper notice displayed at switch points.	Control
11	**Swinging of rail tracks**	
	• Swinging of rail tracks can be avoided by using the new UFR rail type which is connected by flanges suspended from the hanging wall. This rail type has no shackles and suspension chains and has a FoS greater than 5. This will completely eliminate the swinging of the rail tracks during monorail system movements. However, frequent checks on this type of rail installation are necessary to ensure that there is no peeling of sidewalls that may affect the stability of the flanges with time.	Eliminate
12	**Monorail security system**	
	• To avoid the monorail train being set in motion by an unauthorized person or to prevent it from unintentional movement, it is recommended that the manufacturer of the monorail system increases the safeguards on the system. The following safeguards have been suggested: o Each operator must be given a unique code/password which should be entered before operating the monorail system failure to which the system cannot move. o System brakes to be in engaged mode when the system is not moving. o The system should be equipped with manual anchorage for anchoring the system e.g. using chains. The anchorage should also have a locking system which should only be unlocked by the operator.	Control

9.5 Summary

This study has revealed that there are a number of risks and hazards that have the potential to cause injury (or death), system or economic loss and environmental damage during monorail system operations. Identification of the potential hazards is critical in assessing system risks since only what has been identified will be evaluated. Risk assessment conducted on the monorail system hazards facilitates ranking of the hazards in terms of the likelihood and severity of each hazard. The ranking serves as a guide to the order in which these risks should be addressed. The study has also established the potential root causes of monorail system risk and hazard failure through fault-tree analysis. The analysis revealed that proper maintenance of the monorail system and the monorail installations, reduction in production pressure and improving training of personnel on monorail system use are critical in improving the safety of the system. Other root causes of risk and hazard failure include cost saving, poor ground conditions, swinging of rail tracks and negligence. Therefore, in order to improve the health and safety aspects of the monorail system, risk and hazard control strategies have been suggested. The control strategies are aimed at reducing the level of risk by directing corrective measures at potential root causes as opposed to addressing the immediate obvious symptoms.

Chapter 10

10.0 Mine design for monorail system application – Jundee Case Study

10.1 Introduction

In 2004, Newmont Mining Corporation technical group carried out an investigation to determine the potential of "South Deeps" narrow deposits by designing capital developments to the deposits using the conventional 1 in 7 decline gradient. A conceptual mine design was completed for accessing the four optimised areas in the South Deeps. Following the optimisation of the deposits, resources were found to be far from becoming potentially economic. In an effort to improve the economic viability of "South Deeps" deposits, monorail technology is used to design the decline access and other capital developments to these deposits. This Chapter looks at mine design case study using monorail technology to "South Deeps" deposit and the results of the design compared with conventional method. The Nexus deposit is used as a case study area for designing decline access for monorail system application. The mine design for the Nexus deposit was completed using Datamine mining software. It should also be noted that the information used in this Chapter was the best available when this research project commenced.

10.2 Jundee "South Deeps" deposits

The Jundee operations are situated approximately 800 km northeast of Perth in Western Australia. The operations are owned by Newmont Mining Corporation, which is one of the world's largest producers of gold. The Jundee operation began operations in 1995 and is composed of two underground mines as well as

several satellite open pits about 30 km south of the operation. It produced 313,000 ounces of gold in 2006 and reported 1.48 million ounces of gold reserves at year-end. The Nim3 deposit, situated beneath Nim3 open pit (Figure 10.1), is the third largest underground resource of Jundee–Nimary gold field.

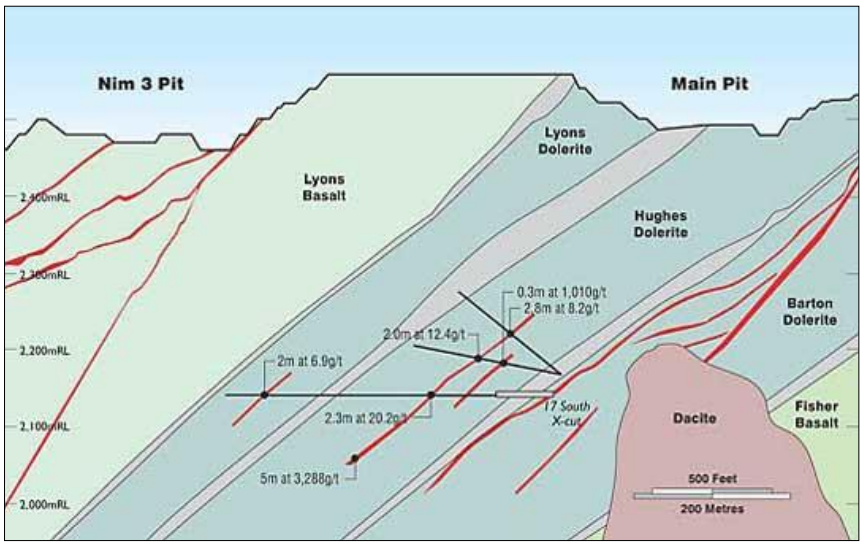

Figure 10.1: Nim3 deposit of Jundee operations (Newmont, 2004)

A number of structures; Nim3 Lyons, Nexus, Midas, Moneyline, Hughes, Cartman and Colloform collectively forms the Nim3 deposit (South Deeps) and was the primary source for Nim3 open cut/underground operations. Figure 10.2 shows the ore bodies of the South Deeps mineralisation.

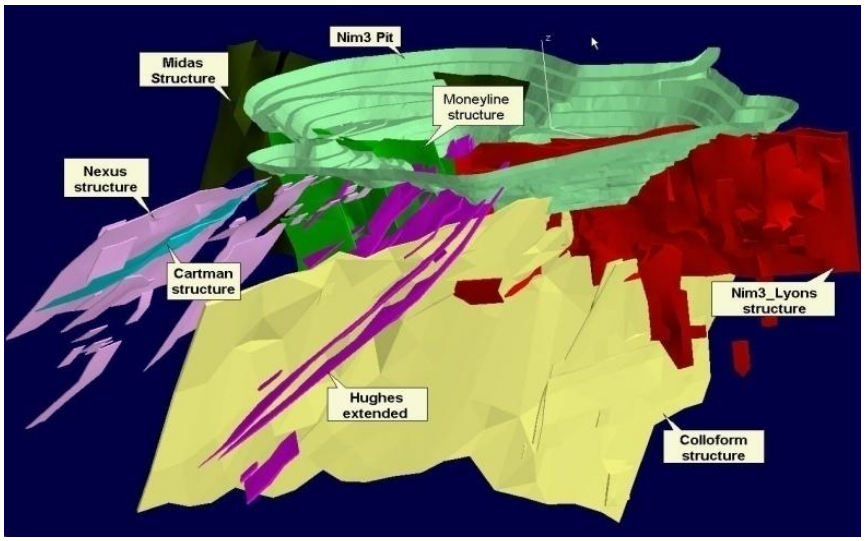

Figure 10.2: Nim3 pit and South Deep deposits (Newmont, 2004)

10.3 The Nexus orebody structure

The Nexus orebody structure strikes north and dips moderately to the west at about 40°. The structure generally lies close to the basal contact with a thick overlying dacitic porphyry body (the Nexus Dacitic Porphyry), which appears to be largely concordant with the local stratigraphy. The Nexus ore body has approximate strike length of 1.1km. About 400m long of the southern portion of the structure is drilled with wide spaced drilling and geological confidence is low. The mineralisation of the Nexus structure is patchy within the corridor between 96550mN and 96800mN. High grade Nexus mineralisation that occurs beneath the Nim3 pit could be modelled only for a short strike length of 125m. The structure beneath Nim3 trends north and dips steeply at 70° to the west.

10.4 Mine design for monorail system application

10.4.1 Mining method

Sublevel open stoping mining method is used for the extraction of the Nexus deposit. The same mining method is applied in similar areas of the mine and has proved to be successful. The orebody characteristics also favour this mining method. Horizontal levels (crosscuts) from the decline to the deposit are developed at 10-m intervals.

10.4.2 Access design to Nexus structures

Access to the Nexus deposits is via a 212m long straight incline, which starts from the box cut entry portal and joins the main Nexus decline at elevation 2390mL. The straight incline is located on the southern centre of the existing Nim3 pit as shown in Figure 10.3. According to Scharf (2007), the minimum decline dimension for one monorail train application is 3.0m x 3.0m. However, decline dimensions of size 4.0m x 4.0m are used in this design to leave enough working space (underneath and on the sidewalls) and to accommodate other mine services, such as, ventilation tubing, air and water pipes and cables. The

main decline to Nexus deposit is developed with gradient 20^0 from 2440mL and spirals down to 2140mL as shown in Figure 10.3.

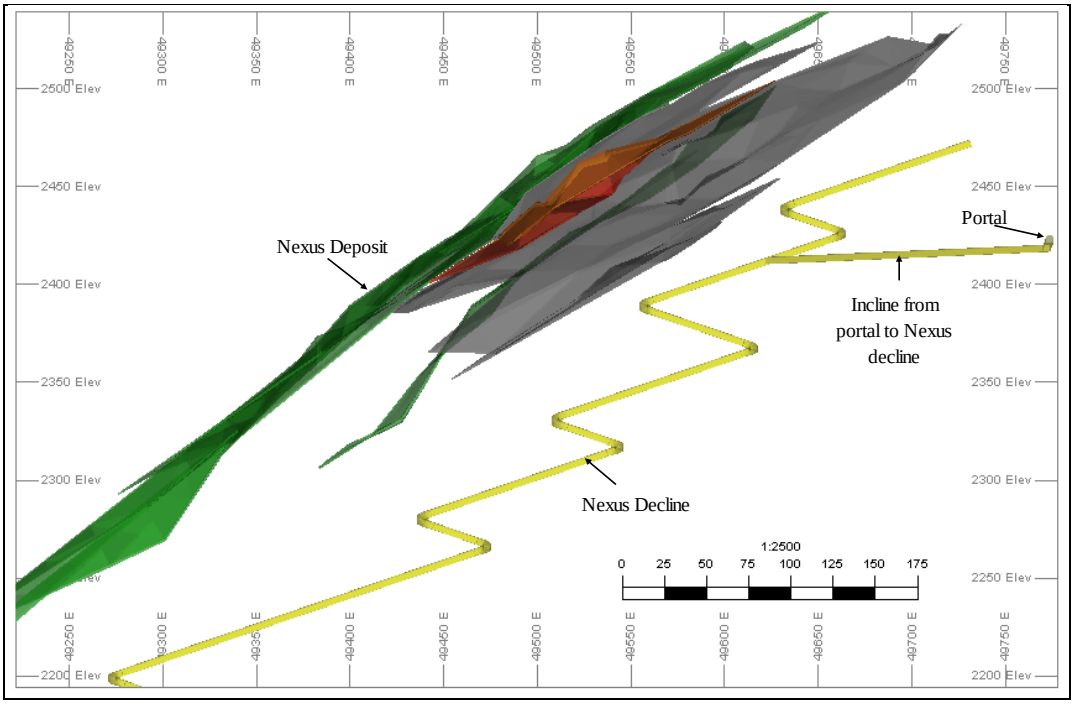

Figure 10.3: Decline design to Nexus structures for monorail system application

According to Scharf (2007), a monorail train can negotiate curves of minimum horizontal radius of 4m. However, to avoid unnecessary stresses on the I-beam rails and on the rollers, horizontal curve radius of 6m is used in this design. Unnecessary stresses may cause excessive wear on the rail tracks and damage to the roller bearings. Varying lengths of straight ramps are also used during the design to provide best access to the orebody.

10.4.3 Design of cross-cuts to Nexus structures

Horizontal development headings exiting the Nexus decline provide access to stopes and draw points of the Nexus deposits. Horizontal crosscuts from the Nexus decline towards the Nexus deposits are designed with dimensions 4m x 4m at 10m interval from 2440mL to 2140mL. A 4m x 4m size of crosscuts was adopted since the monorail network can be extended from the decline to the

crosscuts meaning that there is no need for large openings. A total of 31 crosscuts were designed with a total length of 4990m. Results of the design are shown in Figure 10.4.

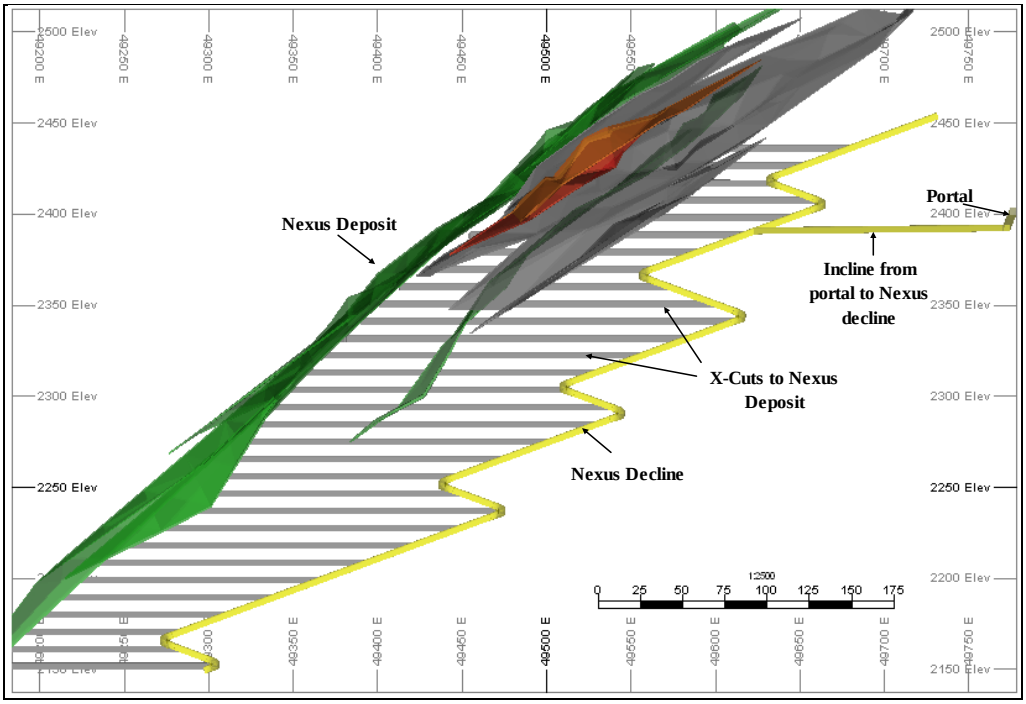

Figure 10.4: Design of crosscuts from Nexus decline to the deposit

10.4.4 Design of intake and exhaust ventilation network

Figure 10.5 shows the designed fresh air intake and exhaust ventilation drives to the Nexus deposits. Both fresh air intake and exhaust access are designed on the footwall side of the deposit to take advantage of the competent ground. According to the designs, fresh air enters Nexus decline from 2390mL and is pumped down to 2140mL by booster fans. Several fresh air intake crosscuts are provided to supply fresh air to intermediate levels. Both fresh air intake and exhaust access are designed with dimensions 2.5m x 2.5m. This size is less than 4.5m x 4.5m (for intake and exhaust crosscuts) and 3.0m x 3.0m (for intake and exhaust raises) used in conventional design. Smaller dimensions are used because the monorail system uses electricity and it is anticipated that there will be less diesel fumes in an underground environment during operations hence there will be a lower demand for ventilation.

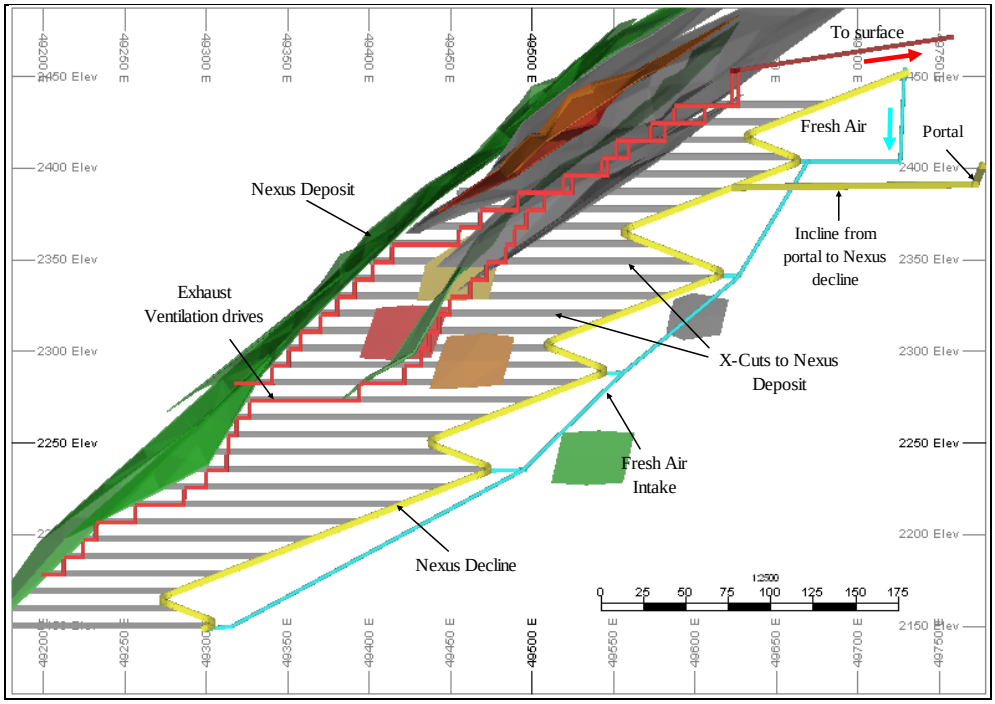

Figure 10.5: Design of intake and exhaust ventilation network to Nexus structures

10.4.5 Waste and ore handling

10.4.5.1 Waste handling

Although the monorail drill-load-haul system is designed for decline development, it can also be used in the development of horizontal headings. As highlighted Section 10.4.3, the use of monorail system in development of horizontal headings can be achieved by extending the rail network into the crosscuts. This means that waste material from the access crosscuts and ventilation headings would be loaded into monorail containers by either the monorail loading system or the LHDs. If LHDs are used, provisions should be made for waste material to be loaded directly into monorail containers. Once waste material is loaded into monorail containers, it is transported to surface by the monorail train.

10.4.5.2 Ore handling

Removal of the ore from stopes may be accomplished by means of LHDs or the monorail system be extended into the crosscuts to the lode (zone of veins of gold). If the LHDs are used to transport ore from the stopes to the monorail system via the crosscuts, special arrangements have to be made to allow the LHD load into the monorail containers in the decline. However, if the monorail system is extended into the crosscuts, LHDs will remove the ore from the stopes to the stockpile located at the end of the crosscut and from here ore will be loaded into the monorail containers using the pneumatic suction system. Alternatively, LHD may be used to load ore from the stockpile into the monorail containers but this will increase the loading time and needs to be avoided.

10.5 Results and analysis of the design

10.5.1 Development meters and tonnage to be removed

Table 10.1 shows development meters and the tonnage to be removed for the designed mine using monorail technology.

Table 10.1: Access development meters and tonnages to be removed

Description	Waste Tonnage (t)	Length (m)
Incline from portal to Nexus Decline	9400	212
Decline from 2440mL to 2140Ml	41600	895
Total	**51000**	**1107**
Crosscuts (a total of 31)	227600	4991
Total	**227600**	**4991**
Fresh air intake access	9800	640
Exhaust access	27000	1650
Total	**36800**	**2290**

As shown in Table 10.1, a total of 1107m is required to develop an incline access from the entry portal to the main Nexus decline as well as the main Nexus decline from 2440 to 2140mL. Results also show that a total of 4990m is required to develop a total of 31 crosscuts while a total of 2290m is required for development of ventilation access to

Nexus deposit. Table 10.1 also reveals that a total of 51000 tonnes (using tonnage factor of 2.85t/m^3) of waste material will be excavated during decline development while a total of 227600 tonnes will be excavated from the crosscuts. Ventilation access would result in excavation of 36800 tonnes of material.

10.5.2 Capital development cost to Nexus structures

Generally, the costs of capital development to access the deposit as well as mine services are considered to be preproduction capital costs and are typically the largest component of mining capital costs. Capital developments also require the longest time period of any mine activity in preparing the mine for production. In this Section, an analysis of the preproduction costs associated with decline development to the Nexus deposits using monorail technology is undertaken. Development costs for monorail system application were calculated on first principle, i.e., development length multiplied by development cost per meter as indicated in Equation 10.1.

$$\text{Development cost} = \text{Development length} \times \text{development cost/m} \quad 10.1$$

This means that after determining the development meters (lengths) for the decline, crosscuts and ventilation access, the development costs were calculated by multiplying the development meters by the development cost per meter as indicated in Table 10.2. The costs used for determining monorail system costs are the same as those used in conventional development according to Newmont (2004).

According to Table 10.2, it would cost approximately A$2.7m to develop a 212-m long incline from entry portal to the main Nexus decline and 895-m long main Nexus decline from 2440mL to 2140mL. The total cost of developing horizontal crosscuts from the decline to Nexus deposit would be approximately A$12m while a total of A$4.4m would be spent on developing ventilation access to the area.

Table 10.2: Capital development costs to Nexus structures using monorail technology

No	Description	Length (m)	Average development Cost (A$/m)	Development cost** (A$'000'000)
Cost of decline access				
1	Incline from portal to Nexus Decline	212	2400	0.5
2	Decline from 2440mL to 2140mL	895	2480	2.2
	Sub-total	**1107**		**2.7**
Cost of crosscut access to Nexus deposit				
1	Crosscuts to Nexus deposits	4991	2450	12
	Sub-total	**4991**		**12**
Cost of ventilation network (Intake Network)				
1	Fresh air intake crosscuts	133	1650	0.2
2	Fresh air intake raise	507	2170	1.1
	Sub-total	**640**		**1.3**
Cost of ventilation network (Exhaust Network)				
1	Exhaust crosscuts	1180	1760	2.1
2	Exhaust raise	470	2070	1.0
	Sub-total	**1650**		**3.1**
	Grand Total			**19.1**

10.5.3 Conventional versus monorail system development meters

Total development meters and waste tonnes obtained during mine design case study for monorail system application were compared with that obtained during a study by Newmont to the same deposit using conventional method. Figure 10.6 shows the results of this comparison.

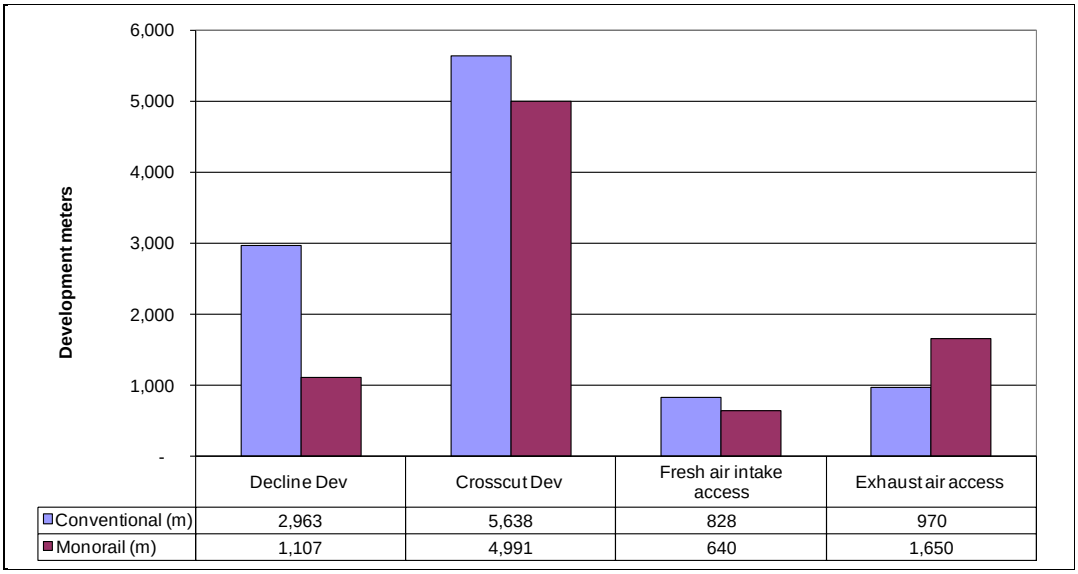

Figure 10.6: Conventional versus monorail system development meters

According to Figure 10.6, the total decline development meters (i.e., from the portal to 2140mL) would be reduced from 2963m using conventional method to 1107m with monorail system application. This represents 62.6% reduction in total decline development meters. The reduction is attributed to an increase in decline gradient from 8^0 to 20^0, which resulted in shorter decline length. It is expected that this reduction would eventually reduce the decline development costs. Furthermore, Figure 10.6 indicates that the total exhaust airway development meters increase from 970m to 1650m representing an increase of 70% for the monorail system. The increase in exhaust development meters results from the fact that exhaust ventilation layout of the mine was redesigned in this study from that originally designed by Newmont. In the redesigned layout, two upcast ventilation networks were provided as compared to one as designed by Newmont. Additionally, since LHDs will be used for ore handling in stoping areas, there is a need to exhaust more fumes from these areas, hence, the increase in development meters.

Figure 10.6 also reveals that the total development meters for horizontal crosscut would be reduced by 647 meters, i.e., from 5638m to 4991m (a reduction of 11.5%). Although this represents a modest reduction in the total

crosscut development meters, the total tonnage reduces by 55.6% (from 513,000 to 227,600 tonnes) as shown in Figure 10.7.

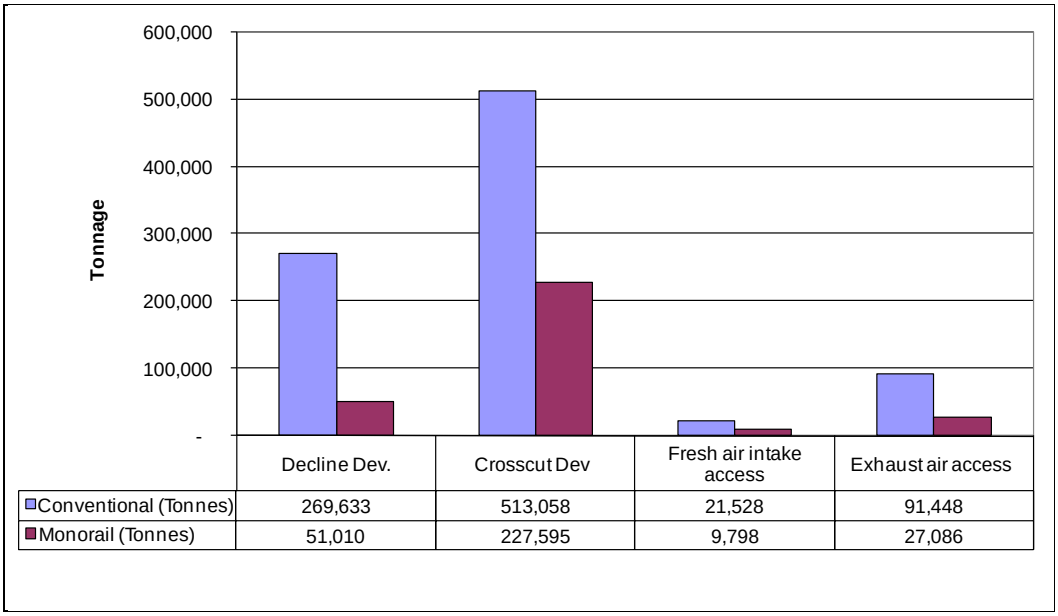

	Decline Dev.	Crosscut Dev	Fresh air intake access	Exhaust air access
Conventional (Tonnes)	269,633	513,058	21,528	91,448
Monorail (Tonnes)	51,010	227,595	9,798	27,086

Figure 10.7: Conventional versus monorail system tonnage to be removed

Results also show that the total tonnage of waste material to be removed from decline development would reduce from 269,000 tonnes (2963m x 91t/m) to 51,000 tonnes (1107m x 46t/m) using conventional method and monorail technology respectively giving a reduction of 81%. The reduction in total tonnage is attributed to the reduced size of the decline from the conventional 5.5mH x 5.5mW to 4mH x 4mW with monorail system application thus reducing the total tonnage per meter from 91t/m to 46t/m. Fresh air intake development meters also reduce from 828m to 640m giving a reduction of 22.7%. The reduction in the size of the fresh air intake developments, i.e., from 3m x 3m to 2.5m x 2.5m, resulted in the reduction in total tonnage of material to be moved from 21,500 tonnes to 9,300 tonnes (a reduction of 56.8%).

10.5.4 Conventional versus monorail system capital development costs

The total costs of capital developments obtained during mine design case study using monorail system were compared with those obtained during a study by Newmont to the same deposits using conventional method. Equation 10.1 was

used to determine the development costs with decline cost per meter and decline lengths as indicated in Table 10.2 and Figure 10.6 respectively. Figure 10.8 shows the results of the comparisons.

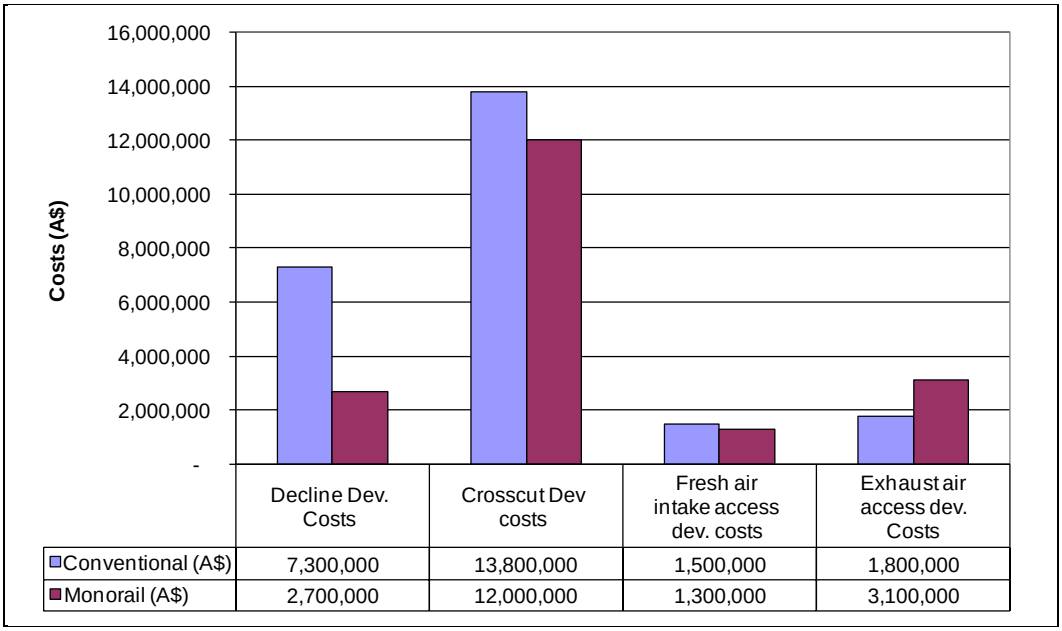

Figure 10.8: Conventional versus monorail system capital development costs

According to Figure 10.8 the total cost of decline development reduces from A$7.3m in conventional development to A$2.7m using monorail technology representing a reduction of 63%. This reduction is attributed to the reduced number of development meters with monorail system application due to steeper gradient as well as the reduced size of the decline. Development costs for horizontal crosscuts also reduce by A$1.8m with application of monorail technology. Compared with conventional method, this represents a reduction of 13% in total crosscut development cost. Figure 10.8 also reveals that the total cost of ventilation access development would increase by 33%. This is due to an increase in exhaust development meters by 70% based on the redesigned mine layout. However, the increase in development costs is minimal compared with the savings that will result from the total development costs. For the monorail development, the estimated total development cost is A$19.1m in comparison with A$24.4m for the conventional development (Figure 10.9).

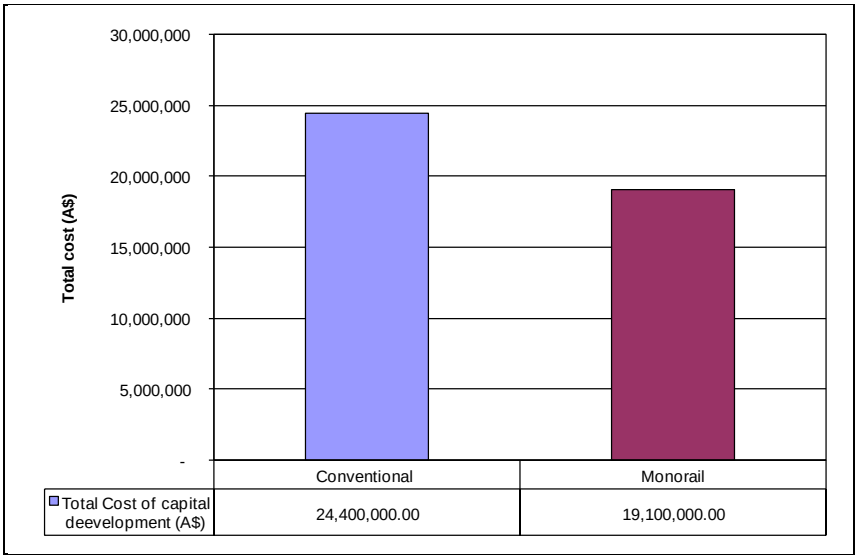

Figure 10.9: Conventional versus monorail system capital cost to access Nexus deposits

10.5.5 Purchase and monorail system installation costs

Capital costs for monorail operations consist of installation of a monorail and purchase of a monorail train. Table 2.7 (Chapter 2) shows capital costs for the purchase of a monorail train with two driver's cabins, four drive units and six lifting beams each with a payload of 30 tonnes. Table 2.8 (Chapter 2) also shows the costs per meter for monorail installation. From Table 2.7, the total cost of purchase of one monorail train (with all accessories) is A$1,316,000 while the total installation cost per meter is estimated at A$577 (Table 2.8). According to the results of the mine design case study, the total decline length from the Nim3 entry portal to Nexus deposit is estimated as 1107m. Therefore, the total cost for purchase and installation of monorail system to Nexus decline is estimated as:

Total cost = [Cost of monorail train] + [Installation cost/meter x decline length] 10.2

Total cost = [A$1,316,000] + [A$577/m × 1107m]

= **A$1,955,000**

Thus, the total cost of decline development to the Nexus deposit with purchase and installation of the monorail system is computed as follows:

Total cost = Cost of capital developments + Total monorail installation cost

= A$19,100,000 + A$1,955,000

= A$21,055,000

Therefore, approximately A$21m is required to develop the decline and install the monorail system to access Nexus deposit. According to Section 10.5.4, the total cost for conventional development is A$24.4m. It should be noted that the development cost for conventional method does not include loading and hauling equipment such as Front End Loader (FEL) as well as dump trucks, i.e., the cost include only development costs. The total cost for conventional development is likely to increase if the cost of FEL and dump trucks are included. Therefore, when compared with the total cost of using the conventional haulage system (without loading and hauling equipment) as evaluated by Newmont (2004), there is still a saving of A$5.3m for capital development to access the same deposit. This represents a reduction of 22% in total capital cost. The saving will even be more if the cost of loading and hauling equipment was included in the conventional method.

10.5.6 Duration of decline development to Nexus structures

According to the simulation results obtained in Chapter 8, the monorail system will have the same advance rate as the conventional system (i.e., 6.66m per day). Since the total length of the decline for the Nexus deposit is known, i.e., 1107m, therefore, using Equation 2.5 (Chapter 2), it would take approximately 166 days (i.e., 1107m ÷ 6.66m/day) to develop the decline to Nexus deposit using monorail technology. In contrast, it would take approximately 445 days (i.e., 2963m ÷ 6.66m/day) to access the same deposit using conventional decline development method.

10.6 Summary

This study has demonstrated that the development of a decline access to Nexus deposits using monorail technology is feasible. Compared with conventional

decline development, results have shown that the monorail system has the potential of reducing the decline length (i.e., spiral decline and straight incline from the portal) to Nexus deposits by over 62.6% and decline costs by 63%. Furthermore, the study has revealed that with the application of the monorail system, there is a potential of reducing the total capital costs by 22% (i.e., cost of developing the decline, straight incline from the portal, crosscuts, ventilation network and installation and purchase of monorail train). Additionally, due to rapid development by the monorail drill-load-haul system resulting from the shorter decline length coupled with smaller decline openings, the duration of decline development reduces by 71.8%. This case study demonstrates that the economics of narrow vein deposits can be improved significantly by using the monorail system.

Chapter 11

11.0 Conclusions and further work

11.1 Conclusions

A distinguishing feature of modern underground hard rock mines in Australia is their seemingly invincible dependence on diesel rubber-tyred machinery based decline development. This system has attained iconic status in the mining industry and it must be acknowledged that the model has in the past served, and in some cases continues to serve, the industry well and will be difficult to displace. However, it has to be recognized that the system suffers from a number of threats including geotechnical problems resulting from bigger cross-sections of the decline, diesel fumes from mining equipment, high ventilation requirements and low advance rates. In contrast, the Electrical Monorail Transport System (EMTS) uses electricity, which provides a solution to some of the challenges faced by current system of decline development. An electro-monorail, combined with the proposed drilling and loading equipment offers a means whereby the mining industry can achieve reductions in green house gas emissions, reduce costs and improve mining rates.

The size of decline openings adopted in conventional mining (5.0m Wide by 5.0m High) is largely driven by the need to accommodate diesel loaders and trucks. The problems associated with 'large' excavations are well known; there is elevated seismic risk, an increased likelihood of large unstable blocks forming, and falling from higher positions, having the potential to cause major damage and injury. Heat pick-up from the greater surface areas exposed can require the

circulation of large volumes of ventilating air, a cost factor often obscured by the overarching ventilation demand of providing sufficient air to cool diesel engines operating underground and simultaneously maintaining adequate breathing air quality. The conventional 1 in 7 decline gradient and turning radius of 20m results in an unnecessarily longer decline whereas a steeper gradient and smaller turning radius results in a shorter decline; hence, an ore body can be accessed more quickly and cheaply. It has to be acknowledged that the capital cost of the monorail system is significantly higher than for a similar payload truck. However, the operating cost of the monorail system at a remote Western Australian mine site using diesel power generation is estimated to be the same as a similar payload underground truck (A$49 per operating hour). Rail components and installation is estimated at A$577 per metre. Interestingly, the operating cost of the monorail would be significantly less than a similar payload truck if the cost of power was significantly reduced to levels occurring in the eastern parts of Australia.

In Chapters 4 and 5, a theoretical analysis of the principles of operation of the monorail drill-and-blast system is undertaken. The stability of the monorail drilling system is critical in ensuring efficiency of the drilling process. By analysing the balance of forces acting on the system, it was possible to determine the minimum and maximum forces required to stabilize the monorail system during drilling operations. The configuration and positioning of the monorail drilling system also has a bearing on the performance of the system. Consequently, the approximate swing and lifting angles that will enable the system to be able to cover the whole drill face during drilling operations have been determined. The use of a vacuum lift system for the transportation of fragmented rock from the face into the hopper is a new development. While it is difficult to determine how the system would perform in the actual production environment, the theory indicates that the system is capable of delivering the required productivity. As a matter of fact, vacuum lift systems have been used in shaft sinking with excellent operating results. The productivity of the monorail system can be increased by integrating the unit operations of drilling, blasting, loading and hauling at the mining face. This is achieved by introducing a

monorail mounted drill and a pneumatic face loading system. This system allows rock to be removed from the development face and loaded into the monorail containers in accelerated mining cycle.

Chapter 6 has revealed the importance of having an adequate support system during monorail system operations. It has been established that for the safety of the personnel as well as the system, high strength roof bolts, suspension chains and steel supports that are able to support the two systems must be installed. Using the developed models, the study has demonstrated that the support system currently in use has adequate strength to support and suspend the two systems. It has also been established that the required strength of roof bolts varies inversely with the decline gradient. However, the strength of suspension chains in the decline and at horizontal curves as well as the strength of roof bolts at horizontal curves remains constant. To reduce or minimise displacements of suspension chains, it is recommended that the velocity of the monorail system at horizontal curves be reduced during motion.

In Chapter 7, automation design for monorail drilling and loading systems processes has been developed. The ultimate aim of automation design is to increase the safety and improve the efficiency of the two systems. The proposed automation system would increase productivity by improving operator performance through control of the system processes. It is hoped that automation of the monorail drilling and loading systems will reduce the total drill-load-haul cycle time hence improving the efficiency of the systems.

The simulation model developed in Chapter 8 confirms the results obtained from the analytical models. Both the monorail and conventional systems for decline development appear to have the similar advance rates (3.3 metres per shift) because both systems depend on one blasting process. However, the total mining cycle is lower for the monorail system, allowing for a further drill and blast cycle within the same time period.

In Chapter 9, hazards and risks that have the potential to cause injury (or death), system or economic loss and environmental damage during monorail system operations have been identified. Risk assessment conducted on the monorail system hazards has ranked the hazards in terms of the likelihood and severity of each hazard. The ranking serves as a guide to the order in which these risks should be addressed. Potential root causes of system risk and hazard failure have also been identified. The major root causes of system failure include lack of maintenance of the monorail system and the monorail installations, production pressure and insufficient training of personnel on monorail system use. Therefore, in order to improve the health and safety aspects of the monorail system, the study has developed risk and hazard control strategies. These strategies are aimed at reducing the level of risk by directing corrective measures at potential root causes as opposed to addressing the immediate obvious symptoms.

In Chapter 10, the application of monorail technology to the development of decline access to the Nexus ore body at Jundee in Western Australia indicates that gains can be made in terms of cost saving and speed of development. Compared with conventional decline development, results show that the monorail system has the potential of reducing the decline length to the deposit by over 62.6%. Further, the study indicates that with the monorail system, there is potential to reduce decline development costs by 22%. Also, due to the reduced mining cycle using the monorail system, the shorter decline length coupled with smaller decline openings, the time it would take to develop the decline reduces by a staggering 71.8%. These results have been collaborated by the computer simulation of the system.

Clearly, the electro-monorail drill-load-haul system is a viable alternative mining system for decline development especially for small to medium low tonnage orebodies. The system can even be used as a second level electrical reticulation component. Other benefits include elimination of diesel powered equipment in the underground environment, lower ground support and haulage costs and potential for rapid decline development.

11.2 Further work

In going forward with this technology, it is proposed that a demonstration system be installed at a mine site in Australia. This will require the cooperation of Scharf SMT, mining companies, and government relevant agencies. The objective of setting up the demonstration system is to provide proof of concept and measure/collect operational data to be used in the subsequent design of a full scale integrated monorail system. If a demonstration system cannot be setup due to operational consideration, the study based on a virtual mine is recommended. The study should include economic comparisons such as Net Present Value (NPV). It is also recommended that time aspects of the proposed system, such as pneumatic loading be studied on laboratory scale.

To further improve advance rates with the monorail system, it is suggested that the new Super Material Abrasive Resistant Tools or SMART*CUT diamond composite bits being developed by CSIRO be used during drilling operations. This technology uses thermally stable diamond composites (TSDC) in the design and manufacture of cutting tools for mining, civil construction and manufacturing (Alehossein, et al., 2009). TSDC has superior wear resistance and exceptional hot hardness characteristics (Boland, et al., 2010; Li, et al., 2008; Li and Boland, 2005). It is more than 1000 times more resistant to abrasive wear than tungsten carbide. TSDC overcame the thermal instabilities limiting traditional diamond composites but it posed a vexing bonding problem. CSIRO has developed a reliable bonding process and is prototyping drill bits and other cutting tools to take advantage of TSDC's unique properties. Laboratory drilling trials have demonstrated that these prototype bits have twice the penetration rate and expend half the energy of traditional rock coring bits. In the manufacturing industries, indexable cutting inserts incorporating TSDC would offer several important advantages over tungsten carbide. Such tools could:

- Operate at higher cutting temperatures;
- Eliminate or at least reduce the need for environmentally damaging cooling fluids; and
- Enable faster and more economical high-speed machining operations.

References

Alan, D. (2003). *Mechanical Engineering: BTEC National Option Units*.' Oxford: Newnes. p. 56. ISBN 0750657618.

Alehossein, H., Li, X. S. and Boland, J. N. (2009). *Towards Improving Rock Cutting Tools Using Thermally Stable Diamond Composites*, Advanced Materials Research, v 76 – 78, p 585-590.

Alwyn, E. A. (1991). *Mineral Deposit Evaluation. A practical Approach. Chapman and Hall,'* ISBN 0417352907. p89.

AS/NZS 4360, (2004). *Standards Australia 2004, Risk Management, Joint Standards Australia/ Standards New Zealand Committe*e, 31 August.

Atlas Copco Manual, (1982). 4th Edition. pp 261.

AusIMM, (2007). *The Mining Glossary.* The essential handbook of mining terminology, Australasian Institute of Mining and Metallurgy, ISBN 9780980425604.

Ayyub, B. M. (2003). *Risk Analysis in Engineering and Economics*; Chapman & Hall / CRC, A CRC Press Company, NY. ISBN 1-58488-395-2.

Aziz, Z. B. and Klinzing, G. E. (1990). *Dense Phase Plug Flow Transfer: The 1-inch Horizontal Flow.* Powder Technology, 62: p. 41-49.

Bankston, J. D. and Baker, F. E. (1994). *Selecting the Proper Pump.* SRAC Publication No. 372.

Biegaj, K. (2002). *Mobile Supersucker Winzing* – Attaining proven prior to capital commitment.

Boland, J. N. Li, X. S., Rassool, R. P., MacRae, C. M., Wilson, N. C., Elbracht, S., Luzin, V., Imperia, P. and Sobott, B. (2010). *Wear Resistance and Microstructural Study of Diamond Coated WC Tools*, Materials Science Forum, Vols. 654-656 pp 2527-2530.

Boyed, J. T. (1993). *Technical Report, Independent Assessment of Coal Mining Operations at Maamba Collieries Limited.* Report 2324.2. Published by John T. Boyd and Company, Mining and Geological Engineers, Pittsburgh, Pennsylvania, United States of America.

Bradley, M. S. A. (1989). *An Improved Method of Predicting Pressure Drop along Pneumatic Conveying Pipelines.* Third International Conference on Bulk

Materials. Storage. Handling and Transportation, Newcastle, N.S.W., June, 27-29 pp. 282-288.

Brazil, M. L. D., Rubinstein, J. H., Thomas, D. A., Weng, J. F. and Wormald, N. C. (2003). *Optimisation in the Design of underground Mine Access.* Orebody Modelling and Strategic Mine Planning Conference. Spectrum Series Volume 14.

Buyens, M. (2005). *Design and application of high speed development system for tracked haulage;* in colloquium: A new Era of Tunnelling? pp 1-15 (The South Africa Institute of Mining and Metallurgy, Johannesburg).

Carl, T. (2002). *Parallel and Distributed Discrete Event Simulation*, *Nova Science Publication.* ISBN 1590333772; ISBN-13: 978-1590333778.

CCPS, (2000). *Center for Chemical Process Safety Chemical Process Quantitative Risk Analysis*, 2nd edn, AIChE, New York.

Chanda, E. K. and Burke, P. A. (2007). *Electro-monorails; an alternative operating system for deep mining.* Australian Centre for Geomechanics Publications; ISBN: 978-0-9804185-2-1.

Chanda, E. K. and Corbett, C. J. (2003). *Underground mining of shallow dipping ore bodies.* Mechanised up dip stoping versus transverse retreat stoping, Proc. 12th International Symposium on Mine Planning and Equipment Selection (MPES), 23 -25 April, Kalgoorlie, Western Australia, CD (The Australasian Institute of Mining and Metallurgy; Melbourne).

Chanda, E. K. and Roberts, M. (2005). *Evaluation of monorail haulage system in metalliferous underground mining*. Proc. Hoist and Haul Conference, 5 – 7 September, Perth, 39 – 44 (The Australasian Institute of Mining and Metallurgy; Melbourne).

Chung, C. A. (2003). *Simulation Modelling Handbook.* A practical approach; Published by CRC Press LLC, ISBN: 9780849312410, ISBN 10: 0849312418.

Dorf, C. R. and Kusiak, A. (1994). *Handbook of design, Manufacturing and Automation*. Wiley-Interscience Publications, ISBN-10: 0471552186; ISBN-13: 978-0471552185.

Dorricott, M. G. and Jones, I. O. (1984). *Vacuum Lift Systems for the Transport of Broken Rock in Shafts*. Paper presented at Regional Conference on 'Gold

Mining, Metallurgy and Geology', The AusIMM Perth and Kalgoorlie Branches.

Ergun, S. (1952). *Fluid flow through packed columns*. Chemical Engineering Progress 48, 89–94.

Ferdinand, P. B., Russel, E. J. and DeWolf, J. T. (2002). *Mechanics of Materials.* International Edition 3rd Edition McGraw-Hill Publishers ISBN: 0071121676.

Fischhoff, B., Lichtenstein, S., Slovic, P., Derby, S. L. and Keeney, R. L. (1981). *Acceptable Risk*. New York: Cambridge University Press.

Fishman, G. S. (2001). *Discrete-Event Simulation: Modelling, Programming and Analysis*. Springer Series in Operations Research. ISBN:0387951601; EAN: 9780387951607.

Franklin, J. and Katsabanis, T. (1996). *Measurement of blast fragmentation*. Proceedings of the fragblast-5 workshop on measurement of blast fragmentation; Balkema / Rotterdam / Brookfield Publication. Montreal, Quebec, Canada 23-24 August. ISBN: 9054108452.

Garvey, P. R. (2009). *Analytical Methods for Risk Management. A system Engineering Perspective*. Chapman and Hall/CRC. Taylor and Francis Group. NY. ISBN: 9781584886372.

Geldart, D. (1973). Types of Gas Fluidization. Powder Technology. **7**: p. 285 - 292.

Gibbons, J. D., Olkin, I., and Sobel, M. (1977). *Selecting an ordering populations; A New statistical methodology*. New York; John Wiley & Sons.

Granholm, S., Kumar, U. and Nilsson, I. (1990). *Raise Mining – a mining method for narrow ore bodies.* Lulea University of Technology, Sweden, Mining Department, 9p.

Graves, R. M. and O'Brien, D.G. (1998). *StarWars Laser Technology Applied to Drilling and Completing Gas Wells*. Paper presented at the 1998 SPE Annual Technicar Conference and Exhibition bald in New Orteans, Lcuisiana, 27-30 September 1998 Copyright 1998, Society of Petroleum Engineers, Inc.

Gunnar, A. Uday, K. and Vagenas. N. (1993). *Mine Mechanisation and Automation*. Proceedings of the second international symposium on mine mechanisation

and automation, Luleå University of Technology, Sweden 7-10 June 1993. A.A Balkema/Totterdam/Brookfield publication ISBN No. 9054103140.

Guse, A. and Weibezhn, K. (1997). *Continuous transport in hard rock mining;* Colloquium – Underground Lateral Transport, 16 April, p 1-6, Randburg, South African Institute of Mining and Metallurgy; Johannesburg.

Hall, A. S., Archer, F. E., and Gilbert, R. I. (1999). *Engineering Statics*. Second Edition. UNSW Press. ISBN 086840425X. pp 209 – 211.

Hartman, H. L. (1992). *Elements of mining*; SME Mining Engineering Handbook. Society for Mining, Metalurgy, and Exploration, Inc, 2nd Edition; ISBN 0873351002. Pp 33.

Hartman, H. L. (2002). *Introductory Mining Engineering.* John Willey and Sons, 2nd Edition; ISBN 0471348511.

Hellerstein J. L., Tilbury, D. M., and Parekh, S. (2004). *Feedback Control of Computing Systems*. John Wiley and Sons. ISBN 0-47-126637-X.

Herbich, J. B. (2000). *Handbook of Dredging Engineering. McGraw-Hill Professional* ISBN:0071343067.

Hilti Corporation, (2004). FL-9494 Schaan, Principality of Liechtenstein, www.hilti.com.

Hirota, M., Sogo, Y., Marutani, T., and Suzuki, M. (2002). *Effect of mechanical properties of powder on pneumatic conveying in inclined pipe.* Powder Technology, 122(2-3): p. 150-155.

Holland, F. A. (1973). *Fluid flow for chemical engineers*. 2nd ed. Edward Arnold Publication London.

http://www.esr.ruhr-uni-bochum.de/rt1/syscontrol/node5.html

http://www.flickr.com

Irving, G.P.E. (1989). *Fluid Mechanics.* 4th Edition, ISBN 013352170-2,

Isokangas, T. and White, B. (1993). *Transportation and haulage practices in the Australasian mineral industry* – underground systems, in Australasian Institute of Mining and Metallurgy, Volume 1, p91-92.

Jagger, L. J. (1997). *Sinking of a twin decline system at 9^0 with Impala Plats Ltd*' – Internal Report, unpublished.

Jones, I. O. (1989). *Pneumatic Conveying in Mines*. Third International Conference on Bulk Materials, Storage, Handling and Transportation Newcastle 27-29 June.

Kano, T. (1985). *Reduction of power consumption in pneumatic conveying of granular material*. Proceedings of pneumatic conveying of bulk and powder conference. Trans Tech Publication. ISBN 0878490639 pp 185 – 192.

Kaplan, S. and Garrick, B. J. (1981). *On the quantitative definition of risk, Risk Analysis*, Vol 1, Issue 1, pp 11 - 27.

Kelman, I. (2002). *Physical flood vulnerability of residential properties in coastal, eastern England*. *PhD Thesis*, University of Cambridge September 2002, U.K.

Kerttu, S. M. (1985). *Pipeliness - The Sealed and Quite Coal Transporters*. The National Engineering Conference, ASEA Pty. Limited, Melbourne. 2 - 8 March.

Klinzing, G. E. (1981). *Gas solid Transport* - McGraw-Hill, New York.

Klinzing, G. E., and Dhodapkar, S. V. (1993). *Pressure fluctuations in pneumatic conveying systems.* International conference on Bulk Material Handling and Transportation; Symposium on Freight pipelines, Wollongong, Australia 6 – 8 July 1992.

Klinzing, G. E., Marcus, R. D., Rizk, F., and Leung, L. S. (1997). *Pneumatic Conveying of Solids - A Theoretical and Practical Approach*. Chapman & Hall.

Kraus, M. N. (1980). *Pneumatic Conveying of bulk materials*. Second Ed. McGraw-Hill Chemical Engineering Publications. New York. ISBN. 070107246.

Kuo, B. C. (1991). *Automatic Control Systems.* 6th ed. New Jersey: Prentice Hall. ISBN 0-13-051046-7.

Law, A. M. (2005). *How to build valid and credible simulation models.* Proceedings of the 2005 Winter Simulation Conference, Tucson, U.S.A.

Lawrence, S. L. (1997). '*Physics for Scientists and Engineers*'. Boston: Jones & Bartlett Publishers. p. 128. ISBN 0867204796.

Lawrence, W. W. (1976). *Of Acceptable Risk*: *Science and the Determination of Safety*. Los Altos, CA: W. Kaufmann.

Leppkes, H. (2004). Personal Communications' September.

Leppkes, H. (2005). *Continuous Transport in Hard Rock Mining*.

Li, X. S. and Boland, J. N. (2005). *The Wear Characteristics of Superhard Composite Materials in Abrasive Cutting Operations*, Wear, Volume 259, Issues 7-12, pp. 1128-1136.

Li, X. S., Boland, J. N. and Guo, H. (2008). *A Comparison of Wear and Cutting Performance between Diamond Composite and Tungsten Carbide Tools*, Industrial Diamond Review, v 68, n 1, , p 51-54.

Liptak, B. (1995). *Instrument Engineers. Handbook: Process Control*. Radnor, Pennsylvania: Chilton Book Company, 20-29. ISBN 0-8019-8242-1.

Liu, H. (2003). *Pipeline Engineering: Fundamentals for the Water and Wastewater Maintenance.* CRC Press ISBN:1587161400.

Mason, J. S., Mills, D., Reed, A. R. and Woodcock, C. R. (1980). *Introduction to pneumatic conveying*. Powder Europa 80, Industrial Awareness Seminar Lecture Notes. International Powder Institute, London, pp 1 – 57.

McCarthy, P. L. and Livingstone, R. (1993). *Shaft of Decline? An Economic Comparison.* Open Pit to Underground: Making the transition. AIG Bulletin 14, 1993 pp 45 – 56.

McGregor, K. (1967). *The drilling of Rock' CR Books Ltd Publication.* pp 59-61,

Medhurst, G. (2004). *An objective assessment of shaft hoisting truck haulage in underground mines.* Report – Sinclair Knight and Merz (http://www.skm.au), 11p.

Meriam, J. L. and Kraige, L. G. (1993). Engineering Mechanics. Volume 1, 3rd Edition. John Wiley & Sons, Inc. p61.

Metzger, O. H. (1940). *U.S. Bureau of Mines Information Circular.* No. 7095, Feb. 1940.

Meyer, S. (2007). Scharf, Germany – Personal communications.

Meyer, S. (2008). Scharf, Germany – Personal communications.

Mills, D. (1990). *Pneumatic Conveying Design Guide*. Butterworth-Heinemann

Mills, D. (2004). *Pneumatic conveying designs.* Butterworth-Heinemann Publications 650 pp ISBN:0750654716.

Mills, D., Mason, J. S. and Stacey, R. B. (1982). *A design study for the Pneumatic conveying of fine particulate material.* Proceedings of Solid ex 82, The Solid Handling Conference. Harrogate, England, pp C-1 to C-75.

Mohammad, M. (2006). *Risk Analysis in Engineering*; Techniques, Tools and Trends. CRC Taylor and Francis Group. NY. ISBN: 1574447947.

Monsees, J. E. and Hansmire, W. H (1992). *Civil works tunnels for vehicles, water and wastewater*; SME Mining Engineering Handbook. Society for Mining, Metalurgy, and Exploration, Inc, 2nd Edition; ISBN 0873351002. Pp 2123.

Morikawa, Y., Tsuji, Y., Matsui, K. and Jittani, Y. (1978). *Pressure Drops due to Pipe Bends in Air-Solids Two Phase Flows:* Circular and Elliptical Bends', Int. J Multiphase Flow, Vol. 4, pp 575-583.

Nance, R. E. (1984). *A tutorial view of simulation model development*. Proceedings of SIMULETTER Winter Simulation Conference April 1984, Vol. *t5,* No 2.

Newmont, (2004). *South Deeps Mining Study Report*. Jundee Mine Planning Group.

Nisture, S. P. (2006). *Engineering Mechanics.* Technical Publications. ISBN 8184310927, 9788184310924. pp 919 pages.

Novak, T. and Kohler J. L. (1998). *Technological innovations in deep coal mine power systems*. IEEE Trans. Ind. Applicant., vol. 34, pp. 196–203.

Oguz, S. and Stefanko, R. (1971). *Evaluation of a monorail mine haulage system.* Special Research Report, The PennState University, Department of Mining Engineering, 106p.

Olaf, J. H. E. (1979). *Automation and remote monitoring and control in mines*. Verlag Glükauf GMBH ESSEN Publication. ISBN No. 3773902883.

Ottjes, J. A., Meeuse, G. C., and Kuijk, V. G. T. L. (1976). *Particle Velocity and Pressure Drop in Horizontal and Vertical Pipes.* Pneumotransport 3.

Ozdimir, L. and Hanna, K. (1995). *Comparing mining techniques and equipment using computer graphics simulation*. Proceedings of the Third International Symposium on Mine mechanisation and automation, Vol. 1, Colorado School of Mines, 12-14, US Bureau of Mines. ISBN No. 0918062969.

Pan, R. and Wypych, P. W. (1992). *Scale-up Procedures for Pneumatic Conveying Design.* Powder Handling and Processing; 4(2): p. 167-172.

Pan, R. and Wypych, P. W. (1997). *Pressure Drop and Slug Velocity in Low-Velocity Pneumatic Conveying of Bulk Solids.* Powder Technology; 94(2): pp123-132.

Parfitt, N. L. C. and Griffin K. G. (1963). *Development in transport of Men and Materials.* The Colliery Guardian Overseas, pp 42 – 53.

Payne, T. and Mitra, R. (2008). *A review of heat issues in underground metalliferous mines*; 12th U.S./North American Mine Ventilation Symposium 2008 – Wallace (ed) The University of New South Wales, Sydney, Australia. ISBN 978-0-615-20009-5, pp197 -201.

Pond, R. (2000). *Telephone conversation with author.* Evansville, IN: Frontier-Kemper Constructors.

Ratnayake, C. (2005). *A Comprehensive Scaling Up Technique for Pneumatic Transport Systems.* PhD Thesis Department of Technology, The Norwegian University of Sceince and Technology (NTNU), Norway.

Rhodes, M. (2001). *Pneumatic Transport of Powders.* Copyright © 2001 Martin Rhodes, Licensed to *ERPT;* Monash *University, Melbourne, Australia.*

Robertson, A. C. (1998). *Trucking in the next Millennium:* in Underground operations Conference, Townsville, 30th June – 3rd July, 51-54 (The Australasian Institute of Mining and Metallurgy; Melbourne).

Ruppretcht, S. M. (2003). *In-stope material handling:* in proceedings Mine Planning and Equipment Selection, 23 -25 April, Kalgoorlie, Western Australia, p 573 - 580 (The Australasian Institute of Mining and Metallurgy; Melbourne).

Samson AG, (2003). Technical Information on '*Terminology and symbols in Controlled engineering.*'

Sandvik Mining and Construction, (2007). Manual. http://www.miningandconstruction.sandvik.com/

Sargent, G. R. (1991). *Simulation Model Verification and Validation.* Proceedings of Winter Simulation Conference.

Scharf, (2007). *EMTS System.* Electric Powered Transport System Brochure.

Schlichting, H. (1960). *Boundary Layer Theory,* 4th edition - McGraw-Hill, New York.

Schmid, C. (2005). Course on Dynamics of multidisplicinary and controlled Systems.(http://www.esr.ruhr-uni-bochum.de/rt1/syscontrol/node5.html)

Shannon, R. E. (1975). *Systems Simulation*: The Art and the Science', Prentice-Hall.

Sharp, J. J. (1988). *Basic Fluid Mechanics.* Buttterworth & Company Ltd, ISBN 040801640X. pp47.

Standridge, C. R. and Tsai J. (1992). *A method for computing discrete event simulation performance measures from traces.* Published by: SAGE Publication; ISBN: 0037 5497/91 USA.

Starr, C. and Whipple C. (1980). *Risk of risk decision*; Science 208: 1114 – 1119;

Sturgul, J. R. (2000). *Mine Design; Examples using Simulation*. SME Publications ISBN 0873351819.

Terence, A. (1997). *Particle size measurement. V*olume 1 – Powder Sampling and particle size measurement 5th Edition, Springer Published 1997, ISBN0412729504.

Thywissen, K. (2006). *Core terminology of disaster reduction: a comparative glossary*. In: Birkmann, J. (Ed.), Measuring Vulnerability to Natural Hazards—Towards Disaster Resilient Societies. UNU Press, Tokyo, New York, Paris.

Toler, V. D. (1965). *Diesel Shuttle Cars in an underground Coal Mines.* Coal Age, p 56 – 58.

Tsuji, Y. (1982). *Prediction of Pressure Drop and Optimal Design of Dilute Phase Pneumatic Conveying Systems.* Pneumatech.

Udo, W. P. and James, A. W. (1993). *Discrete Event Simulation; A Practical Approach*' CRC Press, ISBN 0849371740.

Vincent, T. C. and Miley, W. M. (1993). *Risk Assessment Methods: Approaches for Assessing Health and Environmental Risks*. Published by Springer, 2nd Ed. pp 319 ISBN 0306443821.

Wikipedia, (2007). *Wikipedia.* http://www.wikipedia.org.

World Mining Equipment, (1996).

Wypych, P. W. (1994). *Optimising the design and operation of pneumatic transport systems.* International Mechanical Engineering Congress. Perth Western Australia 15 – 19 May.

Wypych, P. W. and Arnold P. C. (1984). *Feasibility and Efficiency of Dense Phase Pneumatic Transportation.* Transportation Conference, Perth, 30 October - 1 November.

Wypych, P. W. and Pan, R. (1991). *Determination of Air-only pressure Drop in Pneumatic Conveying Systems.* Powder Handling and Processing.

Wypych, P. W., Kennedy O. C., Stebbins K. and Arnold P. C. (1990). *Pneumatic Conveying of Coal.* Paper presented at the International Coal Engineering Conference, Sydney 19-21 Institution of Engineers, Australia.

Yang, W. (1977). *A Verified Theory on Dilute Phase Pneumatic Transport.* Journal of Powder & Bulk Solids Technology, Vol. 1, No.1, Summer pp.89·95.

Zenz, F. A. (1964). *Conveyability of Materials of Mixed Particle Size.* Industrial and Engineering Chemistry, American Chemical Society, 3(1): p. 65-75.

Zenz, F. A. and Othmer, D. F. (1960). *Fluidization and fluid particle systems.* Reinhold, New York.

Every reasonable effort has been made to acknowledge the owners of copyright material. I would be pleased to hear from any copyright owner who has been omitted or incorrectly acknowledged.

Appendix 1

GPSS/H PROGRAM FOR SIMULATING THE MONORAIL DRILLING AND LOADING SYSTEMS

```
*********************************************************************************
```
GPSS/H program for simulating the monorail drilling and loading systems

Written by

Bunda Besa

```
*********************************************************************************
            SIMULATE
MYFILE  FILEDEF     'K:\KAPEYA2a.ATF'
    INTERGER        &DRILL,&LOADS,&NH,&T
    REAL            &LOAD,&CDNS1,&DR,&CDNF,&CDOWN,&LIFT,&OFFLOAD,&DUMP_
                    ,&A,&B,&CUP1,&CUP2,&CUP3,&CUP4,&CUP5,&CUP6, &CDN2A,&BLAST_
                    ,&CUP1A,&CUP2A,&CUP3A,&CUP4A,&CUP5A,&CUP6A,&CUPL1_
                    ,&CUPS2,&CUPW1,&CDN1,&CDN2,&CDN3,&CDN4,&CDN5,&CDN6_
                    ,&CDN3A,&CDN4A,&CDN5A,&CDN6A,&CUPL2,&CUPS1,&CDN1A,
CONT1   FUNCTION    RN2,D3
0.1,3.3/0.6,3.4/1,3.5
CONT2   FUNCTION    RN2,D3
0.1,1.6/0.6,1.7/1,1.8
    GENERATE        ,,,1 (one transaction is created to represent a one monorail)
HOME    BPUTPIC     FILE=MYFILE,LINES=4,AC1,XID1,XID1,XID1
TIME *.****
CREATE MONO1 M*     (monorail loading system created)
CREATE DRILLF D*    (monorail drilling system created)
CREATE WASTE W*     (waste material to be loaded created)
    BPUTPIC    FILE=MYFILE,LINES=2,AC1,XID1
TIME *.****
PLACE W* AT 14 17   (waste material place at face)
    BPUTPIC    FILE=MYFILE,LINES=13,AC1
TIME *.****
CREATE CONT1E CE1
CREATE CONT2E CE2
CREATE CONT3E CE3
CREATE CONT4E CE4
CREATE CONT5E CE5
CREATE CONT6E CE6
CREATE CONT1F CF1
CREATE CONT2F CF2
CREATE CONT3F CF3
CREATE CONT4F CF4
CREATE CONT5F CF5
CREATE CONT6F CF6
    BLET            &A=30/FN(CONT1) (time for drilling system to reach the face)
    BPUTPIC         FILE=MYFILE,LINES=3,AC1,XID1,XID1,&A
TIME *.****
PLACE D* ON PDR
SET D* TRAVEL *.****
    ADVANCE         &A  (drilling system travels to the face 30m from waiting place)
    BPUTPIC         FILE=MYFILE,LINES=3,AC1,XID1,XID1
TIME *.****
PLACE D* AT 15.01 26.79     (coordinates for monorail drilling position)
PLACE M* AT 67.74 50.36     (coordinates for monorail container lowering position)
    BPUTPIC         FILE=MYFILE,LINES=7,AC1
TIME *.****
PLACE CE1 ON C1
PLACE CE2 ON C2
PLACE CE3 ON C3
PLACE CE4 ON C4
PLACE CE5 ON C5
```

```
PLACE CE6 ON C6
      ADVANCE          RVNORM(1,5,0.1) (Loading system prepares to lower containers)
      BLET             &CDOWN=RVNORM(1,10,0.5)
     BPUTPIC           FILE=MYFILE,LINES=7,AC1,&CDOWN,&CDOWN,&CDOWN,&CDOWN,&CDOWN,&CDOWN
TIME *.****
SET CE1 TRAVEL *.****
SET CE2 TRAVEL *.****
SET CE3 TRAVEL *.****
SET CE4 TRAVEL *.****
SET CE5 TRAVEL *.****
SET CE6 TRAVEL *.****
      ADVANCE          &CDOWN (empty containers are lowered down)
      BPUTPIC          FILE=MYFILE,LINES=1,AC1
TIME *.****
      ADVANCE          RVNORM(1,8,0.5) (chains are removed from empty containers)
      BLET             &B=30/FN(CONT1) (time for loading system to travel to loading point)
      BPUTPIC          FILE=MYFILE,LINES=4,AC1,XID1,XID1,XID1,&B
TIME *.****
PLACE M* ON PH
SET D* CLASS DRILL
SET M* TRAVEL *.****
      ADVANCE          &B (monorail loading system travels to the loading point)
      BPUTPIC          FILE=MYFILE,LINES=3,AC1,XID1,XID1
TIME *.****
CREATE ROD RD*
PLACE RD* AT 12 22.5 (monorail drilling system starts drilling the face)
      BLET             &DR=RVNORM(1,360,10) (time to drill one hole)
      BLET             &DRILL=AC1/&DR (number of holes drilled at this time)
      BPUTPIC          FILE=MYFILE,LINES=3,AC1,&DRILL,AC1
TIME *.****
WRITE M4 ***.**
WRITE M8 ***.**
      BPUTPIC          FILE=MYFILE,LINES=1,AC1
TIME *.****
      ADVANCE          RVNORM(1,20,0.1) (suction pipe is connected to the hopper)
      BPUTPIC          FILE=MYFILE,LINES=4,AC1,XID1,XID1,XID1
TIME *.****
CREATE HOPPER HP*
SET M* CLASS MONO1
DESTROY HP*
      BLET             &LOAD=600 (loading/suction time of material in the hopper)
      BPUTPIC          FILE=MYFILE,LINES=5,AC1,XID1,XID1,XID1,XID1,&LOAD
TIME *.****
CREATE ROCK R*
CREATE ROCK1 RH*
PLACE RH* ON EH
SET RH* TRAVEL *.****
      ADVANCE          &LOAD (material is loaded into the hopper)
      BPUTPIC          FILE=MYFILE,LINES=2,AC1,XID1
TIME *.****
DESTROY RH*
      BPUTPIC          FILE=MYFILE,LINES=1,AC1
TIME *.****
      ADVANCE          RVNORM(1,20,0.1) (suction pipe is disconnected from the hopper)
       BLET            &CUP1=3.5/FN(CONT2) (time for loading system to travel to first empty container)
      BPUTPIC          FILE=MYFILE,LINES=3,AC1,XID1,XID1,&CUP1
TIME *.****
PLACE M* ON P1A
SET M* TRAVEL *.****
```

```
      ADVANCE     &CUP1 (loading system travels to position of first empty container 3.5 m from loading point)
      BLET                &OFFLOAD=RVNORM(1,5,0.1)
      BPUTPIC             FILE=MYFILE,LINES=3,AC1,XID1,XID1,&OFFLOAD
TIME *.****
PLACE R* ON C1
SET R* TRAVEL *.****
      ADVANCE             &OFFLOAD (material is offloaded into the container)
      BPUTPIC             FILE=MYFILE,LINES=5,AC1,XID1
TIME *.****
DESTROY R*
SET CE1 CLASS CONT1F
PLACE CF1 ON CC1
DESTROY CE1
      BLET                &LOADS=&LOADS+4 (total tonnes loaded)
      BPUTPIC             FILE=MYFILE,LINES=3,AC1,AC1,&LOADS
TIME *.****
WRITE M1 ***.**
WRITE M2 ***.**
      BLET                &DRILL=AC1/&DR (number of holes drilled at this time)
      BPUTPIC             FILE=MYFILE,LINES=3,AC1,&DRILL,AC1
TIME *.****
WRITE M4 ***.**
WRITE M8 ***.**
      BLET                &CDN1=3.5/FN(CONT1) (time for loading system to travel back to loading point)
      BPUTPIC             FILE=MYFILE,LINES=3,AC1,XID1,XID1,&CDN1
TIME *.****
PLACE M* ON P1B
SET M* TRAVEL *.****
      ADVANCE             &CDN1 (loading system travels back to loading point)
      BPUTPIC             FILE=MYFILE,LINES=1,AC1
TIME *.****
      ADVANCE             RVNORM(1,20,0.1) (suction pipe is reconnected to the hopper)
      BPUTPIC             FILE=MYFILE,LINES=4,AC1,XID1,XID1,XID1
TIME *.****
CREATE HOPPER HP*
SET M* CLASS MONO1
DESTROY HP*
      BLET                &LOAD=600 (loading/suction time of material in the hopper)
      BPUTPIC             FILE=MYFILE,LINES=5,AC1,XID1,XID1,XID1,XID1,&LOAD
TIME *.****
CREATE ROCK R*
CREATE ROCK1 RH*
PLACE RH* ON EH
SET RH* TRAVEL *.****
      ADVANCE             &LOAD (material is loaded into the hopper)
      BPUTPIC             FILE=MYFILE,LINES=2,AC1,XID1
TIME *.****
DESTROY RH*
      BPUTPIC             FILE=MYFILE,LINES=1,AC1
TIME *.****
      ADVANCE             RVNORM(1,20,0.1) (suction pipe is disconnected from the hopper)
      BLET                &CUP2=7/FN(CONT2) (time for loading system to travel to second empty container)
      BPUTPIC             FILE=MYFILE,LINES=3,AC1,XID1,XID1,&CUP2
TIME *.****
PLACE M* ON P2A
SET M* TRAVEL *.****
      ADVANCE             &CUP2 (loading system travels to position of second empty container 7m from loading point)
      BLET                &OFFLOAD=RVNORM(1,5,0.1)
      BPUTPIC             FILE=MYFILE,LINES=3,AC1,XID1,XID1,&OFFLOAD
```

```
TIME *.****
PLACE R* ON C2
SET R* TRAVEL *.****
      ADVANCE          &OFFLOAD (material is offloaded into the container)
      BPUTPIC          FILE=MYFILE,LINES=5,AC1,XID1
TIME *.****
DESTROY R*
SET CE2 CLASS CONT2F
PLACE CF2 ON CC2
DESTROY CE2
      BLET             &LOADS=&LOADS+4 (total tonnes loaded)
      BPUTPIC          FILE=MYFILE,LINES=3,AC1,AC1,&LOADS
TIME *.****
WRITE M1 ***.**
WRITE M2 ***.**
      BLET             &DRILL=AC1/&DR (number of holes drilled at this time)
      BPUTPIC          FILE=MYFILE,LINES=3,AC1,&DRILL,AC1
TIME *.****
WRITE M4 ***.**
WRITE M8 ***.**
       BLET            &CDN2=7/FN(CONT1) (time for loading system to travel back to loading position)
      BPUTPIC          FILE=MYFILE,LINES=3,AC1,XID1,XID1,&CDN2
TIME *.****
PLACE M* ON P2B
SET M* TRAVEL *.****
      ADVANCE          &CDN2  (loading system travels back to loading point)
      BPUTPIC          FILE=MYFILE,LINES=1,AC1
TIME *.****
      ADVANCE          RVNORM(1,20,0.1) (suction pipe is reconnected to the hopper)
      BPUTPIC          FILE=MYFILE,LINES=4,AC1
TIME *.****
CREATE HOPPER HP*
SET M* CLASS MONO1
DESTROY HP*
      BLET             &LOAD=600 (loading/suction time of material in the hopper)
      BPUTPIC          FILE=MYFILE,LINES=5,AC1,XID1,XID1,XID1,XID1,&LOAD
TIME *.****
CREATE ROCK R*
CREATE ROCK1 RH*
PLACE RH* ON EH
SET RH* TRAVEL *.****
      ADVANCE          &LOAD (material is loaded into the hopper)
      BPUTPIC          FILE=MYFILE,LINES=2,AC1,XID1
TIME *.****
DESTROY RH*
      BPUTPIC          FILE=MYFILE,LINES=1,AC1
TIME *.****
       ADVANCE         RVNORM(1,20,0.1) (suction pipe is disconnected from the hopper)
      BLET             &CUP3=10.5/FN(CONT2) (time for loading system to travel to third empty container)
      BPUTPIC    FILE=MYFILE,LINES=3,AC1,XID1,XID1,&CUP3
TIME *.****
PLACE M* ON P3A
SET M* TRAVEL *.****
      ADVANCE          &CUP3 (loading system travels to position of third empty container 10.5m from loading point)
      BLET             &OFFLOAD=RVNORM(1,5,0.1)
      BPUTPIC          FILE=MYFILE,LINES=3,AC1,XID1,XID1,&OFFLOAD
TIME *.****
PLACE R* ON C3
SET R* TRAVEL *.****
```

```
      ADVANCE          &OFFLOAD (material is offloaded into the container)
      BPUTPIC          FILE=MYFILE,LINES=5,AC1,XID1
TIME *.****
DESTROY R*
SET CE3 CLASS CONT3F
PLACE CF3 ON CC3
DESTROY CE3
      BLET             &LOADS=&LOADS+4 (total tonnes loaded)
      BPUTPIC          FILE=MYFILE,LINES=3,AC1,AC1,&LOADS
TIME *.****
WRITE M1 ***.**
WRITE M2 ***.**
      BLET             &DRILL=AC1/&DR (number of holes drilled at this time)
      BPUTPIC          FILE=MYFILE,LINES=3,AC1,&DRILL,AC1
TIME *.****
WRITE M4 ***.**
WRITE M8 ***.**
      BLET             &CDN3=10.5/FN(CONT1) (time for loading system to travel back to loading position)
      BPUTPIC          FILE=MYFILE,LINES=3,AC1,XID1,XID1,&CDN3
TIME *.****
PLACE M* ON P3B
SET M* TRAVEL *.****
      ADVANCE          &CDN3 (loading system travels back to loading point)
      BPUTPIC          FILE=MYFILE,LINES=1,AC1
TIME *.****
      ADVANCE          RVNORM(1,20,0.1) (suction pipe is reconnected to the hopper)
      BPUTPIC          FILE=MYFILE,LINES=4,AC1,XID1,XID1,XID1
TIME *.****
CREATE HOPPER HP*
SET M* CLASS MONO1
DESTROY HP*
      BLET             &LOAD=600 (loading/suction time of material in the hopper)
      BPUTPIC          FILE=MYFILE,LINES=5,AC1,XID1,XID1,XID1,XID1,&LOAD
TIME *.****
CREATE ROCK R*
CREATE ROCK1 RH*
PLACE RH* ON EH
SET RH* TRAVEL *.****
      ADVANCE          &LOAD (material is loaded into the hopper)
      BPUTPIC          FILE=MYFILE,LINES=2,AC1,XID1
TIME *.****
DESTROY RH*
      BPUTPIC          FILE=MYFILE,LINES=1,AC1
TIME *.****
      ADVANCE          RVNORM(1,20,0.1) (suction pipe is disconnected from the hopper)
       BLET            &CUP4=14/FN(CONT2) (time for loading system to travel to fourth empty container)
      BPUTPIC          FILE=MYFILE,LINES=3,AC1,XID1,XID1,&CUP4
TIME *.****
PLACE M* ON P4A
SET M* TRAVEL *.****
      ADVANCE          &CUP4 (loading system travels to position of fourth empty container 14m from loading point)
      BLET             &OFFLOAD=RVNORM(1,5,0.1)
      BPUTPIC          FILE=MYFILE,LINES=3,AC1,XID1,XID1,&OFFLOAD
TIME *.****
PLACE R* ON C4
SET R* TRAVEL *.****
      ADVANCE          &OFFLOAD (material is offloaded into the container)
      BPUTPIC          FILE=MYFILE,LINES=5,AC1,XID1,XID1,XID1,XID1
TIME *.****
```

```
DESTROY R*
SET CE4 CLASS CONT4F
PLACE CF4 ON CC4
DESTROY CE4
      BLET              &LOADS=&LOADS+4 (total tonnes loaded)
      BPUTPIC           FILE=MYFILE,LINES=3,AC1,AC1,&LOADS
TIME *.****
WRITE M1 ***.**
WRITE M2 ***.**
      BLET              &DRILL=AC1/&DR  (number of holes drilled at this time)
      BPUTPIC           FILE=MYFILE,LINES=3,AC1,&DRILL,AC1
TIME *.****
WRITE M4 ***.**
WRITE M8 ***.**
      BLET              &CDN4=14/FN(CONT1) (time for the loading system to travel back to loading position)
      BPUTPIC           FILE=MYFILE,LINES=3,AC1,XID1,XID1,&CDN4
TIME *.****
PLACE M* ON P4B
SET M* TRAVEL *.****
      ADVANCE           &CDN4 (loading system travels back to loading point)
      BPUTPIC           FILE=MYFILE,LINES=1,AC1
TIME *.****
      ADVANCE           RVNORM(1,20,0.1) (suction pipe is reconnected to the hopper)
      BPUTPIC           FILE=MYFILE,LINES=4,AC1,XID1,XID1,XID1
TIME *.****
CREATE HOPPER HP*
SET M* CLASS MONO1
DESTROY HP*
      BLET              &LOAD=600 (loading/suction time of material in the hopper)
      BPUTPIC           FILE=MYFILE,LINES=5,AC1,XID1,XID1,XID1,XID1,&LOAD
TIME *.****
CREATE ROCK R*
CREATE ROCK1 RH*
PLACE RH* ON EH
SET RH* TRAVEL *.****
      ADVANCE           &LOAD (material is loaded into the hopper)
      BPUTPIC           FILE=MYFILE,LINES=2,AC1,XID1
TIME *.****
DESTROY RH*
      BPUTPIC           FILE=MYFILE,LINES=1,AC1
TIME *.****
      ADVANCE           RVNORM(1,20,0.1) (suction pipe is disconnected from the hopper)
      BLET              &CUP5=17.5/FN(CONT2) (time for loading system to travel to fifth empty container)
      BPUTPIC           FILE=MYFILE,LINES=3,AC1,XID1,XID1,&CUP5
TIME *.****
PLACE M* ON P5A
SET M* TRAVEL *.****
      ADVANCE           &CUP5 (loading system travels to position of fifth empty container 17.5m from loading point)
      BLET              &OFFLOAD=RVNORM(1,5,0.1)
      BPUTPIC           FILE=MYFILE,LINES=3,AC1,XID1,XID1,&OFFLOAD
TIME *.****
PLACE R* ON C5
SET R* TRAVEL *.****
      ADVANCE           &OFFLOAD (material is offloaded into the container)
      BPUTPIC           FILE=MYFILE,LINES=5,AC1,XID1,XID1,XID1,XID1
TIME *.****
DESTROY R*
SET CE5 CLASS CONT5F
PLACE CF5 ON CC5
```

```
DESTROY CE5
      BLET              &LOADS=&LOADS+4 (total tonnes loaded)
      BPUTPIC           FILE=MYFILE,LINES=4,AC1,AC1,&LOADS,AC1
TIME *.****
WRITE M1 ***.**
WRITE M2 ***.**
      BLET              &DRILL=AC1/&DR (number of holes drilled at this time)
      BPUTPIC           FILE=MYFILE,LINES=3,AC1,&DRILL,AC1
TIME *.****
WRITE M4 ***.**
WRITE M8 ***.**
      BLET              &CDN5=17.5/FN(CONT1) (time for loading system to travel back to loading position)
      BPUTPIC           FILE=MYFILE,LINES=3,AC1,XID1,XID1,&CDN5
TIME *.****
PLACE M* ON P5B
SET M* TRAVEL *.****
      ADVANCE           &CDN5 (loading system travels back to loading point)
      BPUTPIC           FILE=MYFILE,LINES=1,AC1
TIME *.****
      ADVANCE           RVNORM(1,20,0.1) (suction pipe is reconnected to the hopper)
      BPUTPIC           FILE=MYFILE,LINES=4,AC1,XID1,XID1,XID1
TIME *.****
CREATE HOPPER HP*
SET M* CLASS MONO1
DESTROY HP*
      BLET              &LOAD=600 (loading/suction time of material in the hopper)
      BPUTPIC           FILE=MYFILE,LINES=5,AC1,XID1,XID1,XID1,XID1,&LOAD
TIME *.****
CREATE ROCK R*
CREATE ROCK1 RH*
PLACE RH* ON EH
SET RH* TRAVEL *.****
      ADVANCE           &LOAD (material is loaded into the hopper)
      BPUTPIC           FILE=MYFILE,LINES=2,AC1,XID1
TIME *.****
DESTROY RH*
      BPUTPIC           FILE=MYFILE,LINES=1,AC1
TIME *.****
      ADVANCE           RVNORM(1,20,0.1) (suction pipe is disconnected from the hopper)
      BLET              &CUP6=21/FN(CONT2) (time for loading system to travel to sixth empty container)
      BPUTPIC           FILE=MYFILE,LINES=3,AC1,XID1,XID1,&CUP6
TIME *.****
PLACE M* ON P6A
SET M* TRAVEL *.****
       ADVANCE          &CUP6 (loading system travels to position of sixth empty container 21m from loading point)
      BLET              &OFFLOAD=RVNORM(1,5,0.1)
      BPUTPIC           FILE=MYFILE,LINES=3,AC1,XID1,XID1,&OFFLOAD
TIME *.****
PLACE R* ON C6
SET R* TRAVEL *.****
      ADVANCE           &OFFLOAD (material is offloaded into the container)
      BPUTPIC           FILE=MYFILE,LINES=5,AC1,XID1,XID1,XID1,XID1
TIME *.****
DESTROY R*
SET CE6 CLASS CONT6F
PLACE CF6 ON CC6
DESTROY CE6
      BLET              &T=140
      BLET              &LOADS=&LOADS+4 (total tonnes loaded)
```

```
      BPUTPIC          FILE=MYFILE,LINES=4,AC1,AC1,&LOADS
TIME *.****
WRITE M1 ***.**
WRITE M2 ***.**
      TEST L           &LOADS,&T,DOWN (are total tonnes loaded equal to 140 tonnes?)
      BLET             &DRILL=AC1/&DR (number of holes drilled at this time)
      BPUTPIC          FILE=MYFILE,LINES=3,AC1,&DRILL,AC1
TIME *.****
WRITE M4 ***.**
WRITE M8 ***.**
      BLET             &CDN6=21/FN(CONT1) (time for loading system to travel back to loading position)
      BPUTPIC          FILE=MYFILE,LINES=3,AC1,XID1,XID1,&CDN6
TIME *.****
PLACE M* ON P6B
SET M* TRAVEL *.****
      ADVANCE          &CDN6 (loading system travels back to loading point)
      BPUTPIC          FILE=MYFILE,LINES=1,AC1
TIME *.****
      ADVANCE          RVNORM(1,20,0.1) (hopper is disconnected from monorail train)
       BLET            &CUPL1=30/FN(CONT2) (time for loading system to travel to container lifting position)
      BPUTPIC          FILE=MYFILE,LINES=6,AC1,XID1,XID1,XID1,XID1,XID1,&CUPL1
TIME *.****
PLACE M* ON PL
CREATE HOPPER HP*
SET M* CLASS TRAIN
PLACE HP* AT 22 30
SET M* TRAVEL *.****
      ADVANCE          &CUPL1 (loading system travels to container lifting position 30m from loading point)
UPTOP  BPUTPIC         FILE=MYFILE,LINES=3,AC1,XID1,XID1
TIME *.****
PLACE M* AT 67.74 50.36 (container lifting position)
      BPUTPIC          FILE=MYFILE,LINES=1,AC1
TIME *.****
       ADVANCE         RVNORM(1,8,0.1) (loading system waits for the chains to be connected to containers)
      BLET             &LIFT=RVNORM(1,10,0.5)
      BPUTPIC          FILE=MYFILE,LINES=7,AC1,&LIFT,&LIFT,&LIFT,&LIFT,&LIFT,&LIFT
TIME *.****
SET CF1 TRAVEL *.****
SET CF2 TRAVEL *.****
SET CF3 TRAVEL *.****
SET CF4 TRAVEL *.****
SET CF5 TRAVEL *.****
SET CF6 TRAVEL *.****
      ADVANCE          &LIFT (loaded containers are lifted by the monorail train)
      BPUTPIC          FILE=MYFILE,LINES=7,AC1,XID1
TIME *.****
DESTROY CF1
DESTROY CF2
DESTROY CF3
DESTROY CF4
DESTROY CF5
DESTROY CF6
      BLET             &CUPS1=2000/FN(CONT2) (time for loading system to travel to surface for material dumping)
      BPUTPIC          FILE=MYFILE,LINES=3,AC1,XID1,XID1,&CUPS1
TIME *.****
PLACE M* ON PZ
SET M* TRAVEL &CUPS1
      ADVANCE          &CUPS1 (loaded containers are transported to surface for dumping)
      BPUTPIC          FILE=MYFILE,LINES=2,AC1,XID1
TIME *.****
```

```
PLACE M* AT 419.78 150.04 (monorail dumping position on surface)
      BLET              &DUMP=RVNORM(1,120,30)
      BPUTPIC           FILE=MYFILE,LINES=4,AC1,XID1,XID1,XID1,&DUMP
TIME *.****
CREATE ROCK R*
PLACE R* ON PD1
SET R* TRAVEL *.****
      ADVANCE           &DUMP (material is dumped on suface)
      BPUTPIC           FILE=MYFILE,LINES=2,AC1,XID1
TIME *.****
DESTROY R*
      BLET              &CDNS1=2000/FN(CONT1) (time for loading system to travel back
underground)
      BPUTPIC           FILE=MYFILE,LINES=3,AC1,XID1,XID1,&CDNS1
TIME *.****
PLACE M* ON PZ1
SET M* TRAVEL &CDNS1
      ADVANCE           &CDNS1 (monorail returns underground)
      BPUTPIC           FILE=MYFILE,LINES=2,AC1,XID1
TIME *.****
PLACE M* AT 67.74 50.36 (empty container lowering position)
      BPUTPIC           FILE=MYFILE,LINES=13,AC1
TIME *.****
CREATE CONT1E CE1
CREATE CONT2E CE2
CREATE CONT3E CE3
CREATE CONT4E CE4
CREATE CONT5E CE5
CREATE CONT6E CE6
CREATE CONT1F CF1
CREATE CONT2F CF2
CREATE CONT3F CF3
CREATE CONT4F CF4
CREATE CONT5F CF5
CREATE CONT6F CF6
      BPUTPIC           FILE=MYFILE,LINES=7,AC1
TIME *.****
PLACE CE1 ON C1
PLACE CE2 ON C2
PLACE CE3 ON C3
PLACE CE4 ON C4
PLACE CE5 ON C5
PLACE CE6 ON C6
      ADVANCE           RVNORM(1,5,0.1)
      BPUTPIC           FILE=MYFILE,LINES=7,AC1,&CDOWN,&CDOWN,&CDOWN,&CDOWN,&CDOWN,&CDOWN
TIME *.****
SET CE1 TRAVEL *.****
SET CE2 TRAVEL *.****
SET CE3 TRAVEL *.****
SET CE4 TRAVEL *.****
SET CE5 TRAVEL *.****
SET CE6 TRAVEL *.****
      ADVANCE           &CDOWN (monorail loading system lowers empty containers)
      BPUTPIC           FILE=MYFILE,LINES=1,AC1
TIME *.****
      ADVANCE           RVNORM(1,8,0.1) (chains are disconnected from empty containers)
      BLET              &CDNF=30/FN(CONT1) (time for loading system to travel to loading position)
      BPUTPIC           FILE=MYFILE,LINES=3,AC1,XID1,XID1,&CDNF
TIME *.****
```

```
PLACE M* ON PH
SET M* TRAVEL *.****
      ADVANCE          &CDNF (monorail loading system travels to the loading point 30m from waiting point)
      BPUTPIC          FILE=MYFILE,LINES=1,AC1
TIME *.****
      ADVANCE          RVNORM(1,20,0.1) (hopper is reconnected to the monorail loading system)
      BPUTPIC          FILE=MYFILE,LINES=3,AC1,XID1,XID1
TIME *.****
SET M* CLASS MONO1
DESTROY HP*
      BLET             &LOAD=600 (loading/suction time of material in the hopper)
      BPUTPIC          FILE=MYFILE,LINES=5,AC1,XID1,XID1,XID1,XID1,&LOAD
TIME *.****
CREATE ROCK R*
CREATE ROCK1 RH*
PLACE RH* ON EH
SET RH* TRAVEL *.****
      ADVANCE          &LOAD (loading of material into the hopper completed)
      BPUTPIC          FILE=MYFILE,LINES=2,AC1,XID1
TIME *.****
DESTROY RH*
      BPUTPIC          FILE=MYFILE,LINES=1,AC1
TIME *.****
      ADVANCE          RVNORM(1,20,0.1) (suction pipe is disconnected from the hopper)
      BLET             &CUP1A=3.5/FN(CONT2) (time for loading system to travel to first empty container)
      BPUTPIC          FILE=MYFILE,LINES=3,AC1,XID1,XID1,&CUP1A
TIME *.****
PLACE M* ON P1A
SET M* TRAVEL *.****
      ADVANCE          &CUP1A (loading system travels to position of first empty container 3.5m from loading point)
      BLET             &OFFLOAD=RVNORM(1,5,0.1)
      BPUTPIC          FILE=MYFILE,LINES=3,AC1,XID1,XID1,&OFFLOAD
TIME *.****
PLACE R* ON C1
SET R* TRAVEL *.****
      ADVANCE          &OFFLOAD (material is offloaded into the container)
      BPUTPIC          FILE=MYFILE,LINES=5,AC1,XID1,XID1,XID1,XID1
TIME *.****
DESTROY R*
SET CE1 CLASS CONT1F
PLACE CF1 ON CC1
DESTROY CE1
      BLET             &LOADS=&LOADS+4 (total tonnes loaded)
      BPUTPIC          FILE=MYFILE,LINES=3,AC1,AC1,&LOADS
TIME *.****
WRITE M1 ***.**
WRITE M2 ***.**
      BLET             &DRILL=AC1/&DR (number of holes drilled at this time)
      BPUTPIC          FILE=MYFILE,LINES=3,AC1,&DRILL,AC1
TIME *.****
WRITE M4 ***.**
WRITE M8 ***.**
      BLET             &CDN1A=3.5/FN(CONT1) (time for loading system to travel back to loading point)
      BPUTPIC          FILE=MYFILE,LINES=3,AC1,XID1,XID1,&CDN1A
TIME *.****
PLACE M* ON P1B
SET M* TRAVEL *.****
      ADVANCE          &CDN1A (loading system travels back to loading point)
      BPUTPIC          FILE=MYFILE,LINES=1,AC1
TIME *.****
```

```
      ADVANCE          RVNORM(1,20,0.1) (suction pipe is reconnected to the hopper)
      BLET             &LOAD=600 (loading/suction time of material in the hopper)
      BPUTPIC          FILE=MYFILE,LINES=5,AC1,XID1,XID1,XID1,XID1,&LOAD
TIME *.****
CREATE ROCK R*
CREATE ROCK1 RH*
PLACE RH* ON EH
SET RH* TRAVEL *.****
      ADVANCE          &LOAD (material is loaded into the hopper)
      BPUTPIC          FILE=MYFILE,LINES=2,AC1,XID1
TIME *.****
DESTROY RH*
      BPUTPIC          FILE=MYFILE,LINES=1,AC1
TIME *.****
      ADVANCE          RVNORM(1,20,0.1) (suction pipe is disconnected from the hopper)
      BLET             &CUP2A=7/FN(CONT2) (time for loading system to travel to second empty container)
      BPUTPIC          FILE=MYFILE,LINES=3,AC1,XID1,XID1,&CUP2A
TIME *.****
PLACE M* ON P2A
SET M* TRAVEL *.****
      ADVANCE          &CUP2A (loading system travels to position of second empty container 7m from loading point)
      BLET             &OFFLOAD=RVNORM(1,5,0.1)
      BPUTPIC          FILE=MYFILE,LINES=3,AC1,XID1,XID1,&OFFLOAD
TIME *.****
PLACE R* ON C2
SET R* TRAVEL *.****
      ADVANCE          &OFFLOAD (material is offloaded into the container)
      BPUTPIC          FILE=MYFILE,LINES=5,AC1,XID1,XID1,XID1,XID1
TIME *.****
DESTROY R*
SET CE2 CLASS CONT2F
PLACE CF2 ON CC2
DESTROY CE2
      BLET             &LOADS=&LOADS+4 (total tonnes loaded)
      BPUTPIC          FILE=MYFILE,LINES=3,AC1,AC1,&LOADS,AC1
TIME *.****
WRITE M1 ***.**
WRITE M2 ***.**
      BLET             &DRILL=AC1/&DR (number of holes drilled at this time)
      BPUTPIC          FILE=MYFILE,LINES=3,AC1,&DRILL,AC1
TIME *.****
WRITE M4 ***.**
WRITE M8 ***.**
      BLET             &CDN2A=7/FN(CONT1) (time for the loading system to travel back to loading position)
      BPUTPIC          FILE=MYFILE,LINES=3,AC1,XID1,XID1,&CDN2A
TIME *.****
PLACE M* ON P2B
SET M* TRAVEL *.****
      ADVANCE          &CDN2A (loading system travels back to loading point)
      BPUTPIC          FILE=MYFILE,LINES=1,AC1
TIME *.****
      ADVANCE          RVNORM(1,20,0.1) (suction pipe is reconnected to the hopper)
      BPUTPIC          FILE=MYFILE,LINES=4,AC1,XID1,XID1,XID1
TIME *.****
CREATE HOPPER HP*
SET M* CLASS MONO1
DESTROY HP*
      BLET             &LOAD=600 (loading/suction time of material in the hopper)
      BPUTPIC          FILE=MYFILE,LINES=5,AC1,XID1,XID1,XID1,XID1,&LOAD
```

```
TIME *.****
CREATE ROCK R*
CREATE ROCK1 RH*
PLACE RH* ON EH
SET RH* TRAVEL *.****
      ADVANCE          &LOAD (material is loaded into the hopper)
      BPUTPIC          FILE=MYFILE,LINES=2,AC1,XID1
TIME *.****
DESTROY RH*
      BPUTPIC    FILE=MYFILE,LINES=1,AC1
TIME *.****
      ADVANCE          RVNORM(1,20,0.1) (suction pipe is disconnected from the hopper)
      BLET             &CUP3A=10.5/FN(CONT2) (time for loading system to travel to third empty container)
      BPUTPIC          FILE=MYFILE,LINES=3,AC1,XID1,XID1,&CUP3A
TIME *.****
PLACE M* ON P3A
SET M* TRAVEL *.****
      ADVANCE          &CUP3A (loading system travels to position of third empty container 10.5m from loading point)
      BLET             &OFFLOAD=RVNORM(1,5,0.1)
      BPUTPIC          FILE=MYFILE,LINES=3,AC1,XID1,XID1,&OFFLOAD
TIME *.****
PLACE R* ON C3
SET R* TRAVEL *.****
      ADVANCE          &OFFLOAD (material is offloaded into the container)
      BPUTPIC          FILE=MYFILE,LINES=5,AC1,XID1,XID1,XID1,XID1
TIME *.****
DESTROY R*
SET CE3 CLASS CONT3F
PLACE CF3 ON CC3
DESTROY CE3
      BLET             &LOADS=&LOADS+4 (total tonnes loaded)
      BPUTPIC          FILE=MYFILE,LINES=3,AC1,AC1,&LOADS
TIME *.****
WRITE M1 ***.**
WRITE M2 ***.**
      BLET             &DRILL=AC1/&DR (number of holes drilled at this time)
      BPUTPIC          FILE=MYFILE,LINES=3,AC1,&DRILL,AC1
TIME *.****
WRITE M4 ***.**
WRITE M8 ***.**
      BLET             &CDN3A=10.5/FN(CONT1) (time for the loading system to travel to loading position)
      BPUTPIC          FILE=MYFILE,LINES=3,AC1,XID1,XID1,&CDN3A
TIME *.****
PLACE M* ON P3B
SET M* TRAVEL *.****
      ADVANCE          &CDN3A (loading system travels back to loading point)
      BPUTPIC          FILE=MYFILE,LINES=1,AC1
TIME *.****
      ADVANCE          RVNORM(1,20,0.1) (suction pipe is reconnected to the hopper)
      BPUTPIC          FILE=MYFILE,LINES=4,AC1,XID1,XID1,XID1
TIME *.****
CREATE HOPPER HP*
SET M* CLASS MONO1
DESTROY HP*
      BLET             &LOAD=600 (loading/suction time of material in the hopper)
      BPUTPIC          FILE=MYFILE,LINES=5,AC1,XID1,XID1,XID1,XID1,&LOAD
TIME *.****
CREATE ROCK R*
CREATE ROCK1 RH*
```

```
PLACE RH* ON EH
SET RH* TRAVEL *.****
      ADVANCE          &LOAD (material is loaded into the hopper)
      BPUTPIC          FILE=MYFILE,LINES=2,AC1,XID1
TIME *.****
DESTROY RH*
      BPUTPIC          FILE=MYFILE,LINES=1,AC1
TIME *.****
      ADVANCE          RVNORM(1,20,0.1) (suction pipe is disconnected from the hopper)
      BLET             &CUP4A=14/FN(CONT2) (time for loading system to travel to fourth empty container)
      BPUTPIC          FILE=MYFILE,LINES=3,AC1,XID1,XID1,&CUP4A
TIME *.****
PLACE M* ON P4A
SET M* TRAVEL *.****
      ADVANCE          &CUP4A (loading system travels to position of fourth empty container 14m from loading point)
      BLET             &OFFLOAD=RVNORM(1,5,0.1)
      BPUTPIC          FILE=MYFILE,LINES=3,AC1,XID1,XID1,&OFFLOAD
TIME *.****
PLACE R* ON C4
SET R* TRAVEL *.****
      ADVANCE          &OFFLOAD (material is offloaded into the container)
      BPUTPIC          FILE=MYFILE,LINES=5,AC1,XID1,XID1,XID1,XID1
TIME *.****
DESTROY R*
SET CE4 CLASS CONT4F
PLACE CF4 ON CC4
DESTROY CE4
      BLET             &LOADS=&LOADS+4 (total tonnes loaded)
      BPUTPIC          FILE=MYFILE,LINES=4,AC1,AC1,&LOADS
TIME *.****
WRITE M1 ***.**
WRITE M2 ***.**
      BLET             &DRILL=AC1/&DR (number of holes drilled at this time)
      BPUTPIC          FILE=MYFILE,LINES=3,AC1,&DRILL,AC1
TIME *.****
WRITE M4 ***.**
WRITE M8 ***.**
      BLET             &CDN4A=14/FN(CONT1) (time for loading system to travel back to loading position)
      BPUTPIC          FILE=MYFILE,LINES=3,AC1,XID1,XID1,&CDN4A
TIME *.****
PLACE M* ON P4B
SET M* TRAVEL *.****
      ADVANCE          &CDN4A (loading system travels back to loading point)
      BPUTPIC          FILE=MYFILE,LINES=1,AC1
TIME *.****
      ADVANCE          RVNORM(1,20,0.1) (suction pipe is reconnected to the hopper)
      BLET             &LOAD=600 (loading/suction time of material in the hopper)
      BPUTPIC          FILE=MYFILE,LINES=5,AC1,XID1,XID1,XID1,XID1,&LOAD
TIME *.****
CREATE ROCK R*
CREATE ROCK1 RH*
PLACE RH* ON EH
SET RH* TRAVEL *.****
      ADVANCE          &LOAD (material is loaded into the hopper)
      BPUTPIC          FILE=MYFILE,LINES=2,AC1,XID1
TIME *.****
DESTROY RH*
      BPUTPIC          FILE=MYFILE,LINES=1,AC1
TIME *.****
```

```
      ADVANCE          RVNORM(1,20,0.1) (suction pipe is disconnected from the hopper)
      BLET             &CUP5A=17.5/FN(CONT2) (time for loading system to travel to fifth empty container)
      BPUTPIC          FILE=MYFILE,LINES=3,AC1,XID1,XID1,&CUP5A
TIME *.****
PLACE M* ON P5A
SET M* TRAVEL *.****
      ADVANCE          &CUP5A (loading system travels to position of fifth empty container 17.5m from loading point)
      BLET             &OFFLOAD=RVNORM(1,5,0.1)
      BPUTPIC          FILE=MYFILE,LINES=3,AC1,XID1,XID1,&OFFLOAD
TIME *.****
PLACE R* ON C5
SET R* TRAVEL *.****
      ADVANCE          &OFFLOAD (material is offloaded into the container)
      BPUTPIC          FILE=MYFILE,LINES=5,AC1,XID1,XID1,XID1,XID1
TIME *.****
DESTROY R*
SET CE5 CLASS CONT5F
PLACE CF5 ON CC5
DESTROY CE5
      BLET             &LOADS=&LOADS+4 (total tonnes loaded)
      BPUTPIC          FILE=MYFILE,LINES=3,AC1,AC1,&LOADS
TIME *.****
WRITE M1 ***.**
WRITE M2 ***.**
      BLET             &DRILL=AC1/&DR (number of holes drilled at this time)
      BPUTPIC          FILE=MYFILE,LINES=3,AC1,&DRILL,AC1
TIME *.****
WRITE M4 ***.**
WRITE M8 ***.**
      BLET             &CDN5A=17.5/FN(CONT1) (time for loading system to travel back to loading position)
      BPUTPIC          FILE=MYFILE,LINES=3,AC1,XID1,XID1,&CDN5A
TIME *.****
PLACE M* ON P5B
SET M* TRAVEL *.****
      ADVANCE          &CDN5A (loading system travels back to loading point)
      BPUTPIC          FILE=MYFILE,LINES=1,AC1
TIME *.****
      ADVANCE          RVNORM(1,20,0.1) (suction pipe is reconnected to the hopper)
      BLET             &LOAD=600 (loading/suction time of material in the hopper)
      BPUTPIC          FILE=MYFILE,LINES=5,AC1,XID1,XID1,XID1,XID1,&LOAD
TIME *.****
CREATE ROCK R*
CREATE ROCK1 RH*
PLACE RH* ON EH
SET RH* TRAVEL *.****
      ADVANCE          &LOAD (material is loaded into the hopper)
      BPUTPIC          FILE=MYFILE,LINES=2,AC1,XID1
TIME *.****
DESTROY RH*
      BPUTPIC          FILE=MYFILE,LINES=1,AC1
TIME *.****
      ADVANCE          RVNORM(1,20,0.1) (suction pipe is disconnected from the hopper)
      BLET             &CUP6A=21/FN(CONT2) (time for loading system to travel to sixth empty container)
      BPUTPIC          FILE=MYFILE,LINES=3,AC1,XID1,XID1,&CUP6A
TIME *.****
PLACE M* ON P6A
SET M* TRAVEL *.****
      ADVANCE          &CUP6A (loading system travels to position of sixth empty container 21m from loading point)
      BLET             &OFFLOAD=RVNORM(1,5,0.1)
      BPUTPIC          FILE=MYFILE,LINES=3,AC1,XID1,XID1,&OFFLOAD
```

```
TIME *.****
PLACE R* ON C6
SET R* TRAVEL *.****
      ADVANCE          &OFFLOAD (material is offloaded into the container)
      BPUTPIC          FILE=MYFILE,LINES=5,AC1,XID1,XID1,XID1,XID1
TIME *.****
DESTROY R*
SET CE6 CLASS CONT6F
PLACE CF6 ON CC6
DESTROY CE6
      BLET             &T=140
      BLET             &LOADS=&LOADS+4 (total tonnes loaded)
      BPUTPIC          FILE=MYFILE,LINES=4,AC1,AC1,&LOADS
TIME *.****
WRITE M1 ***.**
WRITE M2 ***.**
      TEST L           &LOADS,&T,DOWN (are tonnes loaded lest than 140 tonnes)
      BLET             &DRILL=AC1/&DR (number of holes drilled at this time)
      BPUTPIC          FILE=MYFILE,LINES=3,AC1,&DRILL,AC1
TIME *.****
WRITE M4 ***.**
WRITE M8 ***.**
      BLET             &CDN6A=21/FN(CONT1) (time for loading system to travel back to loading position)
      BPUTPIC          FILE=MYFILE,LINES=3,AC1,XID1,XID1,&CDN6A
TIME *.****
PLACE M* ON P6B
SET M* TRAVEL *.****
      ADVANCE          &CDN6A (loading system travels back to loading point)
      BPUTPIC          FILE=MYFILE,LINES=1,AC1
TIME *.****
      ADVANCE          RVNORM(1,20,0.1) (hopper is disconnected from monorail train)
      BLET             &CUPL2=30/FN(CONT2) (time for loading system to travel container lifting position)
      BPUTPIC          FILE=MYFILE,LINES=6,AC1,XID1,XID1,XID1,XID1,XID1,&CUPL2
TIME *.****
PLACE M* ON PL
CREATE HOPPER HP*
SET M* CLASS TRAIN
PLACE HP* AT 22 30
SET M* TRAVEL *.****
      ADVANCE          &CUPL2 (loading system travels to lifting position 30m from loading point)
      TRANSFER         ,UPTOP
DOWN  BPUTPIC          FILE=MYFILE,LINES=6,AC1,AC1,&LOADS,XID1,AC1,AC1
TIME *.****
WRITE M1 ***.**
WRITE M2 ***.**
DESTROY W*
WRITE M5 End Cleaning Completed!
WRITE M8 ***.**
      BPUTPIC          FILE=MYFILE,LINES=2,AC1,XID1
TIME *.****
PLACE M* AT 67.74 50.36 (monorail container lifting position)
      BPUTPIC          FILE=MYFILE,LINES=1,AC1
TIME *.****
      ADVANCE          RVNORM(1,8,0.1) (chains are connected to empty containers)
      BLET             &LIFT=RVNORM(1,10,0.1)
      BPUTPIC          FILE=MYFILE,LINES=7,AC1,&LIFT,&LIFT,&LIFT,&LIFT,&LIFT,&LIFT
TIME *.****
SET CF1 TRAVEL *.****
SET CF2 TRAVEL *.****
```

```
SET CF3 TRAVEL *.****
SET CF4 TRAVEL *.****
SET CF5 TRAVEL *.****
SET CF6 TRAVEL *.****
      ADVANCE          &LIFT (loaded containers are lifted)
      BPUTPIC          FILE=MYFILE,LINES=7,AC1,XID1
TIME *.****
DESTROY CF1
DESTROY CF2
DESTROY CF3
DESTROY CF4
DESTROY CF5
DESTROY CF6
      BLET             &CUPS2=2000/FN(CONT2) (time for loading system to travel to surface for material dumping)
      BPUTPIC          FILE=MYFILE,LINES=3,AC1,XID1,XID1,&CUPS2
TIME *.****
PLACE M* ON PZ
SET M* TRAVEL &CUPS2
      ADVANCE          &CUPS2 (loaded containers are transported to surface for dumping)
      BPUTPIC          FILE=MYFILE,LINES=2,AC1,XID1
TIME *.****
PLACE M* AT 419.78 150.04 (monorail discharge point on surface)
      BLET             &DUMP=RVNORM(1,120,30)
      BPUTPIC          FILE=MYFILE,LINES=4,AC1,XID1,XID1,XID1,&DUMP
TIME *.****
CREATE ROCK R*
PLACE R* ON PD1
SET R* TRAVEL *.****
      ADVANCE          &DUMP (material is dumped on  surface)
      BPUTPIC          FILE=MYFILE,LINES=3,AC1,XID1,XID1
TIME *.****
DESTROY R*
DESTROY M*
      BLET             &DRILL=AC1/&DR (number of holes drilled at this time)
FINISH   BPUTPIC       FILE=MYFILE,LINES=3,AC1,&DRILL,AC1
TIME *.****
WRITE M4 ***.**
WRITE M8 ***.**
      BLET             &NH=86 (total number of holes to be drilled)
      BPUTPIC          FILE=MYFILE,LINES=1,AC1
TIME *.****
      TEST G           &DRILL,&NH,FINISH  (are number of holes drilled greater that 86)
      BPUTPIC          FILE=MYFILE,LINES=3,AC1,&NH,XID1
TIME *.****
WRITE M4 ***.**
WRITE M6 Drilling Completed!
      BPUTPIC          FILE=MYFILE,LINES=2,AC1,XID1
TIME *.****
DESTROY RD*
      BPUTPIC          FILE=MYFILE,LINES=2,AC1,XID1
TIME *.****
SET D* CLASS DRILLF
      BLET             &CUPW1=30/FN(CONT2) (time for drilling system to travel to waiting place)
      BPUTPIC          FILE=MYFILE,LINES=3,AC1,XID1,XID1,&CUPW1
TIME *.****
PLACE D* ON PD
SET D* TRAVEL *.****
      ADVANCE          &CUPW1 (drilling system travels to waiting place 30m from face)
      BPUTPIC          FILE=MYFILE,LINES=2,AC1,XID1
```

```
TIME *.****
DESTROY D*
      BLET              &BLAST=RVNORM(1,5400,600)
      BPUTPIC           FILE=MYFILE,LINES=2,AC1,XID1,&BLAST
TIME *.****
WRITE M11 Charging /Monorail Extension begins
      ADVANCE           &BLAST (blasting finishes)
      BPUTPIC           FILE=MYFILE,LINES=2,AC1,AC1
TIME *.****
WRITE M13 ***.**
      BPUTPIC           FILE=MYFILE,LINES=3,AC1,XID1,XID1
TIME *.****
WRITE M12 Charging /Monorail Extension complete!
END
      TRANSFER          ,HOME
      TERMINATE
      GENERATE          60*60*12*30 (Simulate for 30 days)
      TERMINATE         1
      START             1
      END
```

Appendix 2

SCREEN SHOTS OF COMPUTER SIMULATION PROCESS

Screen shots showing (for each loading time, i.e., the time to load material in the hopper), the total time to clean the development face and the number of tonnes loaded. The time it takes to drill and support the face, the number of holes drilled and the total drill-blast-load-haul cycle time for each loading time is also indicated.

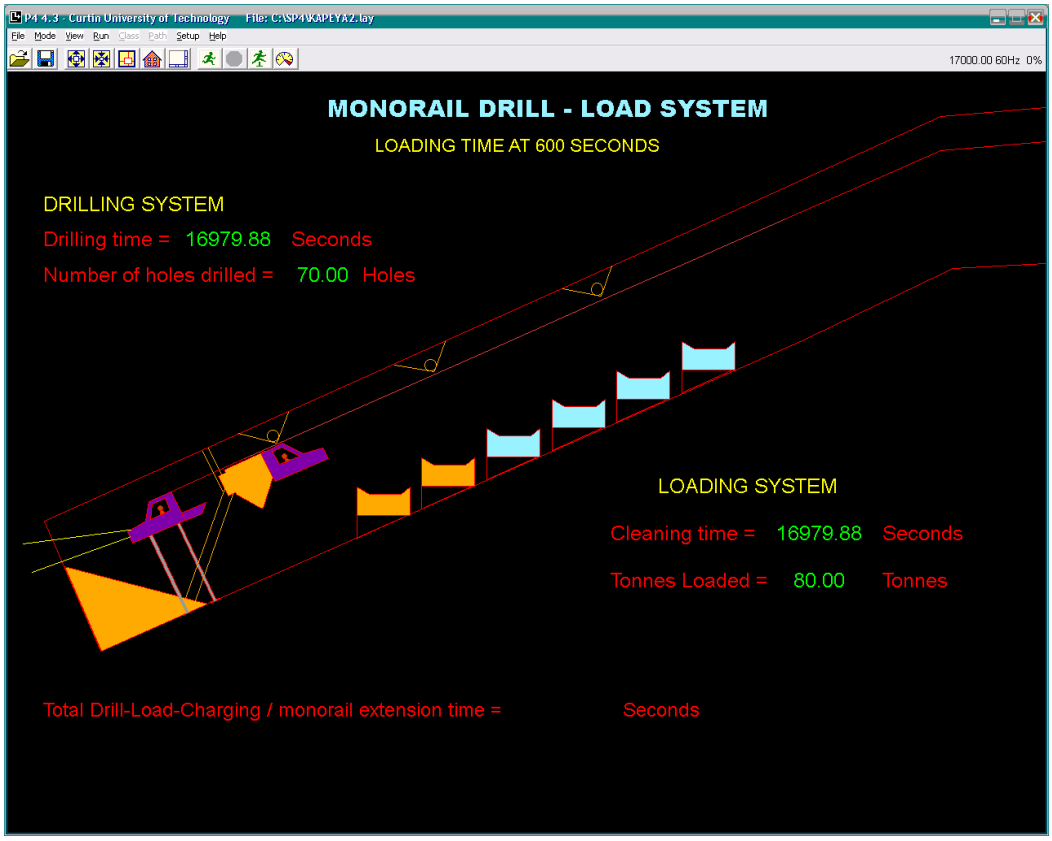

(a)

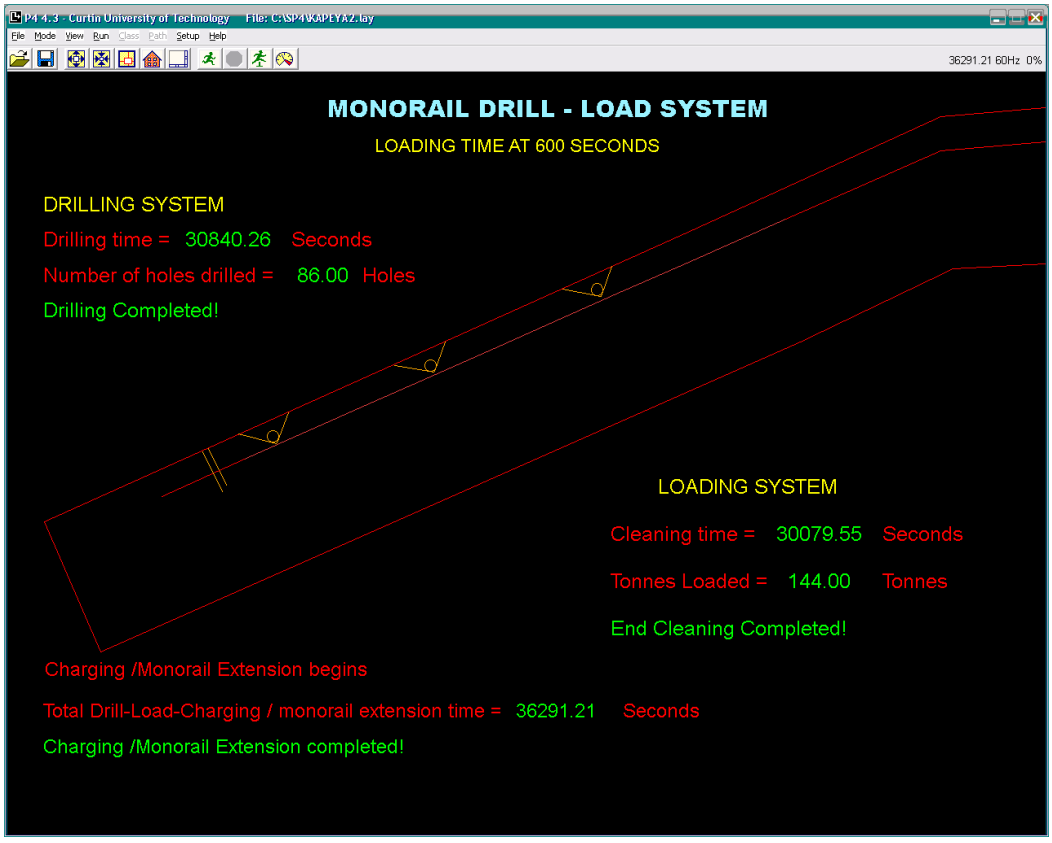

(b)

Figure A1: Loading time 600 sec (a) during loading and drilling (b) after cleaning, drilling and charging

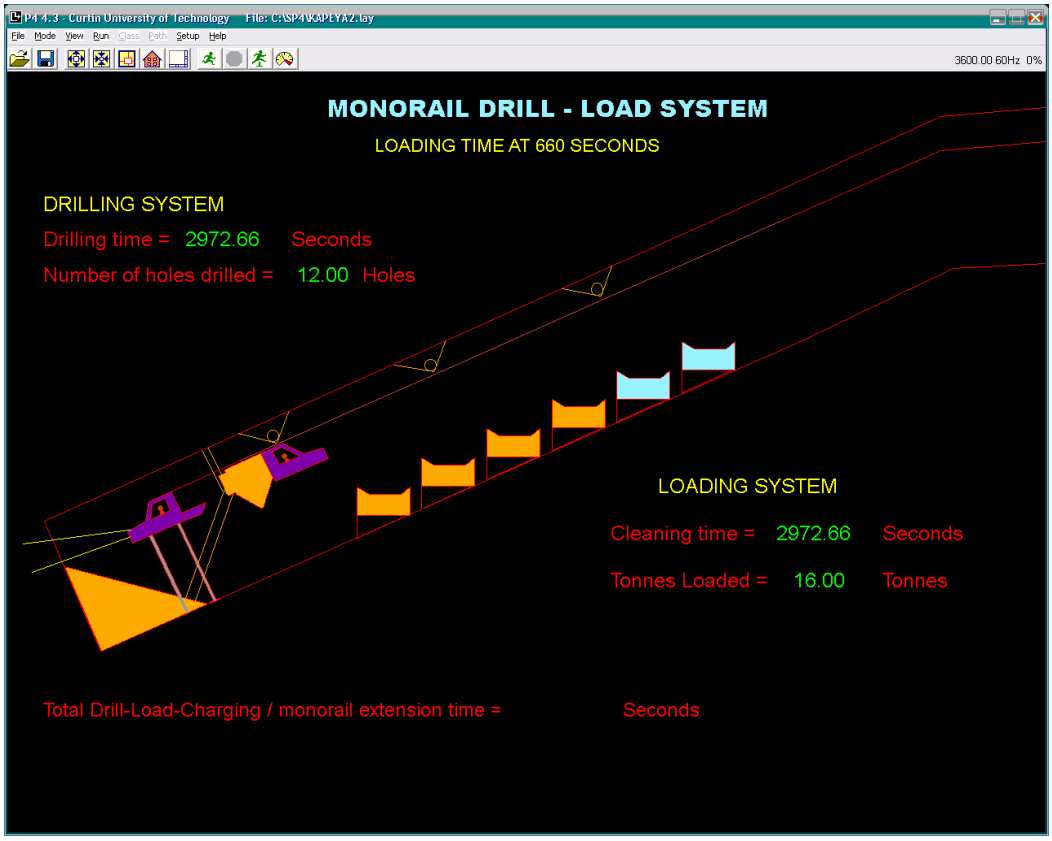

(a)

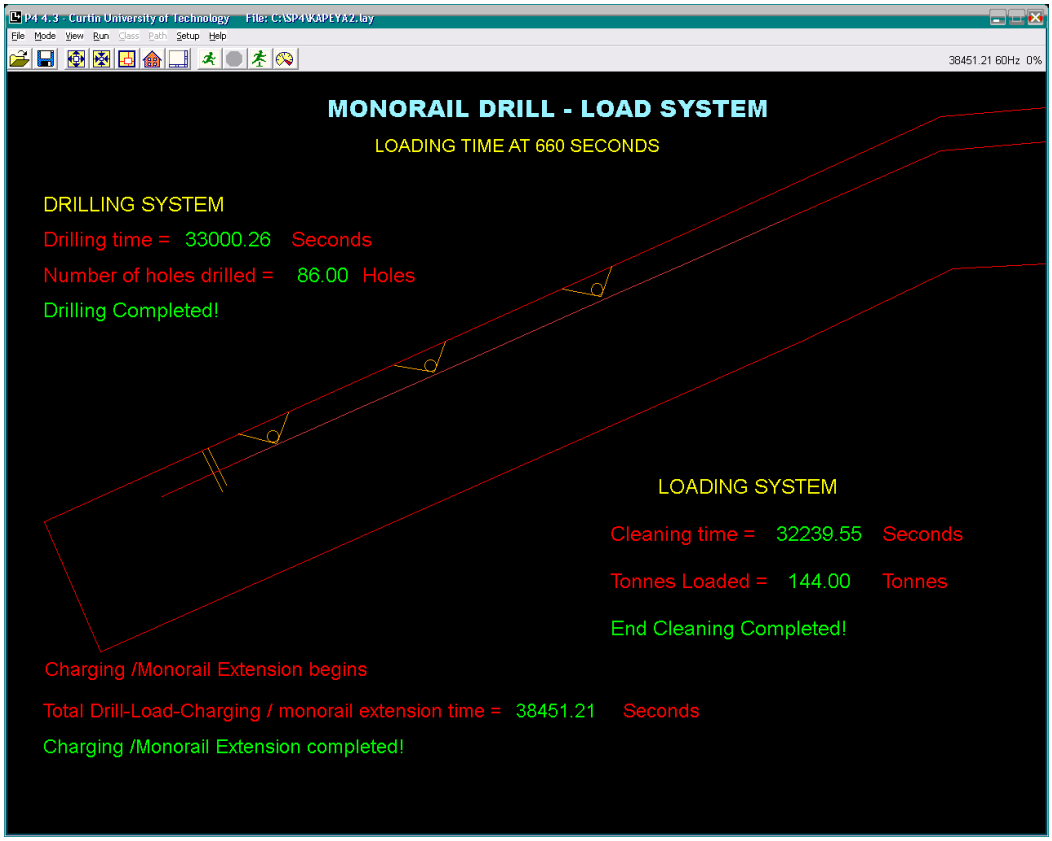

(b)

Figure A2: Loading time 660 sec (a) during face cleaning and drilling (b) after face cleaning, drilling and charging

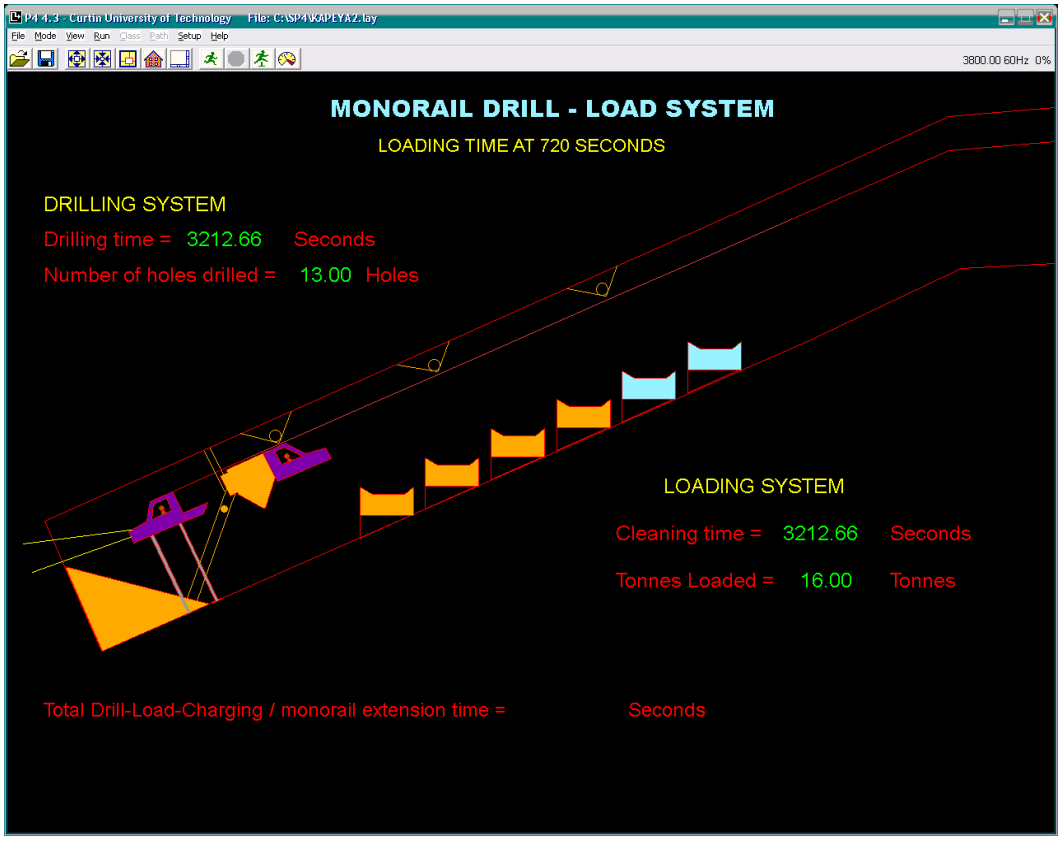

(a)

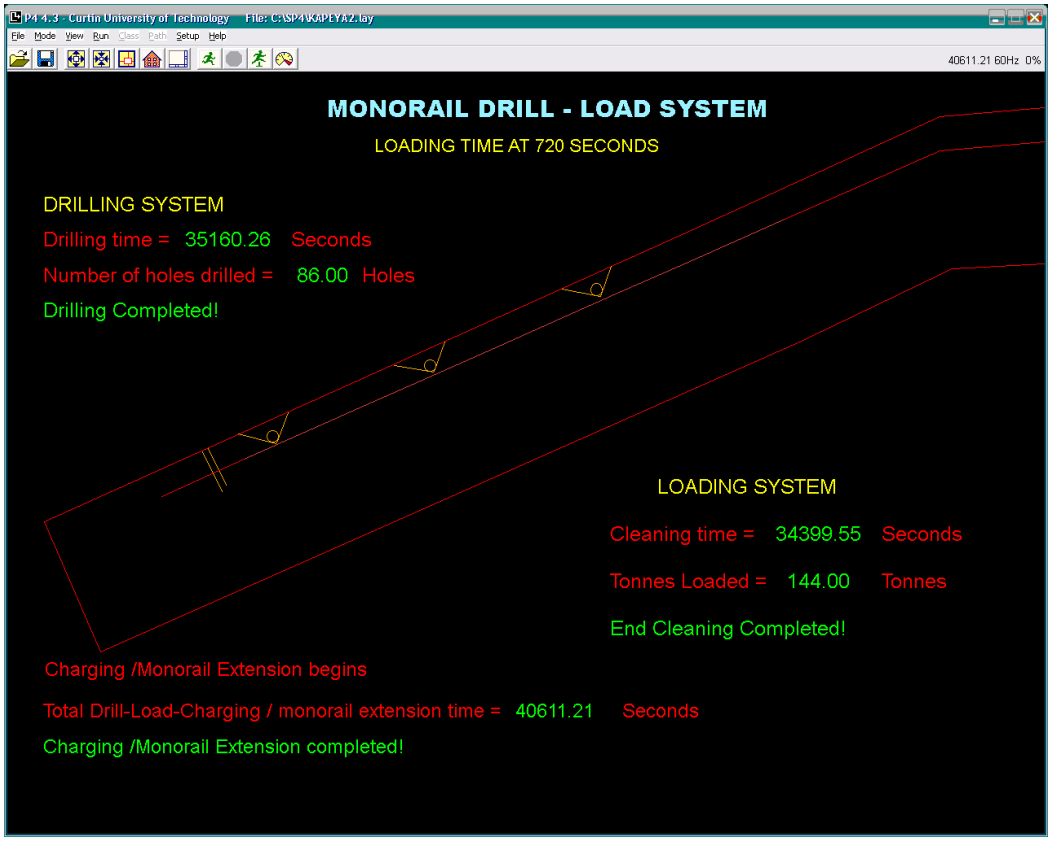

(b)

Figure A3: Loading time 720 sec (a) during face cleaning and drilling (b) after face cleaning, drilling and charging

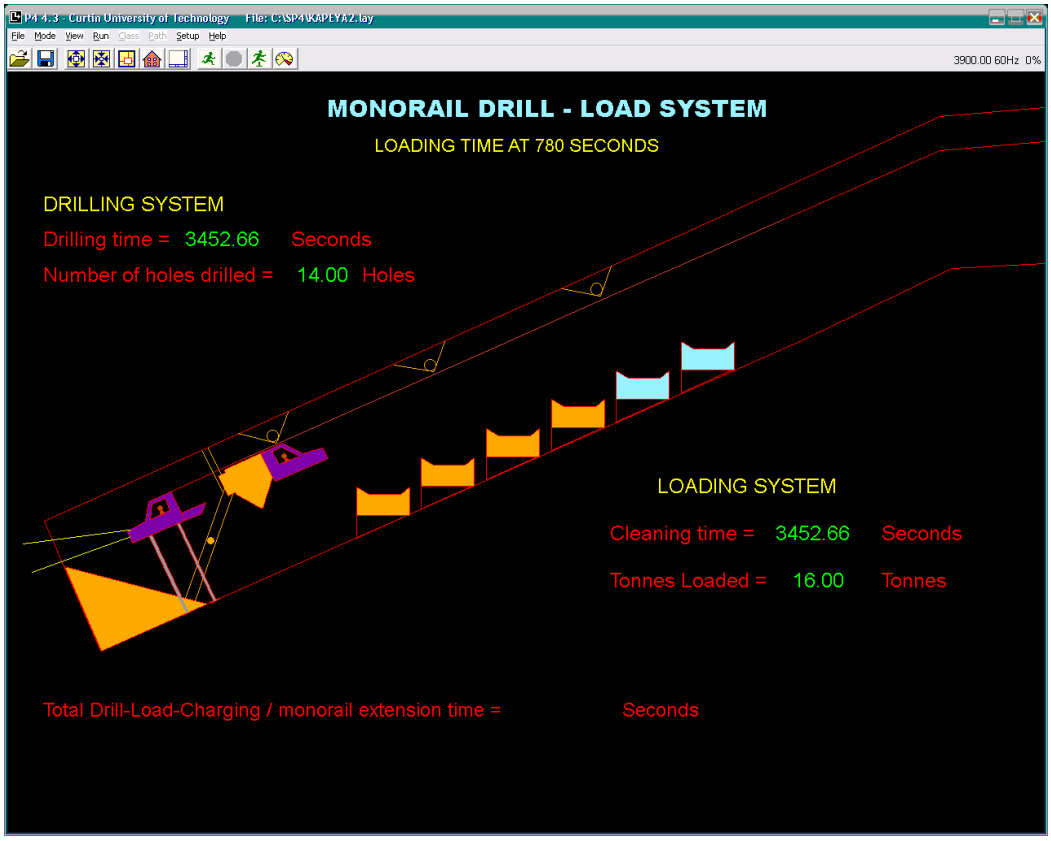

(a)

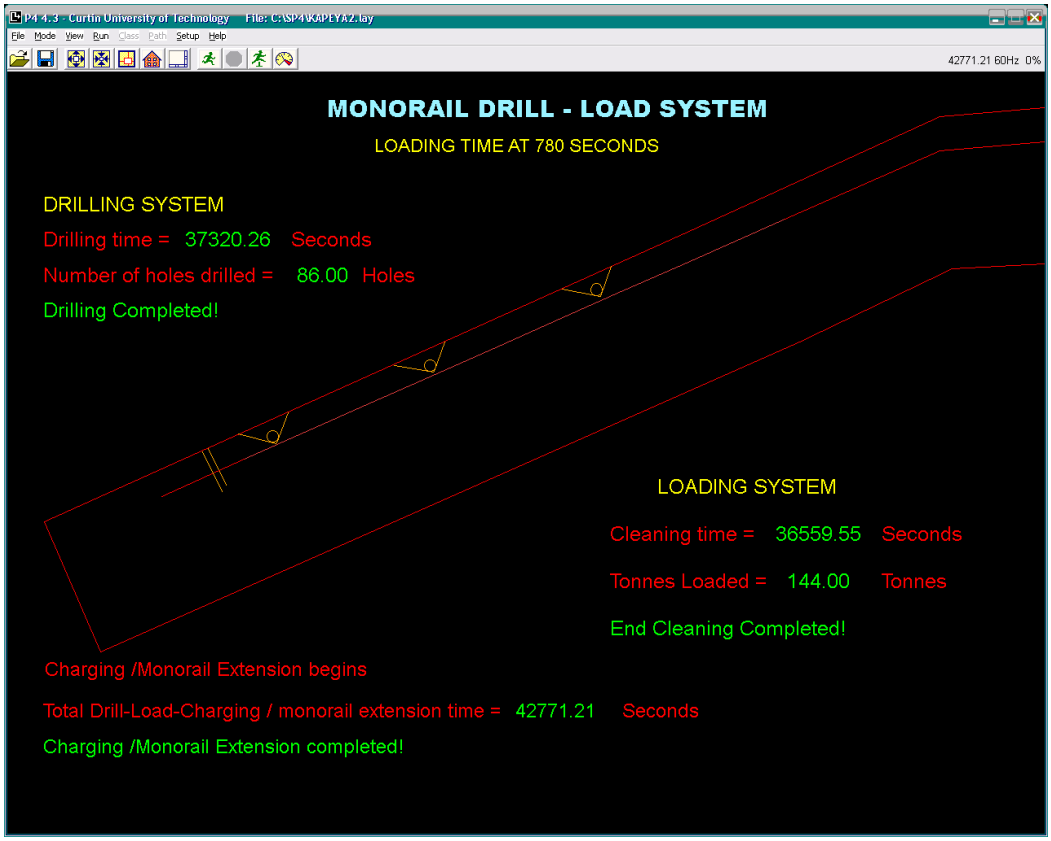

(b)

Figure A4: Loading time 780 sec (a) during face cleaning and drilling (b) after face cleaning, drilling and charging

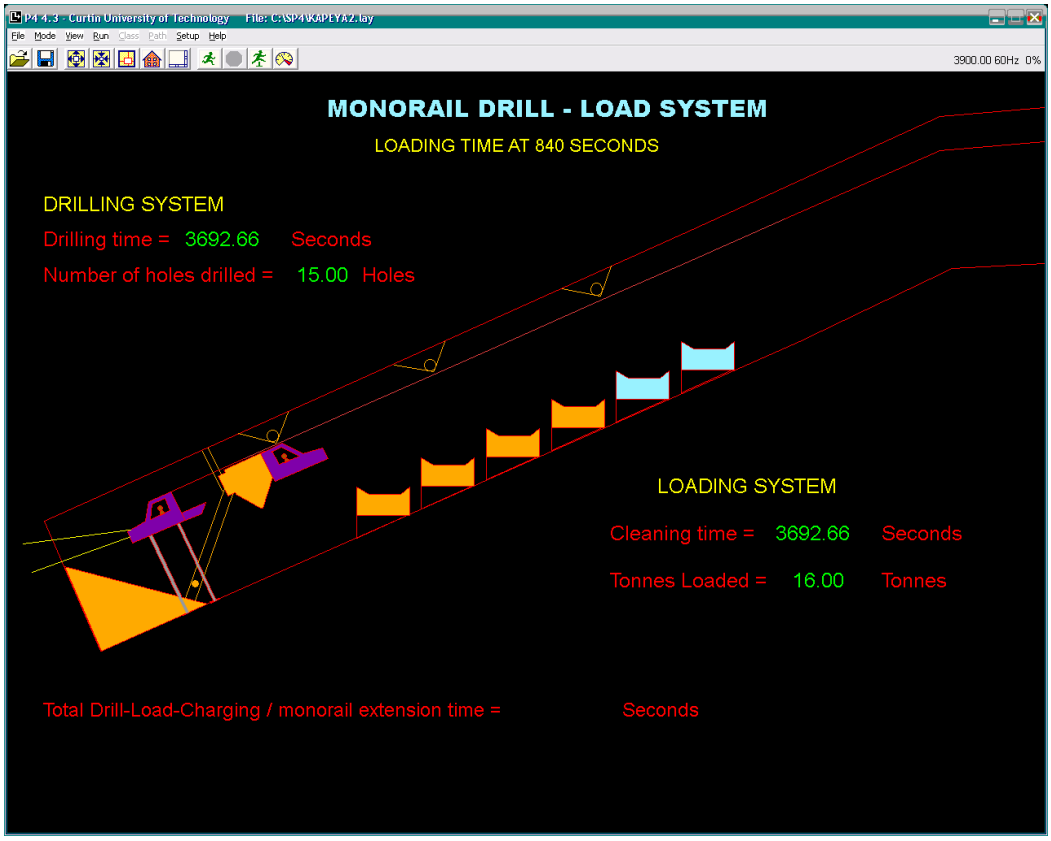

(a)

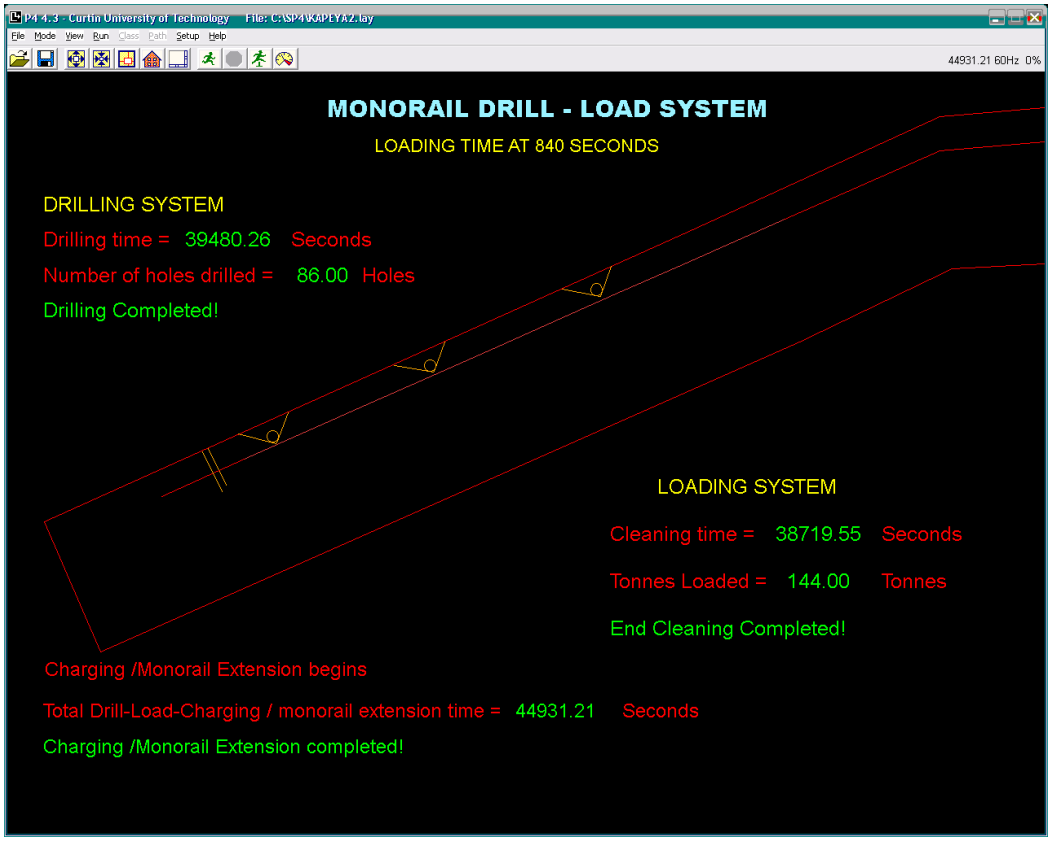

(b)

Figure A5: Loading time 840 sec (a) during face cleaning and drilling (b) after face cleaning, drilling and charging

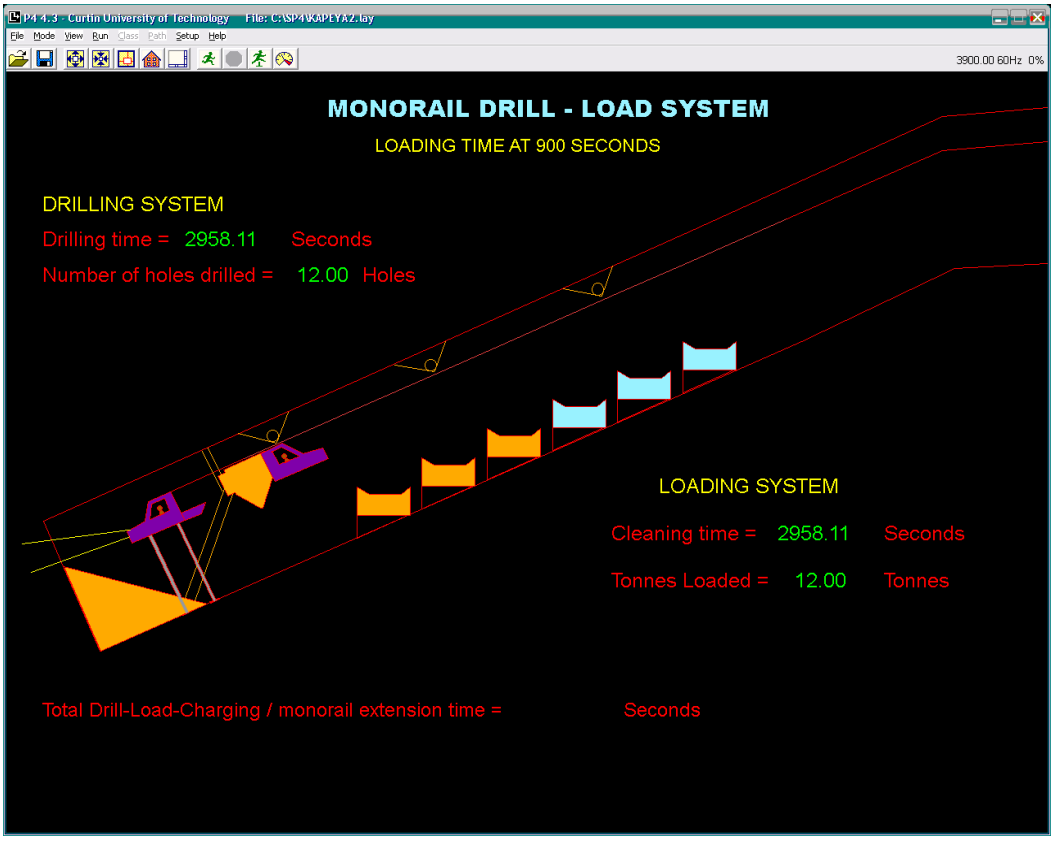

(a)

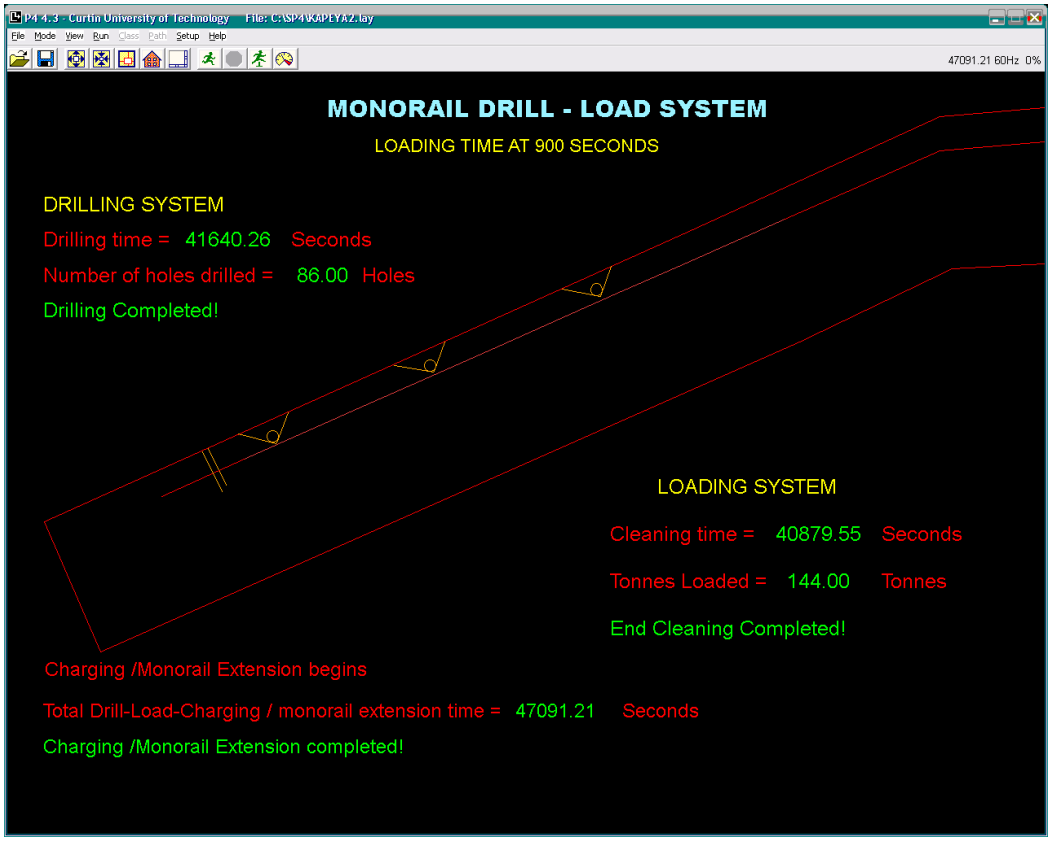

(b)

Figure A6: Loading time 900 sec (a) during face cleaning and drilling (b) after face cleaning, drilling and charging

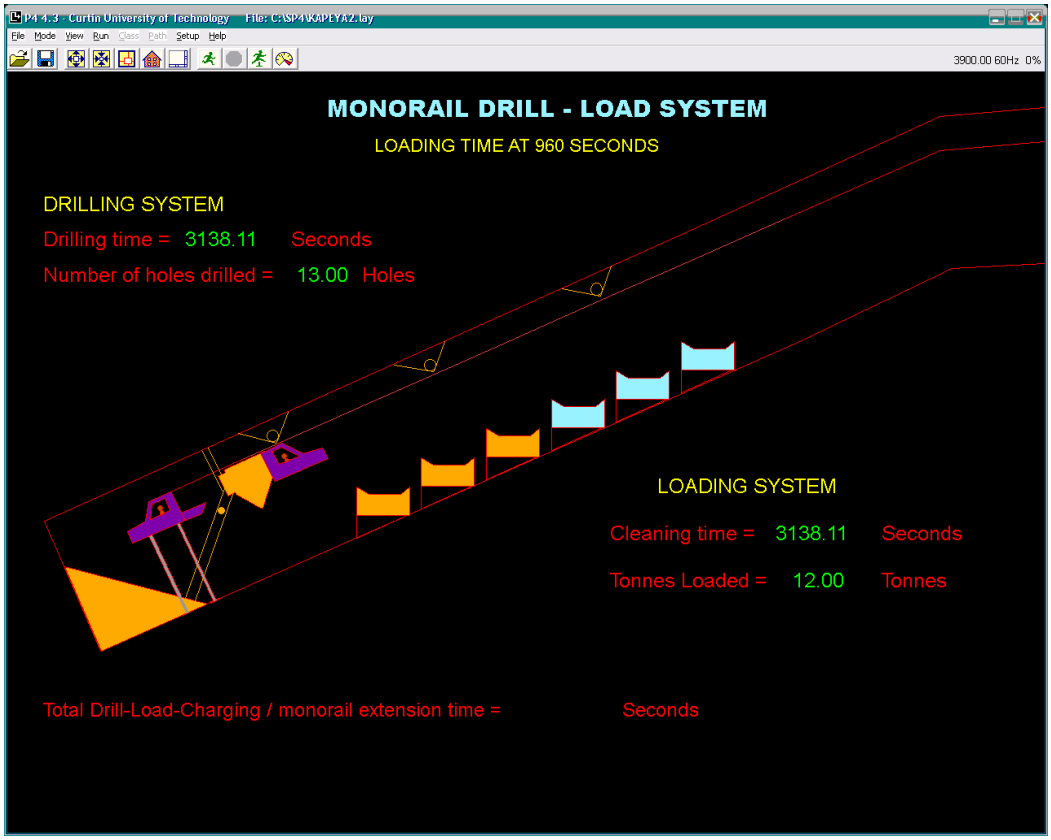

(a)

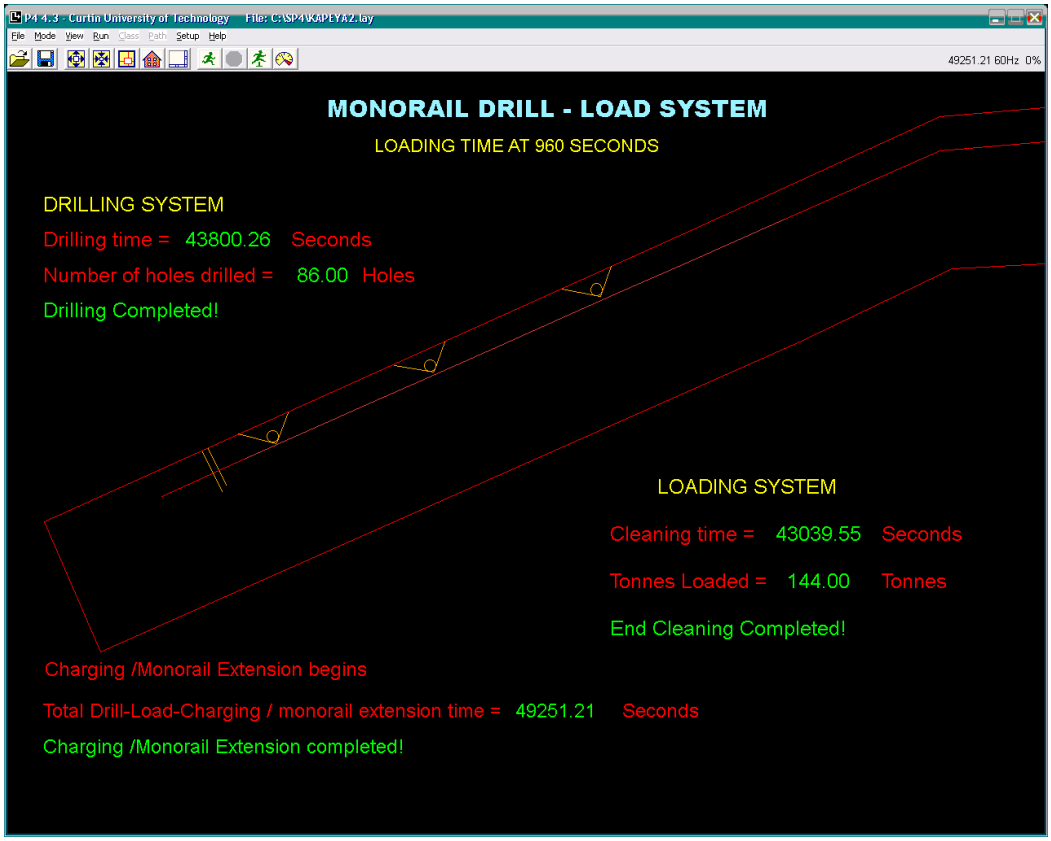

(b)

Figure A7: Loading time 960 sec (a) during face cleaning and drilling (b) after face cleaning, drilling and charging

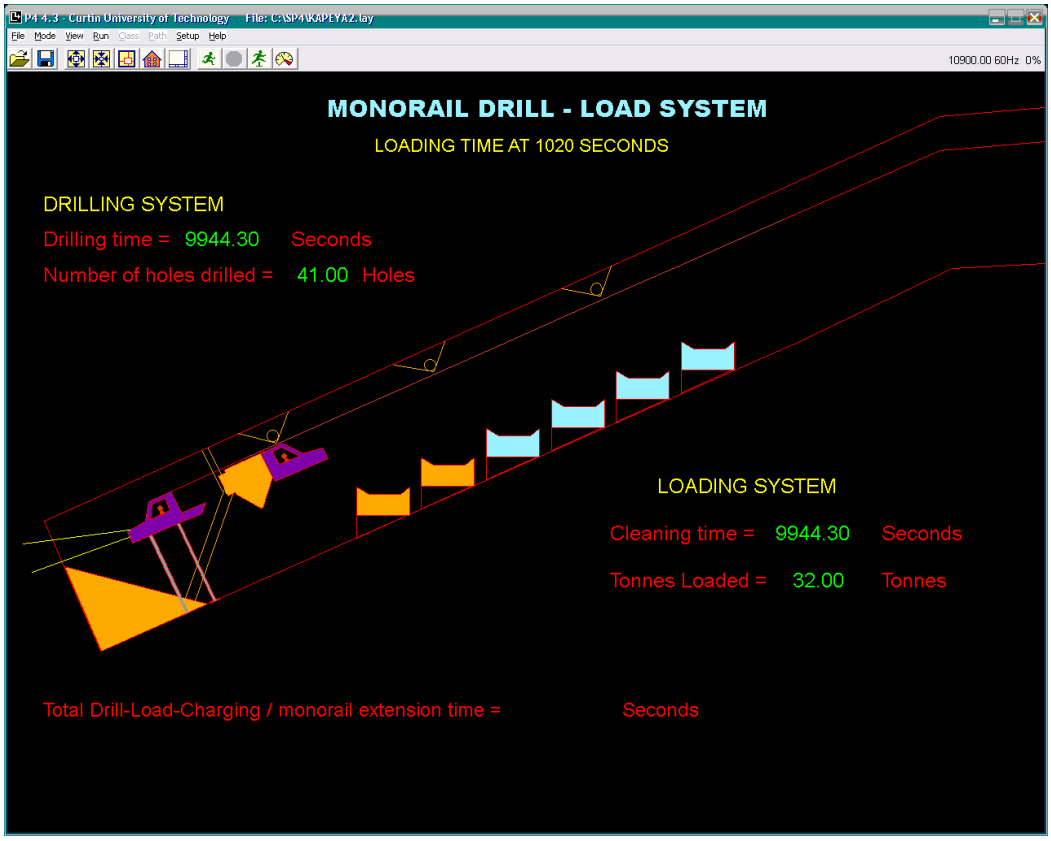

(a)

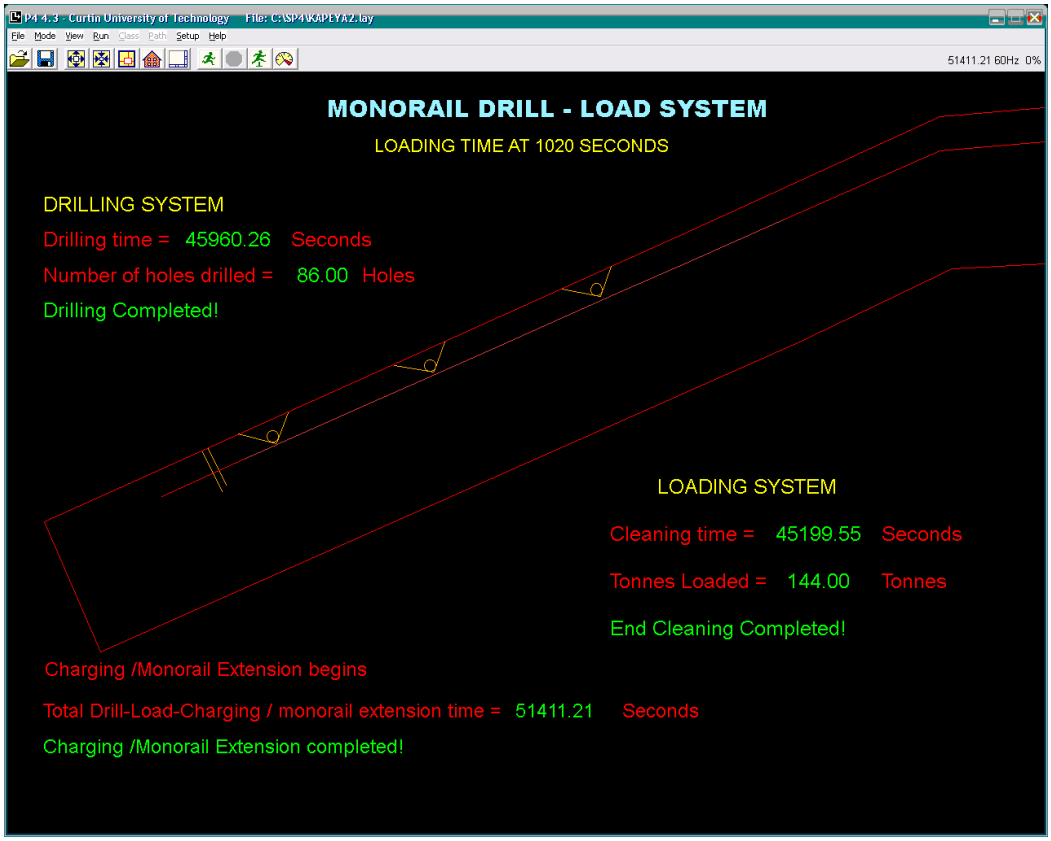

(b)

Figure A8: Loading time 1020 sec (a) during face cleaning and drilling (b) after face cleaning, drilling and charging

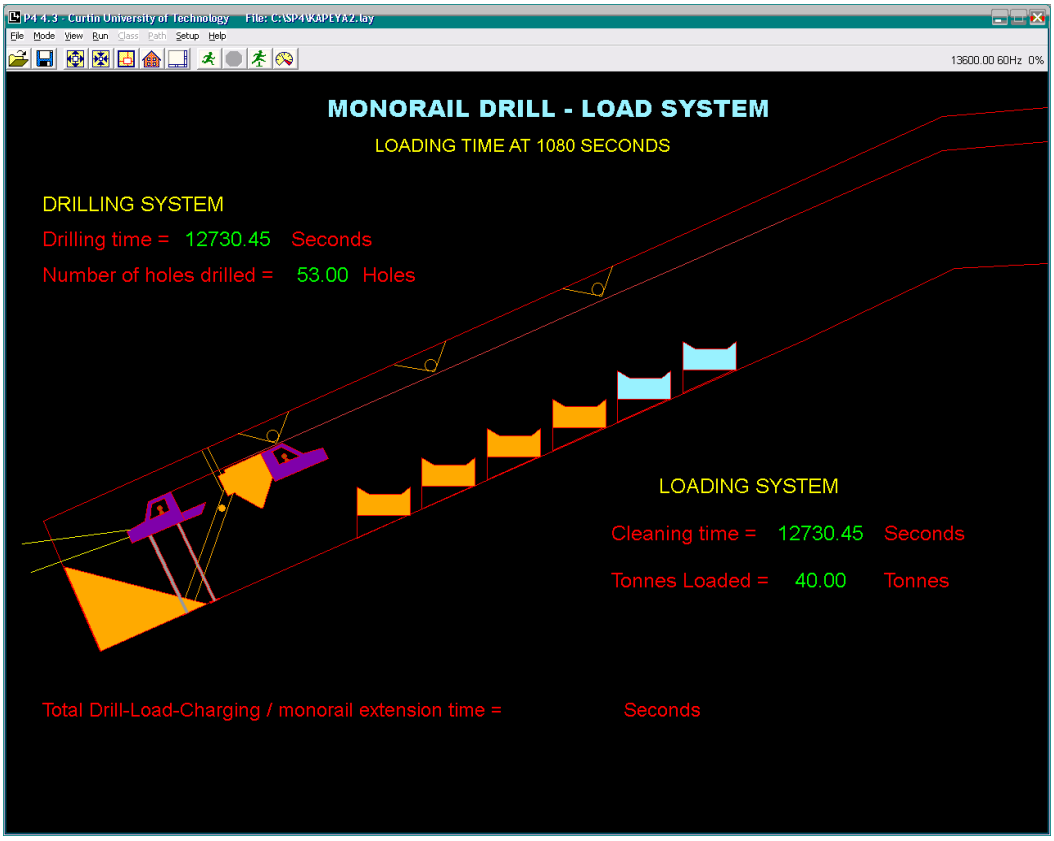

(a)

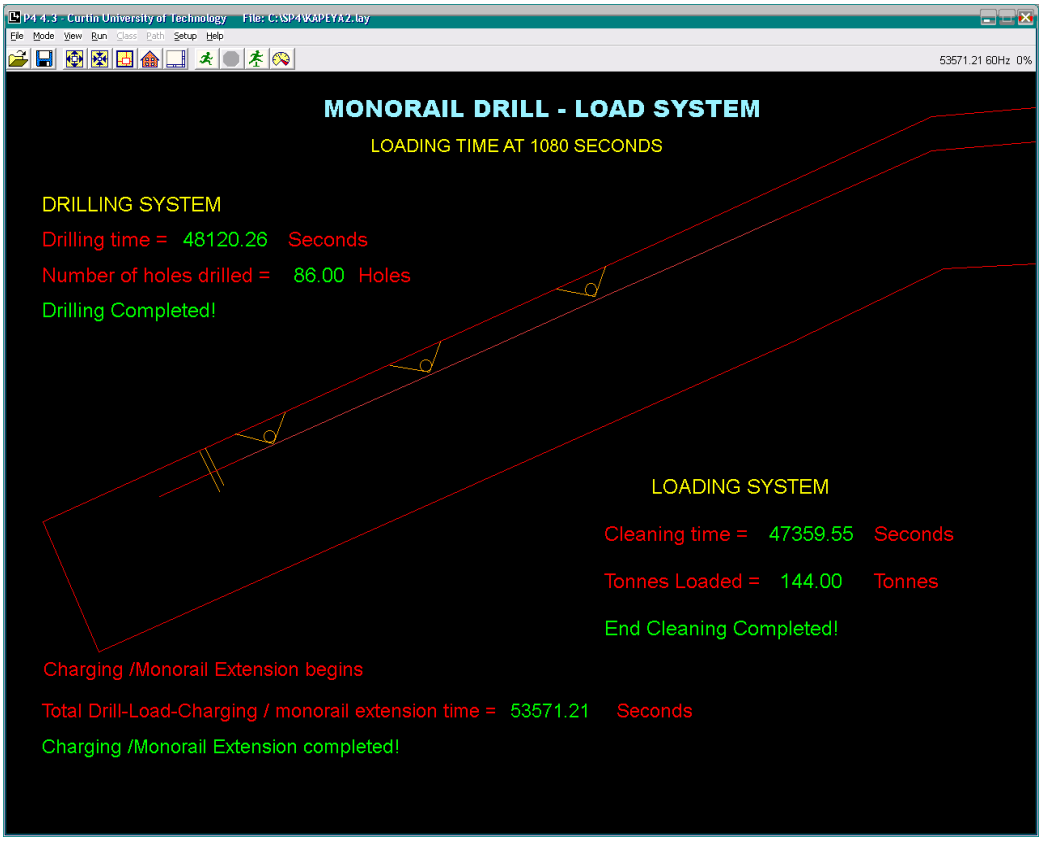

(b)

Figure A9: Loading time 1080 sec (a) during face cleaning and drilling (b) after face cleaning, drilling and charging

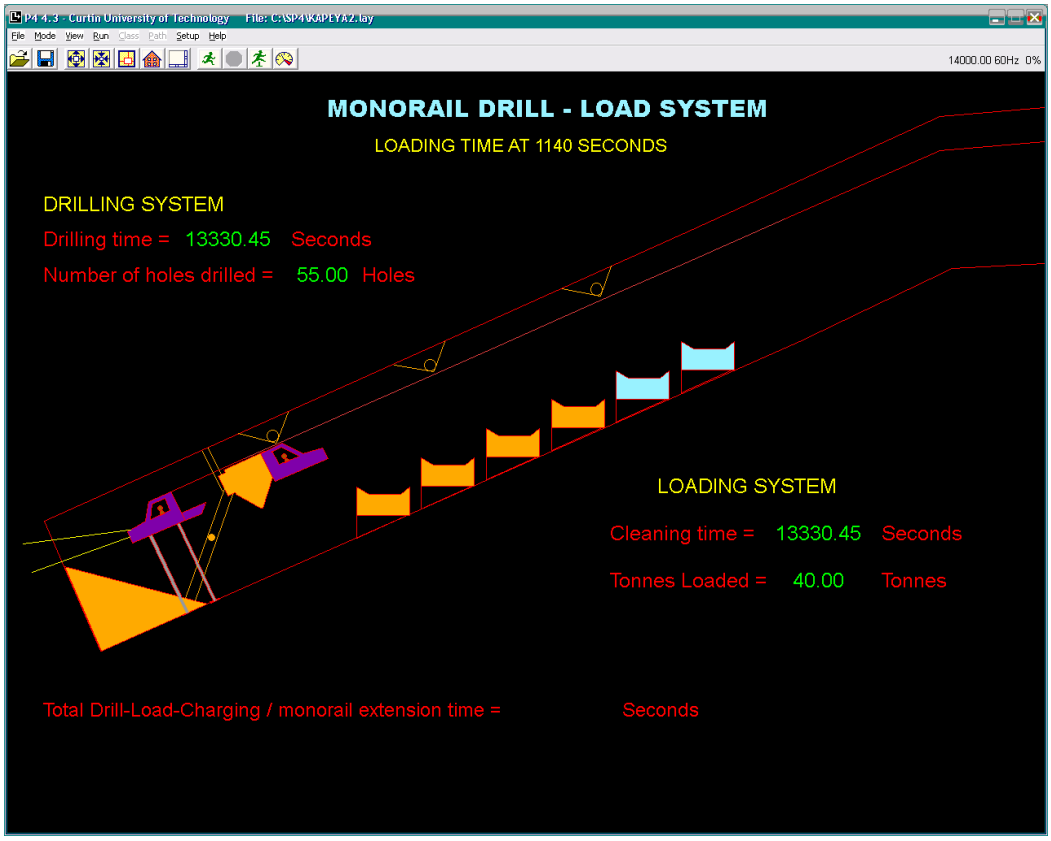

(a)

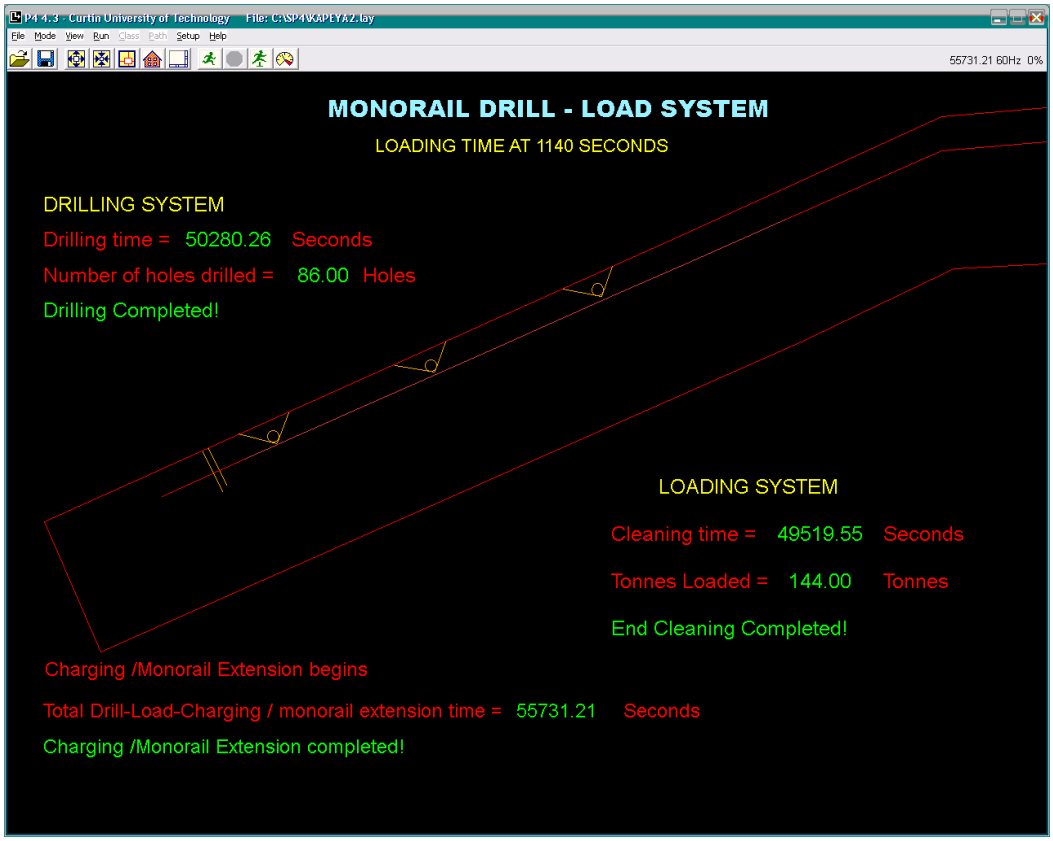

(b)

Figure A10: Loading time 1140 sec (a) during face cleaning and drilling (b) after face cleaning, drilling and charging

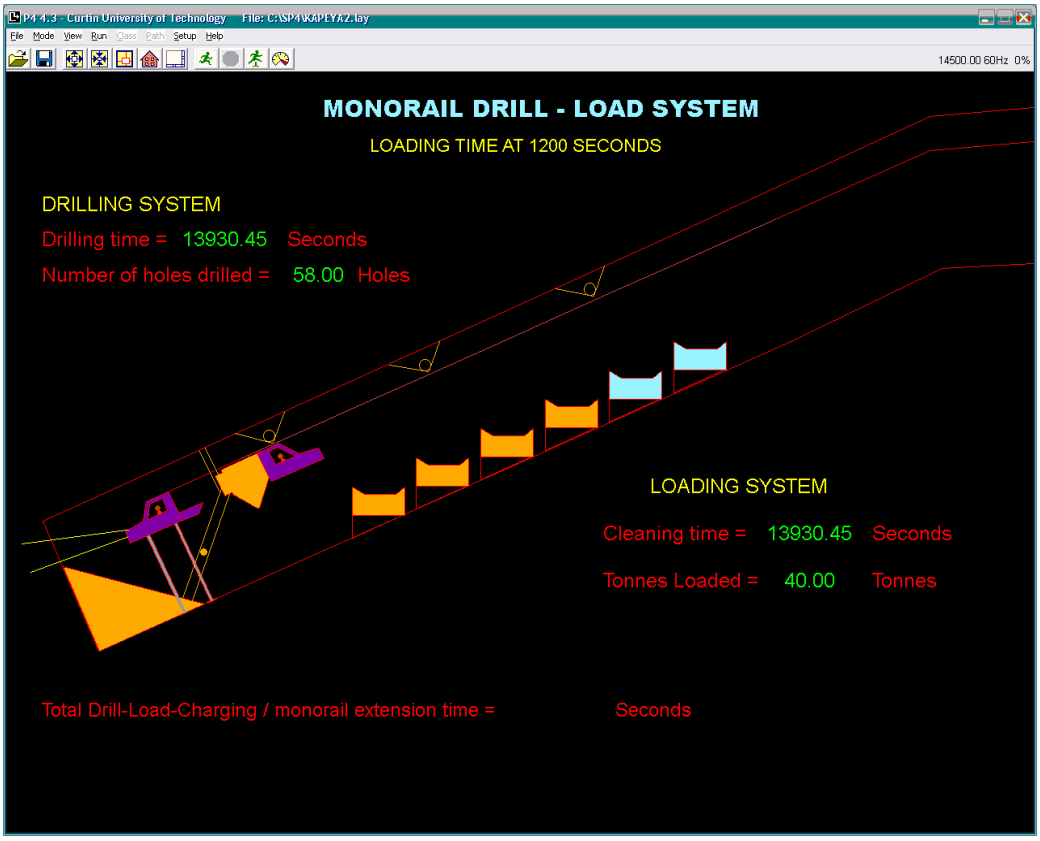

(a)

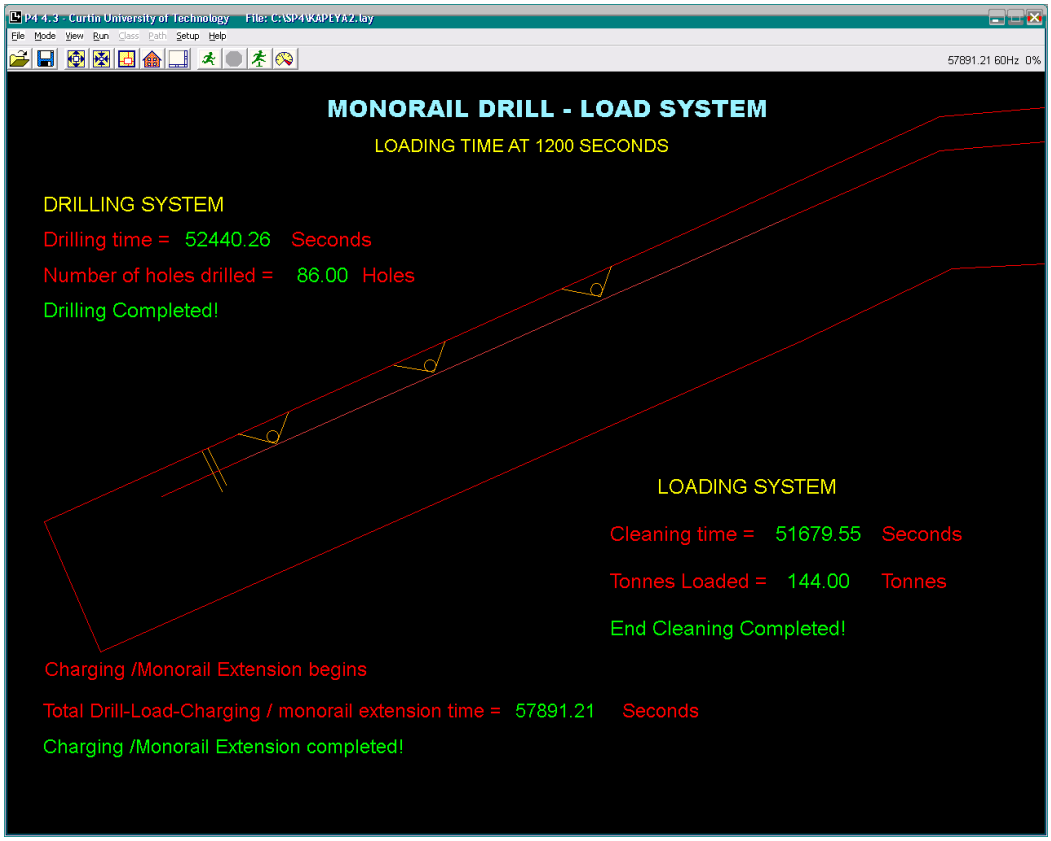

(b)

Figure A11: Loading time 1200 sec (a) during face cleaning and drilling (b) after face cleaning, drilling and charging

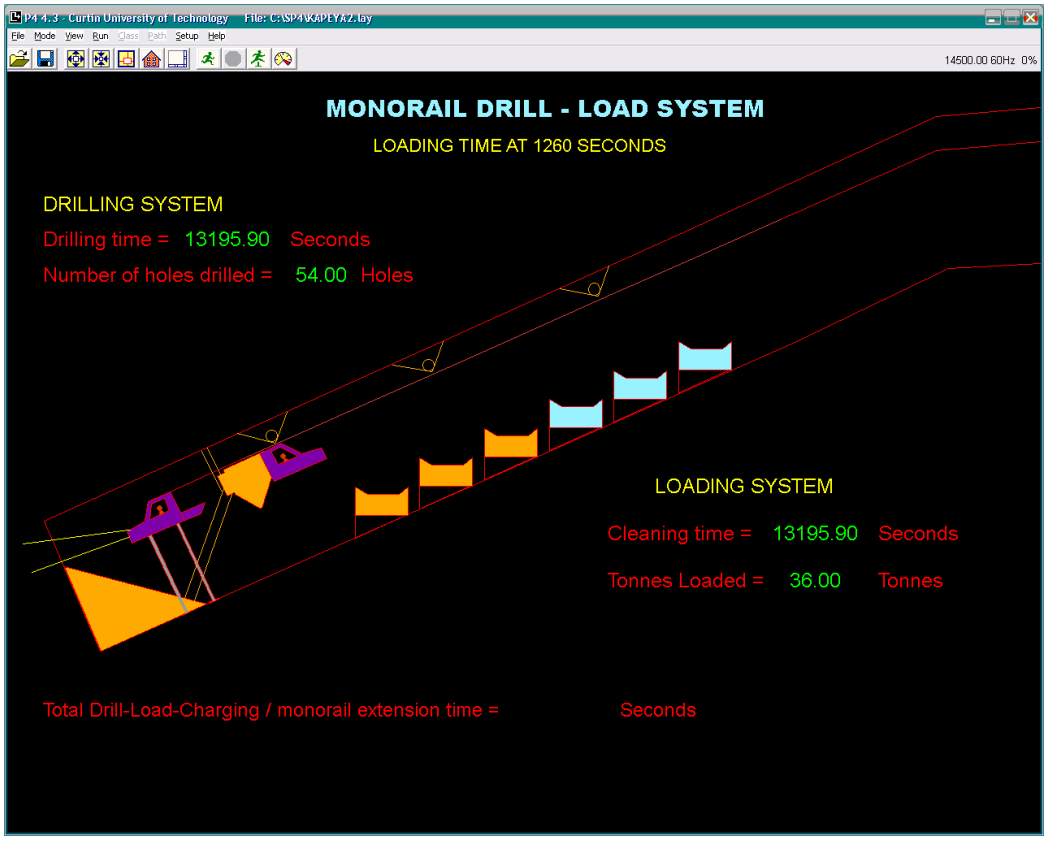

(a)

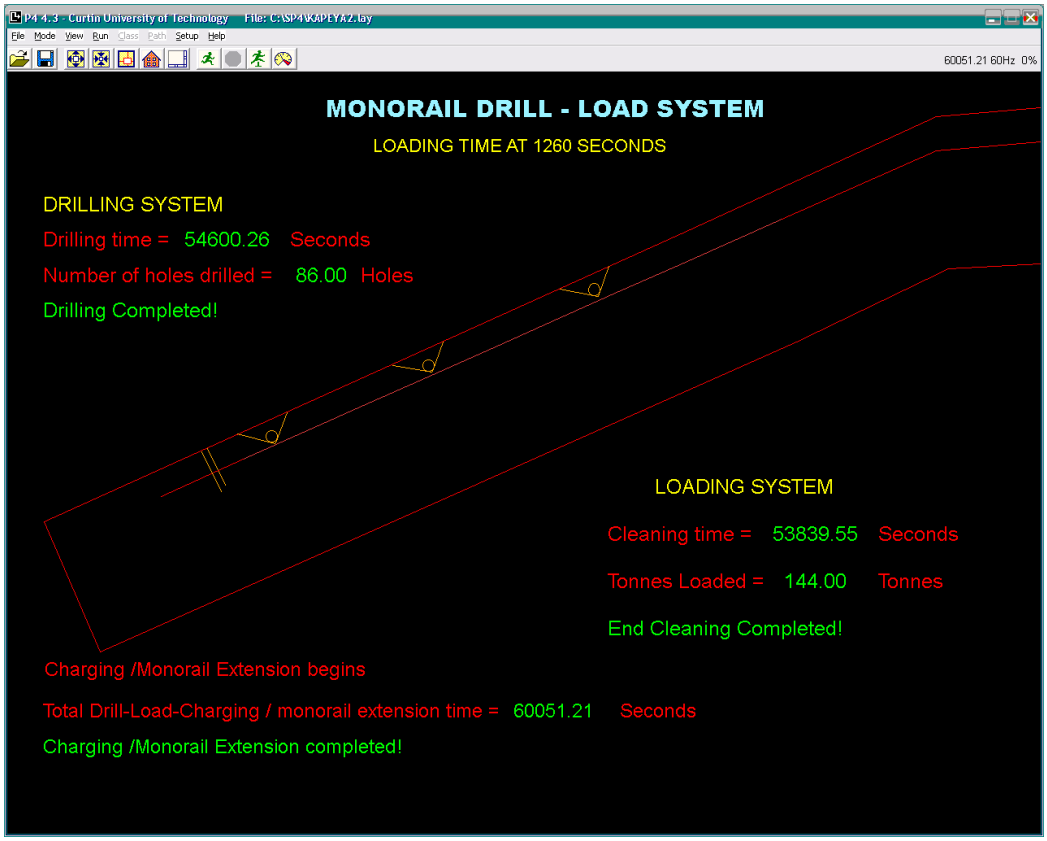

(b)

Figure A12: Loading time 1260 sec (a) during face cleaning and drilling (b) after face cleaning, drilling and charging

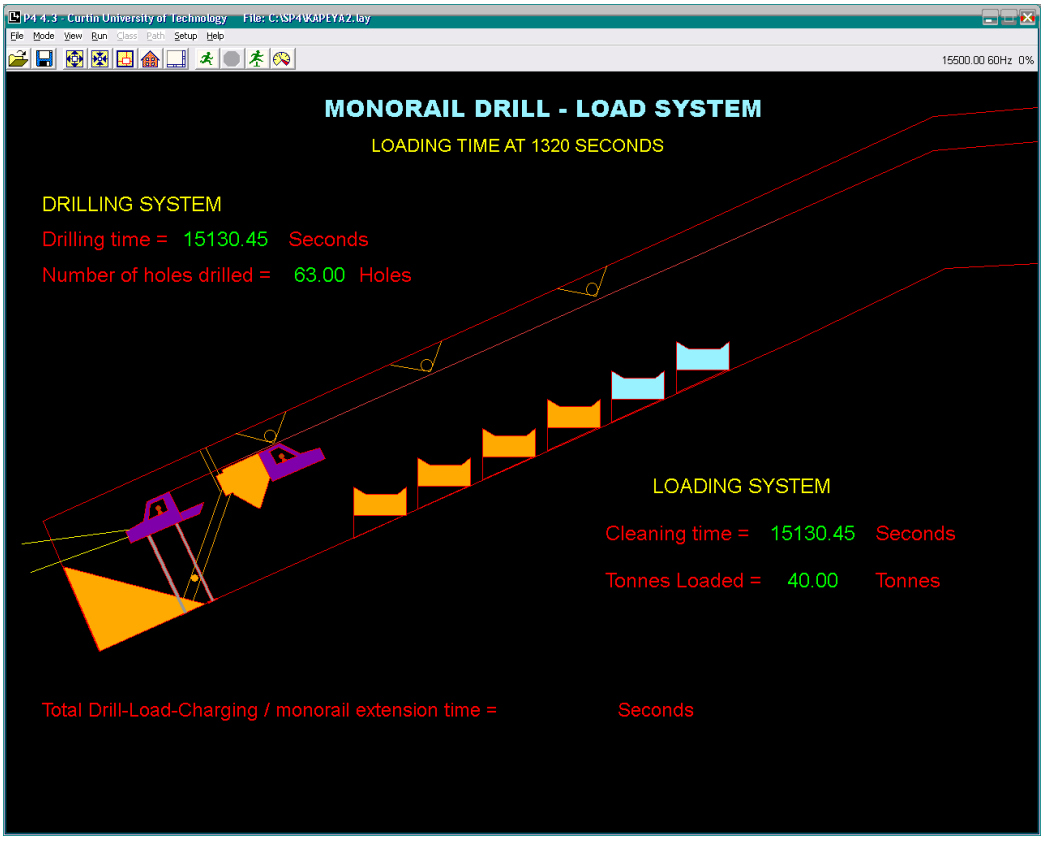

(a)

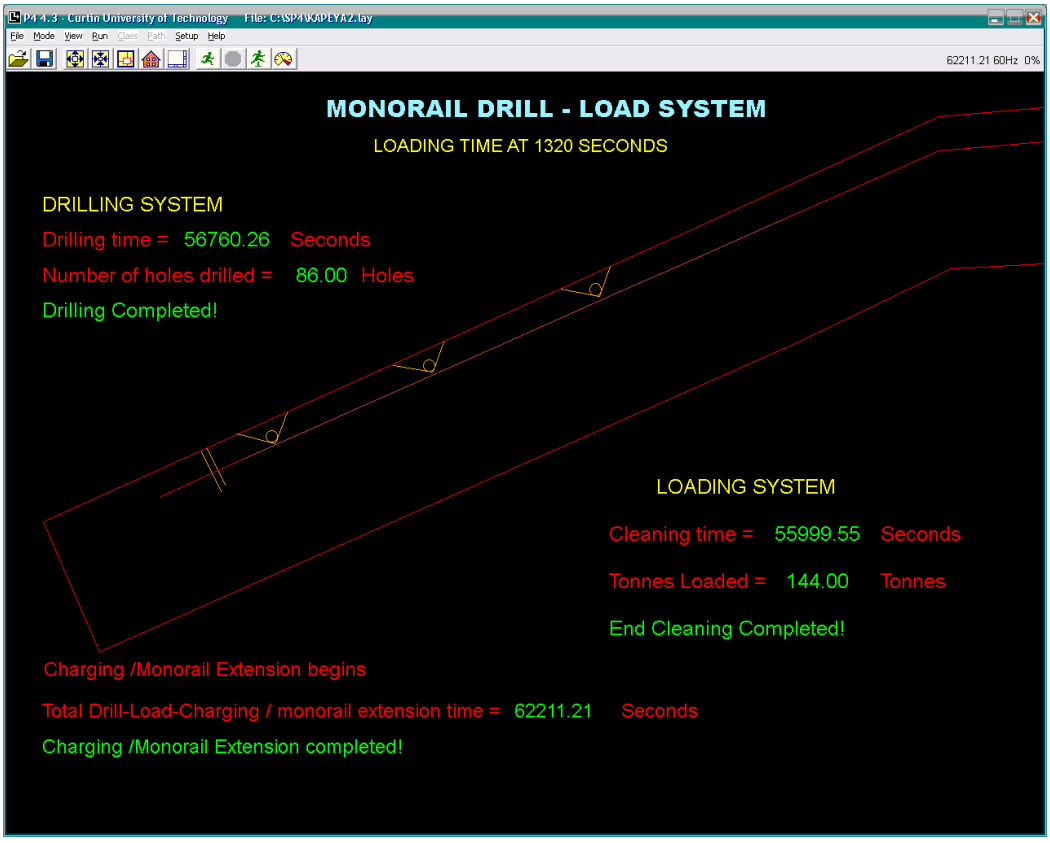

(b)

Figure A13: Loading time 1320 sec (a) during face cleaning and drilling (b) after face cleaning, drilling and charging

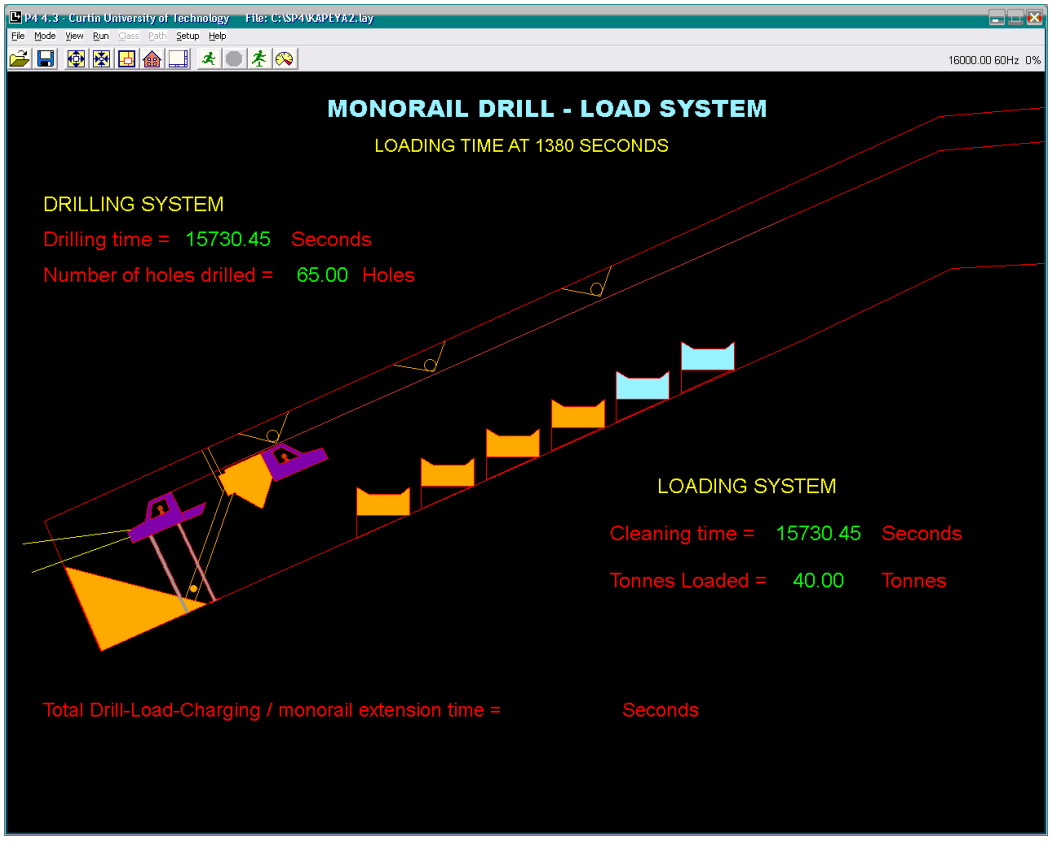

(a)

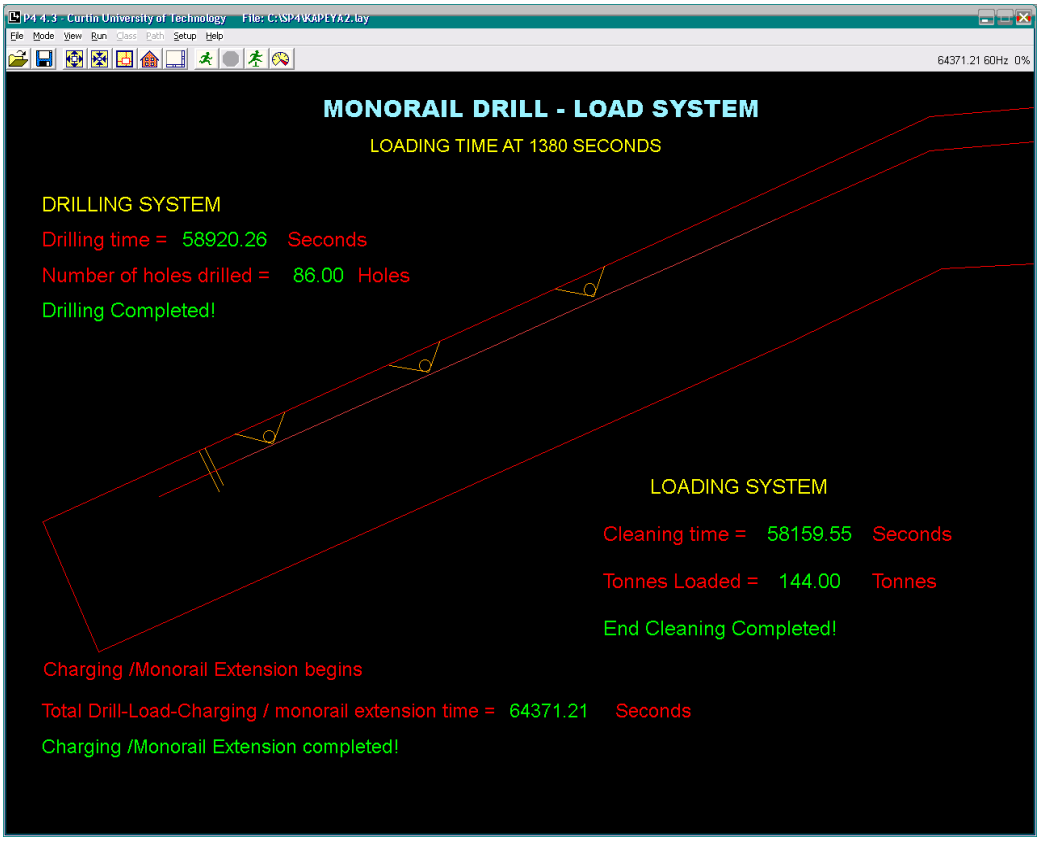

(b)

Figure A14: Loading time 1380 sec (a) during face cleaning and drilling (b) after face cleaning, drilling and charging

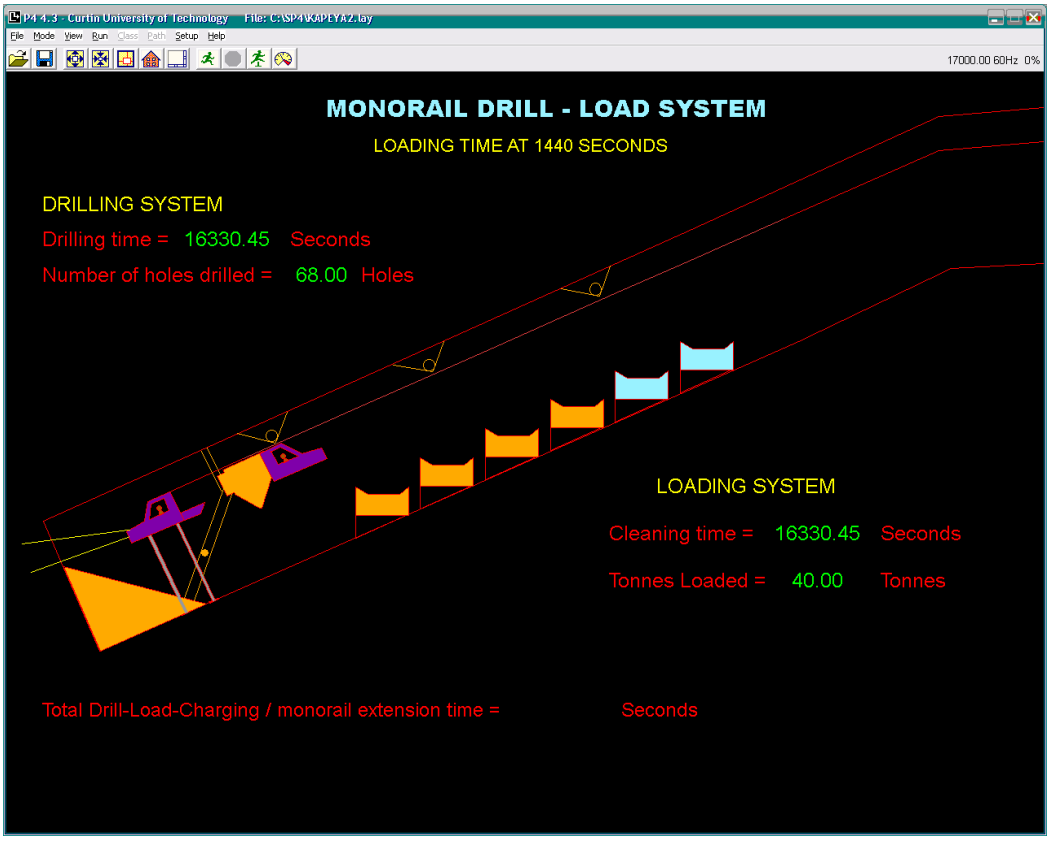

(a)

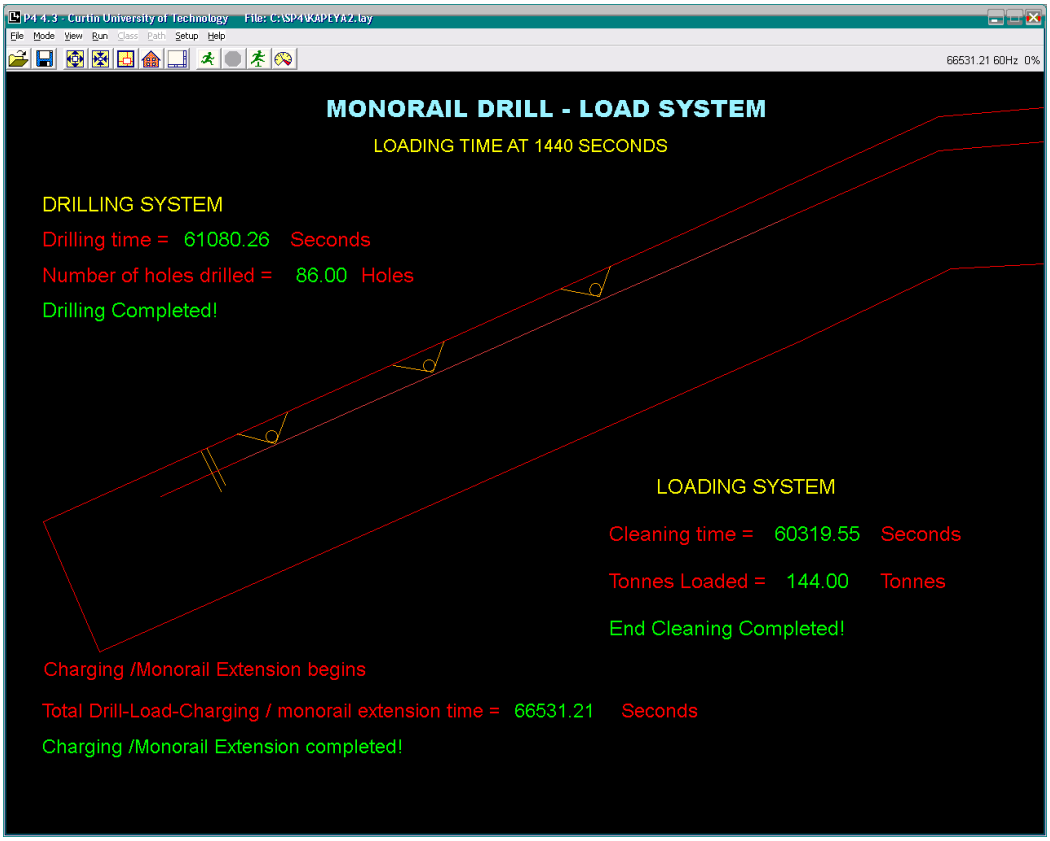

(b)

Figure A15: Loading time 1440 sec (a) during face cleaning and drilling (b) after face cleaning, drilling and charging